The role of upwelling in determining the composition, species distribution and genetic structure of intertidal communities in a time of climate change

A THESIS SUBMITTED IN FULFILMENT OF THE REQUIREMENTS FOR THE DEGREE

OF

DOCTOR OF PHILOSOPHY

OF

RHODES UNIVERSITY

(MARINE BIOLOGY)

BY

Carla Sofia Emídio Rodrigues Lourenço

February 2018

ABSTRACT

Upwelling is an oceanographic process that strongly influences coastal species and the communities they belong to. In upwelling areas, colder, denser, nutrient-rich subsurface waters are transported to the nearshore surface, replacing warmer superficial waters that are advected offshore. Such effects influence the composition and dynamics of coastal communities, for example by affecting species abundance, recruitment, dispersal and distribution. Upwelling areas are key model regions to study the responses of coastal species to climate change because they are characterized by cooler conditions and experience lower warming rates than adjacent regions. In particular, intertidal rocky shore species are ideal coastal sentinel organisms to study distributional changes driven by climate warming because they inhabit the interface between marine and terrestrial habitats and are exposed to extremely severe environmental conditions. In fact, sharp distributional shifts have been reported for multiple intertidal species as a response to ocean warming. Although some studies have investigated the role of upwelling in influencing abundance and distribution of intertidal species, little is known about its potential as refugia against climate warming and the degree to which upwelling shapes species genetic structure is yet not fully understood.

The aim of this thesis is to understand the influence of the Canary Current upwelling system on intertidal community composition, including species distribution and the genetic structure of intertidal species under current climate change. To do this, I investigated community structure of intertidal assemblages along the Atlantic shores of Morocco and Western Sahara, performed large scale surveys on species distribution, evaluated species abundance and frequency of parasitism and examined species genetic patterns. I further coupled biological data with upwelling indices, sea surface temperatures (SST) and the rate of SST warming.

I demonstrate that strong upwelling influences abundance and distribution of intertidal rocky shore species and that upwelling cells can act as refugia from climate change by

ameliorating thermal conditions. Upwelling cells also conserve the genetic diversity of the marine macroalga *Fucus guiryi*, promoting intraspecific genetic diversity by preserving unique genetic lineages. However, no evidence was found that upwelling affects the genetic structure for either *F. guiryi* or the brown mussel *Perna perna*. Instead, the genetic patterns presented in this thesis seem to result from a combination of species' life history traits, population size and habitat suitability. My results also suggest that upwelling intensity affects the frequency of endolithic parasitism on the Mediterranean mussel *Mytilus galloprovincialis*.

In times of climate change, upwelling events provide suitable environmental conditions for species to counter act climatic change. As upwelling is project to intensify in the future, its influence on benthic intertidal species might be greater than previously anticipated.

TABLE OF CONTENTS

TABLE INDEX

FIGURE INDEX

ACKNOWLEDGEMENTS

Quando há quatro anos cruzava pela primeira vez o Saara Ocidental não podia imaginar de todo a aventura que estava prestes a começar. E não falo só dos vários dias a viajar para sul, das mais de 12 horas por dia no carro, das dezenas de vezes que fui parada pela polícia, das idas à esquadra, das vezes que passei por Marroquina ou daquela vez em que cheguei ao carro e tinha os dois pneus da esquerda dilacerados por uma faca. O doutoramento que agora chega ao fim foi todo ele uma grande e desafiante aventura, cheia de peripécias, azares, lágrimas, risos, crescimento pessoal e muita, muita aprendizagem. Mas este não foi de todo um percurso que fiz sozinha. Por isso mesmo, e porque não faria sentido ser de outra forma, quero agradecer a todos os que me acompanharam ao longo dos altos e baixos desta jornada.

Caro Professor Christopher McQuaid, o meu sincero obrigado por me ter dado a oportunidade de embarcar num doutoramento em Rhodes, pelo seu apoio, compreensão, pelas palavras de encorajamento e pelas lições que foram dadas em pequenos comentários – não me esquecerei da diferença entre "variar" e "diferir". Estou também muito agradecida à Doutora Katy Nicastro e ao Doutor Gerardo Zardi, também meus orientadores, pelo constante acompanhamento, pela paciência, por estimularem o meu pensamento crítico, por me deixarem dormir descansada em todas as viagens, pelas intermináveis correcções e por me responderem sempre a "só mais uma pergunta". Por esta altura já deviam saber que eu não faço "só mais uma pergunta".

Esta tese não teria sido possível sem as bolsas de estudo que recebi da NRF – Fundação Nacional de Investigação da África do Sul nem sem o financiamento da FCT – Fundação para a Ciência e Tecnologia em Portugal. Um sincero obrigado à Gwen e à Ticia por agilizarem todos os processos académicos no decorrer destes 4 anos. Estar ausente de Rhodes e não enlouquecer com toda a burocracia só foi possível graças à vossa ajuda.

O sucesso do trabalho em campo e em laboratório, esse, deve-se a um grande número de pessoas. Ritinha do papá, obrigada por toda a ajuda em campo e fora dele. Obrigada por teres sido uma técnica disponível, trabalhadora e que não espera que lhe digam o que há para fazer. Tive vontade de te abandonar em Marrocos algumas vezes, mas depois quem é que conduzia o carro? Pensei melhor. Obrigada à Mariana e ao Pedro pela valiosa ajuda no intertidal e à Mafalda por todas as algas identificadas. Um grande obrigado à Zahira e ao Professor Brahim Sabour por me facilitarem as últimas idas a Marrocos e por me fazerem sentir verdadeiramente em casa. Encontrar-nos-emos de novo, inshallah. Um obrigado à Rosa e à Lica que estiveram sempre disponíveis para

responder a todas as minhas perguntas sobre modelação. André, quem melhor do que tu para me dar explicações de R pelo facebook? Obrigada, Pseudo!
Um obrigado imenso à minha família Farense que me acompanhou nos dias de mau cheiro no laboratório e nas noites estreladas na praia. Aos que já deixaram Faro, aos que vêm de passagem e aos que chegaram há pouco. Tânia Aires, Cristina, Licínia, Nelson, Gonçalo, Joana Macedo, Neiva, Su, (i)Ana, Dinarte. Ao resto da família Algarvia a quem tanto devo e que tornaram o Algarve a minha casa: Inés, Inês, Maló, Alexandra, Bruno, manos Tavares, Diogo, Eva. À Buga, à Saretta e ao Gian (ao Pachá e à Camilla também, obviamente!), grandes amigos e grandes pilares da minha sanidade mental, que me mostram todos os dias que os milhares de km que nos separam não são nada comparados com a nossa amizade. Um obrigado muito especial à mais insana de todas as pessoas da família Farense, uma espécie de irmã mais velha. Perdi conta às horas ao telefone e a tudo o que, sem saberes, fizeste por mim, Xana. Um obrigado certamente não chega, por isso vai de férias que eu fico com a Luninha.
Obrigada Lia por embarcares na Straw Patrol e por me ajudares a deixar o Mundo um pouco melhor do que o encontrámos. Esta aventura tem sido maravilhosa ao teu lado e é tão bom trabalhar contigo.
Estou para sempre grata à minha família em Milfontes, Beja, Montes Velhos e Vendas Novas. A vocês que me perdoaram todas as ausências, todos os aniversários perdidos, todos os Natais a correr, todos os "não vou poder ir, tenho de trabalhar", todas as chamadas que não fiz, todos os abraços que não dei. Em especial, obrigada aos meus sobrinhos - que eu mal vi crescer - por aceitarem sempre, ainda que resignados, que a minha estadia tinha de ser curta. Considero-me bastante feliz e sortuda por fazer parte de uma família com princípios, tão lutadora, e que me permitiu sempre seguir os meus sonhos e fazer as coisas (maioritariamente) à minha maneira. Sou uma melhor pessoa por vossa causa.
À Pi, a mais fiel amiga, que me fez esquecer os dias maus, que me acompanhou noites dentro enquanto escrevia e que me relembra todos os dias que a felicidade está nas pequenas coisas.
A este Algarve, a esta doce Ria Formosa, que roubaram o coração que estaria para sempre destinado à foz do Rio Mira. A este pequeno paraíso, escondido por entre sapais, flamingos e um mar quente, que me fez perceber que a nossa casa é mesmo onde está o nosso coração. A Marrocos, o país que agora também chamo meu, pelas suas gentes prestáveis, pelos cheiros únicos, pela harira – a melhor sopa do Mundo – pelo deserto e por ser sempre a minha casa longe de casa.

Acima de tudo, o agradecimento mais importante de todos, ao meu melhor amigo e companheiro de vida, que tem feito mais do que eu alguma vez poderia pedir. O teu amor fez-me manter a cabeça levantada e o coração forte. Rúben, obrigada por confiares em mim, por aceitares este meu vício pelo trabalho, por todas as vezes que respiraste fundo quando eu stressava, por todos os cães que levei para casa e de quem cuidaste quando eu estava ausente. Obrigada por seres a luz nos períodos mais sombrios, por teres escolhido partir nesta aventura comigo e por nunca me deixares só. E agora, vamos a uma nova aventura! Dobby está livre.

When I was crossing the Western Sahara for the first time 4 years ago I could not imagine the adventure I was about to start. And I am not just talking about those many days driving south, the +12h/day in the car, the dozens of times I was stopped by the police, those days I had to go to police stations, the several times I was mistaken for a Moroccan girl or that one morning when I went to pick up the car and someone had slashed the two left tires. The PhD that now comes to an end has been a huge, challenging adventure, full of mishaps, mischances, tears, laughs, personal growth and so much learning. This was not a solo journey, however, and I cannot miss the chance to thank all those people that walked by my side, through the ups and downs of this adventure.

I would like to express my gratitude to Professor Christopher McQuaid, for supervising me and allowing me to pursue a PhD in Rhodes, for all his support, understanding, for encouraging me to do better and for all the lessons hidden in short comments – I will not forget the difference between 'vary' and 'differ'. I am also grateful to Dr. Katy Nicastro and Dr. Gerardo Zardi, also my supervisors, for the constant guidance, for being patient, for stimulating my critical thinking and initiative, for always letting me sleep the moment I entered the car, for the endless corrections and for always answering me that 'one last question'. You should know by now that it won't be the 'last question'.

The work developed in this thesis would not have been possible without the bursaries granted by NRF – National Research Foundation or without the project funded by FCT – Fundação para a Ciência e Tecnologia (Portugal). I would like to thank Gwen and Ticia for helping me with all the academic processes during these 4 years. Being absent from Rhodes and not going mad with all the paper work has only been possible thanks to you.

The success of all field and lab work is due to a great number of people. Daddy's little Rita – your name in English sounds amazing – thank you for all your help. Thank you for being a great, hard-working technician, and for not sitting and waiting for people to tell you what to do. Sometimes I thought I should just abandon you in Morocco, but who would drive the car then? I thought twice. Many thanks also to Mariana and Pedro for their valuable help in the intertidal and to Mafalda for all the identified algae. I am extremely grateful to Zahira and Professor Brahim Sabour for all their help while travelling in Morocco and for always making me feel home. We will meet again, inshallah. To Rosa and Lica for always being available to help me and answer all my modelling doubts. André, who other than you would teach me how to use R, tutoring me on facebook? Thank you!

My heartfelt gratitude goes to my Faro family, for all those stinky days in the lab and starry nights at the beach. To all those who left Faro, those who pass by and those who have recently arrived. Tânia Aires, Cristina, Licínia, Nelson, Gonçalo, Joana Macedo, Neiva,

Su, (i)Ana, Dinarte. To the remaining Algarvian family, who helped me calling Algarve my home: Inés, Inês, Maló, Alexandra, Bruno, Tavares crew, Diogo, Eva. To Buga, Saretta and Gian (Pachá and Camilla too, obviously!), those great friends who keep me mentally sane, for showing me every single day that the thousands of km that separate us mean nothing compared to our friendship. Special thanks goes to the most insane person of all Faro family members, kind of an older sister. I lost track of the countless hours spent on the phone and of the things you did for me, Xana – even if you did not notice what you were doing. 'Thank you' might not be enough so just go on holidays and leave me taking care of Luninha.

Thank you Lia, for joining Straw Patrol and helping me leave this world a little better than we found it. This has been an amazing ride by your side and I am so happy to have the opportunity to work with you.

I am forever grateful to my family spread around Milfontes, Beja, Montes Velhos and Vendas Novas. You forgave all my absences, all the lost birthdays, every single Christmas I rushed to see you and left the following day, all the phone calls I promised and did not do, all the hugs I still owe you. I would particularly like to thank my nieces and nephew, who grew up without their aunt, for always accepting – although heartbroken – that our time together had to be short. I am so happy and lucky for being part of such a loyal, hard-working family that has always allowed me to pursue my dreams and do things (mostly) my way. I am a better person because of you.

To Pi, the most faithful friend, who made me forget the bad days, who accompanied me all those longs nights writing the thesis and who reminds me every single day that the most simple things can bring the most happiness.

To Algarve, to this sweet Ria Formosa that stole the heart that had been destined to the place where the Mira river meets the ocean. To this small paradise, hidden within salt marshes, among flamingos and a warm sea, for showing me that home is really where our heart is. To Morocco, the country that I now call my own, for its friendly, helpful people, for its unique smells, for harira – the best soup in the World –, for the desert and for always being my home away from home.

Above all, my deepest gratitude goes to my best friend and life companion, who has done so much more than I could ever wish for. Your love has kept my head up and my heart strong. Thank you for trusting me, for accepting how workaholic I am, for your deep breaths under my stress, for all the dogs you took care while I was away. Thank you for being the light in the darkest of times, for joining me in this adventure and for never letting me alone. Now, let the new adventure begin! Dobby is free.

'Words are, in my not-so-humble opinion, our most inexhaustible source of magic.'

J.K.Rowling

Aparecium.

CHAPTER 1

General introduction

Intertidal shores of Sidi Bouzid, Morocco.

1.1 INTRODUCTION

Biogeographical patterns and distributional shifts of species

Biogeography describes 'the distribution of life across space, and how, through time, it has changed' (Whittaker *et al.*, 2005, p4). Species biogeographical patterns are not only the result of species-specific life history traits that influence the ability of an organism to reach and occupy a certain area, they are determined to a large extent by the surrounding environment (Fenberg *et al.*, 2015). Species distribution and abundance are influenced by abiotic factors such as light (Cole & Weltzin, 2005; Frade *et al.*, 2008; Manuel *et al.*, 2013), temperature (Belanger *et al.*, 2012; Lourenço *et al.*, 2016), salinity (Joshi & Ghose, 2003; Josefson, 2016), soil and substratum (Tateno & Takeda, 2003; Steven *et al.*, 2013) and nutrients (Burt *et al.*, 2011; Condit *et al.*, 2013). For example, low light availability prevents the establishment of photoautotrophic species in deciduous forests (Cole & Weltzin, 2005). Temperature also determines species range limits as demonstrated, for example, for mammals (Taulman & Robbins, 2014), reptiles (Medina *et al.*, 2011), insects (Heino, 2001), fish (Perry *et al.*, 2005), bivalves (Morley *et al.*, 2010), trees (Kollas *et al.*, 2014) and algae (Nicastro *et al.*, 2013; Riera *et al.*, 2015).

Biogeographical patterns commonly follow latitudinal gradients (Tuya *et al.*, 2012; Fenberg *et al.*, 2015; Hughes *et al.*, 2016) and consequently, changes in community composition and species distribution have been described as a response to the large scale variation of environmental variables (Fenberg *et al.*, 2015; Klanderud *et al.*, 2015). A well studied example that has long fascinated ecologists is the increasing number of species towards the tropics (Hillebrand, 2004; Jablonski *et al.*, 2006 but see Marshall & Baltzer, 2015). Distinct hypotheses mostly linked either to evolutionary (e.g. different rates of speciation and extinction of species in the tropics and in temperate regions, see Hillebrand, 2004; Jablonski *et al.*, 2006) or ecological processes (e.g. the influence of habitat heterogeneity, reviewed in Schemske & Mittelbach, 2017) have been identified as the presumed drivers of this taxonomic pattern, but still no consensus exists on the factors that cause this biodiversity gradient (Schluter & Pennell, 2017). Nonetheless, changes in environmental conditions are strongly correlated to this equatorward gradient in biodiversity (Francis & Currie, 2003; Mannion *et al.*, 2014; Belmaker & Jetz, 2015).

There is ample evidence, based on historical and present species distribution and environmental data, that species are currently shifting their ranges in response to climate warming due to changes in environmental conditions (e.g. trees, Berger *et al.*, 2007; corals, Yamano *et al.*, 2011; birds, Coristine & Kerr, 2015). Under a changing

environment, species are exposed to novel conditions that either challenge their physiological thresholds, which can ultimately cause range contractions and population extinctions (e.g. Parmesan, 2006; Jones *et al.*, 2010; Coristine & Kerr, 2015) or promote range expansions and increased abundance (e.g. Lourenço *et al.*, 2012; Kooij *et al.*, 2016). Distributional shifts occur generally in three distinct dimensions: 1) over a latitudinal range, as species move polewards or towards the equator (Perry *et al.*, 2005; Parmesan, 2006; Nye *et al.*, 2009), 2) over an elevation gradient, as species move upslope or downslope in mountains (Parmesan & Yohe, 2003; Parmesan, 2006; Lenoir *et al.*, 2010) and, less frequently documented, 3) over a depth gradient, as species move to deeper depths in the ocean or towards shallower areas (Perry *et al.*, 2005; Mueter & Litzow, 2008; Nye *et al.*, 2009).

Under a warming climate scenario, assuming resources, suitable habitat and dispersal capacity allow (Walther *et al.*, 2002; Parmesan, 2006), species may experience distributional shifts, most often towards the poles or higher latitudes, as they try to track the shifting climate (Walther *et al.*, 2002; Parmesan, 2006). This is illustrated by range expansions at the cold leading (higher latitude) edge and range contractions at the warm rear (lower latitude) edge (Cahill *et al.*, 2012; Coristine & Kerr, 2015). Terrestrial taxa are moving polewards approximately three times faster than previously reported (average of 16.9 km/decade in Chen *et al.*, 2011 instead of 6.1 km/decade in Parmesan & Yohe, 2003). Additionally, the largest poleward advances are associated with the highest levels of warming (Chen *et al.*, 2011). Marine taxa exhibit even greater poleward distributional shifts than terrestrial taxa, with species moving polewards on average by 72 km per decade (Poloczanska *et al.*, 2013; see also Sorte *et al.*, 2010). Poleward distributional shifts have been reported in taxa as variable as fish (Perry *et al.*, 2005), invertebrates (Hiddink *et al.*, 2015), algae (Lima *et al.*, 2007a) and birds (Coristine & Kerr, 2015) among others. In mountain ecosystems, as lower elevations warm, some species respond to temperature increases by shifting their distribution in altitude moving upslope as demonstrated for plants (Bergamini *et al.*, 2009; Jump *et al.*, 2012) and for birds (Freeman & Class Freeman, 2014). Conversely, in the marine realm, species may shift in depth, for example by moving deeper to track colder environmental conditions (e.g. fish, Perry *et al.*, 2005; Dulvy *et al.*, 2008; invertebrates, Hiddink *et al.*, 2015, but see also Mueter & Litzow, 2008; Nye *et al.*, 2009).

Overall, climate change-driven distributional shifts may cause novel overlaps in species distributions leading to the coexistence (at least temporarily) of ecologically similar species (Johnson *et al.*, 2011). For example, the volcano barnacle *Tetraclita rubescens* expanded >300 km northwards along the coast of California, overlapping its distribution

on the mid intertidal zone with the native barnacles *Balanus glandula* and *Semibalanus cariosus* (Sanford & Swezey, 2008). Identical, synchronized distributional shifts among coexisting taxa may occur (Kleisner *et al.*, 2016). A survey performed 210 years after Alexander von Humboldt's expedition to the Chimborazo volcano in Ecuador revealed striking changes in the distribution of vegetation zones and in the maximum elevation limits of plants, consistent with increased temperatures and glacier retreat (Morueta-Holme *et al.*, 2015). However, species inhabiting the same area do not necessarily show the same response to warming climate (e.g. Rubal *et al.*, 2013). Contrasting distributional shifts that vary in magnitude and direction, have been described from taxa that share the same habitat, both terrestrial (Lenoir *et al.*, 2010; Chen *et al.*, 2011) and marine (Lima *et al.*, 2007a; Piñeiro-Corbeira *et al.*, 2016; Poloczanska *et al.*, 2016). For example, Lima *et al.* (2007a) showed that 22 out of 39 algal species showed displacement in their range limits along the Portuguese coastline, but the shift was not uniform among taxa. All eight warmwater species shifted northwards while seven of the 14 coldwater species moved north and seven moved south (Lima *et al.*, 2007a). The authors suggested that, although divergent distributional shifts could result from chance alone through stochastic population fluctuations, differences in metabolism (e.g. growth rate and sexual maturity), species interactions (competition, predation) and species-specific physiological constraints (i.e. resilience to adverse conditions) better explained the contradictory distributional patterns.

In addition to tracking a warming climate, species can counter climate change by expressing (heritable) evolutionary adaptations or phenotypic plasticity, allowing them to survive under altered environmental conditions (McCarty, 2001; Visser, 2008; Hoffmann & Sgrò, 2011). This includes, for example, changes in flowering, spawning and breeding dates, growing season, timing of reproduction and the timing of the initiation of larval dormancy (McCarty, 2001; Bradshaw & Holzapfel, 2006). Failure to track or to adapt to a new climate envelope poses serious risks to species persistence (McCarty, 2001; Nicastro *et al.*, 2013; Lourenço *et al.*, 2016). Although clear proof is still needed to establish that warming alone is the main driving force of current global species extinctions (McCarty, 2001; Cahill *et al.*, 2012), organisms are increasingly being exposed to extremely stressful thermal conditions (Helmuth *et al.*, 2016), which may exceed their thermal tolerance limits, leading to sublethal and lethal responses (e.g. Chan *et al.*, 2006; Archambault *et al.*, 2014; Macho *et al.*, 2016). When exposed to temperatures beyond their tolerance thresholds, species frequently experience lower reproductive performance (Zizzari & Ellers, 2011), reduced growth (Pörtner & Knust, 2007), higher metabolic demand (Williams *et al.*, 2005) and lower abundances (Pörtner & Knust, 2007), ultimately resulting in events of mass mortality (Harley, 2008; Jones *et al.*, 2010; Smale *et al.*, 2017).

Evidence of mass mortality culminating in local population extinction in response to increased temperatures is mounting, particularly in the marine realm (Harley, 2011; Nicastro *et al.*, 2013; Lourenço *et al.*, 2016; Smale *et al.*, 2017 but see also Franco *et al.*, 2006). For example, along the western Atlantic, populations of the marine mussel *Mytilus edulis* at the southern edge of its distribution experienced catastrophic mortalities associated with high summer temperatures (Jones *et al.*, 2010). In the South China Sea, the increases of 6 ºC above normal summertime temperatures led to a mass mortality of 40% of the resident coral communities (DeCarlo *et al.*, 2017). Dramatically, a marine heat wave caused the loss of ~2500 km^2 of kelp forests along the Great Southern Reef in Australia, driving a shift towards a regime of algae turfs (Wernberg *et al.*, 2016). Furthermore, species distributions are expected to continue to change worldwide (Erasmus *et al.*, 2002; Peterson *et al.*, 2002; Morin *et al.*, 2008; Cheung *et al.*, 2009; Raybaud *et al.*, 2013; Jueterbock *et al.*, 2013) as 'continued emission of greenhouse gases will cause further warming and long-lasting changes in all components of the climate system' (IPCC, 2014, p56).

Often, populations exhibit distinctive adaptive traits, genetic backgrounds and diverse resistance to environmental stresses along the species range (Pearson *et al.*, 2009; Diekmann & Serrão, 2012; Zardi *et al.*, 2015a). For instance, along the south and eastern shores of South Africa two distinct genetic lineages of the brown mussel *Perna perna* exist, partly overlapping in their distributions (Zardi *et al.*, 2007, 2015a). In addition to distinct genetic backgrounds, recent studies showed that the two lineages differ in their physiological tolerances of sand inundation and high temperatures, in gaping behaviour (periodic closure and opening of the shell) and attachment to the substratum (Zardi *et al.*, 2011a, 2015a; Tagliarolo & McQuaid, 2015). Populations of the sea snail, *Nucella canaliculata*, displayed distinctly different heat tolerances along their distributional range across eastern Pacific shores (Kuo & Sanford, 2009). Specifically, central populations of *N. canaliculata* in California are less heat tolerant than conspecific high-latitude populations in Oregon, which could be explained by genetic-based differences (Kuo & Sanford, 2009). The extinction of local populations containing genetic characteristics and potentially unique adaptive value greatly hampers the long-term preservation of a species' phylogenetic history, genetic diversity and evolutionary potential (Hampe & Petit, 2005; Nicastro *et al.*, 2013; Lourenço *et al.*, 2016).

Historical and contemporary refugia from climate change

The concept of refugia was originally used to refer to locations where species might have survived the last glaciation with reduced numbers and distribution (Bennett & Provan, 2008; Ashcroft, 2010). Not only did these refugial areas offer a buffer against changing climate conditions, they were crucial for species maintenance by serving as sources of recolonization after the cold harsh climate (Hewitt, 2004; Provan & Bennett, 2008). During the Last Glacial Maximum (LGM; 23 000–18 000 years ago), extensive higher latitude areas of Europe and North America were covered by ice sheets and permafrost and the sea level dropped by between 120 and 135 m (Clark & Mix, 2002). As a result, several temperate species suffered a major impact in their geographical distribution and retreated to lower latitude regions where they persisted under less extreme climatic conditions (Gavin *et al.*, 2014). In North America, multiple regions such as Beringia, the Driftless Area, northeastern British Columbia or even the Appalachian Mountains (Loehr *et al.*, 2006; Soltis *et al.*, 2006; reviewed in Beatty & Provan, 2010), which harboured a great variety of species including plants (Beatty & Provan, 2010), mammals (Loehr *et al.*, 2006), fish (Aldenhoven *et al.*, 2010) and reptiles (Soltis *et al.*, 2006) have been proposed as putative glacial refugia. In parallel, the Iberian Peninsula, the Italian Peninsula and the Balkans were the major glacial refugia in Europe (Provan & Bennett, 2008). These Mediterranean regions presumably supported a variety of taxa such as mammals (Meiri *et al.*, 2013; Vilaça *et al.*, 2014), crustaceans (Reniers *et al.*, 2013) and marine gastropods (Albaina *et al.*, 2012), to name a few. Surprisingly, recent studies revealed refugial areas in the northern Mediterranean (e.g. Schmitt & Varga, 2012; Homburg *et al.*, 2013), suggesting that more refugial regions may yet remain to be identified.

Currently, the term refugia has been expanded to include areas that are buffered not from cold glacial conditions, but from interglacial high temperatures (Stewart *et al.*, 2010). In particular, climate refugia are presently seen as 'areas relatively buffered from contemporary climate change over time' (Morelli *et al.*, 2016, p2) that, by providing suitable environmental conditions, enable species persistence in regions threatened by climate change (Keppel *et al.*, 2012; Morelli *et al.*, 2016), acting as safe havens against rising temperatures, promoting species survival and allowing long-term maintenance of global or regional biological and genetic diversity (Riegl & Piller, 2003; Hu & Guillemin, 2016; Lima *et al.*, 2016; Lourenço *et al.*, 2016; Morelli *et al.*, 2016). For example, on a larger scale, talus and mountainous rocky ecosystems of western North America facilitate the persistent of American pikas, *Ochotona princeps*, by offering high diversity wetlands and chilled vegetative areas, which are cooler than the surroundings, and also more

persistent springs (Morelli *et al.*, 2016). On a smaller scale, site-specific topographical complexity, illustrated by the presence of multiple shaded microhabitats, provide thermal refugia to the limpet species *Patella vulgata*, by reducing exposure to high temperatures and consequently leading to lower physiological stress (Lima *et al.*, 2016). In both cases, the cool refugial effect provided by macro or microhabitats strongly influences species density and population size (Lima *et al.*, 2016; Morelli *et al.*, 2016), ultimately potentially dictating species distribution at a geographical scale or species persistence, respectively. Refugial populations are confronted with reductions in the extension of suitable habitats, partial or total isolation and novel ecological boundaries that can decrease migration rates and genetic connectivity among remaining populations, reducing genetic variability and increasing extinction risk (Mock & Miller, 2005; Provan & Bennett, 2008; Lourenço *et al.*, 2016). For example, a refugial population of the plant *Rhododendron ponticum baeticum* in southern Spain is restricted to the coolest and wettest conditions of Sierra del Aljibe, and shows signs of decline (Mejías *et al.*, 2007). In addition, refugial population often present unique genetic information and account for a large part of the species' total gene pool. While typically inhabiting rock pools throughout the entire distributional range, refugial populations of the macroalga *Bifurcaria bifurcata* along northern Africa are highly isolated and fragmented, but they are nonetheless considered important hotspots of genetic diversity due to the unique gene pool associated with the southern distributional range (Neiva *et al.*, 2015).

Refugia can be identified based on multiple lines of evidence such as pollen/fossil records, historical and current species distributions, genetic diversity signatures, climatic conditions, availability of resources, disturbance and species distribution models (Keppel *et al.*, 2012; Gavin *et al.*, 2014). By coupling distributional shifts with data on the genetic diversity and genetic structure of the brown alga *Fucus guiryi*, Lourenço *et al.* (2016) were able to detect important coastal refugial areas for this species along northern African shores. A combination of paleoecological data (pollen and macrofossils) and genetic data (nuclear and chloroplast markers) was used to infer the extent of refugia for the European beech *Fagus sylvatica* (Magri *et al.,* 2006). The results were supported by species distribution models (Gavin *et al.*, 2014).

Delineating the extent and limits of a refugium is manageable when the habitat is associated with sharp topographic features (e.g. mountains; Migliore *et al.*, 2013), but in the marine realm, and in the absence of physical barriers, setting fixed limits is a considerable challenge. Moreover, identifying marine refugia based on fossils records has proven extremely difficult because species such as algae or invertebrates leave little or no fossil record and sea level fluctuation can destroy or obscure fossils (Provan & Bennett,

2008). Although in recent years the potential of marine habitats to act as refugia from climate change has received increasing attention (Chollett & Mumby, 2013; van Hooidonk *et al.*, 2013; Cacciapaglia & van Woesik, 2015; Lourenço *et al.*, 2016), the field remains largely unexplored and deserves deeper investigation. Furthermore, because warming is likely to interact with other variables (e.g. habitat loss, Travis, 2003; ocean acidification, Poloczanska *et al.*, 2016; species interactions, Traill *et al.*, 2010; fishing pressure, Poloczanska *et al.*, 2016), detecting refugial areas is of paramount importance as forthcoming species distributional shifts might be more complex than previously anticipated. Thus, there is an urgent need to identify potential cold refugial areas where species are able to persist under a scenario of climate warming. Riegl & Piller (2003) were the first to propose that such cold refugia could potentially exist in regions affected by upwelling events (see also Graham *et al.,* 2007).

The diverse functional roles of upwelling

During an upwelling event, colder, denser, nutrient-rich subsurface waters are transported to the nearshore surface, replacing warmer superficial waters that are advected offshore by equatorward winds or topographic steering (Narayan *et al.*, 2010; Wang *et al.*, 2015). The enhanced load of nutrients brought to the euphotic zone drives phytoplankton dynamics and determines the cycles of species dominance and phases of succession (Hutchings *et al.*, 1995), leading to high primary production that is responsible for sustaining highly productive fisheries worldwide (Sakko, 1998; Bakun & Weeks, 2008; Kifani *et al.*, 2008; Stock *et al.*, 2017). A number of additional important roles have been attributed to upwelling phenomena, at both the species and the community levels. Specifically, upwelling is an oceanographic process that affects species distributions (Sancinetti *et al.*, 2014), recruitment (Reum *et al.*, 2011), dispersal (Lett *et al.*, 2007), transport and settlement (Barshis *et al.*, 2011). Upwelling can also influence species growth rates (Wieters, 2005; Xavier *et al.*, 2007), structure species biogeographic patterns (Fenberg *et al.*, 2015) and be responsible for promoting speciation (Henriques *et al.*, 2016). At a higher level, upwelling controls coastal community dynamics by influencing species richness, biomass and composition (Lanari & Coutinho, 2014) and has a key role in determining the functional structure of coastal communities (Bosman *et al.*, 1987). However, the degree to which upwelling shapes species genetic structure is not fully understood; experimental evidence has revealed important limitations and inconsistencies leading to divergent hypotheses (e.g. Waters & Roy, 2004; Silva *et al.*, 2009; Barshis *et al.*, 2011). Upwelling intensity may simultaneously explain strong and weak genetic

structure of coastal species. For example, the strong upwelling cell off Cape Ghir has been identified as a major factor driving genetic breaks in marine species along the Moroccan coast, as this phenomenon presumably isolates distinct populations, hindering genetic exchange among them (e.g. Chlaida *et al.*, 2009; Neiva *et al.*, 2015). In clear contrast is the upwelling along the Oregon (USA) coast. In this region, strong upwelling conditions presumably lead to lack of genetic structure of a marine invertebrate species, by increasing larval offshore transport and promoting disruption and admixture among distinct genetic groups prior to larval settlement (Barshis *et al.*, 2011). As discrepancies also arise because comparisons are often made within species or within restricted regions or because seasonal fluctuations of upwelling intensity are not considered, recent studies are currently encompassing larger areas (Reid *et al.*, 2016), using multiple taxa (Kelly & Palumbi, 2010) and considering distinct upwelling seasons (Barshis *et al.*, 2011). By combining previously published and original mitochondrial DNA data, Kelly & Palumbi (2010) analysed the genetic structure of 50 coastal species across the Pacific coast of North America, revealing that the upwelling centre of Cape Mendocino coincides with genetic shifts for species with a variety of dispersal capacities.

Upwelling events are temporally and spatially heterogeneous and are broadly distributed; however, the major upwelling systems are located at the eastern boundaries of both Atlantic and Pacific Oceans, spanning a wide range of latitudes. The Benguela Current system is located off southwestern Africa (~16–35° S; Narayan *et al.*, 2010; García-Reyes *et al.*, 2015), the Humboldt Current system along western South America (~10–40° S; Bakun & Weeks, 2008; Narayan *et al.*, 2010; García-Reyes *et al.*, 2015), the California Current system off western North America (~24–48° N; Narayan *et al.*, 2010; García-Reyes *et al.*, 2015) and the Canary Current system off northwestern Africa and the Iberian Peninsula (~12–43° N; Arístegui *et al.*, 2009; Narayan *et al.*, 2010; García-Reyes *et al.*, 2015). Generally, at higher latitudes coastal upwelling is highly seasonal, starting in spring and extending through summer and early autumn; the opposite downwelling effect occurs primarily during winter (Wang *et al.*, 2015). Towards lower tropical-subtropical latitudes, upwelling is characterized by a marked lack of seasonality, becoming a year-round phenomenon (Wang *et al.*, 2015). For example, Varela *et al.* (2015) detected upwelling-favourable wind conditions throughout the year along the southern regions of the Benguela and the Canary systems, with the highest values occurring during the spring and summer seasons, which was consistent with previous studies (McGregor *et al.*, 2007; Narayan *et al.*, 2010; Patti *et al.*, 2010; Cropper *et al.*, 2014). Despite general concordance among different authors, contradictory understandings may arise between studies if the timing, scale, latitude and methodology applied are different (e.g. Varela *et*

al., 2015 compared to Gómez-Gesteira *et al.*, 2008 and Pardo *et al.*, 2011). While the timing, duration, intensity and spatial heterogeneity of upwelling might be system-specific (Wang *et al.*, 2015), the vigour of coastal upwelling is globally increasing and is expected to further increase worldwide as a result of increased levels of atmospheric CO_2 and global warming (Narayan *et al.*, 2010; Varela *et al.*, 2015; Wang *et al.*, 2015). By the end of the 21st century, at higher latitudes of the Benguela, Canary and Humboldt systems, upwelling is expected to start earlier, end later and become more intense, potentially influencing the geographical distribution of various marine species (Wang *et al.*, 2015).
Although few studies have suggested a putative buffering effect of upwelling areas against climate change (e.g. Riegl & Piller, 2003; Cacciapaglia & van Woesik, 2015), upwelling definitely has a key role in facilitating the persistence of coastal temperate species in the context of global warming (Lourenço *et al.*, 2016). Hu & Guillemin (2016) recognized the refugial effect of upwelling areas in shaping historical and current species distribution previously suggested by Assis *et al.* (2016; for the kelp species *Saccorhiza polyschides*) and Lourenço *et al.* (2016; for the brown alga *F. guiryi*). Hu & Guillemin (2016) additionally highlighted the need for sequential field and genetic studies along coastal upwelling systems worldwide to understand if the buffering effect provided by coastal upwelling is species-specific or can be generalized to other taxa also facing the imminent threat of a warming climate.

The Canary Current system

The Canary Current system (CCS) is the only major upwelling system that encompasses two continents; stretching from cold temperate northern Iberia (~43° N) in Europe to warm tropical Senegal (~12° N; Arístegui *et al.*, 2009) in Africa. The CCS has been the focus of several studies exploring the oceanographic, hydrological and climatological features of the system, based on sea surface temperatures (SST), wind or upwelling indices, covering either its entire extent (Santos *et al.*, 2005; Arístegui *et al.*, 2009; Barton *et al.*, 2013; Benazzouz *et al.*, 2014) or limited regions within the system (Barton *et al.*, 1998; Knoll *et al.*, 2002; Pelegrí *et al.*, 2005; McGregor *et al.*, 2007; Cropper *et al.*, 2014; Sousa *et al.*, 2017a, 2017b). This upwelling system is characterized by great spatial and temporal variability along its range, coupled to large scale variation in wind patterns, resulting in site-specific responses to upwelling phenomena even when locations are subject to similar upwelling conditions (Arístegui *et al.*, 2009; Marcello *et al.*, 2011).
Five different sub-regions have been defined within the CCS based on coastline orientation, coastal freshwater input, characteristics of the dominant water mass,

embayments and the seasonality and strength of upwelling (Arístegui *et al.*, 2009; Fig. 1.1). The northernmost sub-region is the Galician sector (42–43° N), located on the northwestern Spanish coast, which is characterized by the presence of multiple flooded river valleys, capes, a narrow shelf, input of freshwater and summer upwelling (Arístegui *et al.*, 2009), with upwelling maxima occurring between August and early September (Benazzouz *et al.*, 2014). The Portuguese sub-region (37–42° N) covers all the west coast of that country and, like the Galician sector, it is strongly influenced by freshwater input, rivers and capes. This sub-region also presents a narrow continental shelf and upwelling develops during the summer months (Arístegui *et al.*, 2009; Benazzouz *et al.*, 2014). The summer upwelling pattern is interrupted at the Gulf of Cadiz sub-region (33–37° N). There, weak winds and the embayed coastline are generally unfavourable to the development of upwelling (Arístegui *et al.*, 2009), although weak intermittent upwelling has been detected during autumn and winter (Marcello *et al.*, 2011). The Strait of Gibraltar, located in this sub-region, is commonly referred to in the context of Mediterranean-Atlantic water exchange (Arístegui *et al.*, 2009), however, seasonal, spatially restricted upwelling events have also been detected there (at 35.8–35.9° N; Stanichny, 2005). The Moroccan sub-region (21–33° N) is characterized by great mesoscale oceanographic variability due to geographical heterogeneity including a wide shelf, multiple capes and the presence of offshore islands (Canary archipelago; Arístegui *et al.*, 2009; Marcello *et al.*, 2011). In the northern part of this sub-region (26–33° N), upwelling is stronger during summer and autumn (particularly in August-September; Arístegui *et al.*, 2009; Marcello *et al.*, 2011; Benazzouz *et al.*, 2014), while in the southern region (21–26° N) upwelling is quasi-permanent throughout the year (Arístegui *et al.*, 2009; Marcello *et al.*, 2011; Benazzouz *et al.*, 2014), but especially strong from spring to autumn (Marcello *et al.*, 2011). At the southernmost limit of the CCS lies the Mauritanian-Senegalese sub-region (12–21° N), characterized by freshwater input from rivers, a wide continental shelf and the strongest upwelling and highest nutrient concentrations in the entire CCS system. This sub-region is the most productive of the five, experiencing upwelling during winter (varying from late autumn to early spring; Arístegui *et al.*, 2009; Marcello *et al.*, 2011; Benazzouz *et al.*, 2014). Various studies along the CCS have provided broad coverage of the oceanographic processes occurring across its five distinct sub-regions, greatly increasing our knowledge of the region and exposing striking differences regarding the physical environment, circulation patterns and shelf dynamics (Arístegui *et al.*, 2009; Marcello *et al.*, 2011; Benazzouz *et al.*, 2014).

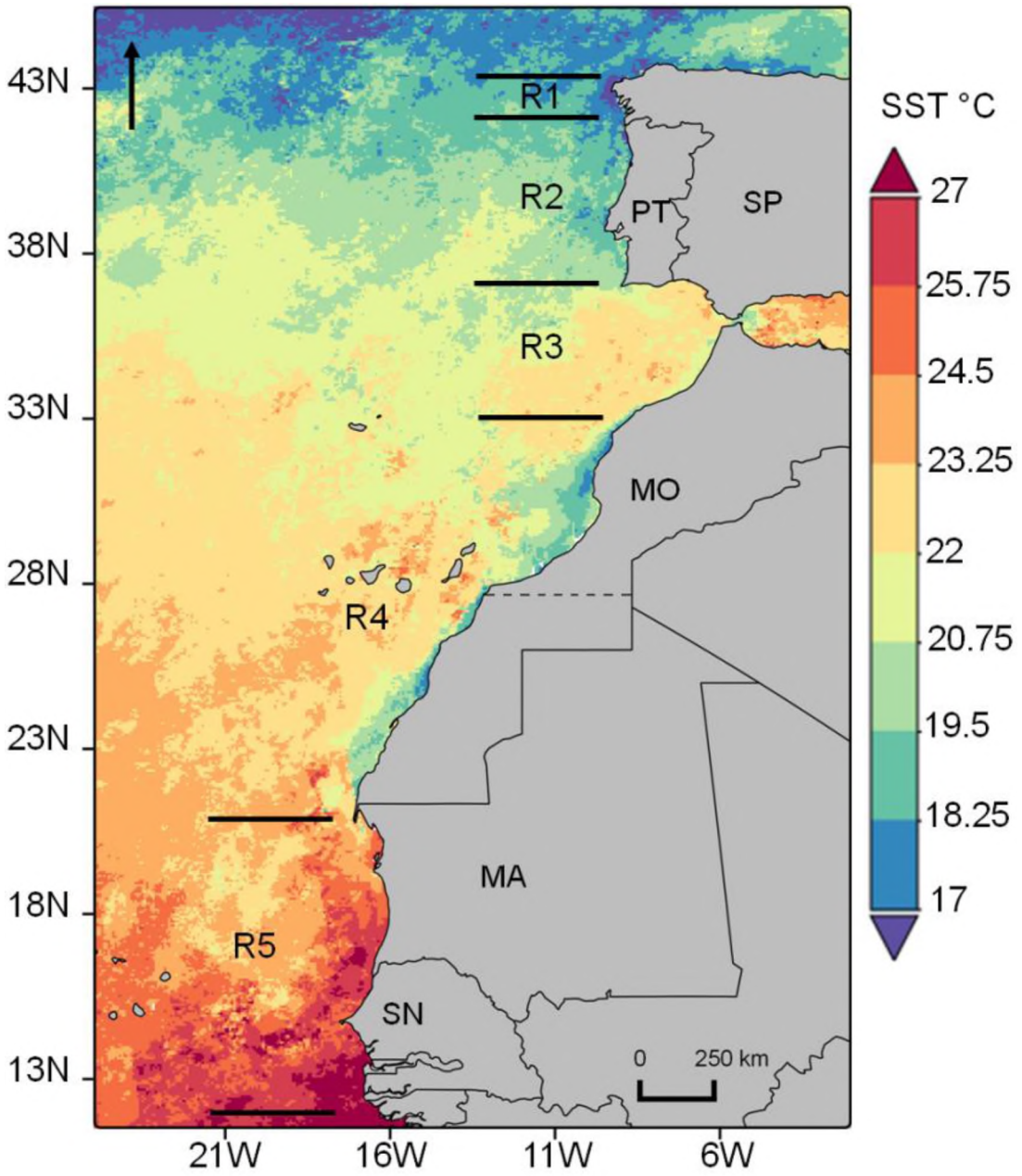

Figure 1.1 – Monthly averaged map of sea surface temperature (SST) of the Canary Current system over June 2017 (modified from Arístegui *et al.*, 2009). The five sub-regions described in the text are depicted as R1, Galician sub-region; R2, Portuguese sub-region; R3, Gulf of Cadiz sub-region; R4, Moroccan sub-region and R5: Mauritanian sub-region. PT: Portugal; SP: Spain; MO: Morocco; MA: Mauritania; SN: Senegal.

The multiple strong, cold upwelling phenomena across the CCS are embedded in a phenomenon of region-wide warming of sea surface temperatures (SST) occurring along the system, of up to 0.73 ºC/decade over the last three decades (Lima & Wethey, 2012). This increase of temperatures has coincided with several changes in species distributions across the region, a biogeographical pattern that has been particularly investigated along the Iberian Peninsula (Lima *et al.,* 2007; Lourenço *et al.*, 2012; Rubal *et al.*, 2013). The Iberian coast constitutes an interface region where numerous cold and warmwater

species reach their southern or northern distributional limits (Boaventura *et al.*, 2002; Pereira *et al.*, 2006; Piñeiro-Corbeira *et al.*, 2016; Gaspar *et al.*, 2017). Since the studies performed by Fischer-Piétte along Iberia in the late 1950's and early 1960's (e.g. Fischer-Piétte, 1958, 1963), many species have been found to exhibit poleward range expansions and contractions in response to a shifting climate, particularly the increase of SST (Lima *et al.,* 2007; Lourenço *et al.*, 2012; Rubal *et al.*, 2013). The brown alga *Himanthalia elongata* showed a 130 km geographical contraction over a five year period (2004–2006 to 2008–2009) along northern Spain (Duarte *et al.*, 2013). Rubal *et al.* (2013) reported a 400 km southern range contraction of the sea snail *Littorina saxatilis* and the dogwhelk *N. lapillus*, and a 185 km poleward range expansion of the pulmonate limpet *Siphonaria pectinata* along Portuguese shores over approximately 70 years. Considerably fewer studies have been performed on biogeographical changes in species distributions within the African sub-regions of the CCS. Some catalogues describing the distributions of specific taxonomic groups along northern African shores have been compiled (algae, Benhissoune *et al.*, 2001, 2002a, 2002b, 2003; John *et al.*, 2004), however a large scale contemporaneous assessment of species distribution has yet to be performed to evaluate distributional shifts within the region. An exception is a recent study of a shift in the distribution of the habitat-structuring species *F. vesiculosus*. This brown alga showed a range contraction of approximately 1250 km from southern Morocco to central Portugal consistent with coastal SST warming (Nicastro *et al.*, 2013).

Patterns of genetic structure in coastal species along Iberian shores have been more extensively investigated (e.g. Barreiro *et al.*, 2006; Ribeiro *et al.*, 2010; Coyer *et al.*, 2011a; Sá-Pinto *et al.*, 2012; Lourenço *et al.*, 2015), although less explored along northern African shores (but see Chlaida *et al.*, 2006; Atarhouch *et al.*, 2007; Quinteiro *et al.*, 2007; Nicastro *et al.*, 2013; Tavares *et al.*, 2017). In the former region, reported high and unique genetic diversity are seen as being crucial to the long-term persistence of species gene pool (Diekmann & Serrão, 2012). Similarly, studies shedding light on the genetic patterns of coastal species inhabiting northern Africa have revealed incredibly strong genetic structure and high genetic diversity from this region (Chlaida *et al.*, 2009; Neiva *et al.*, 2015; Lourenço *et al.*, 2016). For example, Chlaida *et al.* (2009) detected two distinct genetic fish stocks of *Sardina pilchardus* along the Atlantic and Mediterranean coast of Morocco, with a clear genetic cline in the Bay of Agadir area, in western Morocco. Moreover, three distinct genetic clusters of the eelgrass *Zostera noltii* were detected along the Atlantic Moroccan coast, with particularly higher genetic and genotypic diversity in the northern and central locations (Elso *et al.*, 2016).

Intertidal species as climate change sentinels

Intertidal rocky shore species have limited motile abilities and short life spans, while many species also live close to their thermal tolerance limits (Stillman, 2002; Chan *et al.*, 2006; Sunday *et al.*, 2012; see also Walther *et al.*, 2002), so that populations can respond rapidly to environmental change (e.g. Southward *et al.*, 2004). These organisms inhabit regions characterized by strong terrestrial-marine gradients and are usually restricted to compressed intertidal areas on the shore (Helmuth *et al.*, 2002; Harley & Helmuth, 2003; Harley, 2008), where they are exposed to extremely severe environmental conditions involving repeated alternation of marine and terrestrial conditions. Therefore, intertidal rocky shore assemblages are ideal sentinel species to study climate warming-driven changes (e.g. Harley, 2011; Helmuth *et al.*, 2016). For example, over a 52-years interval characterized by significant warming, Harley (2011) documented a 51% reduction in mussel bed extension with an associated 13% rate of local extinction in the Juan de Fuca Strait.

Water temperatures strongly influence large scale distributional shifts of intertidal species and have been identified as major predictors of mortality in intertidal systems (Rivadeneira & Fernández, 2005; Blanchette *et al.*, 2008; Nicastro *et al.*, 2013; Smale *et al.*, 2017). During high tide, intertidal organisms experience the same temperature as seawater, while during low tide periods thermal conditions may be influenced for example by species behaviour (Nicastro *et al.*, 2012) and even niche and habitat occupancy (Helmuth *et al.*, 2006; Lima *et al.*, 2016). Furthermore, water temperature at high tide can also influence intertidal animal body temperature at low tide by setting the baseline from which warming in air occurs (Wethey, 2002). Water temperature is of particular importance for intertidal species because it can have a major influence in their reproductive output, fitness or larval development (e.g Honkoop & van der Meer, 1998; Hicks & McMahon, 2002; Ziadi *et al.*, 2015; Tagliarolo *et al.*, 2016), thus limiting species persistence and distribution.

Additionally, other nearshore abiotic factors (e.g. air temperature, Firth *et al.*, 2011; waves, Martínez *et al.*, 2012), and intra or interspecific interactions (e.g. predation and competition, Walther *et al.,* 2002; parasitism, Zardi *et al.*, 2016) may profoundly affect intertidal species and communities. However, these factors are generally most effective at micro (centimetres – metres) and/or meso (tens of metres – kilometres) spatial scales. As the duration of air exposure and body temperatures of organisms can increase moving shoreward (Gilman *et al.,* 2015), intertidal species at their upper distributional limits are limited by their maximum body temperature, which is strongly influenced by solar

radiation/shading and by air temperature (Helmuth, 1998; Helmuth *et al.* 2011). Any biotic or abiotic factor that minimises thermal stress strongly benefits intertidal species and some of these can be unexpected. For example, parasite-host interactions may benefit host individuals as parasites can buffer the effect of thermal stress (Bates *et al.*, 2011). Phototrophic endolithic parasites excavate mussel shells by chemical dissolution, degrading the outer layer of the shell ultimately resulting in localized shell discolouration (i.e. shell whitening, Kaehler, 1999). Consequently, shell white discoloration augments solar reflectivity, diminishing the absorbed energy, eventually resulting in lower mussel body temperature and leading to reduced mortality rates under heat wave events (Zardi *et al.*, 2016).

Abiotic and biotic factors influencing dispersal and establishment of intertidal species

Oceanographic features such as currents, gyres or upwelling phenomena may act as physical barriers to the dispersal of intertidal species, limiting gene flow between populations (Quinteiro *et al.*, 2007), as well as influencing larval settlement (Connolly & Roughgarden, 1998; Barshis *et al.*, 2011), setting limits that affect species distribution and genetic patterns (Patarnello *et al.*, 2007; Zardi *et al.*, 2007). However, oceanographic barriers might also pass undetected until highlighted by genetic discontinuities (Quesada *et al.*, 1995; Kelly & Palumbi, 2010). A large scale genetic study across northeastern Pacific shores performed on multiple rocky intertidal species revealed a genetic break at Cape Mendoncino, previously missed by genetic sampling (Kelly & Palumbi, 2010). The capacity to disperse and travel long distances is particularly important for intertidal organisms with sessile or sedentary adults (e.g. gastropods, barnacles), because dispersal occurs only during a limited period of the life cycle through the spreading of larvae or propagules (see Kinlan & Gaines, 2003). Hence, planktonic larval duration strongly influences dispersal capacity. Whereas species with long-lived planktonic larvae can be expected to exhibit broader dispersal, greater gene flow and lower genetic structure than species with no or limited dispersal, the capacity to disperse can also be affected by behavioural, demographic and biological processes as well as physical mechanisms (Kelly & Palumbi, 2010; Dawson *et al.*, 2014; D'Aloia *et al.*, 2015). For example, Porri *et al.* (2014) found that mussel larval abundance was linked to the activity of large scale oceanographic meanders as they accumulated larvae onshore or acted as corridors for offshore larval transport, while larval abundance was weakly related to temperature, beam attenuation, fluorescence, depth or zonal velocity. Larval dispersal

may also be potentially influenced by selection (Burgess *et al.*, 2016) and by wind-driven surface currents (McQuaid & Phillips, 2000).

Available suitable substratum and habitat continuity facilitate the maintenance and potential expansion of hard substratum assemblages. In addition to natural substratum, artificial structures further allow species range expansions (Adams *et al.*, 2014; Lodola *et al.*, 2015). For example, when structures are built in areas devoid of natural hard bottom, they provide habitat for larvae that could be lost offshore, potentially promoting previously impossible expansion (Sheehy & Vik, 2010; Adams *et al.*, 2014). Furthermore, if a series of artificial structures is placed along extensive denuded areas they may act as new dispersal pathways, creating a stepping-stone connection between previously unconnected areas (Adams *et al.*, 2014). A vast number of species benefits from artificial manmade structures. Sammarco *et al.* (2012) reported that oil and gas platforms mediated expansion of scleractinian corals in the Gulf of Mexico from natural reef populations. Over the same area, the brown mussel *P. perna* has colonized and expanded its distribution for hundreds of kilometres using man-made structures such as jetties and piers (Hicks & Tunnell, 1993; Hicks & Tunnell, 1995).

Species interactions are also key determinants of intertidal assemblage composition. In line with substratum availability, recipient communities increase the complexity of successful establishment and distribution of intertidal species (Sanford & Swezey, 2008). After dispersal, establishment of hard substratum species might be either facilitated or hampered by species in the recipient assemblages. For example, a newly arriving mussel species might be more susceptible to some native parasites than native established ones (Zardi *et al.*, 2009) but the opposite can also be true (Calvo-Ugarteburu & McQuaid, 1998a, 1998b). Biotic interactions may become even more complex if different habitat conditions are considered. Algae may limit or enhance barnacle recruitment depending on the intertidal height. At mid intertidal wave exposed elevations, the macroalga *Ascophyllum nodosum* limited barnacle recruitment by whiplash effects, while enhancing it in understory habitats on the low shore by minimising water loss and temperature extremes (Beermann *et al.*, 2013).

Intertidal bioengineers and their influence on intertidal assemblages

Intertidal assemblages are commonly dominated by habitat-forming/bioengineer species, organisms that are considered of critical importance regarding the impacts of climate change on intertidal shores. Bioengineer species are organisms that, by modifying habitats and abiotic conditions, often create new environments, increasing spatial

complexity, facilitating the presence of other species and influencing coastal species richness and composition (Borthagaray & Carranza, 2007; Watt & Scrosati, 2013a, 2013b; Arribas *et al.*, 2014). For example, mussel beds are known to form matrices that can harbour several dozens of species (Hammond & Griffiths, 2004; Borthagaray & Carranza, 2007; Silliman *et al.*, 2011; Arribas *et al.*, 2014). When comparing engineered and unmodified habitats, Cole (2010) showed that mussel-engineered habitats exhibited more species, more unique species and different species composition compared with habitats without mussels. A number of studies have shown that algal turfs and canopies also support many infaunal assemblages (Kelaher & Castilla, 2005; Kelaher *et al.*, 2007; Watt & Scrosati, 2013a). This increase in species richness occurs because bioengineers provide conditions not present elsewhere. The effectiveness of bioengineering depends not only on the stress level (Watt & Scrosati, 2013b) and the type of habitat (e.g. wave sheltered vs exposed, Arribas *et al.*, 2014), but also on the abundance of bioengineers (Borthagaray & Carranza, 2007; Watt & Scrosati, 2013b). In fact, species richness is positively correlated or generally increases with bioengineers abundance (Borthagaray & Carranza, 2007; Watt & Scrosati, 2013b). Thus, large scale changes in abundance or disappearance of bioengineers may modify and decrease ecosystem complexity, reducing the diversity and abundance of associated species (Kelaher *et al.*, 2007; Watt & Scrosati, 2013b), presumably affecting all trophic levels. In South Africa, intense harvesting of mussels led to the extirpation of several populations outside marine reserves (Lasiak & Dye, 1989; Ludford *et al.*, 2012), resulting in dramatic changes to the diversity and composition of these assemblages (Lasiak & Field, 1995). Projected losses of bioengineers due to forthcoming climatic changes will most likely result in losses of unique species with further landscape consequences (Cole *et al.*, 2016). While also facing the unpredictable consequences of warming, bioengineers may become of even more critical relevance as climate change develops, by acting as refugia for associated species that may be exposed to harsher environmental conditions (Watt & Scrosati, 2013b).

Thesis overview and study aims

In response to the pressure of climatic changes there has been a growing global interest in qualitatively and quantitatively describing the composition of intertidal communities and how this responds to environmental variables (Blanchette *et al.*, 2008). Sea surface temperatures have been significantly increasing along northern African shores over the last three decades (Lima & Wethey, 2012). Although multiple studies have focused on the climatologic, oceanographic and hydrodynamic patterns of northern African shores (e.g.

McGregor *et al.*, 2007; Marcello *et al.*, 2011; Benazzouz *et al.*, 2014), relatively little is known about how these rocky shore communities are influenced by upwelling.

In this thesis, I applied an integrated approach based on multiple sources of evidence that offers new insights into the ecological and evolutionary significance of upwelling areas under projected climate change. The significance of this thesis extends beyond ecological interest, with comprehensive and global implications for the understanding of the factors driving intertidal community composition, species distribution, genetic patterns, endolithic infestation and host-parasite relationships, as well as representing a solid baseline for future studies focusing on northern African intertidal communities.

Specifically, in chapter 2, I investigated the '*Distributional patterns of benthic intertidal rocky shore species along the Atlantic upwelling-influenced coast of Morocco and Western Sahara'*, in order to determine whether upwelling areas structure the composition of intertidal communities. Additionally, I developed a comprehensive, contemporary record of intertidal species which provides a benchmark for future studies investigating the relationships between climate change and species distributional shifts in the study area. In chapter 3, deepening some results of the previous chapter, I explored the role of '*Upwelling areas as climate change refugia for the distribution and genetic diversity of the marine macroalga Fucus guiryi'*, to assess whether upwelling regions along northern Africa and southern Iberia are able to buffer climate warming effects, promoting the long-term persistence of this species. This allowed me to investigate the evolutionary and ecological ramifications of such a refuge effect. Upwelling phenomena may also dictate coastal species genetic patterns by influencing dispersal. As a consequence, '*The effects of multiple oceanographic barriers to dispersal in the genetic structure of the brown mussel Perna perna*' were investigated in chapter 4 to determine whether oceanographic features (e.g. upwelling cells) and environmental gradients along Atlantic and Mediterranean African and Iberian shores shape the species' sex-specific genetic structure, and determine the environmental factors that better explain the species' native distribution. Chapter 5 explored the '*Upwelling driven-incidence of endolithic infestation and its effects on mussel bed microclimates of Mytilus galloprovincialis'* to explore a potential relationship between upwelling intensity and endolithic-induced infestation gradients on *M. galloprovincialis*. Moreover, I tested the hypothesis that endolith infestation leads to lower mussel body temperatures and ameliorates the microclimate within mussel beds. A synthesis of the major findings of the thesis is provided in chapter 6.

CHAPTER 2

Distributional patterns of benthic intertidal rocky shore species along the Atlantic coast of Morocco and Western Sahara

Intertidal species inhabiting the rocky shores of Nouifed, Western Sahara.

2.1 INTRODUCTION

Evolutionary history, life history traits and environmental factors dictate species biogeographical patterns and distributional ranges over large geographical scales (Fenberg *et al.*, 2015; Bloch & Klingbeil, 2016). In the marine realm, sea surface temperatures (SST), currents, salinity, nutrients, wave exposure and upwelling phenomena are most often considered to be largely responsible for the distributional patterns of coastal marine organisms (Fenberg *et al.*, 2015; Reddin *et al.*, 2015; Cefalì *et al.*, 2016). SST values that exceed the thermal tolerance limits of a species likely prevent it from colonizing novel areas or further expanding its distributional range (Zacherl *et al.*, 2003; Zardi *et al.*, 2007; Stephenson *et al.*, 2009; Lourenço, 2012). There is also ample evidence that by linking or interrupting the connection between adjacent areas, oceanic currents influence species distribution, as they can either promote or hinder larval dispersal and recruitment (e.g. Hare *et al.*, 2005; Ling *et al.*, 2009). Upwelling regimes have the potential to shape the distribution of coastal marine species through a direct influence on inshore/offshore transport and local/regional recruitment of larvae (e.g. Barshis *et al.*, 2011; Moyano *et al.*, 2014; Fenberg *et al.*, 2015), or by delimiting areas that are suitable for species persistence (e.g. climate refugia, Hu & Guillemin, 2016; Lourenço *et al.*, 2016). Notably, upwelled waters are associated with variability in multiple environmental variables (i.e. nutrients, SST, wind, ocean circulation; Narayan *et al.*, 2010; Wang *et al.*, 2015), emphasizing the complexity of how the distribution of organisms is determined.

As upwelling phenomena are spatially and temporally heterogeneous and the vigour of these events is site-specific (e.g. Wang *et al.*, 2015; Sousa *et al.*, 2017a), their effects on intertidal assemblages may also differ and be community-specific, causing, for instance, cascading effects on the composition of the intertidal biota (Nielsen & Navarrete, 2004; Guerry & Menge, 2017). Several studies have shown that variations in upwelling intensity and in upwelling-related variables determine the functional and trophic structure of intertidal communities (Bosman *et al.*, 1987; Broitman *et al.*, 2001; Blanchette *et al.*, 2009; Reddin *et al.*, 2015 but see Kelaher & Castilla, 2005). For example, increased abundance of late-successional corticated algae or ephemeral algae is associated with higher or lower upwelling intensities, respectively (Broitman *et al.*, 2001; Nielsen & Navarrete, 2004). Also, algal cover and herbivore biomass are significantly greater in regions affected by coastal upwelling (Bosman *et al.*, 1987). Despite the large and growing number of studies on nearshore ecosystems worldwide providing valuable clues to the possible driving forces behind intertidal community structure and species distribution (e.g. Nielsen & Navarrete, 2004; Blanchette *et al.*, 2009; Bermejo *et al.*, 2015), more work is

needed to disentangle the effects of upwelling on community composition and understand if described site-specific examples illustrate overall community composition patterns among distinct upwelling systems.

Most studies on the influence of upwelling regimes on coastal marine species have been performed in one of the four Eastern Boundary Upwelling Systems (EBUS): the Benguela Current system off southwestern Africa, the Humboldt Current system along western South America, the California Current system off western North America and the Canary Current system, off northwestern Africa and the Iberian Peninsula (e.g. Hutchings *et al.*, 1995; Bruland *et al.*, 2001; Fenberg *et al.*, 2015). Additionally, the Benguela, Humboldt and California upwelling systems have long been the focus of multiple studies aimed at describing and comparing the biological and environmental structure of intertidal rocky shore communities (e.g. Bustamante & Branch, 1996a; Broitman *et al.*, 2001; Blanchette *et al.*, 2008, 2009). The intertidal fauna and flora of western South African shores, exposed to the Benguela upwelling, are biogeographically distinct from the southern and eastern shore communities (Bustamante & Branch, 1996b; Sink *et al.*, 2005). The discontinuity in community structure around Point Conception across the California Current system coincides with a major oceanographic break that separates two contrasting regions, a northern and a southern region characterized by strong and weak upwelling intensities, respectively (Schoch *et al.*, 2006; Blanchette *et al.*, 2008). Along the Humboldt system, distinct biogeographic provinces have been described with a sharp break in species abundances around 32° S in latitude coinciding with spatial discontinuities in thermal regimes (Broitman *et al.*, 2001; Wieters *et al.*, 2009; Tapia *et al.*, 2014). The Canary Current system remains the least explored of all EBUS. In particular, geographic data on current species distribution along northern African shores are extremely limited. The Census of Marine Life (http://comlmaps.org/mcintyre) has described this coastline as a major biodiversity gap deserving 'improvement of benthic taxonomy' and 'elucidation of the scales of temporal and spatial variability in nearshore habitats'. Although numerous studies have advanced our understanding of the hydrodynamics and the oceanographic features and patterns of this upwelling system (e.g. Marcello *et al.*, 2011; Benazzouz *et al.*, 2014; Cropper *et al.*, 2014; Sousa *et al.*, 2017a) and of the distribution of particular species or groups of species along these shores (e.g. algae, Benhissoune *et al.*, 2001, 2002a, 2002b, 2003), a large scale comprehensive study investigating the biogeographic structure and linking environmental and biological gradients has never been performed.

Within the Canary Current system, distinct ecoregions exist, defined by homogeneous species composition, which are determined by dominant biogeographic variables such as

upwelling, temperature regimes or coastal complexity (Spalding *et al.*, 2007). In particular, Moroccan and Western Sahara shores group together in a single ecoregion (the Saharan upwelling; Spalding *et al.*, 2007) and represent a biogeographic transition where warm and coldwater species reach their northern and southern distributional limits respectively (e.g. Zardi *et al.*, 2011b; Smale *et al.*, 2013; Neiva *et al.*, 2015; Assis *et al.*, 2017). Additionally, this is a region highly affected by ongoing climate change (Belkin, 2009; Lima & Wethey, 2012), where ecosystem-structuring species shift their ranges in response to a warming climate (e.g. the macroalga *Fucus vesiculosus*, Nicastro *et al.*, 2013). The new species records being reported from Morocco (e.g. algae *Neosiphonia ferulacea*, *Polysiphonia funebris*, *Po. subulifera*, Hassoun *et al.*, 2016; *Codium tomentosum var. mucronatum*, *Aglaothamnion pseudobyssoides* Hassoun *et al.*, 2014; and the amphipod *Ampelisca lusitanica*, Belattmania *et al.*, 2017) and the continuous effort to study these shores are not only relevant to the detection of distributional shifts driven by climate change, they also highlight the potential of this region to harbour greater levels of biodiversity than previously recognised.

Inspired by the gap in information and the need for research on benthic intertidal communities along northern African shores (Decker *et al.*, 2003; Brito *et al.*, 2014; Ramos *et al.*, 2015), this chapter aims to describe patterns of diversity and abundance of intertidal rocky shore species along the Atlantic coast of Morocco and Western Sahara and to identify possible upwelling-based drivers that might be related to such patterns. By focusing on the distribution of species belonging to distinct functional groups (i.e. macrophytes, herbivores, filter-feeders, lichens) and site-specific upwelling conditions (i.e. upwelling indices, probability of upwelling, maximum and minimum SST, SST variation) this study is the first to investigate benthic intertidal community structure along the African shores of the Canary Current system. Specifically, the aims of this chapter were to: 1) create a baseline for future studies investigating the distribution of intertidal rocky shores species along northern Africa and climate-driven shifts and 2) assess and relate biological (intertidal community) and environmental (upwelling) structure along the Canary Current system, in order to understand if upwelling-related variables influence the composition of intertidal communities along the study area.

2.2 MATERIAL AND METHODS

2.2.1 Study region

Qualitative and quantitative field surveys were conducted at 12 intertidal rocky shore sites in the Canary Current system (CCS) along the Atlantic shores of Morocco and Western Sahara (Marcello *et al.*, 2011; Benazzouz *et al.*, 2014; Table 2.1). Sites were sampled twice over a 1-year period between September 2013 and October 2014. Sites were equidistantly distributed along the region and selected based on similarity of wave exposure, habitat type, topography and proximity to upwelling cells. Due to inaccessibility of site LB1 during the second survey, the closest accessible rocky shore, site LB2, was selected as its replicate (Table 2.1).

The CCS comprises multiple upwelling cells that vary in timing and intensity (Marcello *et al.*, 2011; Benazzouz *et al.*, 2014). Three main centres of upwelling can be detected through low sea surface temperatures (SST) or upwelling indices along this stretch of coast: the first at 31–32° N (north of Cap Ghir), a second at 26.5–28° N (south of Cap Juby) and a third at 21–25° N (north of Cap Blanc; Marcello *et al.*, 2011; Benazzouz *et al.*, 2014). Adjacent surrounding areas are intermittently affected by upwelling, the effects of which decrease as the distance from the upwelling centres increases (Marcello *et al.*, 2011; Benazzouz *et al.*, 2014). Northern Morocco (33–36° N) shows low seasonality and weak upwelling indices, central and south Morocco and northern Western Sahara (areas between 26–33° N) show the strongest seasonality and the highest upwelling indices (peak during late summer, August–September; Marcello *et al.*, 2011; Benazzouz *et al.*, 2014), while central and southern Western Sahara (21–26° N) show high upwelling indices and very little seasonality (Benazzouz *et al.*, 2014).

Table 2.1 – List of sampling sites along the Atlantic coasts of Morocco and Western Sahara.

Location	Code	Coordinates
Larache	LR	35°11'48.14"N; 06°09'30.61"W
Rabat	RB	34°01'57.26"N; 06°50'27.96"W
Sidi Bouzid	SB	33°13'06.11"N; 08°34'23.19"W
El Beddouza	EB	32°32'42.33"N; 09°16'55.34"W
Essaouira	ES	31°30'42.78"N; 09°46'24.31"W
Imsouane	IM	30°50'24.43"N; 09°49'21.92"W
Mirleft	ML	29°35'06.58"N; 10°02'50.78"W
El Ouatia	TT	28°30'05.58"N; 11°20'06.38"W
Tarfaya	TF	27°45'33.64"N; 13°02'40.40"W
Boujdour	BJ	26°07'38.95"N; 14º30'02.38"W
Nouifed	LB1	24°54'30.29"N; 14º49'45.36"W
Hassi El Kraa	LB2	24°41'06.18"N; 14°54'08.87"W
Dakhla	DK	23°46'06.97"N; 15º55'32.16"W

2.2.2 Biological sampling design

A point-intercept sampling method was used to quantify relative abundance (% cover) of sessile invertebrates, macrophytes and lichen species at each site (adapted from Blanchette *et al.*, 2008). A representative shore section was designated at each site and a measuring tape was laid out from the upper edge of the highest intertidal barnacle zone, perpendicular to the shore, to the lowest level of the low tide (generally the surfgrass zone). The vertical point-intercept transect was divided in 50 equidistant points. Intervals between points were adjusted at each site and depended on the width of the shore. The five taxa under each point, including layering and epibionts, or closest to the point directly attached to the substratum were recorded. Tide pools and inundated areas were not sampled to avoid a misrepresentation of the intertidal height. If an intercept point fell on tide pools/inundated areas, the closest horizontal non-tide pool/inundated area was sampled instead.

When species identification was not possible in the field, specimens were collected for further identification in the laboratory. Algae and lichen specimens were preserved in KEW solution (40% ethanol (70%), 40% seawater, 10% glycerine and 10% formaldehyde (4%)) and sessile invertebrates were preserved in 96% ethanol. A random search of 5 minutes at each site was performed to include species that did not comprise one of the five taxa of each point but were present along the transect. Species were identified and accounted for in the overall qualitative description of the site's community composition, but were not considered in the statistical analyses.

The abundance of target mobile species was estimated using 30 x 30 cm quadrats placed within three zones along the transect following Engle (2008). Specifically, each transect was divided into 1) the low zone, below the mussel zone, 2) the mid zone, centre of the distribution of mussels and 3) the high zone, the area dominated by barnacles and littorinids. Within each zone, three quadrats were randomly placed on the substratum and only the macroinvertebrate target taxa (limpets, gastropods and a pulmonate species) >5mm found within the quadrat were identified and counted. The abundance of littorinids (mostly <5 mm) was only determined in the high zone and the species were sub-sampled in a 7.5 x 10 cm section. When species identification was not possible in the field, specimens were collected and preserved in 96% ethanol for further morphological or genetic identification in the laboratory. Tide pools and inundated areas were not sampled to avoid a misrepresentation of the intertidal height. Only the target taxa found directly on the substratum or as epibionts of other organisms were sampled.

The historical distribution of algae from northern Africa described in the literature and in Algaebase (http://www.algaebase.org/) was used as a baseline for the distributional patterns of the species identified in this chapter. New local records depicted novel descriptions of a species at a site, despite its confirmed presence in the country. A new southern limit was considered when a species was described farther south than its previous historical limit. A new record was considered when the species was first recorded from Moroccan and Western Sahara shores.

2.2.3 Species genetic identification

When identification of macroinvertebrates was not possible from morphological traits (shape/colour/pattern of shell, colour of papillae, colour of the foot), foot tissue (20–30 mg) was dissected from each individual, preserved in 96% ethanol and stored at -20 ºC for DNA extraction. Total genomic DNA extraction was performed using a standard Proteinase K protocol adapted from Sambrook *et al.* (1989).

The universal primers 16SAR 5'-CGCCTGTTTAACAAAAACAT-3' and 16SBR 5'-CCGGTTTGAACTCAGATCACGT-3' (Palumbi, 1996) were used for polymerase chain reaction (PCR) amplification of 16S rRNA gene. PCR was performed in 25 µl containing 1–10 ng of total DNA, 0.2 µM of each primer, 0.2 mM of each dNTP, 1 mM of $MgCl_2$, 1x GoTaq Flexi Buffer (Promega, USA) and 1 U GoTaq DNA Polymerase (Promega, USA). Amplification used an initial denaturation during 5 min at 94 °C followed by 35 cycles of denaturation at 94 °C for 30 s, annealing at 46 °C for 30 s, extension at 72 °C for 30 s and a final extension at 72 °C for 5 min. PCR products were sequenced directly with PCR

primers using the BigDye Terminators version 3.1 Cycle Sequencing Kit (Applied Biosystems, Foster-City, CA) in an ABI PRISM 3130 genetic analyzer (Applied Biosystems).

DNA sequences were visualized using Geneious 4.8.2 (Biomatters Ltd.) and blasted for species confirmation in the National Centre for Biotechnology Information (NCBI) database.

2.2.4 Environmental variables

Site-specific monthly sea surface temperature (SST) data with a 4 km resolution were retrieved from the Moderate Resolution Imaging Spectroradiometer-Aqua (MODIS-Aqua) dataset available from the National Aeronautics Space Administration (NASA) Goddard Earth Sciences (GES) Data and Information Services Center (DISC) for the period from January 2010 to December 2014 using Giovanni, a web-based application developed by the NASA GES DISC. An area of 25 km^2 situated 5 km offshore of each sampling site was selected to investigate annual minimum and maximum SST and SST variation (maximum SST – minimum SST). Annual minimum and maximum SST were obtained by selecting the lowest and highest monthly SST over each year, respectively. Annual minimum and maximum SST and SST variation values were then averaged over the 5-year period considered.

The wind-based upwelling index cross-shore Ekman transport (CSET) was used to estimate upwelling intensity during the period 2010–2014 as in Krug *et al.* (2017). Daily sea surface wind fields (speed and direction) at a spatial resolution of 0.25° were obtained from the Blended Sea Winds dataset (National Climatic Data Centre - National Oceanic and Atmospheric Administration, NCFC-NOAA, http://www.ncdc.noaa.gov/oa/rsad/air-sea/seawinds.html). Blended Sea Winds dataset combines multiple scatterometers standardized across platforms, resulting in high quality temporal and spatial coverage of ocean wind vectors (Zhang *et al.*, 2006). CSET values were estimated for thirteen locations along the meridionally oriented northern African coast (Table 2.1). For each location, CSET values represented the average of a 0.75 x 0.75° box centred on the target location.

The zonal component of the Ekman transport ($CSET_x$), induced by the meridional component of wind-stress (τ_y), was used as an upwelling index for each station. $CSET_x$ ($m^3\ s^{-1}\ km^{-1}$ coastline) was calculated following Bakun (1973), as modified by Alvarez *et al.* (2011):

$$\mathrm{CSET}_x = \frac{1000\ \tau_y}{\rho_w f} = \frac{\rho_a\, c_d}{\rho_w f}\ (W_x^2+W_y^2)^{1/2}\ 1000\ W_y$$

where W represents wind velocity (m s^{-1}), ρ_w is seawater density (1025 kg m^{-3}), ρ_a is air density (1.22 kg m^{-3}), C_d is the drag coefficient ($1.4x10^{-3}$) and *f* is the Coriolis parameter, estimated as 2 Ω sin(θ) where Ω and θ represent the vertical component of the Earth's angular velocity and local latitude, respectively. Negative $CSET_x$ values indicate upwelling-favourable periods with offshore Ekman transport and conversely, positive values indicate downwelling-favourable periods and onshore Ekman transport.

Daily CSET data were first monthly averaged to reduce the influence of daily anomalies. Over each year, the lowest CSET monthly average was identified to obtain the annual minimum. The overall minimum (UImin) and mean (UImean) upwelling indices for the 5-year period (2010–2014) were estimated for each site and used in statistical analyses. The UImin was obtained by selecting the lowest upwelling index of the 5-year period, while the overall UImean was obtained by averaging the five minimum annual CSET (i.e. one value per year). Annual probability of upwelling (UIp in %) was calculated as the average of the monthly frequency of upwelling favourable days (CSET values <0). The overall UIp was the average over the 5-year period.

2.2.5 Data analyses

Site-specific taxon richness was estimated by summing the total number of taxa identified at each site from both transect and quadrat surveys. Species were categorized into functional groups based on their feeding guilds (macrophytes, filter-feeders, herbivores and lichens) as in Blanchette *et al.* (2009).

To examine similarity of biological and environmental data patterns along the study area and understand if the composition of intertidal communities was influenced by upwelling-related variables, the multivariate methods of Clarke (1993) in PRIMER 6.1.3 (Plymouth Routines in Multivariate Ecological Research) software package were used. Taxon abundance was averaged across sampling replicates for each site. The data matrix of taxon abundances was fourth-root transformed to reduce the contribution of very abundant species and increase that of rare species (as in Blanchette *et al.,* 2009). A biological similarity matrix was constructed using the Bray–Curtis similarity coefficient and cluster analysis was performed using a hierarchical method with group-average linking. Environmental data were normalized after fourth-root transformation and a similarity matrix was constructed using Euclidean distance. A SIMPROF test was run for the biological and environmental dendrograms separately using 9999 permutations to indicate significant group structure at the significance level of 5%.

The SIMPER routine was performed to identify the taxa of each group that were most responsible for the differences among groupings, with a cut-off of 25% contribution (Clarke & Gorley, 2006). Sites were assigned to groups defined *a priori* based on SIMPROF analyses of the biological dendrogram.

Two-dimensional, non-metric multidimensional scaling (MDS) was performed on the environmental variables to examine regional segregation among sites (Kruskal & Wish, 1978).

The RELATE routine was used in PRIMER to match the environmental resemblance matrices with the resemblance matrices of taxon richness, abundance of functional groups, taxon abundance based on transects (TAT) and based on quadrats (TAQ) separately, running 9999 permutations under the Spearman rank correlation method at a significance level of 5%.

Distance-based linear models (DistLM) were carried out to determine the contribution of the environmental variables to the variability in community composition. DistLM analyses were performed through a dissimilarity matrix, using the 'all specified' selection procedure under the Akaike Information Criterion (AIC), performing 9999 permutations for taxon richness, abundance of functional groups, TAT, TAQ, and presence/absence for the taxa identified in transects, separately. The environmental variables were analysed individually (marginal tests) and a sequential test was employed to evaluate the cumulative effect of each variable once the previous variable(s) had been accounted for.

2.3 RESULTS

2.3.1 Biological sampling

A total of 186 taxa (26 Ochrophyta, 26 Chlorophyta, 107 Rhodophyta, 1 Annelida, 4 Arthropoda, 2 Ascomycota, 1 Chordata, 3 Cnidaria, 16 Mollusca) inhabiting the intertidal shores of Atlantic Morocco and Western Sahara were identified (Table 2.2, see also Fig. A1–A4 in Appendix). A considerably greater number of algae taxa were identified in comparison with lichens or animals. Algae constituted 85.5% of the identified taxa, while animals and lichens constituted 13.4% and 1.1%, respectively. The surveys reported 376 new local records of algae; new overall southern limits were detected for 25 algal species and nine other algal species were recorded for the first time from the study area. Overall, distribution novelties or changes were described from 89% (141 species) of the algal taxa identified.

Table 2.2 – List of all species recorded along intertidal Atlantic Moroccan and Western Sahara shores. The phylum of each taxa group is depicted in bold. Location codes as is Table 2.1. x, presence; **x**, new local record; [1]new southern limit detected,[2]first record from Morocco and Western Sahara.

Taxon	LR	RB	SB	EB	ES	IM	ML	TT	TF	BJ	LB	DK
Chlorophyta												
Bryopsis duplex					**x**							
Bryopsis plumosa												**x**
Chaetomorpha aerea		x								**x**	**x**	
Chaetomorpha mediterranea						**x**				**x**		
Cladophora albida						**x**						**x**
Cladophora hutchinsiae[1]						**x**				**x**		**x**
Cladophora laetevirens[1]						**x**				**x**		
Cladophora lehmanniana[1]				**x**		**x**		**x**				
Cladophora rupestris[1]										**x**	**x**	
Cladophora sp												**x**
Codium adhaerens					x	**x**	x					
Codium sp		x	x						**x**			
Codium tomentosum var. mucronatum	**x**	x		**x**		**x**	x	**x**	**x**		**x**	**x**
Pedobesia simplex											**x**	
Ulva clathrata						**x**				**x**		
Ulva compressa		x		**x**	x					**x**	**x**	**x**
Ulva fasciata									**x**	**x**		
Ulva flexuosa						**x**						
Ulva intestinalis		x		**x**								
Ulva linza[1]										**x**		
Ulva prolifera		x				**x**				**x**	**x**	

Ulva pseudolinza[2]											x	
Ulva rigida	x	x	x	x	x	x	x	x	x	x	x	x
Ulva sp	x	x			x	x	x		x	x	x	x
Ulvaria obscura[1]			x		x	x	x	x	x	x		x
Valonia utricularis[1]									x	x		
Ochrophyta												
Acinetospora crinita		x				x						
Bifurcaria bifurcata			x	x	x	x						
Cladostephus spongiosus[1]									x			
Colpomenia peregrina	x	x		x		x	x					
Colpomenia sinuosa						x	x			x	x	
Cystoseira humilis			x						x			
Cystoseira sedoides[2]								x				x
Cystoseira sp			x		x	x		x	x	x	x	x
Dictyopteris polypodioides									x			
Dictyota cyanoloma[2]											x	
Dictyota dichotoma	x		x	x	x	x	x	x	x	x	x	
Fucus guiryi			x	x	x	x			x			x
Hincksia mitchelliae						x						
Laminaria ochroleuca			x		x							
Padina pavonica		x				x			x			
Pelvetiopsis brevipes		x										
Phyllariopsis purpurascens			x									
Ralfsia verrucosa[1]	x	x	x	x	x	x	x	x	x	x	x	
Saccorhiza polyschides			x		x							
Sargassum sp			x									
Sargassum vulgare			x									
Sphacelaria cirrosa[1]						x				x		
Sphacelaria fusca						x						
Sphacelaria rigidula			x			x	x					
Sphacelaria tribuloides						x						
Stypocaulon scoparium									x	x		
Rhodophyta												
Ahnfeltiopsis devoniensis[1]		x	x		x		x	x	x	x	x	x
Acrosorium ciliolatum		x	x				x		x	x		
Aglaothamnion hookeri		x	x	x	x							x
Amphiroa beauvoisii		x	x			x						
Amphiroa rigida								x				
Amphiroa vanbossea[2]						x						
Antithamnion cruciatum		x				x	x				x	
Aphanocladia stichidiosa[1]			x			x						
Apoglossum ruscifolium							x					
Asparagopsis armata										x		
Bangia fuscopurpurea												x

Boergeseniella fruticulosa		x	x	**x**		**x**	**x**	**x**	**x**	**x**	**x**	**x**
Boergeseniella thuyoides[1]				**x**					**x**			
Bornetia secundiflora			x					x				
Calliblepharis ciliata									**x**			
Calliblepharis jubata			x		x			x	**x**	**x**		
Callithamnion corymbosum		**x**		**x**								
Callithamnion tetragonum		x	x	**x**	**x**		x	x	**x**	**x**	**x**	**x**
Callithamnion tetricum[1]									**x**			
Callophyllis laciniata[1]			x									**x**
Catenella caespitosa	**x**	x				**x**						
Caulacanthus ustulatus	x	x	x	**x**	x	x	x	x	**x**	**x**	**x**	**x**
Centroceras clavulatum										**x**		
Ceramium ciliatum			x	**x**	x	**x**	x	x	**x**	**x**	**x**	
Ceramium diaphanum		x	**x**			**x**						
Ceramium echionotum			x			**x**	x	x	**x**			
Ceramium gaditanum[1]												**x**
Ceramium sp		x										
Ceramium tenerrimum	**x**											
Ceramium virgatum	x	x	x	x	x	x	x	x	x	x	x	x
Champia compressa[1]							**x**					
Champia parvula		x		**x**	x							
Chondracanthus acicularis	x	x	x	**x**	x	x	x		x	x	x	x
Chondracanthus teedei		x	x		x				**x**			
Chondria coerulescens			x			**x**			**x**			
Chondria dasyphylla			x									
Corallina caespitosa[2]	**x**	**x**	**x**	**x**	**x**	**x**	**x**	**x**	**x**	**x**	**x**	**x**
Crouania attenuata			**x**									
Cryptonemia lomation[1]									**x**			
Cryptonemia seminervis			x									
Dasya corymbifera[1]							**x**					**x**
Dasya hutchinsiae						**x**						**x**
Dasya oceollata			x									
Drachiella spectabilis[2]							**x**					
Ellisolandia elongata	x		x			**x**						
Erythrotrichia carnea						**x**						
Falkenbergia rufolanosa state						**x**	x	x				
Gastroclonium ovatum				**x**			x	x				**x**
Gastroclonium reflexum[1]		**x**	**x**	**x**	x				**x**	**x**	**x**	**x**
Gayliella flaccida				**x**		**x**	**x**	**x**		**x**	**x**	
Gelidium crinale									**x**	**x**		
Gelidium pulchellum	x	x	x						**x**	**x**		
Gelidium pusillum			x			**x**	**x**		**x**	**x**	**x**	**x**
Gelidium sesquipedale			x		x						**x**	
Gelidium sp		x	x						**x**	**x**		
Gelidium spathulatum		x										
Gelidium spinosum									**x**	**x**		

Gigartina pistillata									**x**			
Gracilaria multipartita		x	x	**x**	x				**x**	**x**		
Grateloupia filicina		x										
Grateloupia lanceola	x	x	x	**x**		**x**			**x**			
Gymnogongrus crenulatus	x			x	x				**x**			
Gymnogongrus griffithsiae		x								**x**		
Halopithys incurva			x		x				**x**	**x**		
Halurus equisetifolius				**x**			**x**	**x**	**x**			
Halymenia latifolia[2]									**x**			
Herposiphonia secunda			x		x	**x**	**x**		**x**	**x**	**x**	**x**
Heterosiphonia crispella		**x**										**x**
Hypnea musciformis			x			**x**	x		**x**	**x**		**x**
Hypoglossum hypoglossoides			x	**x**		**x**	**x**		**x**	**x**	**x**	**x**
Jania longifurca					x							**x**
Jania rubens				**x**		**x**			**x**	**x**	**x**	
Laurencia obtusa									**x**	**x**		
Leptosiphonia schousboei			x									
Lithophyllum byssoides	x	x	x	**x**	x	x	x				**x**	
Lithophyllum incrustans	x	x	x	**x**	x	**x**	x	x	**x**	**x**	**x**	**x**
Lomentaria articulata[1]	x		x	x	x				**x**	**x**		
Lophosiphonia reptabunda[1]									**x**	**x**	**x**	**x**
Mastocarpus stellatus								x			**x**	
Melobesia membranacea					x			**x**		**x**		
Mesophyllum lichenoides	x	x	x	**x**	x	**x**	x	x		**x**	**x**	
Neosiphonia collabens		x	x	**x**		**x**	**x**	x	**x**	**x**	**x**	**x**
Neosiphonia ferulacea[2]				**x**			**x**					
Ophidocladus simpliciusculus			x			**x**			**x**		**x**	
Osmundea osmunda			**x**	**x**	**x**				**x**	**x**		**x**
Osmundea pinnatifida		x	x	**x**	x		x		**x**	**x**	**x**	**x**
Osmundea sp							x			**x**	**x**	**x**
Peyssonnelia sp				**x**								
Phyllophora sp			x									
Plocamium cartilagenum			x	**x**	x	**x**	x	x	**x**	**x**	**x**	**x**
Polysiphonia atlantica												**x**
Polysiphonia brodiei[1]						**x**		**x**				
Polysiphonia fucoides[1]			**x**									
Polysiphonia funebris[1]			**x**			**x**			**x**			
Polysiphonia scopulorum[1]											**x**	
Porphyra umbilicalis	**x**	x	**x**	**x**	x						**x**	
Porphyrostromium boryana											**x**	
Pterocladiella capillacea			x		x					**x**		
Pterosiphonia ardreana[2]			**x**	**x**	**x**	**x**	**x**		**x**		**x**	**x**
Pterosiphonia complanata		x	x	**x**		**x**	**x**	**x**		**x**	**x**	
Pterosiphonia parasitica						x						
Pterosiphonia pennata			x	**x**	**x**	**x**			**x**		**x**	**x**
Rhodochorton purpureum									**x**			

Rhodymenia pseudopalmata					x				x	x		
Rhodymenia sp				x								
Stylonema alsidii		x										
Titanoderma pustulatum					x							
Ascomycota												
Lichina pygmaea			x	x	x							
Verrucaria maura	x		x	x	x	x					x	x
Annelida												
Sabelaria alveolata	x	x	x	x	x	x	x	x	x	x	x	x
Arthropoda												
Chthamalus montagui	x	x	x	x	x	x	x	x	x	x	x	x
Chthamalus stellatus	x	x	x	x	x	x	x	x	x	x	x	x
Perforatus perforatus	x	x	x	x	x	x	x	x		x	x	
Pollicipes pollicipes	x	x	x	x	x		x			x	x	x
Chordata												
Pyura herdmani						x	x	x				
Cnidaria												
Actinia equina						x				x		
Actinia fragacea				x			x			x		
Anemonia viridis							x			x		
Mollusca												
Cymbula safiana	x	x	x	x		x		x	x	x	x	x
Echinolittorina punctata	x	x	x	x	x	x	x	x	x	x	x	X
Fissurela nubecula	x	x	x			x	x	x	x	x		X
Gibbula pennanti		x				x		x		x		
Gibbula umbilicalis	x	x	x	x	x	x	x	x	x	x		
Melarhaphe neritoides	x	x	x	x	x	x	x	x	x	x	x	x
Mytilus galloprovincialis	x	x	x	x	x	x	x	x	x	x	x	x
Patella depressa	x	x	x	x	x	x	x	x	x	x	x	x
Patella rustica	x		x		x						x	x
Patella ulyssiponensis	x	x	x	x	x	x	x	x	x	x	x	x
Perna perna	x	x	x	x	x	x	x	x		x	x	x
Phorcus lineatus			x	x	x	x			x	x	x	
Phorcus sauciatus	x	x		x		x	x	x	x	x	x	x
Siphonaria pectinata	x	x	x		x	x	x	x	x	x	x	x
Stramonita haemostoma				x		x			x			
Vexillum zebrinum						x	x			x		

Taxon richness varied along the study area, but did not follow a clear latitudinal gradient (Fig. 2.1). However, the four southernmost sites showed a trend of decreasing taxon richness towards the south. Average taxon richness across all sites was 46, but some sites presented particularly low (29 taxa, sites ML and TT) or high (62 taxa, site TF) richness. Macrophyte, filter-feeder, herbivore and lichen taxa ranged 15–49, 4–8, 6–10 and 0–2, respectively, per site.

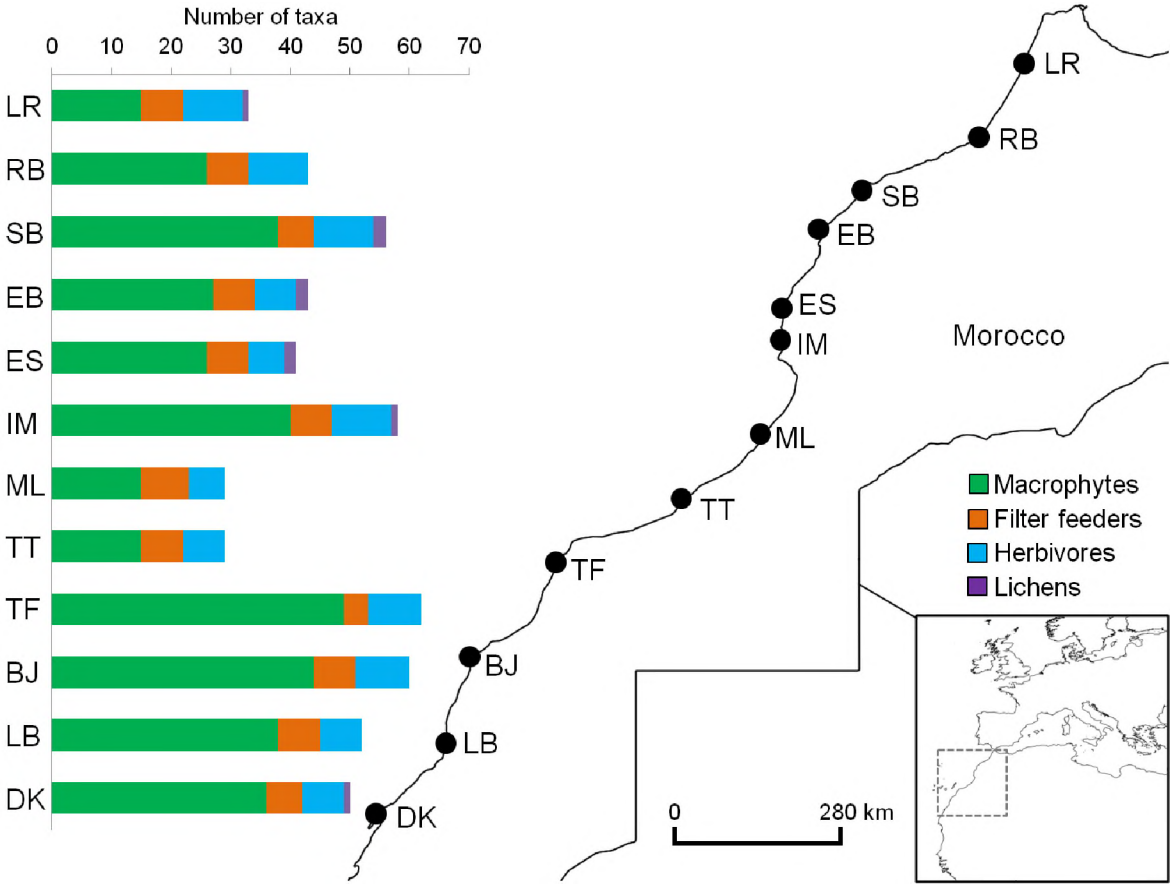

Figure 2.1 – Species richness at 12 sites along the coasts of Morocco and Western Sahara, categorized by functional groups.

Hierarchical cluster analyses based on taxon abundance from the transect (TAT) matrix revealed significant geographic structure, although no significant structure was detected for taxon abundance from quadrats (TAQ; Fig. 2.2). The SIMPROF test performed on TAT data identified three significantly different clusters (groups B1, B2 and B3). Group B1 contains site IM exclusively. Group B2 comprised sites LR, RB, ML and TT at a Bray-Curtis similarity of around 64%. Groups B1 and B2 showed significant similarity of around 55%. Group B3 comprised sites SB, EB and ES and TF, BJ, LB and DK at a similarity of 53%.

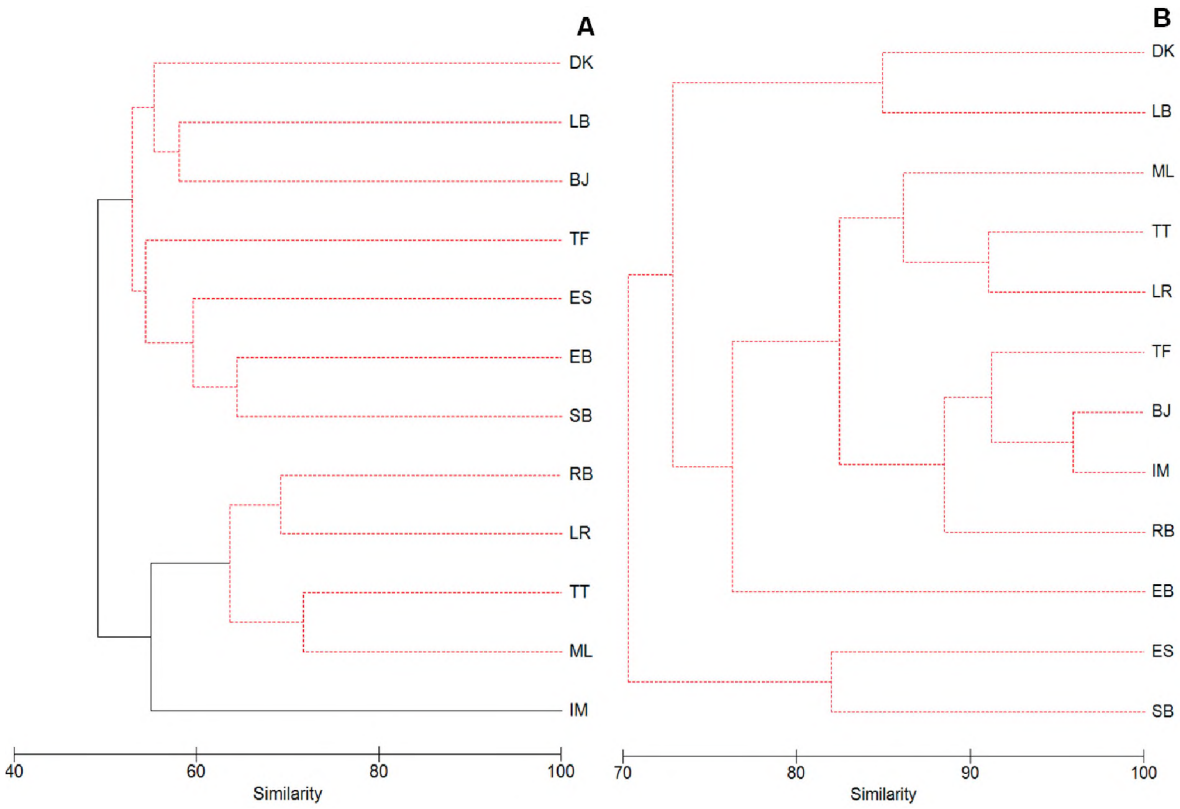

Figure 2.2 – Bray-Curtis similarity dendrograms based on the community composition of A) taxon abundance from transect and B) taxon abundance from quadrat data. Black nodes depict significant clustering (p<0.05).

The SIMPER results showed that a total of 20 algae and two animal taxa contributed the most to the dissimilarities between the three groups (B1B2, B1B3 and B2B3). While seven taxa contributed the most to differences between groups B1 and B2 (dissimilarity of 45.04%), 11 and 12 taxa contributed the most to differences between groups B1 and B3 (dissimilarity of 51.01%) and B2 and B3 (dissimilarity of 50.82%), respectively (Table 2.3).

Table 2.3 – Results of similarities percentages (SIMPER) analyses showing the percentage contributions of the species that contributed the most to dissimilarity between groups.

Taxon	B1B2	B1B3	B2B3
Ellisolandia elongata	2.78	-	-
Verrucaria maura	2.9	-	-
Jania rubens	3.2	2.11	-
Codium adhaerens	3.55	2.72	-
Padina pavonica	3.81	2.86	-
Ulva clathrata	4.21	2.69	-
Bifurcaria bifurcata	4.72	2.68	-
Colpomenia peregrina	-	2.23	-
Pyura herdmani	-	1.88	-
Sphacelaria fusca	-	1.88	-
Perforatus perforatus	-	2.08	1.72
Fucus guiriy	-	2.18	2.86
Osmundea pinnatifida	-	2.96	3.86
Osmundea sp	-	-	1.67
Ralfsia verrucosa	-	-	1.69
Hypoglossum hypoglossoides	-	-	1.78
Lithophyllum byssoides	-	-	1.91
Ulva compressa	-	-	1.92
Neosiphonia collabens	-	-	1.94
Chondracanthus acicularis	-	-	1.95
Plocamium cartilagineum	-	-	2.23
Osmundea osmunda	-	-	2.36

SIMPER contributions based on TAT per site were plotted and highlighted dissimilar distributional arrangements and changes in species abundance among and within groups (Fig. 2.3). Out of the 22 taxa retrieved in SIMPER analyses only two were animals, one was lichen and the remaining 19 were algae. Seven species contributed most to dissimilarities between groups (*Bifurcaria bifurcata*, *Ulva clathrata*, *Osmundea pinnatifida*, *Padina pavonica*, *Codium adhaerens*, *Jania rubens* and *Fucus guiryi*). Abundance of *B. bifurcata* gradually increased from group B3 (site SB) to its maximum abundance in group B1 (site IM; Fig. 2.3) and was absent south of IM. *Ulva clathrata* was exclusive to sites IM (group B1), where it was the most abundant, and BJ (group B3). *Osmundea pinnatifida* was present at all sites of group B3 but absent from the remaining two groups. While *Pa.*

pavonica, *C. adhaerens* and *J. rubens* were relatively abundant in group B1 (site IM) they were absent or extremely rare in the other two groups. Finally, *F. guiryi* was abundant at most sites of group B3, with a gradual increase of abundance from site SB to ES, but the species was absent from groups B1 and B2.

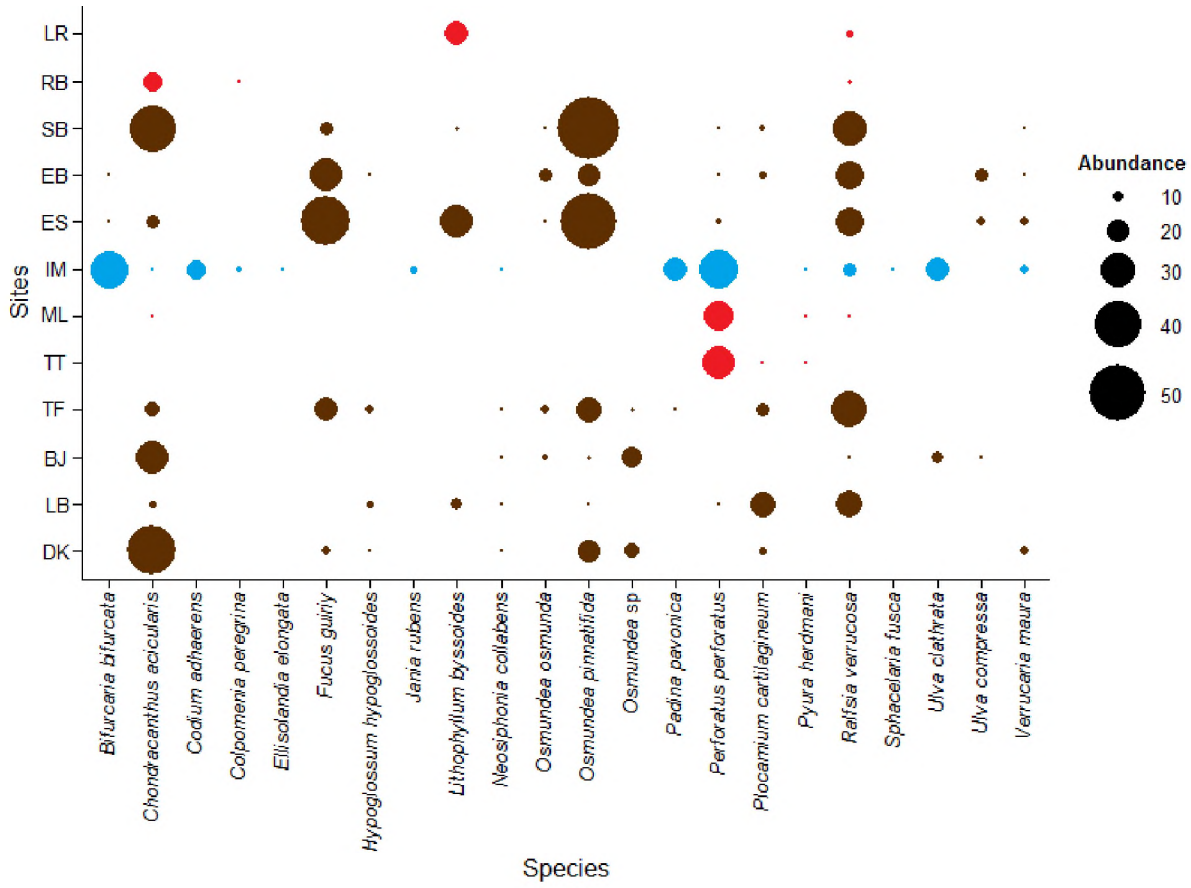

Figure 2.3 – Geographic pattern of distribution and abundance for the species that contributed most to the dissimilarity between groups B1B2, B1B3 and B2B3. Sites belonging to group B1, B2 and B3 are represented in blue, red and brown, respectively. Species abundance is represented by total percentage (%) of presence detected along the 50 points of each transect, averaging the abundance of each of the two replicates at each site. Study sites are as in Table 2.1.

2.3.2 Species genetic identification

A total of 83 sequences were blasted in the National Centre for Biotechnology Information (NCBI) database and compared with available sequences, confirming the presence of 5 species of limpets: *Patella ulyssiponensis* (36 sequences), *Cymbula nigra* (12 sequences), *Pat. depressa* (19 sequences), *Fissurela nubecula* (11 sequences) and *Pat. rustica* (1 sequence); and one pulmonate species, *Siphonaria pectinata* (4 sequences).

2.3.3 Environmental data

The environmental variables were averaged over the 5-year period (2010–2014) for each site (Table 2.4, as described in section 2.2.4) and analysed to detect geographical clustering of sites. The minimum (UImin) and mean (UImean) values of wind-based upwelling indices ranged from -1723.51m^3 s^{-1} km^{-1} coastline (at IM) to -418.99 m^3 s^{-1} km^{-1} coastline (at RB) and -1543.06 m^3 s^{-1} km^{-1} coastline (at IM) and -312.55 m^3 s^{-1} km^{-1} coastline (at RB), respectively. Favourable wind-conditions for upwelling phenomena occurred between 68.9% (at RB) and 95.73% (at DK) of the time of the 5-years period. Maximum and minimum sea surface temperature (SSTmax and SSTmin) ranged between 20.41 °C (at ES) and 23.33 °C (at RB) and between 16.08 °C (at IM) and 17.12 °C (at TF), respectively. SST variation (SSTv) ranged 4.05 °C (at LB) and 6.94 °C (at RB).

Table 2.4 – Summary of the environmental variables analysed at each sampling site. UImin, minimum Upwelling Index; UImean, mean Upwelling Index; UIp, probability of upwelling events; SSTmax, maximum sea surface temperature; SSTmin, minimum sea surface temperature and SSTv, variation of sea surface temperature (maximum-minimum SST). Sampling sites are as in Table 2.1.

Sites	UImin (m^3 s^{-1} km^{-1})	UImean (m^3 s^{-1} km^{-1})	UIp (%)	SSTmax (°C)	SSTmin (°C)	SSTv (°C)
LR	-430.19	-340.36	70.52	22.53	16.17	6.37
RB	-418.99	-312.55	68.94	23.33	16.39	6.94
SB	-820.64	-702.49	77.97	22.76	16.38	6.38
EB	-1077.05	-909.97	80.93	22.23	16.54	5.69
ES	-1611.04	-1441.31	83.24	20.41	16.15	4.26
IM	-1723.51	-1543.06	84.22	20.80	16.08	4.72
ML	-1704.03	-1263.98	83.98	22.16	16.62	5.55
TT	-1140.94	-1014.64	88.16	21.88	16.77	5.11
TF	-1330.26	-1050.61	90.28	21.79	17.12	4.67
BJ	-1301.84	-1209.70	92.66	22.62	16.76	5.86
LB	-1058.47	-953.61	93.26	20.48	16.43	4.05
DK	-1072.76	-924.01	95.73	21.15	16.98	4.17

Hierarchical cluster analysis based on the six environmental variables revealed significant geographical structure which was supported by the non-metric multidimensional (MDS) analysis (Fig. 2.4). The SIMPROF test significantly identified three main groups (E1, E2 and E3). Group E1 contained site IM. Group E2 comprised sites LR, RB, SB and EB (the four northernmost sites). Group E3 comprised sites ES and ML, TT, TF, BJ, LB and DK (central and southern sites).

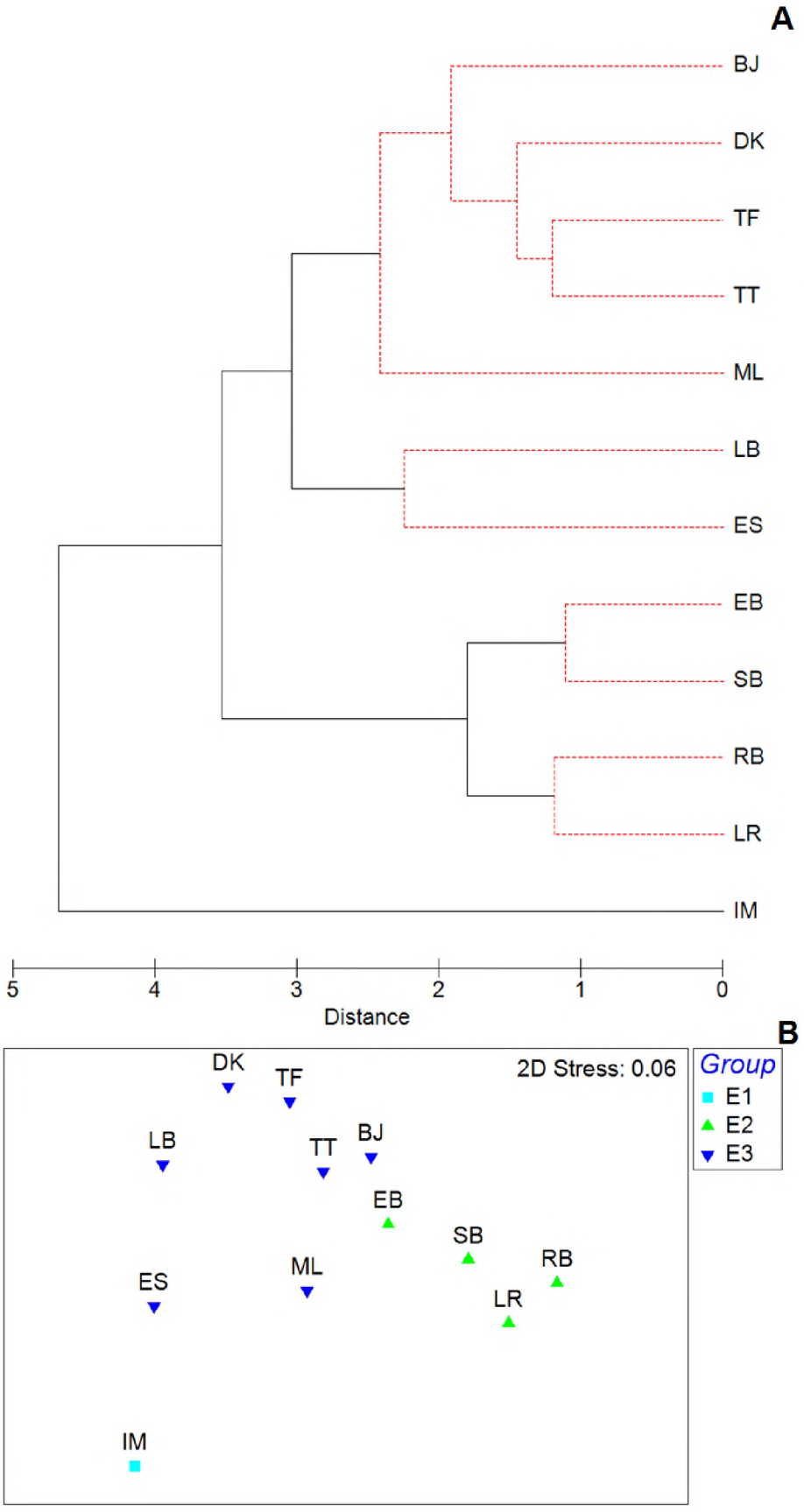

Figure 2.4 – Geographic structure based on environmental data; A) Euclidean distance dendrogram of the similarity of sites based on environmental variables, B) non-metric multidimensional ordination plot from the 12 study sites. Black nodes in the dendrograms depict significant clustering (p<0.05).

2.3.4 Biological-Environmental comparison

The RELATE routine did not identify significant similarity between the environmental variables and taxon richness (Rho=-0.1163, p=0.927), abundance of functional groups (Rho=-0.079, p=0.739), TAT (Rho=0.121, p=0.198) or TAQ (Rho=0.022, p=0.420). However, both biological (transect based) and environmental hierarchical cluster analyses showed similar clustering structure. Site IM was depicted as an outlier group in both cluster analyses. Additionally, both cluster analyses grouped sites LR and RB in B2/E2 and sites ES and TF, BJ, LB and DK in B3/E3.

DistLM did not retrieve any significant contributions of the environmental variables to the variability of taxon richness, abundance of functional groups, TAT or TAQ (marginal and sequential tests on environmental variables all p>0.05, Table 2.5). Although marginal tests on the environmental variables explaining TAQ were all non-significant (all p>0.05, Table 2.5), sequential tests showed that UImin, UImean, UIp and SSTmax together explained 47% of the variation (p=0.040, Table 2.5).

However, a DistLM analysis retrieved a significant contribution of UIp (marginal tests, p=0.0361) to the variability of presence/absence data from taxa identified in transects, explaining ~16% of the variation (Table 2.5).

Table 2.5 – Results of DistLM model. Environmental variables were analysed individually (marginal tests) and sequentially using the 'all specified' selection procedure and the Akaike (AIC) selection criterion. Prop (%) is the proportion of variance in taxon richness, abundance of functional groups, taxa from quadrats and from transects explained by each variable. Significant (p<0.05) values are indicated in bold.

MARGINAL TESTS				**SEQUENTIAL TESTS**			
Taxon richness							
Variable	Pseudo-F	*p*-value	Prop (%)	Pseudo-F	*p*-value	Prop (%)	Cumul.
Ulmin	0.012998	0.9198	0.12981	0.012998	0.9208	0.12981	0.001298
Uimean	0.55436	0.5049	5.2524	3.4548	0.0798	27.702	0.27832
Ulp	1.3626	0.2673	11.992	0.88807	0.379	7.2108	0.35043
SSTmax	0.26808	0.6149	2.6108	0.74211	0.4065	6.2264	0.41269
SSTmin	0.22212	0.6427	2.1729	0.027105	0.8757	0.26413	0.41533
SSTv	0.49801	0.4879	4.7438	2.1704	0.1947	17.697	0.59231
Functional group							
Variable	Pseudo-F	*p*-value	Prop (%)	Pseudo-F	*p*-value	Prop (%)	Cumul.
Ulmin	0.075224	0.8563	0.74663	0.075224	0.8526	0.74663	0.007466
Uimean	0.84733	0.4171	7.8114	2.8365	0.0856	23.785	0.24532
Ulp	0.42341	0.5517	4.0621	0.99913	0.3412	8.3789	0.32911
SSTmax	0.90635	0.3598	8.3103	0.5323	0.5103	4.7412	0.37652
SSTmin	2.1252	0.1742	17.527	0.10476	0.8201	1.0699	0.38722
SSTv	0.34377	0.6037	3.3235	0.18432	0.7203	2.1786	0.409
Quadrats							
Variable	Pseudo-F	*p*-value	Prop (%)	Pseudo-F	*p*-value	Prop (%)	Cumul.
Ulmin	0.53817	0.7095	5.1068	0.53817	0.7122	5.1068	0.051068
Uimean	0.22038	0.913	2.1562	0.67448	0.5889	6.6157	0.11723
Ulp	0.81871	0.5376	7.5675	0.93633	0.4601	9.2495	0.20972
SSTmax	1.8648	0.1375	15.717	3.5266	**0.0404**	26.476	0.47448
SSTmin	0.80664	0.5417	7.4643	0.39312	0.7426	3.2315	0.50679
SSTv	1.6995	0.1605	14.527	1.1109	0.3863	8.9658	0.59645
Transect							
Variable	Pseudo-F	*p*-value	Prop (%)	Pseudo-F	*p*-value	Prop (%)	Cumul.
Ulmin	0.78303	0.7153	7.2617	0.78303	0.7149	7.2617	0.072617
Uimean	0.83759	0.6619	7.7286	0.75381	0.7388	7.1672	0.14429
Ulp	1.6735	0.066	14.336	1.6347	0.0856	14.519	0.28948
SSTmax	0.8457	0.6253	7.7975	1.0522	0.4213	9.2849	0.38232
SSTmin	1.4703	0.1127	12.819	1.1015	0.391	9.5808	0.47813
SSTv	1.0683	0.3428	9.6518	0.98974	0.4567	8.6233	0.56437
Presence/absence from transect							
Variable	Pseudo-F	*p*-value	Prop (%)	Pseudo-F	*p*-value	Prop (%)	Cumul.
Ulmin	0.73365	0.7677	6.835	0.73365	0.7741	6.835	0.06835
Uimean	0.74402	0.7798	6.925	0.8607	0.6409	8.132	0.14967
Ulp	1.8832	**0.0361**	15.848	1.8136	0.0541	15.714	0.30681
SSTmax	0.89442	0.5643	8.2099	1.0795	0.4038	9.2616	0.39943
SSTmin	1.4469	0.1311	12.64	1.2854	0.2722	10.596	0.50539
SSTv	1.1706	0.2775	10.479	1.0226	0.4398	8.3982	0.58937

2.4 DISCUSSION

The results of this chapter suggest that upwelling may influence community structure of intertidal benthic biota of Atlantic Moroccan and Western Sahara shores. Here, I further discuss the intertidal biodiversity of Morocco and Western Sahara territory and the importance of upwelling as a thermal buffer in a context of climate change.

2.4.1 Upwelling influence on intertidal benthic communities

The fact that the distribution and abundance of coastal marine species are strongly influenced by large scale oceanographic processes (Bosman *et al.*, 1987; Broitman *et al.*, 2001; Blanchette *et al.*, 2008) and that the latitudinal variability of environmental or geographical variables enables clear geographical partitions of study regions (e.g. Hutchings *et al.*, 2009), highlights the possibility of finding distinct intertidal communities associated with areas differently influenced by environmental or oceanographic processes. The environmental analysis structured the study area of this chapter into three groups: an outlier location (site IM, group E1, western Morocco), a northern region (sites LR, RB, SB and EB, group E2, northern Morocco) and a southern region (sites ES and ML, TT, TF, BJ, LB and DK, group E3, southern Morocco and Western Sahara). Site IM was most likely identified as an independent group due to the combined effects of the strongest upwelling indices (UI), some of the lowest maximum sea surface temperature (SSTmax) and the lowest minimum SST (SSTmin), highlighting a location characterized by the coldest water conditions and most intense upwelling of the entire study area. In sharp contrast, E2 comprised the weakest UI coupled with the lowest probability of upwelling (UIp) and greatest SST variation, which matches previous studies describing northern Morocco as a region characterized by weak upwelling indices (Marcello *et al.*, 2011; Benazzouz *et al.*, 2014; Cropper *et al.*, 2014). In agreement with the described intense upwelling events and the lack of seasonality along southern Morocco and Western Sahara due to conditions that are favourable to upwelling year-round (Marcello *et al.*, 2011; Benazzouz *et al.*, 2014), E3 revealed strong upwelling indices and the greatest probability of upwelling.

Because they can interrupt the general pattern of warmer or colder SSTs towards the equator or the poles, respectively, oceanographic features such as fronts, currents or upwelling phenomena cause thermal latitudinal discontinuities, influencing the distribution of intertidal assemblages (e.g. Blanchette *et al.*, 2008; Ling *et al.*, 2009). For example, the East Australian Current (EAC) flows south along eastern Australia, the Tasman Sea and

eastern Tasmania, warming intertidal shores along these regions (Ridgway, 2007). This latitudinal thermal discontinuity has major implications for the distribution and composition of rocky shore communities, as the warm tongue of the EAC favours the spread of warm adapted taxa beyond their subtropical distributional range and leads to range contractions of cold adapted ones (Poloczanska *et al.*, 2007; Ling *et al.*, 2009; Wernberg *et al.*, 2011). Latitudinal discontinuities associated with upwelling are key elements in explaining community structure of benthic intertidal biota, as in the case of the Humboldt Current system (Broitman *et al.*, 2001; Wieters *et al.*, 2009; Tapia *et al.*, 2014), the California Current system (Blanchette *et al.*, 2008) and the Benguela Current system (Wieters *et al.*, 2009). Upwelling conditions were proposed as major drivers of biogeographic variation of the intertidal fauna and flora along South Africa (Bustamante & Branch, 1996b; Sink *et al.*, 2005; Xavier *et al.*, 2007). Discontinuities in community structure and species abundance along California and Humboldt Current systems also coincided with regional shifts in upwelling intensities (California, Broitman *et al.*, 2001; Schoch *et al.*, 2006; Blanchette *et al.*, 2008; Humboldt, Wieters *et al.*, 2009; Tapia *et al.*, 2014). In this chapter I demonstrate that under extreme upwelling-related environmental conditions (i.e. the strongest upwelling indices coupled to the lowest SST) upwelling drives changes in species abundance and community composition. The general lack of statistical significance between environmental and biological data and the partial discordance in clustering structure between taxon abundance and upwelling-related variables depicted in this work might suggest that upwelling does not influence nearshore benthic community structure. Indeed, it has been shown that upwelling alone does not affect the abundance of intertidal mussels, the mesoscale variation in faunal assemblages in mussel beds or the number of species associated with mussel beds (Cole & McQuaid, 2010). However, DistLM analyses on taxa abundance in quadrats and on presence/absence and the agreement between environmental and biological dendrograms for site IM suggest that upwelling influences the structure of intertidal communities. This influence seems to be exclusive of the site where environmental variables were exceptionally different from the surrounding locations. Specifically, the strongest upwelling indices and the lowest SST displayed by IM most likely mirror an effect on the abundance of intertidal biota, primarily algae, at this location. In fact, the community patterns described in this chapter largely reflect variations in the relative abundance of taxa rather than changes in species assemblages. This pattern has been previously described by Blanchette *et al.* (2008) from the intertidal shores of the California Current system. In this chapter, many of the species that contributed most to differences between groups did not show large scale presence/absence patterns, but rather had striking differences in abundances, with

particular expression where upwelling was stronger. For example, *Bifurcaria bifurcata*, *Padina pavonica* and *Ulva chlathrata* were relatively abundant in group B1/E1 (i.e. site IM) but extremely rare in the other groups. *Bifurcaria bifurcata* is a warm temperate species distributed from the British Isles to Morocco, restricted to tide pools to escape critical thermal extremes (Neiva *et al.*, 2015). Group B1/E1 most likely provides optimum conditions as a thermal refugium for the persistence of this brown algae, as evidenced by the greatest upwelling indices and lowest minimum and maximum SST at site IM, explaining the great abundance and intertidal cover of *B. bifurcata* there. This is in line with recent evidence highlighting the role of upwelling cells as contemporary refugia for marine species in a context of warming climate (Riegl & Piller, 2003; Hu & Guillemin, 2016; Lourenço *et al.*, 2016). In areas experiencing dramatic ocean warming, upwelling cells buffer the temperature increase on algae populations by delivering cold upwelled waters that counter the effect of warming SST, allowing the long-term maintenance of the species and its genetic diversity, most likely with consequences for the associated biota (Lourenço *et al.*, 2016). Noticeably, the only animal that greatly contributed to differences among sites was the barnacle *Perforatus perforatus*, which was massively more abundant at sites IM, ML and TT than elsewhere. Additionally, the only other animal identified by SIMPER analysis, the ascidian *Pyura herdmani*, occurred only at these three sites. Similarity in upwelling indicators does not seem responsible for the distributional pattern of the two species, because the three sites differ in upwelling indices and SST variables. Interestingly, along the transect *Py. herdmani* was only recorded at the lowest limit of the intertidal but extended into subtidal habitats (pers. obs). Although *Pyura* species are generally reported up to mid intertidal shores (Monteiro *et al.*, 2002; Castilla *et al.*, 2004), *Py. herdmani* might have a greater affinity to subtidal environments and therefore only rarely extends beyond the low shore. Because subtidal shores were not investigated, this species might be present at other sampling sites but have passed undetected because it is excluded from the intertidal area. Abiotic factors such air or substratum temperature might be limiting the vertical distribution of *Py. herdmani* as described for other subtidal-intertidal species (e.g. Harley, 2011; Mislan *et al.*, 2014).

Upwelled waters also enhance algal growth as a result of an increasing input of nutrients (Bosman *et al.*, 1987; Ormond & Banaimoon, 1994). In particular, *U. chlathrata*, an opportunistic foliose alga characterized by fast growth (Gaspar *et al.*, 2017), reached its greatest relative abundance at IM. This suggests a bottom-up effect potentially caused by nutrient-rich upwelling waters associated with this site (Head *et al.*, 1996) that further promoted the spread of the species along the intertidal, supporting previous evidence of the influence of nutrient-rich upwelling waters in promoting growth of foliose algae

(Bustamante *et al.*, 1995). Most importantly, considering that the overall biological dataset is largely dominated by algae, input of nutrients by upwelled waters might attain an even greater importance and be responsible for the observed clustering patterns. The results might therefore be biased in favour of algae and not correctly represent clustering patterns of animals or of the entire intertidal community. While the key role of nutrient-rich upwelling waters in structuring assemblage composition across the Canary Current system (CCS) has been recently demonstrated for pelagic communities (Anabalón *et al.*, 2014), the drivers of community structure of intertidal benthic biota along Moroccan and Western Sahara shores still warrant further investigation. Additional studies, preferably with similar proportion of algae and animals and targeting a range of environmental variables (i.e. upwelling with different intensities), would help disentangling not only the different influences of upwelling indicators (i.e. SST and nutrients) on the intertidal community structure of northern African shores, but also to detect possible bias on structural patterns of intertidal assemblages. Indeed, it has been shown that different taxonomic groups might respond differently to upwelling influence. For example, while algal cover and herbivores biomass is greater at shores of coastal upwelling than where upwelling does not occur, the opposite pattern is described from the cover of sessile filter-feeders (Bosman *et al.*, 1987).

Additionally, local features such as topography are also important small scale drivers of intertidal community composition (Blanchette *et al.*, 2008; Waters *et al.*, 2014). Despite its vast distribution along eastern Atlantic and Mediterranean shores, the brown alga *Pa. pavonica* is mainly found in rocky tide pools (Herbert *et al.*, 2016). The unique topography of site IM, characterized by a gentle intertidal slope with continuous, shallow (<10 cm) tidal pools, is a probable factor explaining the great abundance of this species. Similarly, site-specific physical attributes have previously explained the distribution of species over large geographical scales. For instance, the presence of the sand tolerant anemones *Anthopleura elegantissima* and *Acrosiphonia* spp from the northwest coast of the United States was explained by site-specific physical traits related to sand exposure (Blanchette *et al.*, 2008).

2.4.2 Intertidal biodiversity along the Atlantic shores of Morocco and Western Sahara in a context of climate change

Multiple expeditions have been performed within the CCS since the 19th century describing faunal and floral richness and biodiversity of this large upwelling ecosystem (reviewed in Ramos *et al.*, 2015). In spite of this, northwest African benthic communities

still remain largely under-investigated and the region is among the less known regions of the planet (Decker *et al.*, 2003; Brito *et al.*, 2014; Ramos *et al.*, 2015). Moreover, this region is of great interest because it is experiencing variable, severe and rapid climatic changes in warming trends (Lima & Wethey, 2012). Therefore, monitoring species that inhabit this region is necessary for the successful assessment of the impact of contemporary climate changes on rocky intertidal biota.

The clarification of distributional limits and the novel records reported in this chapter increase our knowledge on the distribution of intertidal benthic species along northern Africa. Moroccan coasts and the Western Sahara territory harbour great intertidal richness (Benhissoune *et al.*, 2001, 2002a, 2002b, 2003; Franchimont & Saadaoui, 2001; John *et al.*, 2004; Unesco, 2015) but most studies investigating the distribution and presence of marine intertidal species have been performed along northwestern Atlantic or Mediterranean Moroccan shores, with much less sampling effort in southern Morocco or the Western Sahara (Franchimont & Saadaoui, 2001). While most species in this work had been previously described from Atlantic Moroccan shores, their distributions in the southern region remained unclear. Following past studies that exhaustively catalogued the distribution of algae along most of my study area, this work clarified the range distribution of 141 algal species, particularly along the southern region, and added nine novel records for Morocco and Western Sahara, reinforcing the idea that more research is needed on benthic intertidal communities (Franchimont & Saadaoui, 2001; Ramos *et al.*, 2015) if one wants to clarify the composition and distribution of benthic intertidal assemblages of northern Africa. In addition to great gaps in algal distribution records, the distribution and description of macroinvertebrates from Moroccan shores remains largely uncertain (Franchimont & Saadaoui, 2001). As all macroinvertebrate species investigated in this study have previously been recorded from the study region and to avoid overestimating distributional novelties due to unclear range distributions, all local records of macroinvertebrates and lichens were not considered novel. Particularly, less information (e.g. the lack of distribution catalogues) is available on the detailed distribution of macroinvertebrate species along Morocco and Western Sahara, hindering the correct assessment of species distribution and distributional changes. For example, the sandworm *Sabelaria alveolata* has been described in multiple studies as being distributed from Scotland to southern Morocco (e.g. Mieszkowska *et al.*, 2006; Dubois *et al.*, 2007; Plicanti *et al.*, 2016). Although its distribution is well described from the northern part of the range (e.g. Dubois *et al.*, 2007; Mieszkowska *et al.*, 2013; Firth *et al.*, 2015), few studies refer to specific locations along the southern range (Ocaña *et al.*, 2005; Rouhi *et al.*, 2007; Muir *et al.*, 2016). Here, I show that *S. alveolata* extends towards the Western

Sahara, as far south as Dakhla (site DK). Similarly, the barnacle species *Chthamalus stellatus* and *Ch. montagui* have been the focus of several studies, with reported distributions from Scotland to northern Morocco and to Senegal, respectively (Southward, 1976; Clavier *et al.*, 2009; Shemesh *et al.*, 2009), but the southern distributional limits remain largely unexplored. In contrast to Shemesh *et al.* (2009) who showed that *Ch. montagui* was the only chthamalid species along northern Africa (three sites examined between northern Morocco and Senegal), in this chapter I provide evidence that the species coexists with *Ch. montagui* along multiple locations of Atlantic Morocco and Western Sahara. This result supports previous work suggesting that the two species could exist along northern African shores (Crisp *et al.*, 1981). While clarifying the distribution of the limpet species *Patella aspera* and *Pat. ulyssiponensis* along northeastern Atlantic shores, Weber & Hawkins (2005) highlighted the need to study the Moroccan populations to determine which species inhabited these shores and to rule out hybridization zones between the two species. Although a large scale survey would clarify the distribution of *Patella* spp described in this work, I did not find (morphological or genetic-based) evidence of the presence of *Pat. aspera* along Moroccan shores, in contrast to the widespread presence of *Pat. ulyssiponensis*, *Pat. depressa* and *Pat. rustica*.

Generally, a cline of increasing species richness can be observed from the poles towards lower latitudes (Gray, 2002; Macpherson, 2002; Brown, 2014 but see Chaudhary *et al.*, 2016). However, no clear latitudinal gradient in taxon richness was observed along the study area. Nevertheless, the greater than average taxon richness at all Western Sahara locations (sites TF, BJ, LB and DK >46 species/site) matches previous studies contrasting the greater biodiversity and species richness of the Western Sahara compared to Moroccan shores (Ramos *et al.*, 2015). Evidence suggests that environmental factors such as productivity, temperature, nutrients and sediments play dominant roles in determining patterns of large scale species richness, through greater supply of energy (Gray, 2002; Macpherson, 2002). However, no single theory alone successfully explains the latitudinal gradient of increasing species richness towards lower latitudes (Schemske & Mittelbach, 2017; Schluter & Pennell, 2017). Both evolutionary processes (e.g. different rates of speciation and extinction of species in the tropics and in temperate regions, see Hillebrand, 2004; Jablonski *et al.*, 2006) and ecological processes (e.g. the influence of habitat heterogeneity, reviewed in Schemske & Mittelbach, 2017) have been identified as the presumed drivers of this taxonomic pattern. Additionally, anthropogenic stressors such as pollution and environmental contamination strongly influence local patterns of species richness (Leopardas *et al.*, 2016). A recent study performed along the Moroccan

coast showed that the diversity of macroalgae was lower closer to the large urban centre of Essaouira, which is affected by untreated sewage, than farther away from this populated area (Sabri *et al.*, 2017). Pollution from urban centres, which are larger and more widespread along the northwest Moroccan coast, could help explain the overall lower taxon richness along the Moroccan coast (sites LR, RB, SB, EB, ES, IM, ML and TT) compared to the Western Sahara (sites TF, BJ, LB and DK). However, such large scale effect on species richness might seem unlikely as the adverse effect of pollution has only been reported at small, local scales rather than at large, regional ones (see Leopardas *et al.*, 2016; Sabri *et al.*, 2017).

Climate change is expected to further alter species richness and community composition worldwide (Molinos *et al.*, 2016; Woodworth-Jefcoats *et al.*, 2016). The CCS is a temperate zone bordered by the Mediterranean Sea, the tropical West African shores and the cool temperate northeastern Atlantic shores (Spalding *et al.*, 2007), and represents a biogeographical transition where several warm and coldwater species meet and reach their northern or southern range limits (e.g. Lima *et al.*, 2007a; Lourenço *et al.*, 2012; Nicastro *et al.*, 2013; Neiva *et al.*, 2015). In particular, Moroccan and Western Saharan shores have experienced a warming of sea surface temperature of 0.02–0.30 and -0.02–0.29 ^{o}C/decade over the last 30 years, respectively (Lima & Wethey, 2012), and are characterized by distributional shifts linked to climatic changes (Nicastro *et al.*, 2013; Lourenço *et al.*, 2016). For instance, the brown alga *Fucus guiryi* has disappeared from large stretches of Moroccan shores and contracted its distribution, most likely as a result of increasing SSTs (Lourenço *et al.*, 2016, see chapter 3). Due to the scarcity of continuous historical data, it remains unknown whether the new southern limits described in this chapter reflect novel range expansions or simply a lack of updated detailed information on species distributions. Nonetheless, it can be anticipated that distributional changes will continue to occur in the future along these northern African shores. Whether species will adapt fast enough to a changing world and shift their environmental niche to track climatic changes remains a critical question (Visser, 2008; Bellard *et al.*, 2012). As a consequence, there is an urgent need to detect areas that, by acting as climatic refugia, allow species to persist under generally unsuitable environmental conditions. Recently, upwelling areas in my study area have been described as climatic buffers that allow species to persist under warming conditions (Hu & Guillemin, 2016; Lourenço *et al.*, 2016). The multiple upwelling cells of the CCS and the large extension of coast that they permanently or intermittently affect (Marcello *et al.*, 2011; Benazzouz *et al.*, 2014; Sousa *et al.*, 2017a) have therefore the potential to act as safe havens for other intertidal species. Although this chapter provides further evidence on the role of upwelling as a

climatic refugium for the brown alga *B. bifurcata*, the refugium role might have been underestimated. For example, no climatic refugia is detected in this chapter for the brown alga *F. guiryi*, although a more thorough survey in chapter 3 clearly demonstrates the role of upwelling in preserving the species. Increasing the number of sampling sites and the frequency of future surveys will help unravelling unexpected climatic refugia for other intertidal species.

A number of studies has focused on understanding how upwelling intensity is changing and will change worldwide in a context of climate change (McGregor *et al.*, 2007; Bakun *et al.*, 2010; Wang *et al.*, 2015; Sousa *et al.*, 2017a). Regardless of the expected increase in upwelling intensity in northern Africa (Wang *et al.*, 2015 but see also Sousa *et al.*, 2017a), which could counterbalance the negative effects associated with climate change (e.g. mass mortality), warming is expected to continue to increase (Collins *et al.*, 2013; IPCC, 2014), threatening intertidal species that already live close to their thermal tolerance limits. This study can therefore serve as a baseline for future studies investigating how intertidal benthic communities shift in one of the most important upwelling systems in the world.

2.4.3 Final remarks

A single biogeographic region has been described for the Atlantic coast of Morocco and Western Sahara together: the Saharan upwelling ecoregion (Spalding *et al.*, 2007; between ~36° N and 21° N). However, the environmental data presented in this chapter suggest further substructure with northern, central and southern partitions. In fact, considering the great extent of this coast and how different regions are differently affected by upwelling, substructure could be anticipated as has been observed for other upwelling systems. Multiple biogeographical regions are described from the California, Humboldt and Benguela Current systems, each of which covers a similar latitudinal coverage of the coast of ~15° (e.g. California Current system: Montereyan, southern California and Ensenadian regions, Blanchette *et al.*, 2008). Nonetheless, the CCS lacks sharp upwelling-driven biogeographical breaks. For example, in contrast to clear northern/southern upwelling/non-upwelling-influenced shores in the California Current system (reviewed in Blanchette *et al.*, 2009), the CCS is characterized by successive stretches of coast encompassed by upwelling cells adjacent to areas that are seldom affected by cold upwelled waters (Marcello *et al.*, 2011; Benazzouz *et al.*, 2014). Under favourable winds, upwelling filaments extend through hundreds of kilometres intermittently delivering colder upwelled waters to non-upwelling areas (Marcello *et al.*, 2011;

Benazzouz *et al.*, 2014). This alongshore spread of upwelled waters may therefore homogenize the influence of upwelling, erasing any sharp compositional breaks in taxa and leading to less striking spatial changes or geographic structure in benthic community composition along northern Africa, as described in this chapter.

Additionally, this work greatly advances our knowledge of the distribution of numerous intertidal benthic species inhabiting northern African shores, particularly along the southern Morocco and Western Sahara, which have remained largely under-explored. The southern range of some of the species analysed in this chapter have remained unclear for at least the past 40 years (e.g. *Ch. montagui* and *Ch. stellatus*, Southward, 1976; Crisp *et al.*, 1981) and the catalogues describing the distribution of algae date from 2001–2004 (Benhissoune *et al.*, 2001, 2002a, 2002b, 2003; John *et al.*, 2004). Taking into account the growing number of studies reporting new species from Moroccan shores (e.g. Sabour *et al.*, 2013; Hassoun *et al.*, 2014, 2016; Belattmania *et al.*, 2017) and describing distributional shifts of intertidal species driven by climate change (Nicastro *et al.*, 2013), there is an urgent need to provide an update on the distribution of intertidal benthic species. While these results provide information on more than 180 species, future research should try to address not only other functional groups that were not included in this study (e.g. carnivores) but also cover the extension of coast of the Western Sahara that was not surveyed here (from Dakhla to Cape Blanc), which is characterized by marked environmental breaks (Marcello *et al.*, 2011; Benazzouz *et al.*, 2014) and might be expected to exhibit changes in species distributions and community structure.

CHAPTER 3

The effect of upwelling areas in the distribution and genetic diversity of the marine macroalga *Fucus guiryi*

F. guiryi interspersed with the black lichen *Lichina pygmaea* in El Beddouza, Morocco.

3.1 INTRODUCTION

Climatic changes affect biogeographic patterns of a wide variety of taxa, causing range shifts and population extinctions (e.g. Nicastro *et al.*, 2013). As a result, the importance of refugia is increasingly recognized (Ashcroft, 2010; Keppel *et al.*, 2012; Gavin *et al.*, 2014). In the past, the term refugium was used to refer to limited spatial locations to which species retreated and where they persisted throughout the Last Glacial Maximum (LGM), subsequently expanding to surrounding areas when climatic conditions improved (Ashcroft, 2010; Keppel *et al.*, 2012; Gavin *et al.*, 2014). Several regions have been identified as glacial refugia for both terrestrial (e.g. Beatty & Provan, 2011; Schmitt & Varga, 2012; Meiri *et al.*, 2013) and marine species (reviewed in Maggs *et al.*, 2008). These areas, while often fragmented at present, were responsible for preserving in the past not only species as distinct biological units, but also their pool of genetic diversity (e.g. Neiva *et al.*, 2014, 2015). Indeed, as a consequence, the low latitude distributional edges of a number of species harbour higher levels of genetic diversity than populations inhabiting central regions (Diekmann & Serrão, 2012; Assis *et al.*, 2013).

Contemporary refugia provide favourable environmental conditions that facilitate species persistence in regions threatened by climate change (Keppel *et al.*, 2012). Analogous to past glacial refugia (e.g. Albaina *et al.*, 2012; Meiri *et al.*, 2013), current refugia from warming have great ecological and evolutionary importance and are safe havens that contribute to the maintenance of regional and global biodiversity by promoting biodiversity conservation and allowing species to avoid local extinction (Riegl & Piller, 2003; Lima *et al.*, 2016; Morelli *et al.*, 2016).

Coastal upwelling delivers cold, nutrient-rich water from the ocean's depths to the surface into the intertidal and nearshore region (Narayan *et al.*, 2010; Wang *et al.*, 2015). Depending on the intensity and duration of upwelling events, areas affected by upwelled waters are exposed to ecological conditions that are temporarily or permanently distinct from those of surrounding regions. Most importantly, the vigour of coastal upwelling is globally increasing as a result of changes in greenhouse gas concentrations, land-sea pressure differences and wind patterns (Bakun *et al.*, 2010; Narayan *et al.*, 2010). The delivery of cold waters by upwelling events is not directly correlated with climate, therefore providing an opportunity for regional decoupling of global warming in refugia, offering insulation from present and projected climatic changes. Although numerous studies have advanced our understanding of the diverse functional roles played by upwelling (e.g. Bosman *et al.*, 1987; Barshis *et al.*, 2011; Rivera *et al.*, 2013), the role of upwelling areas

as refugia in a scenario of global warming has been proposed (Riegl & Piller, 2003; but see Chollett *et al.*, 2010), but remains largely unexplored.

The Iberian and north African Atlantic coastlines are particularly suitable regions for investigating the potential sheltering effect of upwelling. Over the last few decades, sea-surface temperatures (SST) have significantly increased along this coastline, while five interspersed upwelling areas (west coast of Portugal, Strait of Gibraltar, Cape Ghir, Cape Juby, and north of Cape Blanc) show lower or non-significant temperature increase and rather, in some cases, cooling trends (Lima & Wethey, 2012), offering natural experimental replicates. Importantly, these shores form a biogeographical transition region where several warm and coldwater species reach their northern or southern range limits (Lima *et al.*, 2007a; Lourenço *et al.*, 2012; Rubal *et al.*, 2013), therefore offering the opportunity for early identification of distributional expansions and contractions (Lima *et al.*, 2006, 2007a, 2007b; Nicastro *et al.*, 2013; Neiva *et al.*, 2015).

Here, I investigate whether upwelled waters show evidence of acting as refugia in a region heavily affected by recent climatic changes. To do so, I focus on the intertidal canopy-forming brown alga *Fucus guiryi* (Zardi *et al.*, 2011b) and compare its recent biogeographic dynamics and population genetic diversity and structure with the geographic distribution of upwelling areas and warming rates over the last three decades.

3.2 MATERIAL AND METHODS

3.2.1 Model species

Macroalgae of the genus *Fucus* are a dominant feature along temperate to cold North Atlantic intertidal rocky shores. The recently described species *F. guiryi* (previously designated *F. spiralis* var. *platycarpus* and also referred to as *F. spiralis* Low), can be distinguished from its congeners by the presence of sterile rims around the hermaphroditic receptacles, monopodial branching and the absence of air bladders, in addition to physiological and genetic differences (Billard *et al.*, 2010; Zardi *et al.*, 2011b). *Fucus guiryi* is distributed throughout Morocco, the Canary Islands, the Iberian Peninsula and France, northwards to Great Britain and Ireland (reviewed in Zardi *et al.*, 2011b). South of northern Portugal, *F. guiryi* is the only *Fucus* species present on intertidal shores (Ladah *et al.*, 2003 then reported as *F. spiralis*; Zardi *et al.*, 2011b, 2015b).

3.2.2 Study sites

Field work was conducted along the coastlines of southwest (SW) Iberia, Mediterranean and Atlantic Morocco and Western Sahara, which are affected by distinct upwelling cells: the Atlantic Iberian (from the Canary Current (upwelling) System (CCS), affecting SW Portuguese shores; Relvas & Barton, 2002), the northwest (NW) African (also from the CCS, affecting Atlantic Morocco and Western Sahara; Marcello *et al.*, 2011; Benazzouz *et al.*, 2014) and the Strait of Gibraltar (between the Atlantic and Mediterranean shores of Morocco; Stanichny, 2005). Although no permanent barriers exist to delimit these upwelling areas, and the seasonality and intensity of upwelling vary in their timing and across latitudes, upwelling phenomena can be detected through low sea surface temperatures (SST) or high upwelling indices (Marcello *et al.*, 2011; Benazzouz *et al.*, 2014). The distinct upwelling regions comprise five main centres located at: 42–37° N (PT in Fig. 3.1, Portuguese coast; CCS), 35.8–35.9° N, 6–5° W (GB, Strait of Gibraltar upwelling cell); 31–32° N (GH, north of Cap Ghir; CCS), 26.5°–28° N (JB, south of Cap Juby; CCS) and 21–25° N (BL, north of Cap Blanc; CCS). Adjacent surrounding areas experience intermittent effects of upwelling that decrease while moving away from these centres (Marcello *et al.*, 2011; Benazzouz *et al.*, 2014).

Monthly averaged SST data depicting upwelling seasonality during 2012 with a 4 km resolution were retrieved from the Moderate Resolution Imaging Spectroradiometer-Aqua (MODISAqua) dataset available from the National Aeronautics Space Administration

(NASA) Goddard Earth Sciences (GES) Data and Information Services Centre (DISC) and used to illustrate the different upwelling centres along the study area (Fig. 3.1). Visualization was performed using Giovanni, a web-based application developed by the GES DISC.

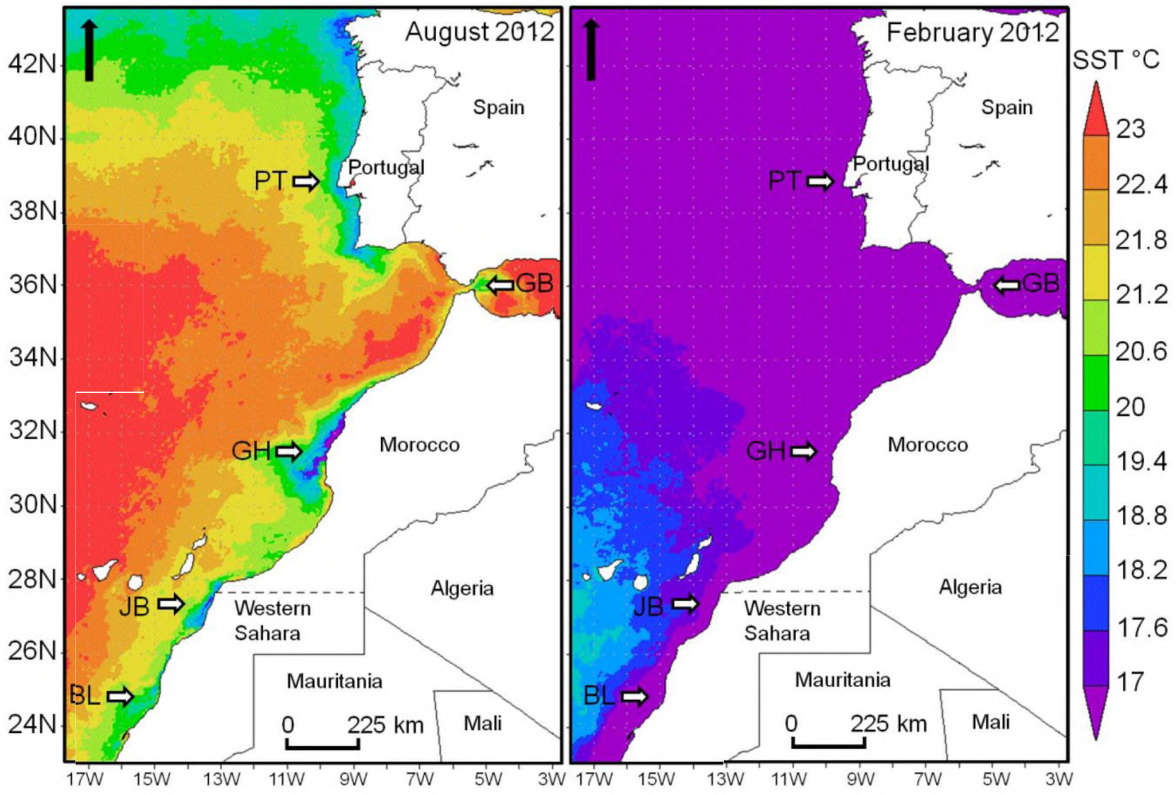

Figure 3.1 – Sea surface temperature (SST) illustrating the five upwelling centres during high (August 2012) and low intensity (February 2012) periods. PT, Portuguese coast; GB, Strait of Gibraltar; GH, north of Cape Ghir; JB, south of Cape Juby and BL, north of Cape Blanc. Longitude and latitude are represented by horizontal and vertical axes, respectively. Gradient coloration corresponds to sea surface temperature variation. All values below 17 °C are shown in purple, whereas 23 °C or higher temperatures are shown in red.

3.2.3 Distribution and southern range contraction of *Fucus guiryi*

To assess range contraction, the distribution of *F. guiryi* along the Mediterranean and Atlantic Iberian and African coasts was investigated through extensive field surveys on rocky intertidal shores during low spring tides between April 2012 and October 2014 (Table 3.1) and compared with historical data described in the literature. During the surveys, locations where the presence of *F. guiryi* was reported in the past were revisited and additional locations for which no data were available were explored; these locations were selected based on habitat preferences of *F. guiryi* (marine intertidal, rocky shores, expose to moderately wave exposed areas, Zardi *et al.*, 2011b, 2015b). Thirty-nine

locations spreading along >2600 km of coastline were surveyed. Two observers assessed the presence or absence of *F. guiryi* by performing approximately 60 min searches across all microhabitats. An additional four non-surveyed locations (Camarinal, Guadalmesi and Punta Carnero; Calaburras R. Bermejo pers. comm.) were retrieved from Bermejo *et al.* (2015), giving a total of 43 study sites.

Historical data on the distribution of *F. guiryi* were assembled from an exhaustive literature review. Literature and information from herbarium collections reporting geographical distribution of *F. spiralis*, *F. spiralis* var. *platycarpus* or mentioning *F. spiralis* Low were considered as reporting *F. guiryi* when populations were described from south of Minho (northern Portugal, see section 3.2.1 Model species). Published literature was screened up until December 2014 using Google Scholar and the ISI Web of Knowledge with the following keywords individually or in combination: Fucus, spiralis, platycarpus, Morocco, Maroc, Sahara, distribution, Atlantic, Mediterranean, Fucales. AlgaeBase (Guiry & Guiry, 2014) was also consulted and distribution records for *F. spiralis* in northern Africa were considered.

Table 3.1 – List of sampling locations along Iberian Peninsula (Portugal, Atlantic and Mediterranean Spain) and northern Africa (Mediterranean and Atlantic Morocco and Western Sahara). Med. refers to Mediterranean, * depicts sampling sites for genetic analyses, *n* refers to sampling size for genetic analyses.

Region	Location	Code	Coordinates	*n*
Portugal	V. N. Milfontes	MF	37°43'09.81"N; 08°47'30.16"W	-
Portugal	Amoreira	AM	37°20'57.30"N; 08°50'49.89"W	-
Portugal	Castelejo	CT	37°06'08.09"N; 08°56'44.99"W	-
Portugal	Arrifes	AB	37°04'34.05"N; 08°16'37.68"W	-
Portugal	Santa Eulália	SE	37°05'12.22"N; 08°12'58.82"W	-
Portugal	Ilha do Farol	FL	36°58'28.87"N; 07°52'02.05"W	-
Portugal	V. R. S. António	VR	37°10'13.57"N; 07°24'09.59"W	-
Atlantic Spain	Cádiz	CD	36°27'58.78"N; 06°15'25.28"W	-
Atlantic Spain	Punta Camarinal[1]	CM	36°05'04.32"N; 05°48'09.48"W	-
Strait of Gibraltar	Paloma Baja	PB*	36°03'41.35"N; 05°43'24.69"W	5
Strait of Gibraltar	Guadalmesi[1]	GM	36°01'45.08"N; 05°32'36.56"W	-
Strait of Gibraltar	Punta Carnero[1]	PC	36°04'39.91"N; 05°25'30.67"W	-
Med. Spain	Torreguadiaro	TG	36°18'00.19"N; 05°16'04.71"W	-
Med. Spain	Calaburras[1]	CL	36°29'28.63"N; 04°41'32.99"W	-
Med. Spain	La Araña	LA	36°42'40.21"N; 04°19'37.96"W	-
Med. Spain	Almuñecar	AL	36°43'39.94"N; 03°41'39.76"W	-
Med. Morocco	Punta Negri	PN	35°16'46.33"N; 03°08'06.63"W	-
Med. Morocco	Punta Afrau	PA	35°12'16.86"N; 03°27'10.68"W	-
Med. Morocco	Cala Iris	CI	35°08'55.02"N; 04°21'38.35"W	-
Med. Morocco	Eddalya	ED*	35°54'51.49"N; 05°27'36.45"W	33
Med. Morocco	Ksar Sghir	KS*	35°49'54.66"N; 05°36'09.96"W	48

Atlantic Morocco	Assilah	AS	35°29'48.95"N; 06°01'11.47"W	-
Atlantic Morocco	Larache	LR	35°11'48.14"N; 06°09'30.61"W	-
Atlantic Morocco	Rabat	RB	34°01'57.26"N; 06°50'27.96"W	-
Atlantic Morocco	Val d'Or	VD*	33°54'09.16"N; 06°59'56.80"W	47
Atlantic Morocco	Casablanca	CB*	33°39'07.22"N; 07°29'03.11"W	40
Atlantic Morocco	Sidi Bouzid	SB*	33°13'06.11"N; 08°34'23.19"W	37
Atlantic Morocco	Oualidia	OL*	32°44'12.23"N; 09°02'44.61"W	45
Atlantic Morocco	El Beddouza	EB*	32°32'42.33"N; 09°16'55.34"W	48
Atlantic Morocco	Souiria	SO	32°03'07.94"N; 09°20'28.37"W	-
Atlantic Morocco	Essaouira	ES*	31°30'42.78"N; 09°46'24.31"W	47
Atlantic Morocco	Imsouane	IM*	30°50'24.43"N; 09°49'21.92"W	22
Atlantic Morocco	Tamri - Cap Ghir	TM	30°37'31.48"N; 09°51'11.51"W	-
Atlantic Morocco	Tamraght-Agadir	TH	30°30'24.03"N; 09°41'15.69"W	-
Atlantic Morocco	Anza-Agadir	AZ	30°26'27.22"N; 09°39'19.99"W	-
Atlantic Morocco	Aglou	AG	29°48'16.15"N; 09°50'08.69"W	-
Atlantic Morocco	Mirleft	ML	29°35'06.58"N; 10°02'50.78"W	-
Atlantic Morocco	Tan Tan plage	TT	28°30'05.58"N; 11°20'06.38"W	-
Atlantic Morocco	Chbika	CH	28°17'42.58"N; 11°32'33.07"W	-
Atlantic Morocco	Tarfaya	TF*	27°45'32.35"N; 13°02'42.15"W	39
Western Sahara	Boujdour[2]	BJ	26°07'38.95"N; 14°30'02.38"W	-
Western Sahara	Nouifed[2]	LB*	24°54'30.29"N; 14°49'45.36"W	48
Western Sahara	Dakhla[2]	DK*	23°46'06.97"N; 15°55'32.16"W	36

[1] Data obtained from Bermejo *et al.* 2015 and Bermejo pers. comm.
[2] No clear historic information about these locations could be retrieved

3.2.4 Sea surface temperature rate of change

A subset of 40 points was used to investigate rates of change of coastal SST (warming/cooling data, °C/decade from January 1982 to December 2011) across the study area. Average rate of change was calculated as the slope of the linear regression of seasonal de-trended SSTs versus time. Data were obtained from the Worldwide Coastal Warming Assessment webpage (http://www.coastalwarming.com/data.html; Lima & Wethey, 2012) and the selected points were located immediately offshore of each surveyed site with the exception of two groups of sites that were very close together, for which only one point was available.

Data were analysed by one-way ANOVA in STATISTICA 7.1 (StatSoft, 2005) under the null hypothesis of no difference between sites where *F. guiryi* was or was not recorded. The analyses consisted of presence (2 levels, presence or absence) as a fixed factor and rate of SST change as the dependent variable.

3.2.5 Cover occupancy

Visual estimates of cover occupancy of *F. guiryi* along upper intertidal shores were used to investigate the extent of this species at each surveyed site (sites as in Table 3.1; adapted from Bermejo *et al.*, 2015). The visual inspection was based on an occupancy scale ranging from 0 to 5: 0–no cover/species is absent; 1–negligible cover/ rare scattered individuals; 2–little cover/ abundant scattered individuals; 3–intermediate cover/ abundant patches; 4–large cover/ almost continuous belts; 5–massive cover/ continuous belts. Cover occupancy from the four non-surveyed locations were retrieved from Bermejo *et al.* (2015).

3.2.6 Genetic data

Blade tissue was collected from distinct individuals between April 2012 and October 2014 from 13 locations (n=22–48, except PB n=5, Table 3.1), preserved in silica gel and used to investigate the genetic structure of *F. guiryi* in Morocco and Western Sahara. Four additional populations from central and southern Portugal (ER, LZ, AR, CT; n=48 each) analysed by Zardi *et al.* (2015b) were included to frame the genetic diversity of this region within the species' overall genetic structure. North of these sites, genetic structure becomes influenced by hybridization with sympatric sister species (*F. vesiculosus* and *F. spiralis*, Zardi *et al.*, 2011b, 2015b). Total genomic DNA was extracted using the CTAB method following Hoarau *et al.* (2007). Nine microsatellite loci, L20, L58, L38, L94, L78 (Engel *et al.*, 2003), F26II (Wallace *et al.*, 2004), F9, F42 and F58 (Coyer *et al.*, 2009) were amplified as in Perrin *et al.* (2007; for L20, L58, L38, L94, L78) and modified from Wallace *et al.* (2004; for F26II) and Coyer *et al.* (2009; for F9, F42 and F58). PCR products were run in 2 % agarose gel during an electrophoresis of about 30 min at 120 V and 400 A. Genotyping was performed following Perrin *et al.* (2007; for L20, L58, L38, L94, L78) and modified from Wallace *et al.* (2004; for F26II) and Coyer *et al.* (2009; for F9, F42 and F58) in an ABI PRISM 3130 genetic analyser (Applied Biosystems). Four multiplex designs were used during genotyping process: run 1 included L20, L38 and L94 loci; run 2 included L58 and L78 loci; run 3 included F42 and F26II while run 4 included F9 and F58 loci.

3.2.6.1 Genetic analyses

Allele sizes were scored using STRand 2.4.59 software (http://www.vgl.ucdavis.edu/informatics/STRand), binned with the Ruby 1.9.3 package tandem 1.09 (Matschiner & Salzburger, 2009) and manually reviewed for ambiguities. MICRO-CHECKER 2.2.3 (van Oosterhout *et al.*, 2004) was used to test for stuttering, null alleles and large allele dropout at each locus and for individuals collected at the same location (hereafter referred to as population). Two datasets were tested: 1) including all nine loci and 2) excluding F58 due to high amount of missing data. All loci had less than 5% of missing data with the exception of F58 (13.5%). Because results were similar between datasets, the dataset with all loci was used in the following analyses.

For each population, observed (H_O) and expected (H_E) heterozygosity and inbreeding coefficients (F_{IS}; Weir & Cockerham, 1984) were estimated, and deviations from Hardy-Weinberg equilibrium were tested for significance with 10 000 permutations using GENETIX 4.05 (Belkhir *et al.*, 2004). Allelic richness (Â) was estimated for each population and standardized to the two smallest sample sizes (n=5 and n=22), using GENETIX 4.05 and standArich 1.02 package (http://www.ccmar.ualg.pt/maree/software.php?soft=sarich) in R (R Core Team, 2012). Missing data were replaced by the most common alleles when calculating standardized Â. Allelic frequencies for each population and marker were plotted using standArich 1.02, depicting unique private alleles at each sampling site. Genetic differentiation between pairs of populations was estimated as F_{ST} (Weir & Cockerham, 1984; and its p-values) using GENETIX 4.05 and as Jost's D (Jost, 2008) using the R package DEMEtics 0.8.7 (Gerlach *et al.*, 2010), with significance tested using 1000 bootstraps and corrected by the q-value for multiple comparisons with qvalue 2.0.0 package in R (R Core Team, 2012). STRUCTURE 2.3.4. software (Pritchard *et al.*, 2000) was run to infer the presence of distinct clusters of populations. The analysis was run without prior information on populations, assuming an admixture model and correlated allele frequencies. The number of possible clusters (K) assessed was 1 to 18 (maximum number of populations plus one) and 11 independent runs with 100 000 Markov Chain Monte Carlo (MCMC) iterations and 50 000 burn-in were performed for each K. STRUCTURE HARVESTER 0.6.94 (Earl & von Holdt, 2012) estimated the most probable number of K calculating ΔK as in Evanno *et al.* (2005). CLUMPP 1.1.2 software (Jakobsson & Rosenberg, 2007) was used to find the consensus of the 11 replicated runs of the selected K. The optimal alignment matrix across replicates was plotted with Ruby 1.9.3 package Bar Plotter 1.0 (http://evolution.unibas.ch/salzburger/software.htm). A discriminant analysis of principal

components (DAPC) based on the matrix of individual genotypes with nine microsatellite loci was performed with adegenet 1.4.2 package (Jombart, 2008) in R (R Core Team, 2012) to characterize the global genetic variation of the study area. To avoid overfitting of the model by using an excessive number of principal components, the function *optim.a.score* was used and five principal components were retained. DAPC was run with individuals assigned to their prior sampling populations and the function *find.cluster* was subsequently used to determine the number of clusters (K) in the dataset. The chosen number of clusters is the minimum K after which the Bayesian Information Criterion changes by a negligible amount (Jombart *et al.*, 2010). Each individual was then assigned to a single cluster and a new DAPC was run without information of their prior sampling location. A hierarchical analysis of molecular variance (AMOVA) was conducted in Arlequin 3.11 (Excoffier *et al.*, 2005) to evaluate levels of differentiation and investigate population genetic structure, including all sites and running 10 100 permutations. To understand how genetic variation is partitioned between clusters, among populations within clusters and within populations, groups were designated *a priori* based on STRUCTURE 2.3.4 results and each sampled population was incorporated in a single cluster. Lastly, to compare the level of diversity among clusters and within upwelling areas, estimates of H_O and H_E, Â and number of unique alleles were calculated. Populations were sorted into upwelling groups based on their geographical location and proximity to upwelling centres. The upwelling group PT is composed of ER, LZ, AR and CT; GB comprises PB, ED and KS; GH includes VD, CB, SB, OL, EB, ES and IM; JB is composed entirely of TF and BL is constituted by LB and DK (location codes as in Fig. 3.1 and Table 3.1).

3.3 RESULTS

3.3.1 Distribution and southern range contraction of *Fucus guiryi*

Field surveys revealed a considerable change in the southern range limit of *Fucus guiryi* (Fig. 3.2A). From the 43 studied sites, 24 had past species presence/absence records and 19 were novel. Overall, the species was reported at 23 sites. Eight sites had hosted this macroalga, but no longer did so, although suitable rocky intertidal habitat was available. While the species disappeared from only one location from southwestern Iberian shores, the major change in *F. guiryi* range distribution was its disappearance from all Spanish and Moroccan Mediterranean studied locations, except CL. The absence of the species at additional sites not covered by the historical records, along with the study of Bermejo *et al.* (2015) confirmed a marked distributional shift of the species in this region. The northern and southern coasts of Morocco experienced the disappearance of three populations of *F. guiryi*. The coastal locations hosting *F. guiryi* populations were either close to or in the centre of upwelling areas (Fig. 3.2A).

3.3.2 Sea surface temperature rate of change

All sites showed significant (p<0.05) rates of change of sea surface temperature (SST) except SO, ES and LB, which showed the lowest rates of warming in the entire study area and are located near Cape Ghir and Cape Blanc upwelling centres. In fact, cooling was detected at LB (-0.04 ^{o}C/decade), although this was non-significant. The highest warming was in the Mediterranean Sea (PA, 0.32 ^{o}C/decade; Fig. 3.2B). Moreover, sites where *F. guiryi* is absent or has gone extinct showed significantly higher warming rates than sites where the species is currently present (p<0.001).

3.3.3 Cover occupancy

Most of the locations at which the species was present showed negligible or little cover and only one site was characterized by full cover of *F. guiryi* (Fig. 3.2C). Along southwestern Iberia, cover occupancy decreased towards the south from intermediate levels in southwestern Portugal at MF to zero at FL. The populations located in the Strait of Gibraltar area generally had little cover occupancy and the remaining Mediterranean population (CL) showed negligible cover. The northwestern shores of Morocco showed the highest values and variability of cover. From north to south, cover increased from zero

to a maximum at ES (near the centre of upwelling) and decreased again to negligible cover occupancy values at IM. In southern Morocco and Western Sahara, despite being towards the southern distributional limit for the species, the few isolated locations where *F. guiryi* was present had either intermediate (LB and DK) or large cover occupancy (TF) and were all located inside or near centres of upwelling.

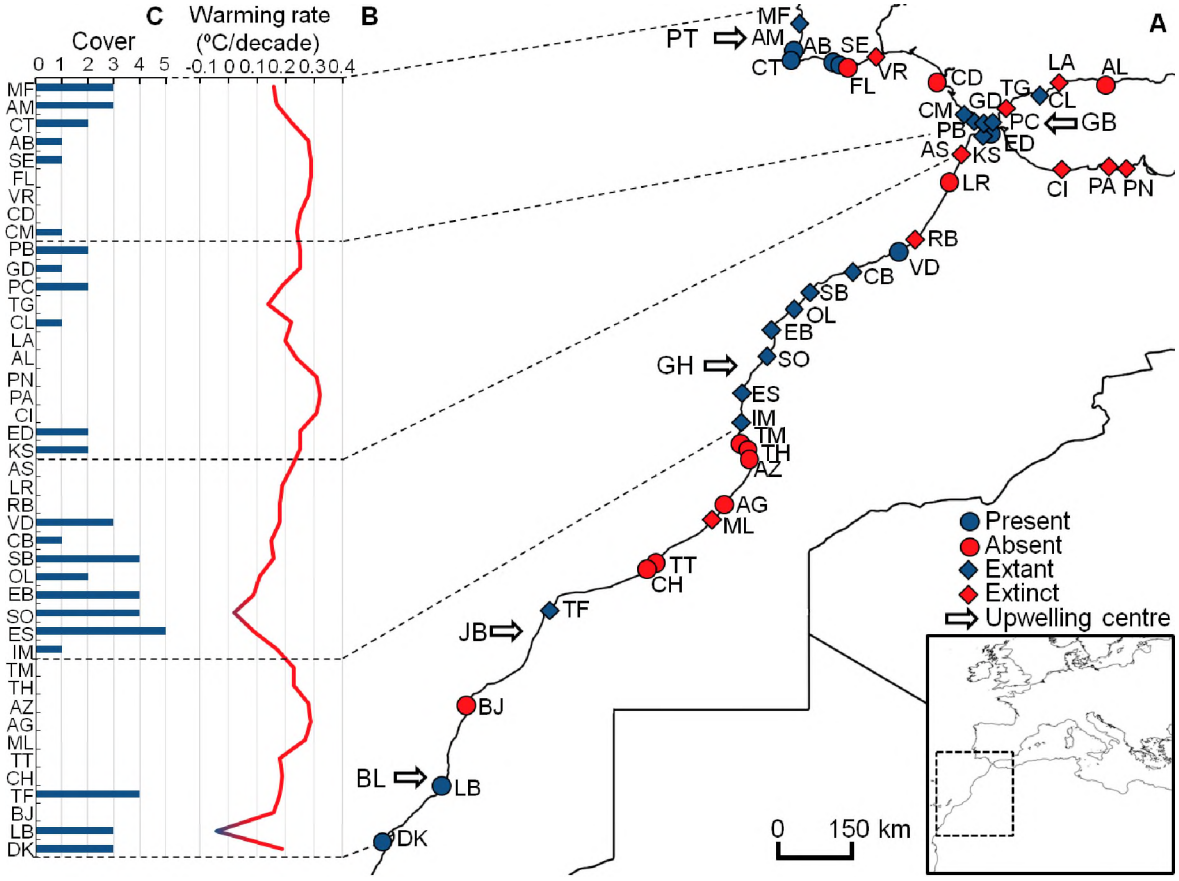

Figure 3.2 – Demography of *F. guiryi* along the study area: A) Range distribution of *F. guiryi*, B) sea surface temperatures (SST) rate of change and C) species cover. Contemporary presence (blue) and absence (red) of *F. guiryi* is based on field surveys (April 2012 to October 2014) and depicted with circles; results compared with published records and herbarium collections are in diamond markers and indicate extinct (red; previously recorded in the literature but absent from present surveys) or extant (blue; recorded in the literature and surveys) populations. Arrows indicate main upwelling centres in the study area: PT, Portuguese coast; GB, Strait of Gibraltar; GH, north of Cape Ghir; JB, south of Cape Juby and BL, north of Cape Blanc. Coastal SST warming/cooling data covered the last three decades (°C/decade; 1982 to 2011; Lima & Wethey, 2012). Red and blue lines of SST rate of change refer to warming and cooling, respectively. Cover occupancy ranges from 0 to 5.

3.3.4 Genetic analyses

The 17 Mediterranean and Atlantic populations included 38 different alleles from 681 individuals. The total number of alleles per locus ranged from 1 to 18 (see Table 3.2). There was no evidence for large allele drop-out at any locus, but potential stuttering and null alleles at a frequency higher than 0.2 were suggested for L20, L94, F26II and F9 by MICRO-CHECKER 2.2.3. All these loci have been used in previous studies (Perrin *et al.*, 2007; Coyer *et al.*, 2011a, 2011b; Zardi *et al.*, 2013, 2015b), some of which also suggested potential null alleles (Perrin *et al.*, 2007). However, because the presence of null alleles was not consistent across populations or loci, except for F26II, this may not reflect real null alleles (Perrin *et al.*, 2007).

Table 3.2 – Allelic diversity at each population of *F. guiryi* and for each locus. Location codes and cluster assignment as in Table 3.1 and Fig. 3.3, respectively.

Population	Cluster	L20	L38	L94	L58	L78	F42	F26II	F9	F58
ER	1	168	188	162	122/124	150	190	367/387/389	181	185
LZ	1	162/168	188	162	122	150	190	367/383/387/389/391	181	185
AR	2	162/168	188/197	162	122	150	190	367/385/387/389	181	185
CT	2	162/168	188/197	162	122	150	190	367/385	181	185
PB	3	150	188	162	122	150	190/193	367/371/385	177	185/187
ED	3	150/171	188	156/162	122	150	193	369/371/383	177	187
KS	3	150	188	162	122	150	193	369/371/373	177	187
VD	4	171/174	188/197	162	122	150	190	371/373/375/383/389	181	185
CB	4	171	188/197	162	122	150	190	371/373/375	181	185
SB	4	171	188	162	122	150	190	371/373/375/423/425	181	185
OL	4	171	188	162	122	150	190	369/371/373	181	185
EB	4	171	188	162	122	150	190	371/373/375	181	185
ES	4	135/168/171	188	162	122	150	190/193	371/375/377/393/395/397	181	185
IM	4	171	188	162	122	150	190	393/397	181	185
TF	1	168/171	188	162	122	150	190	349/371/373/385/387	181/211	185
LB	2	162	188	162	122	150	190	369	181	185
DK	1	168/171	188	162	122	150	190	371/385/389/391/405	181	185

Moreover, the selfing hermaphroditic reproductive strategy of *F. guiryi* (Perrin *et al.*, 2007; then named *F. spiralis*) likely causes an excess of homozygotes, by unequal transmission of different alleles and lack of outcrossing; apparent null alleles are therefore likely. Inbreeding and localized recruitment result in apparent high frequencies of null alleles (e.g. Costantini *et al.*, 2007). These considerations justify the inclusion of all loci in further analyses. Population genetic diversity estimated as allelic richness standardized to the smallest populations $\hat{A}_{(5;\ 22)}$ varied between 1.0 and 1.4 or 1.8, and one population (LB) was monomorphic at all loci. Eleven unique alleles were present over seven populations (Table 3.3). While ER, ED, VD and DK presented one unique allele each, SB and TF comprised two, and three unique alleles were exclusive to ES. Gene diversity levels estimated as expected heterozygosities (H_E) were always low (0.000–0.189). Observed heterozygosities (H_O) were significantly lower than expected, resulting in a marked heterozygosity deficit ($0.888 < F_{IS} < 1$; $p<0.001$).

Table 3.3 – Genetic analyses of *F. guiryi* populations along southern Iberia and northern Africa including *n*, number of individuals per population; H_E, expected heterozygosity; H_O, observed heterozygosity; Â, allelic richness represented by mean number of alleles per locus per population; Â(n) allelic richness standardized to the smallest sample size; UA, unique alleles; F_{IS}, inbreeding coefficient. Location codes as in Table 3.1. ER, LZ, AR and CT were retrieved from Zardi *et al.* (2015b).

Population	*n*	H_E	H_O	Â	$\hat{A}_{(5)}$	$\hat{A}_{(22)}$	UA	F_{IS}
ER	47	0.063	0.007	1.333	1.111	1.267	1	0.888
LZ	48	0.104	0.000	1.556	1.244	1.378	0	1.000
AR	43	0.112	0.005	1.556	1.222	1.467	0	0.955
CT	48	0.047	0.005	1.333	1.000	1.200	0	0.903
PB	5	0.178	0.000	1.444	1.444	-	0	1.000
ED	33	0.148	0.007	1.444	1.311	1.444	1	0.952
KS	48	0.038	0.000	1.222	1.089	1.156	0	1.000
VD	47	0.189	0.000	1.667	1.422	1.644	1	1.000
CB	40	0.039	0.000	1.333	1.111	1.267	0	1.000
SB	37	0.067	0.003	1.444	1.178	1.356	2	0.956
OL	45	0.022	0.000	1.222	1.022	1.200	0	1.000
EB	48	0.043	0.000	1.222	1.089	1.156	0	1.000
ES	47	0.148	0.000	1.889	1.378	1.800	3	1.000
IM	22	0.054	0.000	1.111	1.111	1.111	0	1.000
TF	39	0.189	0.000	1.667	1.444	1.600	2	1.000
LB	48	0.000	0.000	1.000	1.000	1.000	0	1.000
DK	36	0.100	0.000	1.556	1.200	1.489	1	1.000

Most of the genetic structure observed between populations and regions was due to differences at loci L20, F26II, F9 and F58. Moreover, locus L78 was fixed in all populations. F_{ST} values ranging from 0.087 to 0.965 were significant (p<0.005) for all pairwise comparisons and supported genetic subdivisions (Table 3.4). Jost's D ranged from 0.006 to 0.698 and depicted similarly significant (p<0.01) genetic differentiation (Table 3.4).

Table 3.4 – Pairwise F_{ST} (above) and Jost's D (below) comparisons of *F. guiryi* populations along southern Iberia and northern Africa. All *p*-values of F_{ST} and Jost's D were corrected and significant ($p<0.005$ and $p<0.01$, respectively). Location codes as in Table 3.1.

	ER	LZ	AR	CT	PB	ED	KS	VD	CB	SB	OL	EB	ES	IM	TF	LB	DK
ER	-	0.087	0.673	0.819	0.788	0.833	0.908	0.525	0.765	0.703	0.804	0.759	0.489	0.725	0.417	0.858	0.349
LZ	0.020	-	0.603	0.741	0.703	0.793	0.870	0.443	0.666	0.600	0.706	0.664	0.398	0.608	0.345	0.743	0.215
AR	0.241	0.242	-	0.440	0.754	0.817	0.887	0.432	0.761	0.719	0.795	0.766	0.600	0.720	0.548	0.796	0.627
CT	0.307	0.290	0.092	-	0.860	0.871	0.934	0.561	0.862	0.822	0.889	0.858	0.707	0.842	0.654	0.891	0.768
PB	0.334	0.348	0.485	0.432	-	0.515	0.633	0.603	0.846	0.787	0.888	0.844	0.622	0.794	0.527	0.953	0.715
ED	0.590	0.589	0.698	0.691	0.282	-	0.599	0.706	0.806	0.786	0.846	0.826	0.712	0.781	0.687	0.891	0.781
KS	0.556	0.556	0.664	0.657	0.148	0.160	-	0.809	0.919	0.906	0.942	0.924	0.824	0.921	0.802	0.965	0.880
VD	0.234	0.219	0.247	0.246	0.442	0.522	0.577	-	0.411	0.336	0.442	0.383	0.257	0.365	0.364	0.659	0.348
CB	0.222	0.222	0.328	0.320	0.370	0.401	0.444	0.151	-	0.488	0.657	0.574	0.390	0.590	0.489	0.920	0.626
SB	0.222	0.222	0.331	0.323	0.402	0.471	0.542	0.140	0.096	-	0.577	0.437	0.224	0.430	0.422	0.863	0.544
OL	0.222	0.222	0.331	0.323	0.403	0.471	0.519	0.141	0.080	0.101	-	0.096	0.470	0.681	0.515	0.950	0.683
EB	0.222	0.222	0.331	0.323	0.406	0.478	0.528	0.125	0.088	0.086	0.006	-	0.351	0.563	0.474	0.902	0.626
ES	0.189	0.188	0.310	0.322	0.386	0.465	0.527	0.120	0.112	0.073	0.127	0.097	-	0.305	0.301	0.688	0.346
IM	0.222	0.222	0.331	0.323	0.406	0.480	0.556	0.173	0.111	0.111	0.111	0.111	0.112	-	0.416	0.918	0.559
TF	0.173	0.176	0.260	0.280	0.339	0.517	0.544	0.232	0.185	0.191	0.169	0.169	0.167	0.194	-	0.682	0.318
LB	0.222	0.204	0.247	0.213	0.407	0.531	0.553	0.264	0.222	0.222	0.219	0.222	0.224	0.222	0.261	-	0.796
DK	0.084	0.066	0.259	0.307	0.399	0.543	0.551	0.149	0.175	0.179	0.179	0.179	0.147	0.179	0.146	0.222	-

Bayesian admixture analyses implemented in STRUCTURE 2.3.4 revealed K=4 defined clusters, corresponding to 1) central Portugal (ER, LZ), southern Morocco (TF) and Western Sahara (DK), 2) southern Portugal (AR, CT) and Western Sahara (LB), 3) Strait of Gibraltar (PB, ED, KS) and 4) northwestern and western Morocco (VD, CB, SB, OL, EB, ES, IM; Fig. 3.3A). Three populations (VD, ES and TF) showed high levels of admixture between two clusters (59 and 38% of clusters 4 and 1, respectively for VD; 69 and 22% of clusters 4 and 1 for ES and 52 and 42% of clusters 1 and 4 for TF).

DAPC confirmed the above results, suggesting four distinct groups and highlighting a strong differentiation between Strait of Gibraltar and the remaining clusters (Fig. 3.3B, Fig. A5-A6 in Appendix). The proportion of overall correct assignment of individuals to their prior populations was very high (0.77). The posterior assignment of individuals into each cluster was similar to the STRUCTURE 2.3.4 results. Cluster 1 was widespread along the entire study area, covering central and southern Portugal, Strait of Gibraltar, Morocco and Western Sahara (total of nine locations). Cluster 2 was present in central and south Portugal and Western Sahara. In contrast, clusters 3 and 4 were exclusive to the Strait of Gibraltar or Morocco and Western Sahara, respectively, and were not found outside of these upwelling areas (Fig. 3.3C).

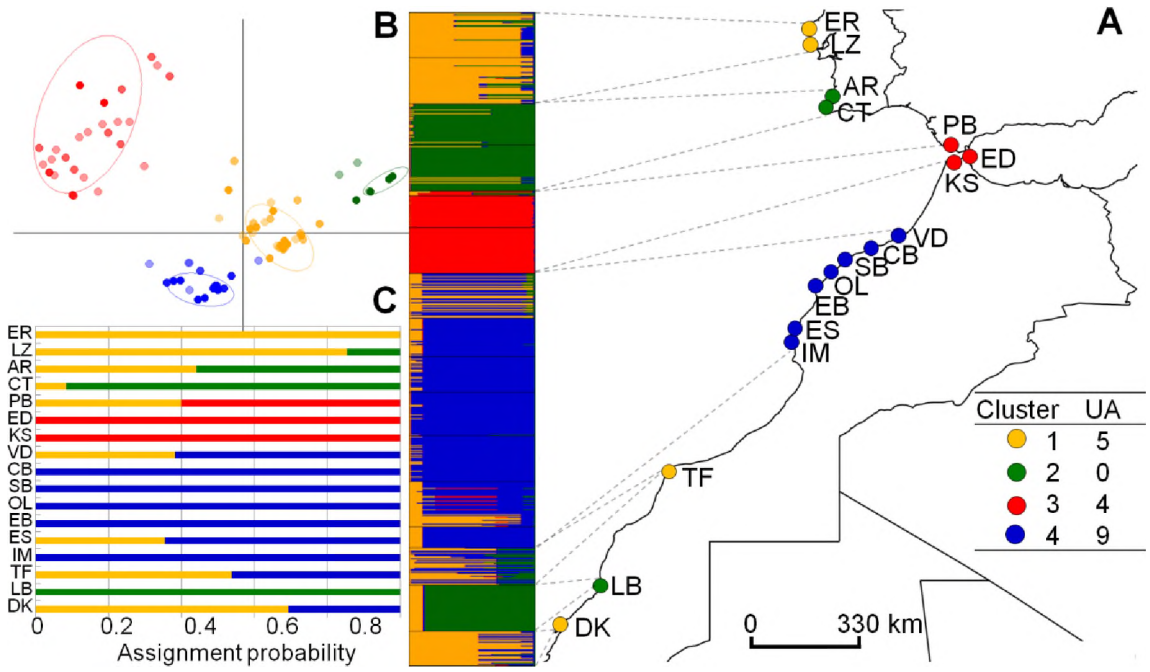

Figure 3.3 – Genetic structure of *F. guiryi* populations along southern Iberia and northern Africa. A) Bayesian analysis summary plot (each bar represents one individual) obtained from STRUCTURE software indicating that clustering of populations is best described by four clusters, i.e. K=4. Solid circles in the map represent the main genetic cluster of each location. UA, unique alleles. B) DAPC scatter plot of *a posteriori* K=4 clusters. Each individual was assigned to a cluster and solid dots correspond to overlapping of several individuals. C) DAPC assignment probability of clusters to each population. In all sections, each colour corresponds to the inferred cluster. Location codes as in Table 3.1.

AMOVA attributed most of the genetic variation among clusters (47%; $p<0.001$), while the other 27% and 26% occurred within populations ($p<0.001$) and among populations within clusters ($p<0.001$; Table 3.5).

Table 3.5 – Hierarchical analysis of molecular variance (AMOVA) results for *F. guiryi* populations from southern Iberia and northern Africa using K=4 clusters as depicted by STRUCTURE. Each population was assigned to a single cluster.

Source of variation	df	Sum of square	Variance components	Percentage of variation	F-statistics	*p*-value
Among clusters	3	726.589	0.660	47.43	FCT=0.474	<0.001
Among populations within clusters	13	371.320	0.360	25.86	FSC=0.492	<0.001
Within populations	1345	499.976	0.372	26.71	FST=0.733	<0.001
Total	1361	1597.885	1.392			

Allelic richness by upwelling and by clusters (Table 3.6) indicated Cape Ghir (GH) and cluster 4 as the most diverse ($\hat{A}_{(39)}$=2.33 and $\hat{A}_{(36)}$=2.11) and Cape Blanc (BL) and cluster 2 as the least diverse ($\hat{A}_{(39)}$=1.60 and $\hat{A}_{(36)}$=1.64). Cape Ghir and cluster 4 also had the highest number of unique or private alleles (UA=9), while either the Portuguese upwelling or the Cape Blanc upwelling showed the lowest (UA=1) and cluster 2 none (UA=0).

Table 3.6 – Genetic analyses of *F. guiryi* populations from southern Iberia and northern Africa by upwelling and by cluster for K=4 clusters. *n*, number of individuals per cluster; H_E, expected heterozygosity; H_O, observed heterozygosity; $\hat{A}$, allelic richness; $\hat{A}_{(n)}$ standardized allelic richness to the smallest sample size; UA, unique alleles. Each population was assigned to a single cluster. Upwelling and cluster codes as in Fig. 3.2 and Fig. 3.3, respectively.

	n	H_E	H_O	A	$\hat{A}_{(39)}$/ $\hat{A}_{(36)}$	UA
Upwelling						
PT	186	0.1948	0.0042	1.889	1.778	1
GB	86	0.1601	0.0027	2	1.778	4
GH	286	0.1368	0.0004	2.778	2.333	9
JB	39	0.1893	0	1.667	1.667	2
BL	84	0.1272	0	1.778	1.6	1
Cluster						
1	170	0.1503	0.002	2.444	2.089	5
2	139	0.157	0.0032	1.667	1.644	0
3	86	0.1601	0.0027	2	1.844	4
4	286	0.1368	0.0004	2.778	2.111	9

3.4 DISCUSSION

Ongoing change in sea surface temperature (SST) is regarded as a dominant and pervasive component of climate change, having an impact on species and intraspecific diversity across coastal ecosystems worldwide (e.g. Jones *et al.*, 2010; Nicastro *et al.*, 2013). In this study I provide evidence that upwelling areas represent contemporary climatic refugia by buffering some populations within a species against ongoing range contraction that is correlated with climate warming. Furthermore, I show that these refugia harbour distinct genetic pools, thereby representing important evolutionary potential for the species as a whole.

3.4.1 Contraction of *Fucus guiryi* distribution into upwelling areas

Sea surface temperature of 71% of the world's shores has increased significantly over the last three decades (Lima & Wethey, 2012). However, this trend is spatially highly heterogeneous, mostly because local and regional phenomena can override and modulate the large scale effect of climate (e.g. Lima & Wethey, 2012). The stretch of coast investigated in this study exemplifies the large scale heterogeneity of coastal SST and warming trends; the general latitudinal thermal cline is interrupted by interspersed areas of upwelling that vary in strength and frequency. Most importantly, SST has significantly increased along most of the stretch of coast studied here (between 0.09 and 0.32 °C/decade for my sampling sites, Lima & Wethey, 2012), but this effect has been strongest in areas distant from upwelling centres.

I show that the intertidal macroalga *F. guiryi* has experienced a recent range contraction of the trailing southern edge of its distribution along extensive stretches of the Atlantic and Mediterranean coasts. However, this large scale shift has not been latitudinally homogeneous from south to north, but rather fragmented. Along the retreating front, extant populations persist within regions affected by upwelling. In contrast, *F. guiryi* is absent or has disappeared from contiguous non-upwelled waters that have experienced significant recent warming.

Once abundant and widespread (e.g. Seoane-Camba, 1965; Conde & Seoane, 1982; Margalet *et al.*, 1993; González García & Conde Poyales, 1994), *F. guiryi* has now disappeared from both the European and the African coastlines of the western Mediterranean. My results show that similar extensive population extinctions of *F. guiryi* associated with recent warming trends have occurred along the Atlantic shores of Iberia and Morocco. The significantly higher SST warming rates in areas where *F. guiryi* is

absent or has disappeared compared with locations where it still persists suggest that warming trends underlie local extinction events. In addition to SST warming, several related or unrelated factors may have contributed to the observed range contraction. These include abiotic (e.g. air temperature, waves; Firth *et al.*, 2011; Riera *et al.*, 2015), biotic (e.g. grazing, competition; Walther *et al.*, 2002) or anthropogenic (e.g. pollution, Borowitzka, 1972) factors. However, many studies have highlighted the role of water temperatures as the main determinant of large scale range shifts (e.g. Rivadeneira & Fernández, 2005; Jones *et al.*, 2010; Nicastro *et al.*, 2013; Smale & Wernberg, 2013). It is not clear whether seasonal thermal extremes or chronic exposure to stressful thermal conditions caused the range contraction of *F. guiryi*. Extreme climatic events such as marine heat waves can drive marginal populations to extinction (Smale & Wernberg, 2013), but annual mean and maximum water temperatures are also responsible for mortality events in the intertidal zone (Rivadeneira & Fernández, 2005; Jones *et al.*, 2010). Thermal stress can also strongly regulate population dynamics by impairing reproduction (Riera *et al.*, 2015) and algal growth (Short *et al.*, 2015). As populations of an intertidal canopy-forming species suffer a reduction in reproduction and growth, overall abundance is affected (Riera *et al.*, 2015) and algal cover diminishes, in turn decreasing individual survival and increasing vulnerability to additional stressors (Brawley & Johnson, 1991).

The absence of detailed information about the past distribution of *F. guiryi* in Western Sahara and southern Morocco hinders my assessment of distributional shifts in this region. Nevertheless, my survey shows that the few known isolated populations (TF, LB and DK) are located within upwelling centres (JB and BL), supporting the idea of the importance of upwelling in mitigating warming effects. Most importantly, populations of this fucoid persist within shores affected by upwelled water regardless of upwelling intensity, frequency or geographic area. Notably, the single extant Mediterranean population (CL) and the few populations still present in southern Portugal (SE and AB) consist of rare scattered specimens (a few tens of individuals in each population) dispersed along the upper intertidal, reflecting a marked decrease compared to the extensive and continuous canopies that prevailed until a few decades ago (Fig. 3.4 and R. Bermejo pers. comm.).

Although numerous studies have advanced our understanding of the effects of upwelling on marine systems (e.g. Menge *et al.*, 2004; Nielsen & Navarrete, 2004; Thompson *et al.*, 2012), the refugial potential of upwelling areas in a scenario of global warming has been only hypothesised (corals, Riegl & Piller, 2003 and deep-water kelp, Ladah *et al.*, 2003 but see Chollett *et al.*, 2010). In this study I do not aim to investigate which of the distinct

components of upwelled waters are more important in providing shelter against ongoing warming. Multiple determinants directly or indirectly related to upwelling may be involved, including SST (Assis *et al.*, 2016), nutrient supply (Pereira *et al.*, 2015) and the moderation of biotic interactions (e.g. grazing and competition, Menge *et al.*, 2004; Nielsen & Navarrete, 2004; Thompson *et al.*, 2012). Despite this limitation, I argue that the assessment of multiple upwelling and non-upwelling areas has provided a strong test for the ecological (and evolutionary, see below) role of upwelling as refugia that extends beyond site specificity.

Figure 3.4 – *Fucus guiryi* cover in 2004 (above) and in 2010 (below) at Santa Eulália (SE in Table 3.1; Fig. 3.2A), southern Portugal during summer.

Interestingly, although other intertidal organisms have shown large scale distributional shifts within the same study area, they did not find refuge within upwelling areas (e.g. Lima *et al.*, 2007a; Rubal *et al.*, 2013). For example, the southern limit of the congeneric *F. vesiculosus* has shifted over the past 30 years from southern Morocco to central Portugal (Nicastro *et al.*, 2013). Although species distributional modelling identified SST as the most important environmental predictor for the distribution of *F. vesiculosus* (Assis *et al.*, 2014), populations in upwelling areas have also gone extinct. The lack of a refuge effect has been attributed to short term SST anomalies that, despite being less frequent within upwelling areas, might be strong enough to have caused *F. vesiculosus* extinction. *Fucus vesiculosus* range distribution partially overlaps with that of *F. guiryi*, but the southernmost range limits of the two species are distinct. Presently, *F. vesiculosus*, a cold temperate water species, occurs from central Portugal (but with few extant, isolated patches in southern Iberia) and North Carolina to the White Sea, Greenland and Canada (Nicastro *et al.*, 2013; Assis *et al.*, 2014), while *F. guiryi*, a southern warmwater species, ranges from the Western Sahara to the United Kingdom (Zardi *et al.*, 2011b, 2015b; this study). These contrasting geographical distributions indicate distinctive temperature optima which ultimately suggest distinct species thermal tolerances and adaptive potential. Taken together with my results, this highlights the fact that the protective effect of upwelling is not applicable to the entire community but it is restricted by species-specific properties of resilience in the face of environmental stressors.

3.4.2 Upwelling areas are reservoirs of genetic diversity

The integration of intra-specific genetic information with distributional data is profoundly important for an understanding of the impact of climate change on species. A combined approach can help to target future conservation needs that are specific to particular lineages in geographically restricted portions of a species' range. When genetic diversity of a retreating species is geographically skewed, specific portions of its genetic variability could be under threat, potentially affecting the ability of the species as a whole to adapt to a changing environment and thus increasing its risk of extinction. Here, I identified major genetic discontinuities that are geographically structured along the distributional range of *F. guiryi*. Phylogeographic analyses revealed four distinct genetic groups refuged within the five upwelling centres. The Portuguese and Cape Blanc upwelling filament each sustained two distinct lineages (clusters 1 and 2), while the Strait of Gibraltar upwelling, the west Moroccan upwelling off Cape Ghir and the Cape Juby upwelling each supported one unique genetic entity (clusters 3, 4 and 1 respectively). This highlights the crucial role

played by upwelling areas not only for the persistence of a species as a whole, but also for the maintenance of distinct genetic lineages and unique alleles, each nearly endemic to a particular upwelling cell.

Of the four lineages recovered, cluster 4 (Cape Ghir upwelling area) appears to be a relevant genetic resource for the species. The high number of unique alleles and the genetic diversity of clade 4 suggest that this region is a key refugial area for the species with long-term stability, where population persistence and the accumulation of unique mutations are favoured.

In addition, the cluster associated with the Strait of Gibraltar upwelling (cluster 3) revealed the greatest spatial genetic differentiation of all clusters. Given that the species was historically distributed along the Mediterranean coastline, this differentiation, partially caused by the presence of several unique alleles, might reflect an area that was separated from the Atlantic for a prolonged period, causing a distinct lineage to persist in protracted isolation.

Genetic clusters associated with specific environmental regimes may display different physiological tolerances to environmental stress, and thus have unique adaptive potential that can be important for species survival (Pearson *et al.*, 2009; Zardi *et al.*, 2013; Saada *et al.*, 2016). In the sister species *F. vesiculosus*, the genetic clade inhabiting southern, warmer latitudes has greater resilience to heat stress than the neighbouring, northern lineage (Saada *et al.*, 2016). Potentially, each of the *F. guiryi* lineages described here could display unique ecophysiological responses to their environment, widening the ecological implications of these climatic refugia.

Although not of primary interest in this study, other patterns of genetic differentiation are worth highlighting. Firstly, although it is generally accepted that central populations have higher levels of genetic diversity compared with peripheral ones (Eckert *et al.*, 2008), *F. guiryi* genetic signatures add weight to recent, mounting evidence describing the reverse (Bush *et al.*, 2011; Diekmann & Serrão, 2012; Assis *et al.*, 2013; Zardi *et al.*, 2015b). *Fucus guiryi* range edge populations, such as VD, ES and TF, showed higher genetic diversity compared to populations from the more central locations ER and LZ. This pattern could be the result of ongoing genetic admixture between populations from neighbouring clusters and/or past gene exchange with extinct populations that occurred when the species was continuously distributed along the coastline (i.e. at non-upwelling sites, such as southern Portugal and the Strait of Gibraltar).

Moreover, genetic analyses clustered together Portuguese and south Moroccan/Western Sahara populations of *F. guiryi*. Genetic similarity between these distant geographic regions could have resulted from 1) dispersal from Portugal to south Morocco/Western

Sahara or vice-versa or 2) random genetic convergence. Gene flow of direct-developing structural seaweeds, such as *F. guiry*, is limited, mainly driven by dispersal via rafting of fertile thalli (Norton, 1992; Kalvas & Kautsky, 1998; Coleman & Brawley, 2005; McKenzie & Bellgrove, 2008), and is shaped by density-barrier effects (Petit *et al.*, 2003; Neiva *et al.*, 2012). Prevailing north-to-south oceanographic currents that govern the study area (Martins *et al.*, 2002) could drive asymmetric connectivity in the same direction; however, the dispersal distance and higher genetic richness at the southern than at the northern edge (for cluster 1) make this seem unlikely.

Alternatively, convergence could result from similar, random genetic changes (Losos, 2011). Given the very low polymorphism and the fragmented nature of the populations in south Morocco and Western Sahara, genetic drift could have caused allele sizes of populations from opposite regions to randomly converge. This is supported by the frequency pattern of two specific markers (F26 and L20) that most likely are the main two drivers of the genetic similarity.

3.4.3 Final remarks

Increased upwelling intensities have been observed over the last few decades (McGregor *et al.*, 2007; Narayan *et al.*, 2010; Cropper *et al.*, 2014) and are predicted to increase further as a response to climatic changes (e.g. Bakun *et al.*, 2010; Cropper *et al.*, 2014; Wang *et al.*, 2015). I can thus anticipate that the contemporary refugial effect reported in this study might even grow, irrespective of the individual nature of each upwelling centre, whether the permanent (100s km) one off Cape Ghir or the small, intermittent one in the Strait of Gibraltar. Concurrently, warming rates are predicted to rise further (Collins *et al.*, 2013, IPCC, 2014) along this stretch of coast, placing populations at the edges of these upwelling centres under increasing threat.

While the effects of upwelling centres as refugia may be species specific, in this case there are likely to be bottom-up cascading effects on the ecosystem as a whole. Canopy-forming bioengineer species, such as *F. guiryi*, increase local species richness and diversity, particularly in stressful environments (Watt & Scrosati, 2013b). Consequently, the described climatic refugia for *F. guiryi* are likely to indirectly stabilize intertidal species composition, trophic linkages and thus overall ecosystem functioning. In summary, I suggest that upwelling centres are potentially important in maintaining not only the existence of species, which is particularly important in the case of ecological engineers, but also the genetic diversity of species, with long term evolutionary implications.

CHAPTER 4

The effects of multiple oceanographic barriers to dispersal in the genetic structure of the brown mussel *Perna perna*

The brown mussel *P. perna* on the intertidal shores of Praia do Farol, Portugal.

4.1 INTRODUCTION

The physical environment influences species distribution patterns and shapes the genetic structure of their populations (Harley *et al.*, 2006; Zardi *et al.*, 2011a; Nicastro *et al.*, 2013; Fenberg *et al.*, 2015). In the marine realm, species' distributional arrangements and genetic discontinuities are often caused by dispersal barriers (e.g. upwelling, currents) and environmental gradients (e.g. temperature, salinity) that interrupt or limit demographic connectivity among populations (Teske *et al.*, 2008; Zardi *et al.*, 2011a; Assis *et al.*, 2015; Fenberg *et al.*, 2015). Importantly, there is increasing modelling and experimental evidence that pronounced alterations to oceanographic features due to climatic change are rearranging species' genetic patterns and distributions globally (Assis *et al.*, 2014; Martínez *et al.*, 2015).

Species inhabiting a specific bioregion do not all necessarily show the same genetic breaks as some are able to sustain high levels of gene flow among populations regardless of the presence of oceanographic barriers (Neethling *et al.*, 2008; Kelly & Palumbi, 2010; Villamor *et al.*, 2014). The absence of genetic structure has been related, for instance, to species life history traits, such as the presence of a pelagic phase and larval behaviour (Neethling *et al.*, 2008; Kelly & Palumbi, 2010; Villamor *et al.*, 2014). Historical events are also key drivers of genetic patterns (Grosberg & Cunningham, 2001). For example, there is ample evidence that, during the Last Glacial Maximum (LGM), species retreated to restricted glacial refugia areas, persisting throughout unsuitable conditions to reveal contemporary genetic signatures that are the result of accumulated genetic diversity (Provan & Maggs, 2012; Neiva *et al.*, 2015).

The Mediterranean Sea and the northeastern Atlantic are ideal regions to study the effects of dispersal barriers and environmental gradients on species distribution and genetic patterns. In the Mediterranean basin, the Strait of Sicily connects the Western and the Eastern Mediterranean regions (Robinson *et al.*, 1991), represents a geographical break for several species (Bianchi *et al.*, 2002; Coll *et al.*, 2010) and is a driver of genetic differentiation (Buonomo *et al.*, 2017). The Almeria-Oran Front (AOF, stretching from Almeria, Spain to Oran, Algeria) separates the Western Mediterranean region from the Alboran Sea (Atlantic-Mediterranean waters, Tintore *et al.*, 1988), affecting the genetic structure of several species inhabiting both sides of the front (Patarnello *et al.*, 2007). Towards the Atlantic, the Strait of Gibraltar is the meeting point where Atlantic water enters the Mediterranean Sea at the surface, overriding the denser Mediterranean water mass (Tintore *et al.*, 1988) and forming the focus of several studies of the effect of regional oceanographic barriers on genetic structure (reviewed in Patarnello *et al.*, 2007). Along the Atlantic coast of Morocco, upwelling off Cape Ghir has been proposed as a

hydrographic barrier that separates fish stocks (*Sardina pilchardus*, Chlaida *et al.*, 2009) and shapes the genetic structure of intertidal organisms (e. g. *Mytilus galloprovincialis*, Jaziri & Benazzou, 2002; *Bifurcaria bifurcata*, Neiva *et al.*, 2015). Likewise, a genetic break has been detected close to Cape Boujdour in two fish ecotypes (*Engraulis encrasicolus*, Ouazzani *et al.*, 2017). Other upwelling areas or capes along this stretch of coast such as upwelling off Cape Juby and upwelling off Cape Blanc (Marcello *et al.*, 2011) may potentially affect species' population dynamics. Additionally, the Mediterranean and northeastern Atlantic coasts have also seen contractions and expansions of warm and coldwater species, particularly along Portuguese shores (Pereira *et al.*, 2006; Lima *et al.*, 2007a), as a response to recent increases in sea surface temperatures (SST; up to 0.4 °C/decade, Lima & Wethey, 2012). For example, two species of the brown algal genus *Fucus* (*F. vesiculosus* and *F. guiryi*) have exhibited major distributional contractions along Atlantic and Mediterranean Iberian and northern African shores linked to rates of SST warming over the last three decades (Nicastro *et al.*, 2013; Assis *et al.*, 2014; Lourenço *et al.*, 2016).

Recently a northward expansion of the intertidal brown mussel *Perna perna* was described from north Africa to southern Iberia (Lourenço *et al.*, 2012). This dominant habitat-forming species occurs naturally throughout northern Africa, from Tunisia to Senegal, in Ivory Coast and Ghana, along the west African (from Congo Republic to Walvis Bay, Namibia; GI Zardi and KR Nicastro, pers. comm.) and east African coasts (from central Mozambique to False Bay, South Africa) and the west coast of Madagascar (Berry, 1978; Cayré, 1978; Zabi, 1982; Otchere *et al.*, 2003; Sidoumou *et al.*, 2006; Wood *et al.*, 2007). With an Indo-Pacific origin and later expansion to the Mediterranean and the Atlantic (Cunha *et al.*, 2014), *P. perna* is described from Sri Lanka, southern India, Yemen and Oman (Badawy & Al-Harthy, 1991; Szefer & Geldon, 1997; Cunha *et al.*, 2014). Moreover, the Brown mussel has invaded the United States, Mexico, Venezuela, Brazil and Uruguay (Berry, 1978; Vakily, 1989 and references therein; Hicks & Tunnell, 1993, 1995; Wood *et al.*, 2007). The genetic structure of this species is known to be affected by oceanographic features in South Africa. There, the Agulhas current helps to maintain a geographical separation between two very distinct genetic lineages of *P. perna* (the eastern and the western lineages) by preventing larval dispersal and thus enhancing local adaption (Zardi *et al.*, 2007, 2011a, 2015a). The eastern lineage extends from Kenton-on-Sea towards Mozambique, while the western lineage extends from Cape Agulhas to Haga-Haga (Zardi *et al.*, 2007, 2015a). The two lineages overlap in their distributions on the southeast coast of South Africa over approximately 200 km (Zardi *et al.*, 2007, 2015a). Interestingly, also in South Africa, Teske *et al.* (2012) reported sex-specific

differences in the genetic structure of *P. perna*, with significant structuring in females but not in males.

The occurrence of several distinct oceanographic features across the northeastern Atlantic and the Mediterranean Sea, the fact that these are drivers of the genetic structure in some species, and ongoing environmental changes set the basis for this chapter. Here, I combine extensive field survey, multimarker genetic analyses and environmental niche modelling to investigate the factors dictating the distribution and the drivers of genetic structure on *P. perna* along northeastern Atlantic and Mediterranean shores. Specifically I 1) use mitochondrial and nuclear markers to understand if genetic structure is strongly influenced by oceanographic features (e.g. dominant currents and upwelling systems) and if they affect the genetic structure of the two sexes differently, 2) perform environmental niche modelling along the entire native range of the species to assess its potential and realized niches and the environmental variables that most affect its distribution across the northeastern Atlantic and Mediterranean shores. Finally, the distribution of *P. perna* along South African shores was used as an ideal case study to disentangle the relative roles of strongly correlated environmental variables on shaping the distribution of *P. perna*. The South African coastline covers a wide range of very distinct climatic and oceanic conditions that can be divided into three major biogeographic regions (Emanuel *et al.*, 1992). These are the subtropical East Coast, the warm temperate South Coast and the cool temperate West Coast. Interestingly, *P. perna* dominates intertidal shores in the subtropical and warm temperate bioregions but it is absent from the cold waters of the Benguela system on the west coast (Zardi *et al.*, 2007; Tagliarolo *et al.*, 2016).

4.2 MATERIAL AND METHODS

4.2.1 Distribution of *Perna perna* along the Atlantic and Mediterranean Iberian Peninsula

The distribution of *P. perna* along the Atlantic and Mediterranean Iberian Peninsula (from the northwestern Portuguese Atlantic coast, Viana do Castelo 41º41'57.85"N; 08°51'23.81"W, to the Mediterranean Spanish coastline, Cullera 39º11'16.26"N; 00º13'17.20"W; Table 4.1) was investigated through extensive field surveys during low spring tides between November 2011 and July 2016 at 49 natural or manmade (e. g., pontoons, pilings and seawalls) hard substratum intertidal habitats. At each location, two observers assessed the presence or absence of *P. perna* by performing approximately 60 min searches across all microhabitats. Because *Mytilus galloprovincialis* is the dominant intertidal mussel species of these shores and is known to co-exist with *P. perna* in temperate regions (Abada-Boudjema & Davin, 1995; Zardi *et al.*, 2007) its conspicuous presence was considered an indication of suitable habitat for *P. perna*.

Table 4.1 – Atlantic and Mediterranean surveyed locations along Iberian shores. Presence of *M. galloprovincialis* depicts potential suitable locations for *P. perna.*

Country	Location	Coordinates	*M. galloprovincialis* presence
Portugal	Viana do Castelo	41º41'57.85"N; 08°51'23.81"W	Present
Portugal	Ericeira	38º57'21.03"N; 09°25'00.97"W	Present
Portugal	Foz do Lizandro	38º56'28.13"N; 09°25'02.28"W	Present
Portugal	Malhão	37º46'44.64"N; 08°48'09.35"W	Present
Portugal	V. N. Milfontes	37º43'04.79"N; 08°47'27.73"W	Present
Portugal	Amoreira	37º20'59.18"N; 08°50'53.15"W	Present
Portugal	Castelejo	37º06'08.00"N; 08°56'44.29"W	Present
Portugal	Sagres	37º00'23.69"N; 08°56'55.80"W	Present
Portugal	Lagos	37º05'55.10"N; 08°40'02.38"W	Present
Portugal	Alvor	37º07'44.45"N; 08°35'47.71"W	Present
Portugal	Pintadinho	37º06'32.07"N; 08°31'11.63"W	Present
Portugal	Albufeira	37º05'21.03"N; 08°11'29.76"W	Present
Portugal	Vilamoura	37º04'05.50"N; 08º06'42.64"W	Present
Portugal	Farol	36º58'29.95"N; 07º51'42.17"W	Present
Portugal	Tavira	37º06'41.06"N; 07º36'57.99"W	Present
Portugal	V. R. S. António	37º10'03.78"N; 07º24'09.03"W	Present
Spain	Punta del Moral	37º10'57.76"N; 07º19'46.83"W	Present
Spain	Punta Umbria	37º09'53.78"N; 06º56'54.38"W	Present
Spain	Huelva	37º07'45.19"N; 06º51'09.43"W	Absent
Spain	Rota	36º36'55.50"N; 06º21'27.85"W	Absent

Spain	Puerto Sherry	36º34'48.65"N; 06º15'55.07"W	Absent
Spain	Barbate	36º11'00.22"N; 05º56'10.82"W	Absent
Spain	Atlanterra	36º05'24.78"N; 05º48'43.02"W	Present
Spain	Paloma Baja	36º03'49.70"N; 05º43'39.89"W	Absent
Spain	Tarifa	36º00'27.89"N; 05º36'26.09"W	Absent
Spain	Los Palmones	36º10'34.28"N; 05º25'28.26"W	Present
Spain	Torreguadiaro	36º18'00.14"N; 05º16'04.77"W	Present
Spain	La Araña	36º42'41.35"N; 04º19'37.50"W	Present
Spain	Almuñecar	36º43'39.84"N; 03º41'39.86"W	Present
Spain	Balerma	36º41'56.20"N; 02º51'33.99"W	Present
Spain	Roquetas de Mar	36º45'27.41"N; 02º36'15.26"W	Absent
Spain	Aguadulce	36º48'40.91"N; 02º34'00.66"W	Absent
Spain	Cabo de Gata	36º44'00.26"N; 02º12'14.70"W	Present
Spain	La Isleta	36º47'53.54"N; 02º03'42.64"W	Absent
Spain	Garrucha	37º10'21.02"N; 01º49'18.30"W	Absent
Spain	Villaricos	37º14'49.74"N; 01º46'15.80"W	Absent
Spain	Aguilas	37º24'15.16"N; 01º33'56.64"W	Absent
Spain	Calabardina	37º25'53.29"N; 01º30'27.11"W	Absent
Spain	Cape Cope	37º26'12.49"N; 01º29'02.88"W	Absent
Spain	Puerto de Mazarron	37º33'28.51"N; 01º17'10.24"W	Absent
Spain	Portman	37º34'50.35"N; 00º51'13.23"W	Absent
Spain	Cape Palos	37º38'00.94"N; 00º41'23.95"W	Absent
Spain	Guardamar del Segura	38º06'37.33"N; 00º38'27.07"W	Absent
Spain	Santa Pola	38º11'18.94"N; 00º33'06.45"W	Absent
Spain	Alicante	38º21'07.64"N; 00º24'40.40"W	Absent
Spain	Calpe	38º38'25.71"N; 00º03'56.53"E	Absent
Spain	Cape de la Nau	38º43'51.27"N; 00º13'08.85"E	Absent
Spain	Dénia	38º57'50.66"N; 00º07'43.58"W	Present
Spain	Cullera	39º11'16.26"N; 00º13'17.20"W	Present

4.2.2 Genetic diversity and genetic structure of *P. perna* across oceanographic barriers

Perna perna individuals (*n*=13–34 except two populations with *n*=2 and *n*=4) were collected between November 2011 and March 2014 from 27 locations (Table 4.2).

Table 4.2 – List of sampling sites for genetic samples of *P. perna* populations. *n*, sample size; * locations used to investigate sex-specific genetic patterns.

Country/Territory	Location	Code	*n*	Coordinates
Tunisia	Korbous	KR	30	36°49'29.04"N; 10°33'59.97"E
Tunisia	Bizerte	BZ	32	37°15'10.41"N; 09°56'41.15"E
Algeria	Annaba bay	AN	22	36°50'32.48"N; 07°51'17.48"E
Morocco	Punta Negri	PN	31	35º16'46.33"N; 03º08'06.63"W
Spain	Cape Gata	CG	13	36º44'00.26"N; 02º12'14.70"W
Spain	Balerma	BM*	31	36º41'56.20"N; 02º51'33.99"W
Spain	Almuñecar	AM	31	36º43'39.84"N; 03º41'39.86"W
Spain	La Araña	LA	30	36º42'41.35"N; 04º19'37.50"W
Spain	Torreguadiaro	TG	31	36º18'00.14"N; 05º16'04.77"W
Spain	Los Palmones	LP	2	36º10'34.28"N; 05º25'28.26"W
Spain	Atlanterra	AT	26	36º05'24.78"N; 05º48'43.02"W
Spain	Punta del Moral	PM	22	37º10'57.76"N; 07º19'46.83"W
Portugal	Tavira	TV	29	37º06'41.06"N; 07º36'57.99"W
Portugal	Vilamoura	VL	29	37º04'05.50"N; 08º06'42.64"W
Portugal	Sagres	SG	4	37º00'23.69"N; 08º56'55.80"W
Morocco	Larache	LR*	30	35°11'48.14"N; 06°09'30.61"W
Morocco	Rabat	RB	32	34°01'57.26"N; 06°50'27.96"W
Morocco	Casablanca	CB	30	33°39'07.22"N; 07°29'03.11"W
Morocco	Sidi Bouzid	SB	33	33°13'06.11"N; 08°34'23.19"W
Morocco	El Beddouza	EB	34	32°32'42.33"N; 09°16'55.34"W
Morocco	Essaouira	ES*	30	31°30'42.78"N; 09°46'24.31"W
Morocco	Imsouane	IM*	29	30°50'24.43"N; 09°49'21.92"W
Morocco	Mirleft	ML*	30	29°35'06.58"N; 10°02'50.78"W
Morocco	Tan Tan plage	TT*	30	28°30'05.58"N; 11°20'06.38"W
Western Sahara	Boujdour	BJ*	29	26º07'38.95"N; 14º30'02.38"W
Western Sahara	Nouifed	LB*	30	24º54'30.29"N; 14º49'45.36"W
Western Sahara	Dakhla	DK*	30	23º46'06.97"N; 15º55'32.16"W

Mantle tissue (20–30 mg) was dissected from each individual, preserved in 96% ethanol and stored at -20ºC. Total genomic DNA extraction was performed using a standard Proteinase K protocol adapted from Sambrook *et al.* (1989). The primers LCOI 1490, 5'-GGT CAA CAA ATC ATA AAG ATA TTG G-3' and HCO 2198, 5'-TAA ACT TCA GGG TGA CCA AAA AAT CA-3' (Folmer *et al.*, 1994) were used for polymerase chain reaction (PCR) amplification of Cox1 region. PCR amplification was performed in a 25 µl reaction volume containing 10 to 100 ng of total DNA, 0.2 µM of each primer, 0.08 mM of each dNTP, 2mM of $MgCl_2$, 1x GoTaq Flexi Buffer (Promega, USA) and 1 U GoTaq DNA Polymerase (Promega, USA). Amplification used an initial denaturation during 2 min at 94 °C followed by 35 cycles of denaturation at 94 °C for 60 s, annealing at 55 °C for 60 s, extension at 72 °C for 90 s and a final extension at 72 °C for 5 min. PCR products ran in 1.5% agarose gel during an electrophoresis of about 45 min at 120 V and 400 A to ensure

that all samples were amplified. PCR products were then purified for sequencing using ExoSap (USB Co., USA) and sequenced directly with PCR primers using the BigDye Terminators version 3.1 Cycle Sequencing Kit (Applied Biosystems, Foster-City, CA) in an ABI PRISM 3130 genetic analyzer (Applied Biosystems). Eight microsatellite loci P01, P02, P05, P08, P16, P20, P26 and P27 were amplified as in Coelho *et al.* (2012). PCR products run in 2 % agarose gel during an electrophoresis of about 30 min at 120 V and 400 A. Two multiplex and one simplex designs were used during genotyping process: run 1 included P08, P16, P20 and P26 loci; run 2 included P01, P05 and P27 loci while P02 was genotyped alone. Genotyping conditions were performed as in Coelho *et al.* (2012) in an ABI PRISM 3130 genetic analyzer (Applied Biosystems).

4.2.2.1 Genetic analyses

I applied a multimarker approach to increase the power to detect genetic discontinuities (Pérez-Portela *et al.*, 2017). Additionally, by combining mitochondrial (slower mutation rate; maternally-inherited) and nuclear (higher mutation rate; biparentally-inherited) markers, I aimed to understand whether historical and/or contemporary oceanographic barriers are responsible for restricting gene flow in *P. perna* (see Teske *et al.*, 2014; Pérez-Portela *et al.*, 2017) and if sex-specific genetic patterns exist.

4.2.2.1.1 Mitochondrial DNA

DNA sequences were visualized, edited and aligned using Geneious 4.8.2 (Biomatters Ltd.). DnaSP 5.0 (Librado & Rozas, 2009) was used to evaluate haplotype (*h*) and nucleotide (π, Nei, 1987) diversities for individuals collected at the same location (hereafter referred to as a population). Total numbers of haplotypes (H) and unique haplotypes (UH) were estimated for each population in DNAcollapser from FaBox (Villesen, 2007).

The Akaike Information Criterion corrected for small sample sizes (AICc) was used in jModelTest 0.1.1 (Posada, 2008) to select the best fitting model of sequence evolution to analyse the dataset in Arlequin 3.11 (Excoffier *et al.*, 2005). Genetic differentiation between pairs of populations was calculated by estimating ϕ_{ST} (analogous of FST, (Weir & Cockerham, 1984) based on haplotype frequency. Statistical significance was assessed by performing 10 100 permutations under the null hypothesis of no differentiation, and adjusted with q-value correction (Storey, 2002) implemented in R (R Core Team, 2012). Spatial analysis of shared alleles (SAShA, Kelly *et al.*, 2010) was used to complement ϕ_{ST}

differentiation values as it detects alleles that might be restricted to a geographical area by comparing the observed spatial co-occurrence of alleles with the expected geographical distribution under panmixia. Observed distributions of geographic distances between pairs of alleles are compared with the expected null distribution under panmixia. Statistical significance was determined by 1000 permutations of the haplotype matrix, keeping row and column sums constant. The minimum geographic distance between pairs of locations was measured in kilometres using the path ruler tool in Google Earth, from a height of 20 km.

To test the effect of oceanographic features on the genetic structure of *P. perna*, populations (Table 4.2) were divided in seven groups according to the oceanographic barriers described in the literature. These were: Eastern Mediterranean (EM; populations KR, BZ), Western Mediterranean (WM; population AN), Alboran Sea (AS; populations PN, CG, BM, AM, LA, TG and LP), Atlantic Iberia (AI; populations AT, PM, TV, VL and SG), Northwestern Morocco (NM; populations LR, RB, CB, SB, EB and ES), Southern Morocco (SM; IM, ML, TT and BJ) and Western Sahara (WS; population LB and DK). EM is separated from WM by the Strait of Sicily; WM is separated from AS by the Almeria-Oran Front. The Strait of Gibraltar separates AS from AI and NM. Upwelling cells at Cape Ghir and Cape Boujdour separate NM from SM and SM from WS, respectively (Fig. 4.1).

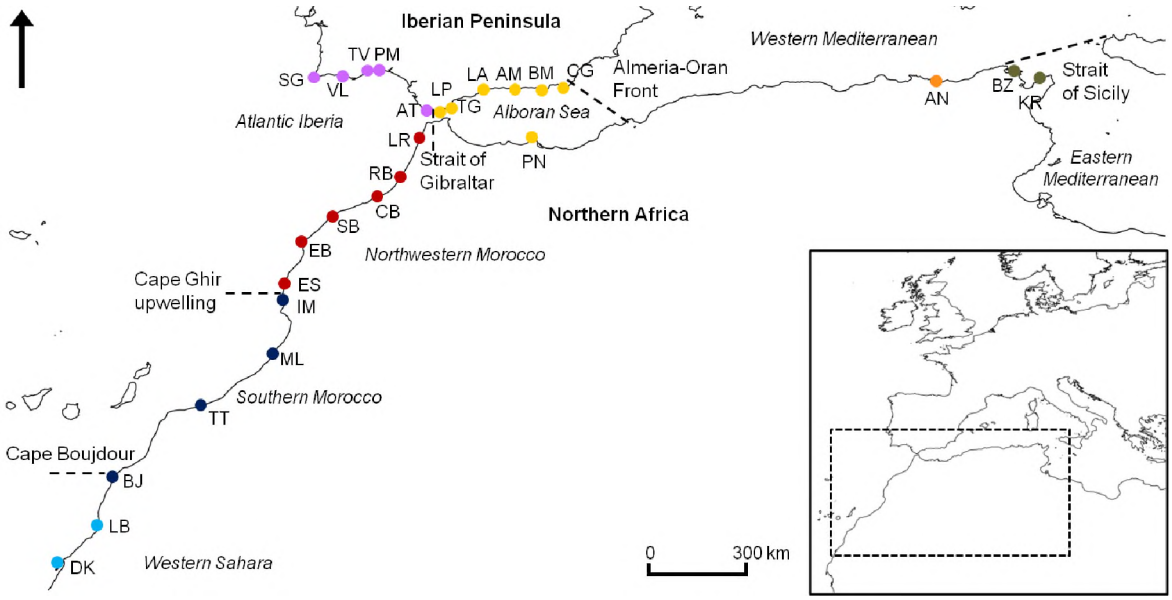

Figure 4.1 – Geographical distribution of sampled populations of *P. perna* and the potential oceanographic barriers for dispersal. Dotted lines represent oceanographic barriers and separate potential genetic groups. Eastern Mediterranean, populations KR, BZ; Western Mediterranean, population AN; Alboran Sea, populations PN, CG, BM, AM, LA, TG and LP; Atlantic Iberia, populations AT, PM, TV, VL and SG; Northwestern Morocco, populations LR, RB, CB, SB, EB and ES; Southern Morocco, populations IM, ML, TT and BJ; Western Sahara, population LB and DK. Location codes as in Table 4.2.

To evaluate population genetic structure, a hierarchical analysis of molecular variance (AMOVA) was conducted in Arlequin 3.11 using 10 100 permutations. To understand how genetic variation is partitioned between distinct groups, among populations within groups and within populations, the seven groups described above were designated *a priori* (EM, WM, AS, IB, NM, SM and WS).

Intraspecific genealogical relationships between groups and the relative frequency of haplotypes were determined by a median-joining haplotype network built on Network 4.5.0.2 (Bandelt *et al.*, 1999). The resulting haplotype network combines minimum-spanning networks and median vectors under a parsimony criterion. Median vectors represent hypothesized or extant unsampled haplotypes, required to connect existing haplotypes with maximum parsimony within the network (Quinteiro *et al.*, 2007).

Cox1 sequences generated and analysed during the current study were deposited in GenBank with the accession numbers KY514494–KY515223.

4.2.2.1.2 Microsatellite markers

Allele sizes were scored using STRand software (http://www.vgl.ucdavis.edu/informatics/STRand), binned with the standArich package in R (R Core Team, 2012) and manually reviewed for ambiguities. MICRO-CHECKER (van Oosterhout *et al.*, 2004) was used to test for stuttering, null alleles and large allele dropout at each locus and population. All loci had less than 5% of missing data with the exception of P16 (22%), which was excluded from the following analyses.

Observed (H_O) and expected (H_E) heterozygosity, inbreeding coefficient (F_{IS}, Weir & Cockerham, 1984) and allelic richness (Â) were estimated for each population. Allelic richness (Â) was additionally standardized to two of the smallest sample sizes using GENETIX 4.05 (Belkhir *et al.*, 2004) and FSTAT (Goudet, 1995). Allelic frequencies for each marker and population were plotted using standArich. Deviations from Hardy-Weinberg equilibrium were tested running 10 000 permutations using GENETIX 4.05. Pairwise genetic differentiation was estimated as F_{ST} (Weir & Cockerham, 1984) and as Jost's D (Jost, 2008) using diveRsity package (Keenan *et al.*, 2013) in R, with significance tested 1000 bootstrap. Pairwise genetic distance between populations was estimated based on the proportion of shared alleles (Bowcock *et al.*, 1994) according to (Jin & Chakraborty, 1994) using Populations 1.2.30 (Langella, 2002) running 999 bootstrap. A neighbour-joining (NJ) phylogenetic tree was constructed using MEGA5 (Tamura *et al.*, 2011).

STRUCTURE 2.3.4 software (Pritchard *et al.*, 2000) estimated population structure and inferred the number of clusters in the dataset, considering no prior information on populations. An admixture model and correlated allele frequencies were assumed. The number of possible clusters (K) assessed ranged from 1 to 28 (maximum number of populations plus one) and five independent runs with 100 000 Markov Chain Monte Carlo (MCMC) iterations and 50 000 burn-in were performed for each K. STRUCTURE HARVESTER 0.6.94 (Earl & von Holdt, 2012) estimated the most probable value of K calculating ΔK as in Evanno et al. (2005). CLUMPP 1.1.2 software (Jakobsson & Rosenberg, 2007) was used to find the consensus of the five replicated runs of the selected K. The replicate consensus was plotted with Ruby package Bar Plotter (http://evolution.unibas.ch/salzburger/software.htm). A discriminant analysis of principal components (DAPC) was performed in R (R Core Team, 2012) with adegenet 1.4.2 (Jombart, 2008) based on the matrix of individual genotypes with seven microsatellite loci, to characterize the genetic variation of the study area. Each individual was assigned to its sampling population. The function *find.cluster* returned the best fitting number of clusters (K) in the dataset, correspondent to the minimum K after which the Bayesian Information Criterion changes by a negligible amount (Jombart *et al.*, 2010).
A hierarchical analysis of molecular variance (AMOVA) was conducted in Arlequin 3.11 running 10 100 permutations, to understand hierarchical population structure with groups designated *a priori* based on potential oceanographic barriers as described above.

4.2.3 Sex-specific genetic structure of *P. perna*

A subsample of nine locations distributed along the survey area was used to investigate if sex-specific differences exist in genetic structure of *P. perna* populations (Table 4.2). If equal numbers of males and females were not obtained during previous collections, sampling continued until 14–15 individuals of each sex were sampled. *Perna perna* mussels can be classified as males or females based on gonad colouration: males present white gonads while females show red-orange gonads (Yap *et al.*, 1979 but see Petes *et al.*, 2008). Whenever colour-based identification was not possible, a piece of gonad tissue was observed under the microscope to determine the sex by the presence of eggs or sperm.

4.2.3.1 Genetic analyses

To compare genetic diversity and structure within and between sexes and understand if genetic patterns of *P. perna* were sex-biased, *h*, π, H, PH, ϕ_{ST} were estimated and AMOVA performed using mtDNA COI sequences from nine populations where sex identification had been previously performed, following procedures described in 4.2.2.1.1. H_O and H_E, Â, number of unique alleles, F_{IS}, F_{ST}, Jost's D, AMOVA and STRUCTURE analyses were also performed using the seven microsatellite markers as described in 4.2.2.1.2. Analyses were performed for each group separately.

4.2.4 Ecological niche modelling of *P. perna* native distribution

4.2.4.1 Data on native occurrence

A total of 118 presences were compiled from extensive field surveys and from records in the existing literature where the species is native (i.e. the African continent, southern Iberia and the Arabian Peninsula, Table A1 in Appendix). As the number of true absences detected in the field was relatively low (52) and biased towards the areas where most of the field surveys were available (i.e. South Africa, Morocco and the Iberian Peninsula), pseudo-absences from non-surveyed areas were randomly added and included in the models. The use of pseudo-absences is particularly useful as a surrogate for accurate absence data when performing presence-absence models; pseudo-absence models also avoid overoptimistic predictions, a common characteristic of presence-only approaches (Engler *et al.*, 2004; Chefaoui & Lobo, 2008). The selection method to generate pseudo-absence data conditions the predictions of the model (Engler *et al.*, 2004; Chefaoui & Lobo, 2008). By performing a random selection of pseudo-absences the modelled range is not overpredicted, allowing a better assessment of the variables affecting the realized distribution of the species (Chefaoui & Lobo, 2008).
The intertidal area was delimited by extracting the coastal cells covering a range from -2 to 1 m from the General Bathymetric Chart of the Oceans (GEBCO) gridded bathymetric data set with a spatial resolution of 30 arc-seconds (http://www.gebco.net/).

4.2.4.2 Environmental variables

The most meaningful environmental variables commonly known to influence and used to model the distribution of intertidal species (Jones *et al.*, 2010; Assis *et al.*, 2015; Fenberg

et al., 2015) were obtained from Bio-ORACLE dataset (Tyberghein *et al.*, 2012) at a spatial resolution of 5 arcmin (9.2 km). These included minimum and maximum surface air temperature (SAT, Jueterbock *et al.*, 2013), minimum and maximum sea surface temperature (SST), nutrients (nitrate and phosphate concentrations), salinity and mean cloud cover fraction (Table 4.3). Significant wave height (2009–2015) was obtained from Aviso (http://www.aviso.altimetry.fr; Table 4.3). All variables and species' records were georeferenced to the same resolution (9.2 km). Correlation among predictors was verified using Pearson's correlation coefficient=|0.7| as a cut-off.

Table 4.3 – Environmental variables used to model *P. perna* likelihood of presence. SST indicates sea surface temperature. SAT indicates surface air temperature.

	Study area		Presences	
Predictors (units)	**Min–Max**	**Mean**	**Min–Max**	**Mean**
Cloud cover fraction	0.069–0.943	0.531	0.251–0.872	0.49
Waves (m)	0.388–5.774	2.008	0.625–3.829	2.183
Minimum SST (°C)	-1.585–28.827	17.403	13.817–25.977	17.316
Maximum SST (°C)	6.979–37.600	27.335	18.908–31.705	24.028
Minimum SAT (°C)	-7.757–25.477	12.414	5.925–23.069	13.878
Maximum SAT (°C)	8.298–35.289	28.169	22.055–34.562	26.511
Salinity	1.634–41.475	34.66	33.953–37.277	35.827
Nitrate (µmol/L)	0.003–12.494	1.355	0.548–6.695	2.12
Phosphate (µmol/L)	0.0184–1.3965	0.229	0.049–0.995	0.33

4.2.4.3 Niche modelling and variable importance

The environmental niche of *P. perna* was modelled using six presence-absence techniques: generalized additive model (GAM), generalized boosting model (GBM), generalized linear model (GLM), flexible discriminant analysis (FDA), randomForest (RF), and multiple adaptive regression splines (MARS) using biomod2 package (Thuiller *et al.*, 2014) in R. Pseudo-absences were selected at random to complement absence data surveyed in the field. A proportion presence/absence of 1:10 (as in Chefaoui *et al.*, 2016) corresponding to a total amount of 1180 absences (52 true absences + 1128 pseudo-absences) was used, for a study region of 20 057 cells of coastal areas. Cross-validation was performed by randomly splitting the data records into training (70 %) and test (30%) datasets. Moreover, the area under the receiver operating characteristic (ROC) curve (AUC), the ROC-derived sensitivity and specificity values (Fielding & Bell, 1997), and the true skill statistic (TSS, Allouche *et al.*, 2006), using the threshold which optimized ROC and TSS scores (Thuiller *et al.*, 2014), were used to evaluate the models. Each of the six algorithms ran 50 iterations and a 'committee averaging' ensemble model was performed

averaging the binary predictions of models with TSS>0.7 to predict the probability of occurrence of the species.

The relative contribution of each variable was calculated by estimating the correlation between each model without a variable and the full model (Liaw & Wiener, 2002), running three permutations. The subtraction of 1 minus the correlation was calculated and each predictor was scored 0–1 (lowest to highest importance; Thuiller *et al.*, 2014). Subsequently, a mean of the scores of the three permutations was calculated for each variable.

4.2.4.3.1 Data analysis

To disentangle the individual significance of minimum SST and SAT on *P. perna* distribution, subsets of nine locations equitably distributed along approximately 2200 km of the cool temperate southwest (CT) and the warm temperate (WT) southern African provinces (Emanuel *et al.*, 1992) were selected (Fig. 4.2). *Perna perna* has been extensively investigated along these shores where a wide distributional gap has been described (*P. perna* is absent from CT but present in WT, Zardi *et al.,* 2007). The absence and presence of *P. perna* along the CT and the WT regions, respectively, coupled to SST and SAT data allows a better understanding of the environmental factors setting the distributional limits of this species. While all nine absence records from the CT were included, three different subsets of nine locations along WT were selected. Only the range of the western lineage of *P. perna* was considered here. The extents of coastlines and the distances between locations were estimated on Google Earth at an altitude of 100 m.

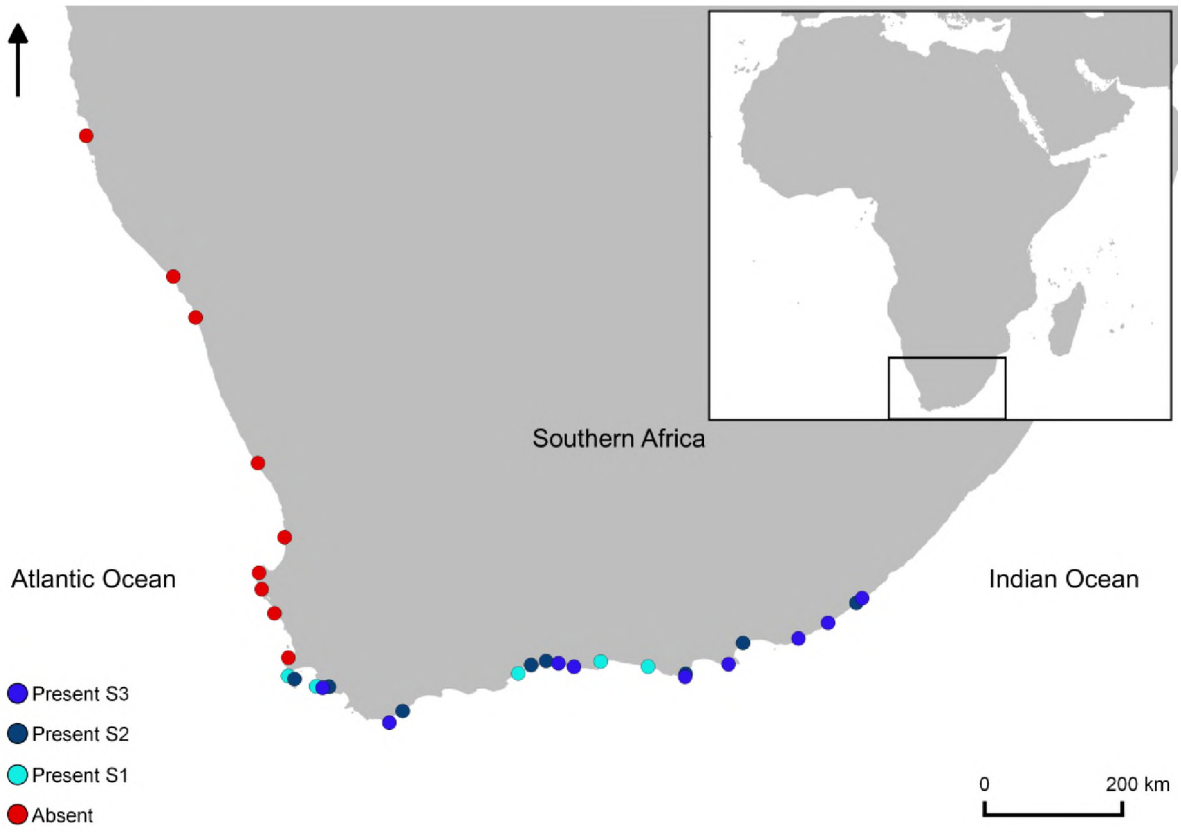

Figure 4.2 – Geographical distribution of the southern African sampling sites used to compare the temperature conditions where *P. perna* is either absent (red) or present (blue). Different shades of blue represent the three distinct subsets (S1, S2 and S3) of presence data.

One-way ANOVA was used to test the null hypothesis that minimum SST and minimum SAT did not differ significantly between the two regions in South Africa where *P. perna* is absent or present. The design consisted of one factor: Record (two levels, fixed) and the analyses were performed three times. All tests and respective significance values were performed with STATISTICA 7.1 (StatSoft, 2005). When data did not fulfill the pre-requisites for parametric analysis (Cochran's Test or Shapiro-Wilk's W), analyses were performed using PERMANOVA (Anderson, 2001; McArdle & Anderson, 2001) running 999 permutations.

4.3 RESULTS

4.3.1 Distribution of *Perna perna* along the Atlantic and Mediterranean Iberian Peninsula

Surveys along the Iberian Peninsula showed that out of the 49 surveyed sites, while *Mytilus galloprovincialis* was present at 27 locations, *P. perna* was only detected at 14, despite the existence of favourable substratum conditions (Fig. 4.3). Castelejo, southwest Iberia (Portugal), was the northwesternmost location where the Brown mussel was found. North of Castelejo, individuals of this species were not detected, although *M. galloprovincialis* was still abundant. Into the Mediterranean, both species were reported as far east as Cape Gata, the easternmost limit of the Brown mussel. After a gap along the southeast coast of Iberia where intertidal mussels were entirely absent, only *M. galloprovincialis* reappeared (present in Dénia and Cullera, see Table 4.1).

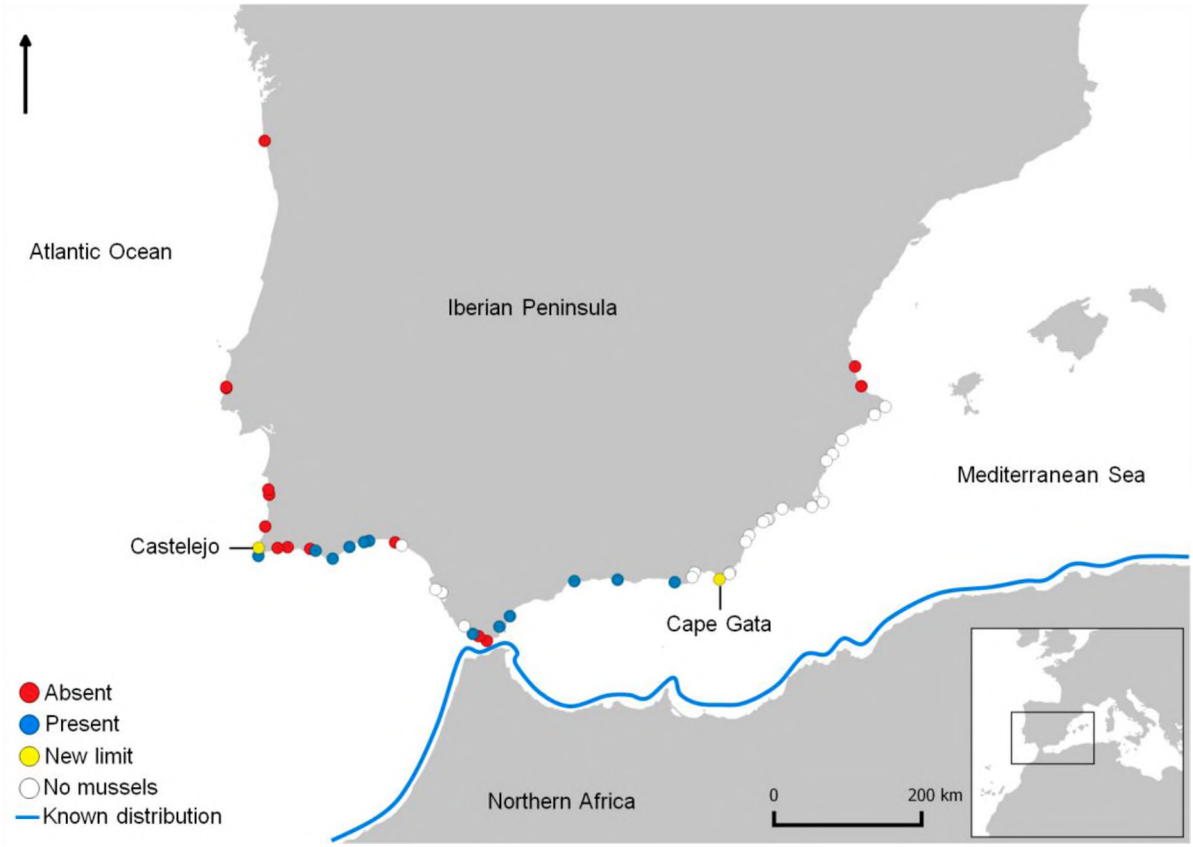

Figure 4.3 – *Perna perna* range expansion along the Iberian Peninsula. Presence and absence of *P. perna* are marked by blue and red dots, respectively. White dots represent surveyed sites where no mussels were found and yellow dots represent the new range limits of the *P. perna* distribution. The thick blue line illustrates the previously known distribution of *P. perna* along northern Africa. Surveyed locations are described in Table 4.1, from north to south and west to east. Arrow indicates north.

4.3.2 Genetic diversity and genetic structure of *P. perna* across oceanographic barriers

4.3.2.1 Mitochondrial DNA–Cox1

Sequences of *P. perna* (615 bp Cox1 region) from 730 specimens revealed 127 haplotypes and 112 polymorphic sites (Table 4.4). PN and LR showed the highest number of overall haplotypes (17) while LP showed the lowest (2), likely due to the very small sample size. BZ and LR presented the highest number of unique haplotypes (8) and KR, CG and CB did not show any unique haplotypes. Whereas 94 haplotypes were private, 33 were shared among populations. Haplotype and nucleotide diversities varied between 0.481 (PM) and 1.0 (LP) and between 0.0010 (PM) and 0.0049 (LP), respectively.

Table 4.4 – Genetic diversity of Cox1 gene of *P. perna* populations. *n*, sample size; H, number of haplotypes; UH, number of unique haplotypes; *h*, haplotype diversity (±SD); π, nucleotide diversity (±SD). Location codes as in Table 4.2.

Population	*n*	H	UH	*h*	π
KR	30	8	0	0.729 ± 0.065	0.0022 ± 0.0004
BZ	32	15	8	0.821 ± 0.062	0.0030 ± 0.0005
AN	22	8	3	0.753 ± 0.069	0.0022 ± 0.0005
PN	31	17	6	0.912 ± 0.036	0.0028 ± 0.0003
CG	13	5	0	0.731 ± 0.096	0.0024 ± 0.0007
BM	31	10	5	0.714 ± 0.070	0.0022 ± 0.0006
AM	31	13	5	0.733 ± 0.085	0.0020 ± 0.0004
LA	30	14	6	0.844 ± 0.056	0.0030 ± 0.0005
TG	31	8	3	0.735 ± 0.062	0.0025 ± 0.0005
LP	2	2	1	1.000 ± 0.500	0.0049 ± 0.0024
AT	26	8	3	0.575 ± 0.113	0.0016 ± 0.0004
PM	22	7	1	0.481 ± 0.131	0.0010 ± 0.0004
TV	29	12	5	0.791 ± 0.073	0.0026 ± 0.0005
VL	29	10	4	0.687 ± 0.091	0.0022 ± 0.0005
SG	4	3	1	0.833 ± 0.222	0.0030 ± 0.0009
LR	30	17	8	0.864 ± 0.058	0.0032 ± 0.0005
RB	32	13	4	0.784 ± 0.066	0.0024 ± 0.0004
CB	30	10	0	0.699 ± 0.085	0.0021 ± 0.0004
SB	33	14	2	0.805 ± 0.064	0.0028 ± 0.0006
EB	34	15	3	0.750 ± 0.080	0.0021 ± 0.0004
ES	30	11	5	0.678 ± 0.094	0.0020 ± 0.0004
IM	29	9	4	0.648 ± 0.096	0.0013 ± 0.0003
ML	30	9	5	0.598 ± 0.103	0.0022 ± 0.0005
TT	30	12	2	0.745 ± 0.082	0.0020 ± 0.0004
BJ	29	9	2	0.613 ± 0.102	0.0013 ± 0.0003
LB	30	10	5	0.754 ± 0.063	0.0022 ± 0.0004
DK	30	8	3	0.756 ± 0.055	0.0027 ± 0.0005

Pairwise ϕ_{ST} values were non-significant across all populations (p>0.05; Table 4.5) and ranged from 0 to 0.432; the highest estimate was found between PM and LP. High pairwise ϕ_{ST} values were recovered from populations with extremely low sampling sizes (e.g. LP, n=2 0.039–0.432 and SG, n=4 0.048–0.349).

Table 4.5 – Pairwise ϕ_{ST} comparison of *P. perna* populations. All *p*-values were corrected for multiple comparisons and non-significant. Location codes as in Table 4.2.

	KR	BZ	AN	PN	CG	BM	AM	LA	TG	LP	AT	PM	TV	VL	SG	LR	RB	CB	SB	EB	ES	IM	ML	TT	BJ	LB	DK
KR	-	0.000	0.008	0.000	0.000	0.000	0.025	0.000	0.013	0.195	0.017	0.027	0.000	0.000	0.127	0.000	0.000	0.000	0.000	0.011	0.013	0.030	0.000	0.014	0.029	0.000	0.000
BZ		-	0.000	0.000	0.000	0.000	0.006	0.000	0.000	0.115	0.000	0.002	0.000	0.000	0.121	0.000	0.000	0.000	0.000	0.000	0.008	0.000	0.000	0.000	0.000	0.000	0.000
AN			-	0.000	0.000	0.000	0.026	0.006	0.000	0.216	0.014	0.058	0.029	0.015	0.256	0.020	0.000	0.002	0.000	0.011	0.054	0.019	0.026	0.020	0.026	0.000	0.000
PN				-	0.000	0.000	0.000	0.000	0.000	0.114	0.000	0.000	0.000	0.000	0.155	0.002	0.000	0.000	0.000	0.000	0.004	0.000	0.000	0.000	0.000	0.000	0.002
CG					-	0.000	0.006	0.000	0.000	0.082	0.008	0.085	0.000	0.014	0.236	0.017	0.000	0.000	0.000	0.024	0.037	0.043	0.003	0.026	0.040	0.000	0.000
BM						-	0.020	0.001	0.000	0.219	0.004	0.025	0.018	0.002	0.219	0.007	0.000	0.000	0.000	0.002	0.033	0.005	0.014	0.006	0.010	0.000	0.000
AM							-	0.000	0.009	0.153	0.000	0.012	0.000	0.013	0.255	0.018	0.000	0.000	0.000	0.002	0.000	0.015	0.000	0.000	0.000	0.022	0.037
LA								-	0.000	0.039	0.000	0.014	0.000	0.000	0.127	0.000	0.000	0.000	0.000	0.001	0.000	0.017	0.000	0.000	0.004	0.000	0.000
TG									-	0.142	0.000	0.046	0.013	0.020	0.234	0.025	0.000	0.000	0.000	0.012	0.032	0.011	0.015	0.002	0.016	0.000	0.012
LP										-	0.252	0.432	0.063	0.212	0.201	0.087	0.156	0.197	0.092	0.225	0.167	0.390	0.128	0.225	0.350	0.229	0.158
AT											-	0.005	0.000	0.000	0.300	0.008	0.000	0.000	0.000	0.000	0.000	0.000	0.000	0.000	0.000	0.005	0.026
PM												-	0.014	0.000	0.324	0.000	0.005	0.003	0.008	0.000	0.000	0.005	0.006	0.000	0.000	0.026	0.044
TV													-	0.000	0.113	0.000	0.000	0.000	0.000	0.006	0.000	0.031	0.000	0.003	0.015	0.010	0.008
VL														-	0.138	0.000	0.000	0.000	0.000	0.000	0.000	0.006	0.000	0.000	0.006	0.000	0.000
SG															-	0.048	0.192	0.189	0.146	0.210	0.172	0.349	0.177	0.217	0.332	0.196	0.113
LR																-	0.000	0.000	0.000	0.001	0.000	0.013	0.000	0.004	0.012	0.000	0.000
RB																	-	0.000	0.000	0.000	0.006	0.000	0.000	0.000	0.000	0.000	0.003
CB																		-	0.000	0.000	0.000	0.000	0.000	0.000	0.000	0.000	0.000
SB																			-	0.000	0.001	0.006	0.000	0.000	0.000	0.000	0.002
EB																				-	0.005	0.000	0.000	0.000	0.000	0.002	0.020
ES																					-	0.028	0.000	0.000	0.005	0.028	0.031
IM																						-	0.020	0.000	0.000	0.009	0.038
ML																							-	0.001	0.005	0.011	0.013
TT																								-	0.000	0.006	0.027
BJ																									-	0.015	0.041
LB																										-	0.000
DK																											-

Spatial analysis of shared alleles (SAShA) indicated that the observed distribution of geographical distance between pairs of haplotypes (OM) was not statistically different from the expectation (EM) under panmixia (OM=885.30 km, EM=892.06 km, p=0.773).
The Akaike Information Criterion corrected for small sample sizes (AICc) selected TrN+G as the best-fit model to be implemented in Arlequin software (gamma shape=0.932). AMOVA analyses attributed most of the variation to within populations (99.52%, p=0.126; Table 4.6). Only 0.5% of the variation occurred among groups (p=0.006)

Table 4.6 – AMOVA from the 27 populations of *P. perna* distributed over seven distinct groups based on mitochondrial Cox1 gene.

Source of variation	df	Sum of squares	Variance components	Percentage of variation	Φ-statistics	*p*-value
Among groups	6	6.327	0.0037	0.53	0.0053	0.006
Among populations within groups	20	13.717	-0.0004	-0.05	-0.0005	0.505
Within populations	703	488.654	0.6951	99.52	0.005	0.126
Total	729	508.699	0.6985			

The median-joining haplotype network reconstruction of *P. perna* revealed one single clade, and no genetic differentiation between *a priori* expected distinct groups distributed along southern Iberian and northern Africa (Fig. 4.4A). The star-shaped network presented two main central haplotypes widespread at all groups (Fig. 4.4B). Generally, both shared and private peripheral haplotypes differed from the centre by one or two mutational steps. Haplotypes were shared irrespective of the geographic distance between groups (i.e. haplotypes shared between WM and AI or between WM and WS).

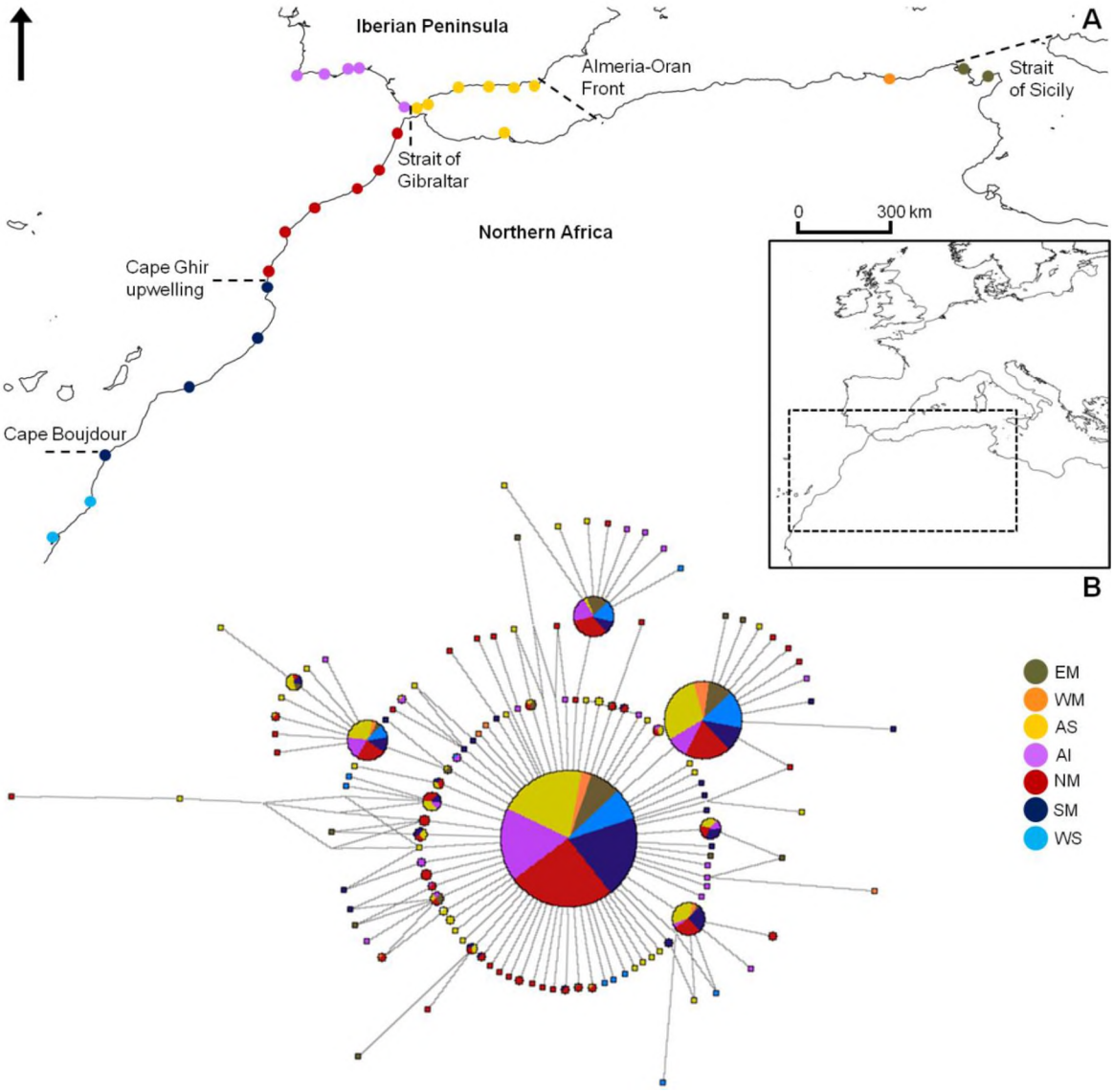

Figure 4.4 – Genetic structure of *P. perna* across northeastern Atlantic and Mediterranean shores. A) Geographical distribution of *P. perna* populations and expected genetic structure according to oceanographic barriers to dispersal described in the literature. B) Median-joining haplotype network of Cox1 gene. Circle size is proportional to haplotype frequency. Colours indicate the group origin of a haplotype. Gray line represents the number of mutational steps.

4.3.2.2 Microsatellite markers

Out of 732 individuals, 373 alleles were detected in seven loci. The total number of alleles per locus ranged from 12 to 134. Excluding locus P16, there was no clear evidence for large allele drop-out, stuttering or null alleles at a frequency higher than 0.2. Expected (H_E) and observed (H_O) heterozygosities varied between 0.536 (CB) and 0.796 (LP) and 0.643 (SG) and 0.773 (AN), respectively, resulting in a minor heterozygosity deficit (F_{IS} ranged from 0 to 0.128). Population genetic diversity standardized to the smallest sample

sizes, $\hat{A}_{(2)}$ and $\hat{A}_{(22)}$, varied between 2.714 (LP) and 3.123 (CB) and between 11.966 (IM) and 14.714 (PM), respectively. A total of 105 unique alleles were described with CB reporting the highest number (10; Table 4.7).

Table 4.7 – Genetic analyses of *P. perna* populations based on nuclear microsatellite markers. *n*, number of individuals per population; H_E, expected heterozygosity; H_O, observed heterozygosity; $\hat{A}$, allelic richness represented by mean number of alleles per locus per population; $\hat{A}_{(n)}$ allelic richness standardized to smallest sample sizes; F_{IS}, inbreeding coefficient; UA, unique alleles. Significant values of F_{IS} are in bold. * $p<0.05$; ** $p<0.01$. Location codes as in Table 4.2.

Population	*n*	H_E	H_O	$\hat{A}$	$\hat{A}_{(2)}$	$\hat{A}_{(22)}$	F_{IS}	UA
KR	30	0.776	0.737	15.714	3.061	13.483	**0.067****	7
BZ	32	0.770	0.712	15.857	3.011	13.190	**0.091****	4
AN	22	0.761	0.773	13.429	2.972	13.429	0.009	1
PN	31	0.754	0.743	16	2.977	13.422	0.032	7
CG	13	0.747	0.747	9.857	2.998	-	0.039	0
BM	32	0.753	0.736	17	3.004	14.012	0.039	7
AM	33	0.749	0.690	17	2.980	13.817	**0.093****	2
LA	30	0.765	0.743	15.571	3.031	13.438	**0.046***	4
TG	33	0.751	0.703	15.714	2.977	12.876	**0.079****	7
LP	2	0.536	0.714	2.714	2.714	-	0	0
AT	26	0.783	0.769	15.714	3.102	14.360	0.039	2
PM	22	0.767	0.716	14.714	3.052	14.714	**0.090****	4
TV	27	0.750	0.740	13.857	2.982	12.557	0.032	0
VL	27	0.780	0.773	15.714	3.088	14.227	0.028	1
SG	4	0.607	0.643	4.5714	2.812	-	0.085	1
LR	30	0.780	0.744	16.429	3.098	14.027	**0.063****	4
RB	32	0.779	0.751	16	3.046	13.411	**0.052***	4
CB	29	0.796	0.708	16.429	3.123	14.394	**0.128****	10
SB	33	0.754	0.701	17.143	3.012	14.046	**0.085****	3
EB	34	0.769	0.731	16.429	3.021	13.354	**0.064****	6
ES	30	0.751	0.712	15.286	2.976	13.063	**0.069****	6
IM	30	0.728	0.726	13.857	2.899	11.966	0.019	5
ML	30	0.757	0.763	16.429	3.014	13.965	0.008	1
TT	30	0.751	0.762	16	2.987	13.629	0.003	5
BJ	30	0.769	0.731	15.571	3.006	13.247	**0.066***	2
LB	30	0.765	0.730	15.429	3.012	13.228	**0.063***	6
DK	30	0.733	0.695	15.857	2.915	13.457	**0.069***	6

F_{ST} and Jost's D ranged from 0 to 0.034 and from 0 to 0.041, respectively (Table 4.8), and showed no significant differences in any pairwise comparisons (F_{ST} lower and upper 95% confidence interval limits ranged from -0.174 to -0.004 and from 0.005 to 0.209, respectively; Jost's D lower and upper 95% confidence interval limits ranged from -0.179 to -0.007 and from 0.022 to 0.279, respectively; Table A2 in Appendix).

Table 4.8 – Pairwise F_{ST} (above) and Jost's D (below) comparisons of *P. perna* populations. Location codes as in Table 4.2.

	KR	BZ	OR	PN	CG	BM	AM	LA	TG	LP	AT	PM	TV	VL	SG	LR	RB	CB	SB	EB	ES	IM	ML	TT	BJ	LB	DK
KR	-	0.000	0.001	0.001	0.000	0.000	0.001	0.000	0.000	0.000	0.000	0.000	0.001	0.000	0.021	0.000	0.000	0.000	0.002	0.000	0.000	0.004	0.004	0.000	0.001	0.000	0.000
BZ	0.000	-	0.000	0.003	0.000	0.000	0.000	0.000	0.002	0.000	0.000	0.000	0.000	0.000	0.019	0.000	0.000	0.001	0.000	0.000	0.000	0.000	0.000	0.000	0.000	0.000	0.000
OR	0.001	0.004	-	0.000	0.000	0.000	0.000	0.000	0.000	0.000	0.000	0.000	0.009	0.000	0.006	0.001	0.000	0.000	0.000	0.000	0.000	0.003	0.006	0.003	0.002	0.000	0.000
PN	0.007	0.016	0.002	-	0.000	0.001	0.000	0.000	0.001	0.000	0.000	0.006	0.011	0.001	0.012	0.002	0.003	0.000	0.009	0.004	0.001	0.010	0.011	0.003	0.006	0.003	0.000
CG	0.005	0.000	0.000	0.003	-	0.000	0.000	0.000	0.000	0.000	0.000	0.000	0.000	0.000	0.012	0.000	0.000	0.000	0.000	0.000	0.000	0.000	0.000	0.000	0.000	0.000	0.000
BM	0.000	0.000	0.000	0.005	0.001	-	0.000	0.000	0.000	0.000	0.000	0.000	0.004	0.000	0.005	0.000	0.000	0.000	0.000	0.000	0.000	0.000	0.001	0.000	0.007	0.000	0.000
AM	0.000	0.000	0.002	0.001	0.001	0.000	-	0.000	0.002	0.000	0.000	0.000	0.000	0.000	0.005	0.000	0.000	0.000	0.001	0.002	0.000	0.001	0.000	0.000	0.005	0.000	0.000
LA	0.000	0.000	0.000	0.000	0.001	0.000	0.000	-	0.000	0.000	0.000	0.000	0.004	0.000	0.005	0.000	0.000	0.000	0.000	0.000	0.000	0.001	0.000	0.000	0.002	0.000	0.000
TG	0.000	0.000	0.000	0.004	0.003	0.000	0.000	0.000	-	0.000	0.003	0.003	0.005	0.000	0.021	0.000	0.004	0.001	0.001	0.000	0.000	0.007	0.004	0.001	0.001	0.000	0.002
LP	0.000	0.000	0.000	0.000	0.000	0.000	0.000	0.000	0.000	-	0.000	0.000	0.000	0.000	0.000	0.000	0.000	0.000	0.000	0.000	0.000	0.000	0.000	0.000	0.000	0.000	0.000
AT	0.000	0.000	0.000	0.000	0.000	0.000	0.000	0.000	0.000	0.000	-	0.000	0.002	0.000	0.008	0.000	0.000	0.000	0.003	0.000	0.002	0.000	0.002	0.000	0.007	0.000	0.000
PM	0.000	0.000	0.001	0.002	0.002	0.000	0.000	0.001	0.003	0.000	0.000	-	0.000	0.000	0.024	0.000	0.000	0.005	0.000	0.000	0.000	0.000	0.000	0.000	0.000	0.000	0.000
TV	0.001	0.000	0.013	0.039	0.003	0.003	0.001	0.006	0.019	0.000	0.000	0.007	-	0.000	0.027	0.000	0.002	0.003	0.006	0.009	0.002	0.003	0.000	0.000	0.001	0.000	0.007
VL	0.000	0.000	0.004	0.001	0.007	0.000	0.000	0.000	0.000	0.000	0.000	0.000	0.000	-	0.024	0.000	0.000	0.000	0.001	0.000	0.000	0.004	0.000	0.000	0.000	0.000	0.001
SG	0.001	0.000	0.001	0.008	0.001	0.000	0.000	0.000	0.000	0.000	0.000	0.006	0.000	0.008	-	0.009	0.009	0.000	0.003	0.010	0.018	0.025	0.024	0.018	0.034	0.021	0.011
LR	0.000	0.001	0.000	0.004	0.000	0.000	0.000	0.000	0.001	0.000	0.000	0.000	0.002	0.000	0.000	-	0.000	0.000	0.000	0.000	0.001	0.001	0.000	0.000	0.002	0.000	0.000
RB	0.001	0.000	0.001	0.014	0.000	0.000	0.000	0.000	0.005	0.000	0.000	0.005	0.000	0.007	0.000	0.001	-	0.000	0.001	0.000	0.000	0.000	0.000	0.000	0.003	0.000	0.000
CB	0.000	0.003	0.001	0.009	0.002	0.000	0.000	0.000	0.000	0.000	0.000	0.001	0.003	0.000	0.000	0.000	0.000	-	0.005	0.001	0.003	0.007	0.005	0.000	0.007	0.000	0.000
SB	0.003	0.001	0.004	0.010	0.000	0.002	0.011	0.000	0.000	0.000	0.000	0.002	0.028	0.000	0.000	0.000	0.008	0.015	-	0.000	0.000	0.001	0.000	0.000	0.000	0.000	0.003
EB	0.002	0.004	0.000	0.017	0.006	0.001	0.006	0.000	0.000	0.000	0.000	0.003	0.041	0.003	0.003	0.002	0.000	0.006	0.000	-	0.002	0.001	0.001	0.000	0.005	0.000	0.000
ES	0.001	0.000	0.000	0.000	0.000	0.000	0.000	0.000	0.000	0.000	0.000	0.000	0.007	0.000	0.000	0.000	0.000	0.001	0.000	0.002	-	0.003	0.001	0.001	0.000	0.000	0.000
IM	0.002	0.001	0.003	0.026	0.002	0.000	0.007	0.001	0.008	0.000	0.000	0.000	0.002	0.013	0.002	0.002	0.000	0.009	0.006	0.005	0.012	-	0.000	0.000	0.007	0.000	0.003
ML	0.004	0.000	0.015	0.007	0.002	0.000	0.000	0.000	0.000	0.000	0.000	0.000	0.000	0.000	0.009	0.000	0.003	0.006	0.000	0.004	0.000	0.003	-	0.000	0.004	0.000	0.002
TT	0.000	0.000	0.007	0.000	0.001	0.000	0.000	0.000	0.000	0.000	0.000	0.000	0.004	0.004	0.000	0.000	0.000	0.001	0.000	0.007	0.006	0.000	0.000	-	0.003	0.000	0.000
BJ	0.005	0.002	0.000	0.014	0.002	0.012	0.012	0.004	0.006	0.000	0.003	0.004	0.009	0.004	0.008	0.002	0.006	0.010	0.001	0.013	0.001	0.016	0.016	0.010	-	0.000	0.006
LB	0.000	0.001	0.000	0.014	0.000	0.000	0.000	0.000	0.000	0.000	0.000	0.002	0.002	0.000	0.005	0.000	0.000	0.000	0.003	0.000	0.000	0.001	0.003	0.000	0.000	-	0.000
DK	0.002	0.001	0.002	0.004	0.001	0.000	0.000	0.000	0.000	0.000	0.000	0.000	0.027	0.002	0.002	0.005	0.001	0.001	0.000	0.000	0.000	0.010	0.002	0.000	0.015	0.001	-

The neighbour-joining tree based on proportion of shared alleles evidenced the absence of a geographical topology (Fig. 4.5).

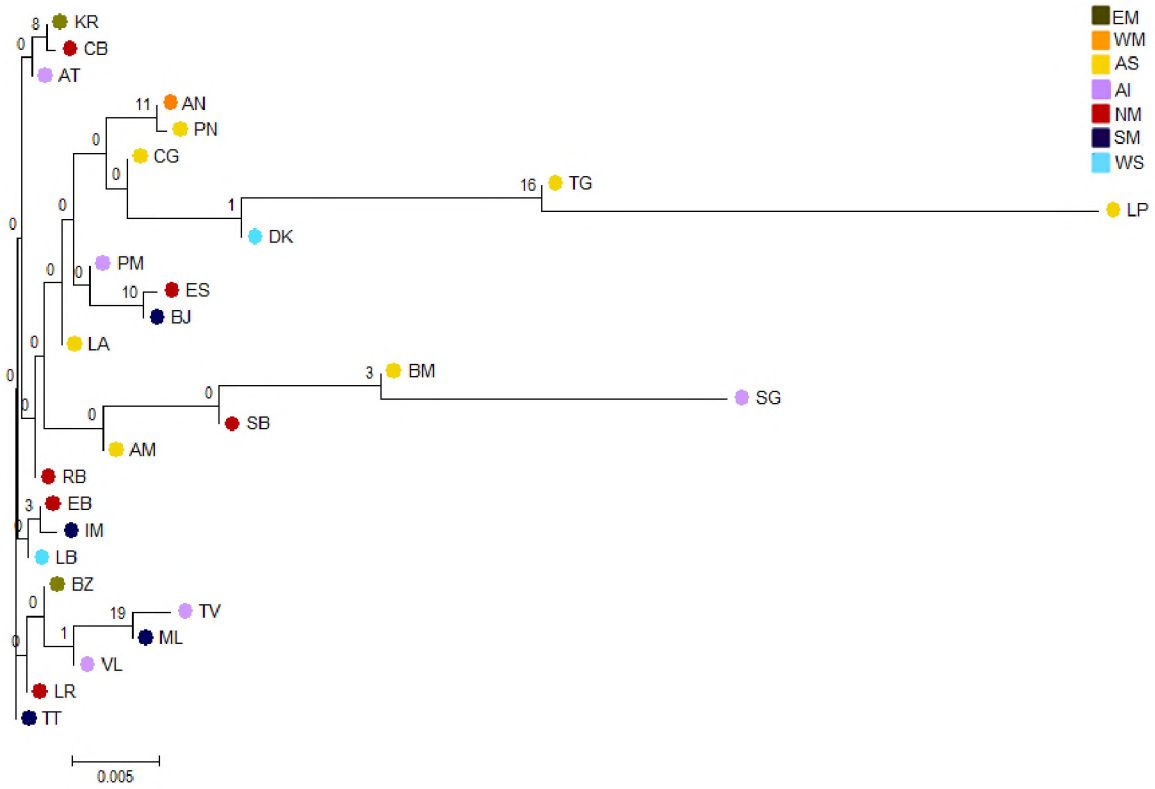

Figure 4.5 – Unrooted neighbour-joining tree of the pairwise genetic distance between populations of *P. perna* across northeastern Atlantic and Mediterranean shores based on proportion of shared alleles of seven microsatellite loci. Colours depict distinct expected oceanographic groups. EM, Eastern Mediterranean; WM, Western Mediterranean; AS, Alboran Sea; AI, Atlantic Iberia; NM, Northwestern Morocco; SM, Southern Morocco; WS, Western Sahara. Location codes as in Table 4.2.

Bayesian admixture analyses implemented in STRUCTURE did not reveal any clear geographical clustering (Fig. 4.6). The log probability of the data (L(K)) returned from the Bayesian admixture analyses suggested K=1 as the best fitting K (Fig. 4.6). Although using the ΔK method (Evanno *et al.*, 2005) proposed K=2 as the best fitting K, the two proposed resolved clusters were consistently present at all populations, thus excluding any geographical and genetic separation. The incongruence between both methods might be explained by the fact that ΔK does not estimate K=1, but L(K) of K=2 suggested the second best fitting K after K=1. All these considerations allow us to select K=1 as the best fitting K for my data.

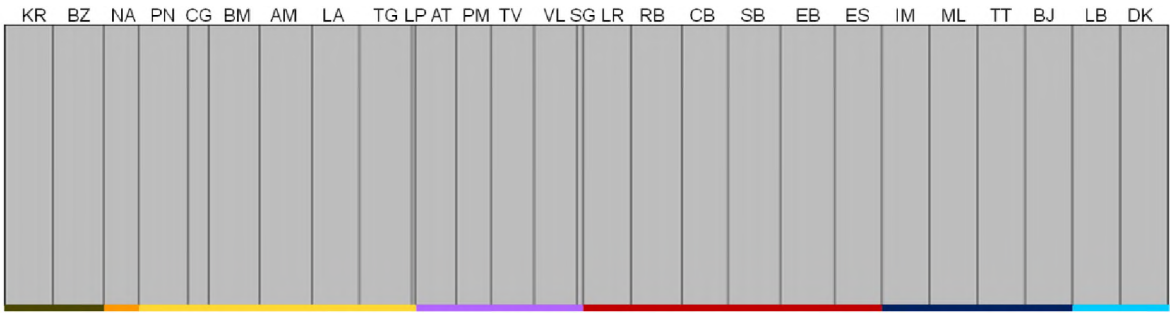

Figure 4.6 – Bayesian analysis summary plot (each bar represents one individual) of the 27 populations of *P. perna* obtained from STRUCTURE i.e. K = 1. Coloured bars depict expected genetic clusters. Bars of different widths indicate different sample sizes for the populations and are composed of single bars for each individual.

AMOVA indicated that most of the genetic variation arose within populations (99.96%; *p*=0.728, Table 4.9).

Table 4.9 – AMOVA from the 27 populations of *P. perna* distributed over seven distinct groups based on mitochondrial Cox1 gene and seven nuclear microsatellites.

Source of variation	df	Sum of squares	Variance components	Percentage of variation	ϕ-statistics	*p*-value
Among groups	6	16.79	0.0004	0.02	0.0002	0.351
Among populations within groups	20	54.17	0.0007	0.03	0.0003	0.76
Within populations	1437	3836.05	2.6695	99.96	0.0004	0.728
Total	1463	3907.01	2.6707			

Discriminant analyses of principal components (DAPC) suggested K=9 as the best fitting number of clusters (Fig. 4.7A). All clusters were distributed across the entire study area, revealing no spatial differentiation among groups (Fig. 4.7B).

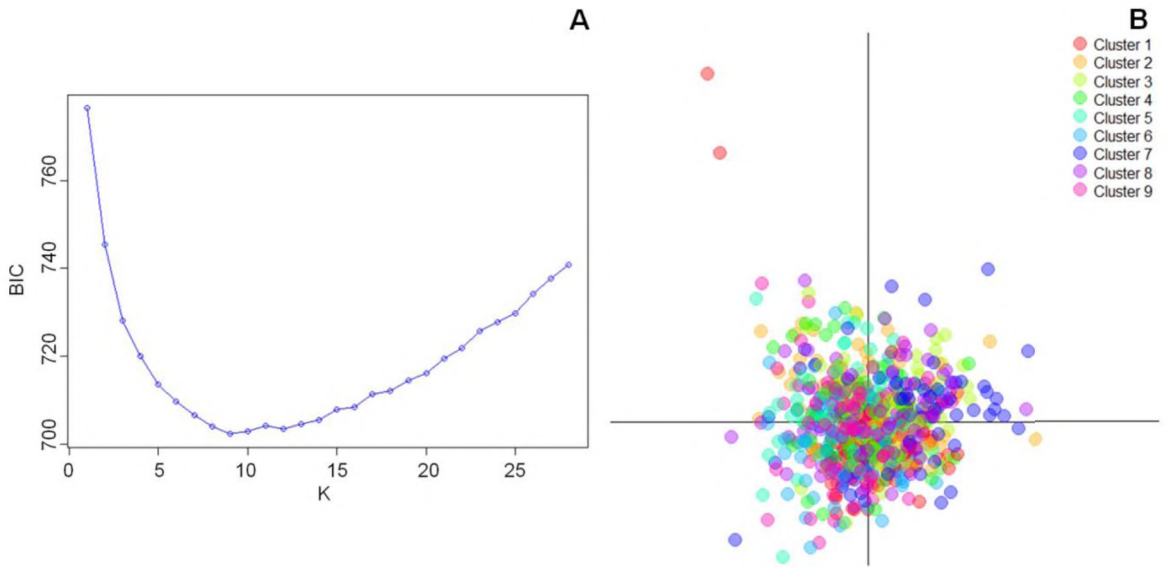

Figure 4.7 – Discriminant analyses of principal components (DAPC) results. A) Selection of best fitting K (K=9) based on Bayesian Information Criterion (BIC), B) DAPC spatial plot of the 27 populations of *P. perna* distributed through nine clusters. Colours correspond to distinct clusters. Each individual was assigned to a cluster and solid dots correspond to the overlapping of several individuals.

4.3.3 Sex-specific genetic structure of *P. perna*

4.3.3.1 Mitochondrial DNA

Sequences of male (*n*=133) and female (*n*=135) *P. perna* (615 bp Cox1 region) revealed 34 and 36 haplotypes, respectively (Table 4.10). LR showed the highest number of overall haplotypes for both males (11) and females (9), while BJ (for males) and DK (for females) showed the lowest (5 and 4, respectively). LR presented the highest number of unique haplotypes (8) in the male dataset while BJ did not show any unique haplotype. The greatest number of unique haplotypes in the female dataset corresponded to LR and TT (6), whereas DK showed the lowest number of unique haplotypes (1). Haplotype and nucleotide diversities varied between 0.648 (ML) and 0.933 (LR) and between 0.0014 (IM) and 0.0040 (LR), respectively in the male dataset. Female haplotype and nucleotide diversities varied between 0.562 (ML) and 0.800 (LR) and between 0.0011 (BJ) and 0.0026 (LR), respectively.

Table 4.10 – Genetic diversity of Cox1 gene of *P. perna* male and female datasets. *n*, sample size; H, number of haplotypes; UH, number of unique haplotypes; *h*, haplotype diversity (±SD); π, nucleotide diversity (±SD). Location codes as in Table 4.2.

Population	*n*	H	UH	*h*	π
Males	133	34	28	0.755 ± 0.035	0.0023 ± 0.0002
BM	15	6	4	0.705 ± 0.114	0.0023 ± 0.0008
LR	15	11	8	0.933 ± 0.054	0.0040 ± 0.0007
ES	15	7	3	0.724 ± 0.121	0.0019 ± 0.0005
IM	14	6	3	0.681 ± 0.132	0.0014 ± 0.0004
ML	15	6	3	0.648 ± 0.134	0.0022 ± 0.0006
TT	15	6	1	0.800 ± 0.077	0.0020 ± 0.0004
BJ	14	5	0	0.659 ± 0.123	0.0015 ± 0.0004
LB	15	6	3	0.762 ± 0.081	0.0021 ± 0.0005
DK	15	7	3	0.838 ± 0.068	0.0032 ± 0.0006
Females	135	36	30	0.671 ± 0.045	0.0020 ± 0.0002
BM	15	6	3	0.743 ± 0.094	0.0022 ± 0.0007
LR	15	9	6	0.800 ± 0.108	0.0026 ± 0.0006
ES	15	6	3	0.648 ± 0.134	0.0020 ± 0.0006
IM	15	5	3	0.638 ± 0.129	0.0012 ± 0.0003
ML	15	5	2	0.562 ± 0.143	0.0021 ± 0.0007
TT	15	7	6	0.657 ± 0.138	0.0020 ± 0.0007
BJ	15	6	4	0.571 ± 0.149	0.0011 ± 0.0004
LB	15	7	3	0.724 ± 0.121	0.0021 ± 0.0006
DK	15	4	1	0.695 ± 0.081	0.0022 ± 0.0006

Non-significant low pairwise ϕ_{ST} values were found across all populations for both datasets (Table A3 in Appendix) ranging from 0 to 0.0.15 (males) and from 0 and 0.101 (females).

AMOVA analyses attributed most of the variation within populations for both male and female datasets (males 99.76% *p*=0.33; females 98.96% *p*=0.12; Table A4 in Appendix).

4.3.3.2 Microsatellite markers

The male and female datasets of *P. perna* including nine populations presented 216 and 217 different alleles, respectively. The total number of alleles per locus ranged from 7 to 84 in the male dataset and varied between 8 and 83 within the female dataset. Male and female allelic richness varied between 10 (IM) and 11.714 (ML) and between 9.714 (IM) and 11.714 (LR), respectively. The male dataset included 57 unique alleles ranging from 8 (BM) to 14 (ML), while the female dataset comprised 59 unique alleles, varying between 5 (LB) and 16 (TT; Table 4.11). Expected (H_E) and observed (H_O) heterozygosities of the male dataset varied between 0.703 (IM) and 0.778 (BJ) and 0.714 (IM) and 0.805 (BJ), respectively. The inbreeding coefficient F_{IS} was always non-significant and ranged from -

0.032 to 0.042. Female H_E and H_O varied between 0.704 (DK) and 0.769 (LR) and 0.648 (DK) and 0.752 (TT), respectively. Most populations showed a significant positive inbreeding coefficient (F_{IS}) ranging from 0.027 to 0.155.

Table 4.11 – Genetic analyses of *P. perna* populations by sex. *n*, number of individuals per group; H_E, expected heterozygosity; H_O, observed heterozygosity; Â, allelic richness; F_{IS}, inbreeding coefficient; UA, unique alleles. Location codes as in Table 4.2.

Population	*n*	H_E	H_O	Â	F_{IS}	UA
Males	135	0.761	0.759	30.857	0.007	57
BM	15	0.726	0.752	10.857	-0.001	8
LR	15	0.757	0.754	10.714	0.038	9
ES	15	0.73	0.726	10.429	0.042	9
IM	15	0.703	0.714	10	0.018	13
ML	15	0.751	0.8	11.714	-0.032	14
TT	15	0.723	0.771	11.143	-0.032	12
BJ	15	0.778	0.805	11.143	0.000	10
LB	15	0.748	0.766	11	0.011	12
DK	15	0.732	0.743	10.714	0.020	9
Females	135	0.767	0.705	31.300	0.084**	59
BM	15	0.747	0.695	11.143	0.104**	13
LR	15	0.769	0.733	11.714	0.081*	8
ES	15	0.753	0.699	10.571	0.105**	11
IM	15	0.734	0.739	9.714	0.027	8
ML	15	0.741	0.727	10.429	0.055	7
TT	15	0.752	0.752	11.143	0.034	16
BJ	15	0.742	0.653	10.571	0.155**	10
LB	15	0.758	0.693	10.571	0.121**	5
DK	15	0.704	0.648	10.714	0.114**	11

Male and female F_{ST} values ranging from 0 to 0.015 and 0 and 0.010, respectively were non-significant (p>0.05) for all pairwise comparisons and did not support genetic subdivisions (Table A5 in Appendix). Jost's D ranged from 0 to 0.145 and 0 and 0.111 for male and female datasets and all the pairwise comparisons were non-significant (p>0.05; Table A5 in Appendix).

AMOVA attributed all the genetic variation of male and female individuals within populations (100%; p=0.580 and p=0.879, respectively; Table A6 in Appendix).

Bayesian admixture analyses implemented in STRUCTURE did not reveal any clear geographical clustering independently of the sex dataset. Evanno *et al.* (2005) method ΔK proposed K=3 for males and K=6 for females as the best fitting K, but the resolved clusters were consistently present at all populations and the log probability of both datasets (L(K)) suggested K=1 (Fig. A7–A8 in Appendix).

4.3.4 Environmental niche modelling

Pearson's correlation test revealed strong correlation between sea surface temperature (SST) and surface air temperature (SAT) and between nitrate and phosphate concentrations. Although the discarding of correlated variables may be an arbitrary procedure (Chefaoui *et al.*, 2016), the most ecologically representative variables for intertidal species were prioritized (e.g. Jones *et al.*, 2010, i.e. SST and nitrate concentration). After Pearson's correlation test minimum and maximum SST, nitrate concentration, salinity, cloud cover and the significant wave height were selected to perform the analyses.

The ensemble produced with the best models (TSS>0.7) resulted in an accurate overall description of *P. perna* native distribution, including its expanding front towards southern Iberia (Fig. 4.8). Along northern Africa, the niche model predicted a distribution from central Senegal north into the Mediterranean, as far as central-eastern Tunisia (Fig. 4.8A). In addition, the prediction indicated that suitable habitat could potentially be found from southeastern Spain to central Portugal. While the probability of *P. perna* being present on Mediterranean Spanish shores was high, towards the Atlantic the predicted likelihood decreased. On southwestern Iberian shores, the species is absent from several locations where it could be expected (Fig. 4.8B). Surprisingly, short portions of potential suitable habitat were detected along the warm equatorial Africa (in Ghana and Ivory Coast) and the Arabian Peninsula (Yemen and Oman) under the effect of upwelling cells.

RandomForest (RF) performed better than other techniques (AUC=0.939 ± 0.018 and TSS=0.775 ± 0.044, Table 4.12). The evaluation of the ensemble produced the following ROC-derived scores: AUC=0.968, sensitivity=99.099, and specificity=88.928; TSS=0.879, sensitivity=99.099, specificity=88.839, revealing an excellent prediction (AUC>0.9) and a high agreement between observed and modelled distribution of *P. perna* (sensitivity~100). By obtaining the highest score (0.26), minimum SST was the predictor that best explained the distribution of *P. perna* (Fig. 4.8C), when modelled alone in comparison with other predictors.

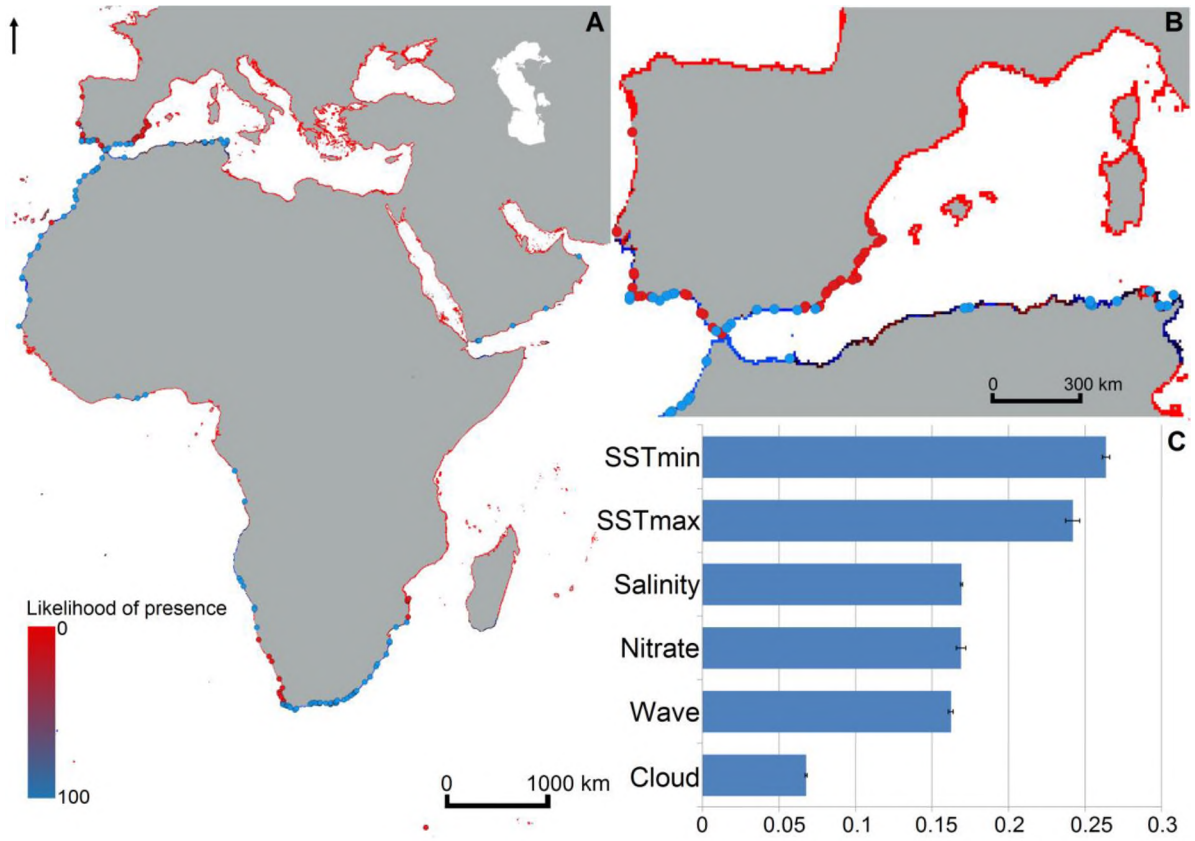

Figure 4.8 – Predicted native distribution for the brown mussel *P. perna* derived by averaging an ensemble of presence-absence algorithms. A) overall distribution, B) *P. perna* distribution along the expanding front in the Northern Hemisphere, C) Mean scores of the relative importance of the environmental variables obtained from the ensemble. Blue and red dots represent presence and absence data, respectively, obtained from field surveys and records in the literature (see Table A1 in Appendix).

Table 4.12 – Mean validation scores obtained using each of the distinct techniques (GLM, GBM, GAM, FDA, MARS and RF).

Model	AUC mean (±SD)	ROC sensitivity	ROC specificity	TSS mean (±SD)	Sensitivity (±SD)	Specificity (±SD)
GLM	0.901 ±0.022	86.182 ± 7.892	83.694 ± 6.395	0.689 ± 0.049	83.939 ± 7.579	84.792 ± 6.078
GBM	0.931 ±0.021	87.515 ± 5.829	87.745 ± 4.851	0.744 ± 0.059	85.757 ± 6.879	88.451 ± 4.338
GAM	0.903 ±0.025	89.758 ± 6.119	81.370 ± 4.660	0.699 ± 0.049	88.545 ± 6.429	81.311 ± 5.471
FDA	0.879 ±0.030	78.727 ± 7.231	87.260 ± 6.424	0.652 ± 0.064	76.303 ± 6.864	88.502 ± 4.241
MARS	0.879 ±0.099	82.121 ± 15.049	84.213 ± 7.620	0.657 ± 0.112	80.182 ± 14.632	85.311 ± 7.167
RF	0.939 ±0.018	92.424 ± 5.095	86.026 ± 4.060	0.775 ± 0.044	90.848 ± 4.762	86.417 ± 3.823

4.3.4.1 Case study: South Africa

Minimum SST was significantly lower where *P. perna* is absent compared to where the species is present (all trials $p<0.001$, Table 4.13, Fig. 4.9). In contrast, minimum SAT did not show any significant difference between the two groups of locations (trial 1 $p=0.796$;

trial 2 p=0.511; Trial 3 p=0.063; Table 4.13). Although only one subset is shown (Fig. 4.9), the results were consistent for all three.

Table 4.13 – One-way ANOVA on the effect of minimum sea surface temperature (SST min) and surface air temperature (SAT min) on *P. perna* presence/absence along the warm temperate and cool temperate southwest South African provinces at three trials (Trial 1, Trial 2 and Trial 3). Statistical significant values are depicted in bold.

	Trial 1				Trial 2				Trial 3			
Source	**df**	**MS**	**F-ratio**	***p*-value**	**df**	**MS**	**F-ratio**	***p*-value**	**df**	**MS**	**F-ratio**	***p*-value**
SST min												
Record	1	29.668	28.147	**0.000071**	1	35.149	31.860	**0.000037**	1	46.263	46.658	**0.000004**
Error	16	1.054			16	1.103			16	0.992		
SAT min												
Record	1	0.0775	0.0709	0.796	1	0.722	0.4607	0.511	1	6.5342	3.9276	0.063
Error	16	1.0929			16	1.5672			16	1.6637		

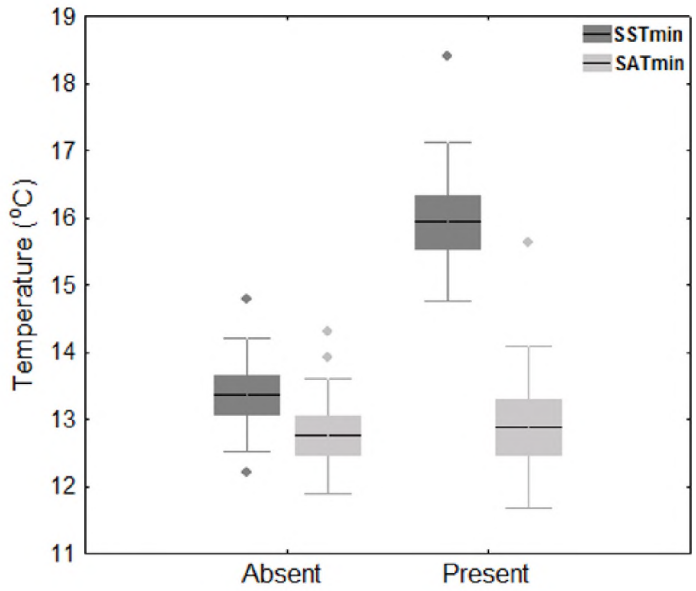

Figure 4.9 – Box-plot of minimum sea surface temperature (SST) and surface air temperature (SAT) of the two South African regions where *P. perna* is absent (cold water) or present (warm water). Box-plot depicts the mean (horizontal line), the standard error (bottom and top of the box) and the standard deviation (whiskers). Diamonds indicate outliers.

4.4 DISCUSSION

The results of this chapter indicate a lack of genetic differentiation of *Perna perna* populations across the study area (>4000 km), irrespective of an individual's sex. Moreover, the niche modelling framework highlights the key role of minimum sea surface temperature (SST) in shaping *P. perna* distributional range limits along its native areas including the southern Iberian expanding front.

4.4.1 Lack of genetic structure in the face of multiple oceanographic barriers

In marine organisms with sessile or highly sedentary adults, genetic structuring is often directly linked to dispersal barriers influencing the transport of planktonic propagules (Zardi *et al.*, 2007; Zhan *et al.*, 2009), though barriers for dispersal do not affect all species equally (Kelly & Palumbi, 2010; Villamor *et al.*, 2014).

The general assumption is that an extended dispersal phase coupled with very large population sizes will result in high levels of connectivity over large geographic scales and across biogeographic provinces (Kinlan & Gaines, 2003; Shanks *et al.*, 2003). In recent years, however, several studies have challenged this view, showing significant genetic structure in organisms with long pelagic larval stages (Sunday *et al.*, 2014; Varney *et al.*, 2016). For example, South African *P. perna* populations are characterised by marked genetic heterogeneity at both meso and macro spatial scales. At large scales, strong genetic division between two geographically defined groups of populations (temperate vs subtropical/tropical) in southern Africa are highlighted by mitochondrial (Cox1, Zardi *et al.*, 2007) and nuclear (ITS, Cunha *et al.*, 2014; microsatellites, Zardi *et al.*, 2015a) markers, though this appears to reflect the evolutionary history of the species. At smaller scales, mitochondrial data show that populations within the temperate group that occupy different bays are genetically distinct from each other and from populations on the open coast (Nicastro *et al.*, 2008).

In contrast to expected large scale genetic discontinuities in the face of numerous potential oceanographic dispersal barriers and selective environmental gradients along the study area, my multilocus approach unequivocally pointed to a northeastern Atlantic and Mediterranean panmictic population of *P. perna*. Previous studies have reported oceanographic barriers and genetic discontinuities at 1) the Strait of Gibraltar, meeting point between Atlantic and Mediterranean (Alboran Sea) waters (Patarnello *et al.*, 2007; Fratini *et al.*, 2016), 2) the Almeria-Oran front, separating the Alboran Sea from Western (European and African) Mediterranean (Patarnello *et al.*, 2007), 3) the Strait of Sicily,

connecting Western and Eastern Mediterranean (Buonomo *et al.*, 2017), 4) Cape Ghir upwelling (Jaziri & Benazzou, 2002; Neiva *et al.*, 2015) and around 5) Cape Boujdour (Ouazzani *et al.*, 2017). These known oceanographic barriers did not, however, cause genetic discontinuities in *P. perna*. The unexpected lack of genetic structure in *P. perna* across the oceanographic barriers described most likely results from a combination of the species' life history traits, habitat continuity and stepping stone movements. *Perna perna* is a broadcast spawner with a pelagic phase of 2–3 weeks (Vakily, 1989), a period that might be extended as a result of larval and postlarval behaviour (Bayne, 1965; Sigurdsson, 1976), and its distribution across northern Africa extends continuously through thousands of kilometres, from Tunisia to Senegal.

Habitat continuity and stepping-stone dynamics influence species genetic structure (Alberto *et al.*, 2010; Buonomo *et al.*, 2017). The dispersal capacity of *P. perna* due to its long planktonic phase, combined with its large continuous distribution and habitat continuity likely account for the lack of genetic structure, by enabling individuals to reach locations hundreds of kilometres apart through stepping-stone movement steps and consequently mixing gene pools. Additionally, hydrological features such as oceanic currents may enhance or limit large scale genetic homogenization of a species' gene pool (Lacerda *et al.*, 2016; Lal *et al.*, 2017). The slope currents contouring northern Africa and southern Iberia (Millot, 1999; Arístegui *et al.*, 2009) may therefore play a role in enhancing *P. perna* dispersal by promoting larval transportation and homogenizing the gene pool across the study area.

Evidence of panmixia has previously been provided for other species across some of the regions considered in this study (e. g. mitochondrial marker (D loop): fish species *Diplodus sargus*, *Pagellus bogaraveo*, *Pagrus pagrus* and *Scomber japonicas,* Patarnello *et al.*, 2007; mitochondrial markers (Cox1 and 16S), abalone *Haliotis tuberculata*, and chitons *Chiton olivaceus,* Fernández *et al.*, 2015). While I explain the genetic pattern of *P. perna* in terms of life history traits and ecological variables, other panmitic genetic signatures have been explained as unlikely to be due to dispersal, but rather the result of fluctuations in populations size (i.e. extinction/colonization and migration) and historical demography (Patarnello *et al.*, 2007; Fernández *et al.*, 2015).

Despite general evidence of panmixia across several taxa (Patarnello *et al.*, 2007; Fernández *et al.*, 2015), rangewide panmixia is extremely rare (but see Neethling *et al.*, 2008; Oomen *et al.*, 2011). The panmitic genetic pattern described from northern Africa and southern Iberia strongly contrasts with the genetic pattern observed from South African populations of *P. perna*. In South Africa, the Brown mussel shows a pronounced genetic break which corresponds to a marked biogeographic disjunction (temperate-

subtropical provinces), separating two distinct genetic lineages (Zardi *et al.*, 2007). Although *P. perna* shows similar life history traits, habitat continuity and stepping stone dynamics in both northern and southern Africa, the genetic structure in South Africa has a historical origin (Cunha *et al.*, 2014) and is presently maintained by the nearshore influence of the powerful Agulhas current, preventing larval dispersal and thus promoting local adaption (Zardi *et al.*, 2007, 2011a, 2015a). Along northern Africa and southern Iberia, neither historical nor contemporaneous genetic discontinuities were detected, as shown by the complete agreement between markers with varying rates of evolution (mitochondrial and nuclear markers).

Species genetic structure might be erroneously interpreted if sex-specific genetic differentiation exists within populations (see Teske *et al.*, 2012). Biparentally-inherited nuclear DNA (e.g. microsatellites) and maternally-inherited mitochondrial DNA (Female-mtDNA) have been used in conjunction to clarify hidden patterns of genetic structure, revealing discrepancies between markers (Palumbi & Baker, 1994; Lyrholm *et al.*, 1999 but see Escorza-Treviño & Dizon, 2000), which likely result from sex-specific differences in dispersal. In this study, in addition to identical genetic patterns depicted by mitochondrial and nuclear markers, no genetic differentiation has been observed for either males or females. Such lack of genetic heterogeneity contradicts the genetic structure described for female *P. perna* from South Africa using mtDNA (Teske *et al.*, 2012). Nicastro *et al.* (2008) showed that coastal topography helps shape *P. perna* genetic structure. Hence, the contrasting habitats, sheltered in South Africa (in Teske *et al.*, 2012) and open coast in northern Africa and southern Iberia, could provide a logic explanation for the conflicting genetic patterns. Unless post-settlement factors alter the genetic background by causing sex-biased mortality (see Teske *et al.*, 2012), genetic differences between males and females are unlikely to arise because dispersal is not expected to differ between sexes (Riginos *et al.*, 2004).

4.4.2 Minimum SST explains *P. perna* northern native range limits

The Iberian Peninsula is an interface region where several cold and warmwater species reach their southern or northern distributional limits (Pereira *et al.*, 2006; Lima *et al.*, 2007a), with several new distributional patterns resulting from range expansions and contractions being attributed to warming SST (e.g. the phaeophyte *Fucus vesiculosus,* Nicastro *et al.*, 2013; the pulmonate limpet *Siphonaria pectinata,* Rubal *et al.*, 2013, but see Lima *et al.*, 2009). The brown mussel *P. perna* has been intermittently recorded from Portuguese shores (Callapez *et al.*, 2012; Lourenço *et al.*, 2012) from fossil records,

kitchen middens and museum specimens dating from the Ancient Neolithic (8000–5000 BP), the Medieval Warm Period (12th century), the late 19th (1888–1899) and the early 20th (1938) centuries (Callapez *et al.*, 2012). These occurrences coincided with warmer periods of SST (see Eiríksson *et al.*, 2006; Mann *et al.*, 2009; Callapez *et al.*, 2012) and mirror a close relationship between the successive Iberian colonisation events of *P. perna* and major warmings of SST (Callapez *et al.*, 2012). Given how rising SST has shaped the distribution of *P. perna* both now and in the past, further poleward colonisation as warming continues can be expected (Collins *et al.*, 2013). Such distributional changes have already been demonstrated for other intertidal species across the study region. For example, the pulmonate limpet *S. pectinata* has expanded its distribution 185 km northwards since 1940, presumably driven by an increase in SST (Rubal *et al.*, 2013). Similarly, new northern limits for the limpet *Patella rustica* (Lima *et al.*, 2006) and macroalgae such as *Codium adhaerens* and *Padina pavonica* on Atlantic Iberian shores have been related to warming of SST (Lima *et al.*, 2007a).

Seawater temperature, whether minimum, mean, maximum SST or bottom water temperature, is a key variable in explaining the modelled distribution of nearshore species. In some case studies, SST has been found to be the main environmental contributor in the projection of species distribution (e.g. gastropod species *Littorina saxatilis*, the crab *Carcinus maenas* and the tunicate species *Styela clava*, de Rivera *et al.*, 2011). More often, even if not the most significant contributor, water temperature still remains one of the top environmental predictors explaining nearshore species distribution (Dennis & Hellberg, 2010; Reiss *et al.*, 2011; Assis *et al.*, 2015; Leidenberger *et al.*, 2015; Chefaoui *et al.*, 2016). For example, out of 24 variables considered, SST is within the top range distribution predictors of two intertidal gastropod cryptic species of the genus *Melampus* (Dennis & Hellberg, 2010). Moreover, bottom water temperature and depth have the greatest impact on the distribution of 14 benthic species out of 10 environmental variables modelled (Reiss *et al.*, 2011). The results of this study further support the determinant role of SST in explaining the distributions of nearshore organisms. Minimum SST was the predictor that best explained the native distribution of *P. perna*. The sharp drop in SST at Cape Gata (Tintore *et al.*, 1988; Folkard *et al.*, 1994) sets the northeastern limit of *P. perna* Iberian distribution, highlights the lack of suitable conditions farther east and is consistent with a preference for subtropical conditions. As SST and surface air temperature (SAT) are commonly linked to latitudinal gradients, difficulties arise when trying to tease apart their separate effects on biogeographic patterns (Mieszkowska *et al.*, 2006). Although SST and SAT were positively correlated across the entire native distribution, additional analyses of thermal regimes in South Africa provide an ideal

scenario to disentangle the relative significance of SAT and SST. South African shores are characterised by sharp environmental clines associated with abrupt species distributional changes (Emanuel *et al.*, 1992). *Perna perna* is absent from the cool west temperate province (minimum SST ranging 12.2–14.8 ºC, Fig. 4.9; winter SST 13–15 ºC, Demarcq *et al.*, 2003) but distributed across the southern warm temperate one (minimum SST ranging 14.5–18.7 ºC, Fig. 4.9; winter SST 15–19 ºC, Demarcq *et al.*, 2003). The west coast of South Africa is permanently affected by the cold waters of the Benguela upwelling system, which have been proposed as important variables limiting *P. perna* distribution (Zardi *et al.*, 2007). In contrast, the southwesterly flowing Agulhas current transports warm water along the east and south coasts of South Africa (Lutjeharms, 2006), offering suitable conditions for *P. perna*. My results show that minimum SST values are significantly lower along the west than the south coast, while SAT shows no such pattern. My findings support previous studies indicating SST as a major predictor of intertidal species distribution, increase our understanding of the role of minimum SST and SAT in setting species range limits at a regional level and emphasise the importance of low SST in limiting *P. perna* distribution in the Iberian Peninsula. The inability of *P. perna* to persist under cold water conditions can be the result of sub lethal effects on its metabolism. Extremely low densities of rare adult *P. perna* individuals along the west coast of South Africa, indicating that the species can survive after settlement but it is unable to reproduce under low SST, even where food availability is particularly high (Tagliarolo *et al.*, 2016).

Maximum SST also influences range distribution and habitat suitability of intertidal organisms (Jones *et al.*, 2010; Jones *et al.*, 2012). Towards equatorial Africa, *P. perna* records are scarce, and the few documented native populations (Zabi, 1982; Otchere *et al.*, 2003) are restricted to colder upwelling areas in Ghana and Ivory Coast (Picaut, 1983). Unsuitable higher equatorial SST, above optimal/maximum SST (18.9–31.7 ºC, Table 4.3), most likely prevents *P. perna* persistence. This hypothesis confirms previous results showing the limiting effect of maximum SST on intertidal species distribution (e.g *Himanthalia elongata*, Martínez *et al.*, 2012; *Undaria pinnatifida*, James *et al.*, 2015). Additionally, the distributional gradients of marine species have also been explained by changes in salinity (e.g. Jaspers *et al.*, 2011), nutrients as nitrate (e.g. Underwood *et al.*, 1998) or waves (e.g. Bustamante & Branch, 1996a). Low cloud cover can also lead to an increase of organisms' body temperature which can interact with other biological parameters and ultimately control species distribution (Hofmann & Somero, 1995).

Total agreement between modelled and observed distributions reflects complete occupation of the species' potential niche (Assis *et al.*, 2015). This has been shown for

the invasive distribution of the blue mussel *Mytilus galloprovincialis* along the shores of South Africa (Assis *et al.*, 2015). *Mytilus galloprovincialis* arrived on South African shores in the late 1970s (Griffiths *et al.*, 1992) and has now occupied all suitable habitats which corresponds to about 2800 km of coast (Assis *et al.*, 2015). In the present study, an extremely high, nearly complete agreement between observed and modelled niche ranges was obtained (sensitivity=99.099), although this is marginally lower than the previous example. The slight disagreement between observed and predicted niche ranges implies that some suitable habitats still remain unoccupied and that additional abiotic or biotic factors may affect the distribution of *P. perna*. The northwesternmost observed Iberian distributional limit of *P. perna*, Castelejo (Portugal), is approximately 180 km south of the predicted limit (Cape Roca), depicting a stretch of coast that has not yet been colonised despite the existence of suitable environmental conditions. Considering the great dispersal capacity of *P. perna* and its ability to cross oceanographic barriers (see above), it could be expected that the entire realized niche would be occupied. Plausible explanations for this discrepancy include insufficient time for colonisation or biological interaction. *Perna perna* specimens could be absent from most southwest Portuguese shores due to a slow occupation of the potential niche. However, the species is characterized by highly invasive behaviour, spreading for hundreds of km under suitable environmental conditions (Hicks & Tunnell, 1993, 1995). Alternatively, *P. perna*, could be ecologically excluded from suitable habitat. Interaction with recipient communities is a major determinant of the success of establishment of a species reaching a new region (Sanford & Swezey, 2008). Along most northern and southern parts of the African coastline and also in southern Iberia, *P. perna* coexists with *M. galloprovincialis* (for South Africa: Zardi *et al.*, 2006a, 2007; Nicastro *et al.*, 2009; for northern Africa: Shafee, 1989; Abada-Boudjema & Davin, 1995; for Iberia: Lourenço *et al.*, 2012). *Mytilus galloprovincialis* exhibits competitive dominance over South African intertidal species (*Aulacomya ater* and *Choromytilus meridionalis*, Hockey & van Erkom Schurink, 1992; Robinson et al., 2007), including *P. perna* (at least at upper intertidal levels, Bownes & McQuaid, 2006). Hence, the Brown mussel might be similarly outcompeted by *M. galloprovincialis* from southwest Portugal by means of higher recruitment rates (Harris *et al.*, 1998), faster growth (Hockey & van Erkom Schurink, 1992) and/or greater colonisation ability (Erlandsson *et al.*, 2006), hindering successful habitat occupation.

The easternmost population of *P. perna* in northern Africa is 213 km north of the realized southern limit. Moving south, the Brown mussel could be expected from southern Madagascar and Somalia, for approximately 630 km and 180 km of coast, respectively. Unfortunately, unequivocal evidence of *P. perna* from these regions is lacking. Despite

the strong support given by presence/absence records of this study and the ensemble framework itself, additional field surveys in areas predicted by the ensemble framework as likely to host *P. perna* (eastern Tunisia, southern Madagascar and Somalia) would highly benefit a complete understanding of the variables affecting *P. perna* distribution.

4.4.3 Final remarks

In this chapter I report the most extensive genetic continuity so far observed for an intertidal organism distributed across northeastern Atlantic and Mediterranean shores (>4000 km), despite the existence of several oceanographic barriers to dispersal previously described in the literature. Moreover, I report a lack of sex-specific genetic structure along the study area for the brown mussel *P. perna*, which contradicts the genetic structure described for female *P. perna* from South Africa (Teske *et al.*, 2012).

Historical records of the presence of *P. perna* in Iberia during past warm periods reinforce the key role of SST in shaping its distribution and range limits. It is expected that forthcoming warming of SST will continue to allow the species to extend further north, unless additional biotic or abiotic agents are able to successfully displace the species from the intertidal zone.

This chapter highlights the importance of adopting a multidisciplinary approach based on species distribution, genetic characterization and ecological niche modelling if one wishes to understand how species distributions and range limits are likely to respond to climate warming. I also emphasise that this approach identifies potential distributions; realised ranges will reflect the additional effects of biological interactions.

Additional field surveys of areas with suitable, but unoccupied habitat will provide a better understanding of the complementary factors influencing *P. perna* range distribution. It is likely that *P. perna* distribution over southern Iberia will be influenced by biological constraints similar to those experienced in other parts of the world (Bownes & McQuaid, 2006; Rius & McQuaid, 2006). However, local intertidal communities and environmental conditions can unpredictably alter distribution patterns, stressing the importance of a future monitoring to clarify the range of *P. perna*.

CHAPTER 5

Upwelling driven-incidence of endolithic infestation and its effects on mussel bed microclimates of *Mytilus galloprovincialis*

Endolithic infestation of the mussel *M. galloprovincialis*.

5.1 INTRODUCTION

Organisms commonly form groups that mitigate either rates of predation or environmental stresses. Such aggregations have long been described as evolutionarily advantageous as the members benefit from increased survivorship and reproductive success, but the advantages of protection against predators and environmental conditions are balanced against the need to compete for resources and the possibility of increased risk of disease (Parrish & Edelstein-Keshet, 1999; Fellous & Salvaudon, 2009). Intertidal marine organisms frequently form patchy or very dense aggregations to cope with harsh environmental conditions. By aggregating, sea snails minimize desiccation stress and experience a reduction in dislodgement caused by water movement (e.g. Feare, 1971; Garrity, 1984; Rojas *et al.*, 2013). Similarly, mussel beds improve individual growth and resistance to waves (van de Koppel *et al.*, 2008).

As bioengineers, mussels are important to the functioning of intertidal ecosystems. Mussel beds provide shelter, substratum and food resources; they increase habitat complexity and alter intertidal humidity and temperature conditions (Ricciardi *et al.*, 1997; Thiel & Ullrich, 2002; O'Donnell, 2008; Nicastro *et al.*, 2012), thus enhancing species richness and species density and shaping trophic networks (Ricciardi *et al.*, 1997; Christianen *et al.*, 2016). The thermoregulatory effects of these aggregations are particularly relevant in the context of climate change. Intertidal mussels inhabit areas within a strong terrestrial-marine gradient, where they are exposed on a daily basis to dramatic environmental changes (Helmuth *et al.*, 2006, 2016; Lathlean *et al.*, 2016a) and live close to their thermal tolerance limits, potentially facing mass mortalities and population extinctions driven by rising temperatures (Jones *et al.*, 2010; Harley, 2011). Moreover, the thermal environment of mussel aggregations is not static but undergoes small scale variations due to species-specific behaviour (Nicastro *et al.*, 2012) or interactions among distinct microhabitat components (Helmuth, 1998). For example, gaping (periodic valve movement during emersion) by the brown mussel *Perna perna* leads to decreased temperatures and increased humidity within mussel aggregations (Nicastro *et al.*, 2012). Similarly, shading by neighbours results in distinct microclimates for solitary or aggregated mussels (Helmuth, 1998) and wind-induced convection may lower mussels' body temperatures (Helmuth *et al.*, 2011). Additionally, it has also been shown that the body temperature of individual mussels is altered by the action of endolithic parasites (Zardi *et al.*, 2016).

Phototrophic endolithic parasitism is a widespread phenomenon in mussels. Photosynthetic endoliths are metabolically dependent on their hosts as they excavate the host shell through chemical dissolution, converting carbonate ions from calcite into carbon

dioxide, which they require for photosynthesis (Garcia-Pichel *et al.*, 2010). This chemical dissolution degrades the outer layer of mussel shells leading to localized shell discolouration (i.e. shell whitening, Kaehler, 1999). With extreme infestation events, shell whitening may cover the entire shell (Kaehler, 1999). Such white discoloration enhances solar reflectivity, diminishing the absorbed energy, eventually leading to a reduction of mussel body temperature (Zardi *et al.*, 2016). Although the cooling effect of endolithic parasitism has been shown for mussels within aggregations and in solitary individuals (Zardi *et al.*, 2016), how infestation alters environmental conditions within mussel beds and whether endolith-induced cooling extends to neighbouring mussels have never been studied. Interestingly, the prevalence of infestation on mussels may differ greatly locally and regionally, dictated by factors that damage the outer layer of the shell (e.g. sand erosion) and light availability (Kaehler, 1999; Zardi *et al.*, 2009; Marquet *et al.*, 2013; Ćurin *et al.*, 2014). Mussels in wave-exposed sites exhibit higher endolithic infestation than mussels in bays, presumably because sediment load caused by waves removes the outer layer of mussel shells (i.e. the proteinaceous periostracum), facilitating endolithic infestation (Zardi *et al.*, 2009). At small scales, endolithic infestation on mussels has also been shown to differ significantly between shaded and non-shaded areas, with greatest incidence of infestation where irradiance is strongest (Zardi *et al.*, 2009). Thus, environmental variables that control light availability at a larger scale than within the intertidal habitat, such as cloud cover, may dictate geographical patterns of endolithic infestation. Light availability follows a latitudinal gradient, increasing towards lower latitudes as cloud cover decreases (Wetherald & Manabe, 1980; Warren *et al.*, 1986). Also, decreased solar irradiance and fog occurrence have been linked to upwelling phenomena as cold upwelled waters cool the atmosphere above the sea surface causing water vapour to condense (Tont, 1975, 1981; Olivier & Stockton, 1989; Cereceda *et al.*, 2002; Cermak, 2012).

The Iberian Peninsula and the Moroccan shores constitute a quasi-continuous stretch of coastline characterized by a latitudinal gradient with multiple upwelling cells, interspersed by areas that are seldom affected by upwelled waters (Marcello *et al.*, 2011; Benazzouz *et al.*, 2014). This is an ideal region to investigate the variation of endolithic infestation on intertidal mussels, and thus set the context for the aims of this study.

Here, I explore large scale infestation severity to understand whether endolithic infestation follows a latitudinal gradient and varies in parallel with upwelling intensity and investigate the thermal properties of infested and non-infested beds of the mussel *Mytilus galloprovincialis*. Specifically, I 1) sampled along >10^{o} latitude of coast to understand if the degree of infestation increases as latitude decreases and if it differs between upwelling

and non upwelling areas, 2) simulated artificial mussel beds to investigate if mussel beds made up of infested individuals exhibit decreased temperatures and increased humidity within the interstitial spaces and 3) mussels surrounded by infested mussels experience lower body temperatures than those surrounded by non-infested mussels.

5.2 MATERIAL AND METHODS

5.2.1 Study area and model species

This chapter targeted the temperate intertidal mussel *Mytilus galloprovincialis* collected from 12 sites distributed along ~1000 km of the southwestern (SW) and southern Portugal coastlines and the Atlantic coast of Morocco (from Malhão, SW Portugal, site MA, 37°46'56.47"N 08°48'08.30"W to El Ouatia, southern Morocco, site TT, 28°30'05.58"N 11°20'06.38"W; Table 5.1). Sampling took place in May–June 2016. All locations were moderately exposed intertidal rocky shores, experiencing low tide at approximately the same time of day. Only monolayered mussel beds (i.e. mussels attached directly to the substratum) in sun-exposed areas (i.e. surfaces exposed to solar radiation 60% of the day; Zardi *et al.*, 2009) were considered.

Table 5.1 – Sampling locations, organized from north to south.

Country	Location	Code	Coordinates
Portugal	Malhão	MA	37°46'56.47"N; 08°48'08.30"W
Portugal	Castelejo	CT	37°06'08.09"N; 08°56'44.99"W
Portugal	Vilamoura	VL	37°04′19.70"N; 08°07′19.71"W
Portugal	Farol	FL	36°58′29.38"N; 07°51′42.51"W
Morocco	Larache	LR	35°11'48.14"N; 06°09'30.61"W
Morocco	Rabat	RB	34°01'57.26"N; 06°50'27.96"W
Morocco	Sidi Bouzid	SB	33°13'06.11"N; 08°34'23.19"W
Morocco	El Beddouza	EB	32°32'42.33"N; 09°16'55.34"W
Morocco	Essaouira	ES	31°30'42.78"N; 09°46'24.31"W
Morocco	Imsouane	IM	30°50'24.43"N; 09°49'21.92"W
Morocco	Mirleft	ML	29°35'06.58"N; 10°02'50.78"W
Morocco	El Ouatia	TT	28°30'05.58"N; 11°20'06.38"W

5.2.2 Degree of infestation along Portugal and Morocco

At each site, three quadrats (15 x 15 cm) were haphazardly sampled from areas with 100% mussel cover in the centre of the *M. galloprovincialis* zone. Mussels were measured and separated into 10-mm size classes according to shell length (SL) and the degree of endolithic infestation was evaluated following the classification of Kaehler (1999): Group A, shells with clean, intact periostracum and distinct periostracal striations; Group B, shells with central portion of surface eroding, outer striations on periostracum becoming indistinct; Group C, shells with erosion spreading past central portion, grooves and pits appearing on the shell surface; Group D, shells heavily pitted and becoming deformed,

outer striations on periostracum almost completely absent; Group E, shells extremely pitted, deformed and brittle, eventually with holes.

5.2.2.1 Calculation of upwelling index

The cross-shore Ekman transport (CSET), a wind-based upwelling index, was used to estimate upwelling intensity between 2011 and 2015 as in Krug *et al.* (2017). Daily sea surface wind fields (speed and direction) were obtained from the Blended Sea Winds dataset (National Climatic Data Centre - National Oceanic and Atmospheric Administration, NCFC-NOAA, http://www.ncdc.noaa.gov/oa/rsad/air-sea/seawinds.html) at a spatial resolution of 0.25°. The Blended Sea Winds dataset combines various scatterometres standardized across platforms, which results in a high quality of temporal and spatial coverage of ocean wind vectors (Zhang *et al.*, 2006). CSET values were estimated for 12 locations along the Portuguese and Moroccan coasts (Table 5.1). The western coast of Portugal and the Atlantic coast of Morocco are meridionally (north-south) oriented; conversely, the southern Portuguese coast is zonally (west-east) oriented. CSET values represented the average of a 0.75 x 0.75° box centred at each target location.
The zonal component of the Ekman transport ($CSET_x$), induced by the meridional component of wind-stress (τ_y), was used as an upwelling index over the stations of Morocco and western Portugal. The meridional component of the Ekman transport ($CSET_y$), induced by the zonal component of wind-stress (τ_x), was used as an upwelling index over the southern Portuguese stations. $CSET_x$ and $CSET_y$ ($m^3\ s^{-1}\ km^{-1}$ coastline) were calculated according to (Bakun, 1973; Alvarez *et al.*, 2011):

$$\mathrm{CSET}_x = \frac{1000\ \tau_y}{\rho_w f} = \frac{\rho_a\, c_d}{\rho_w f}\ (W_x^2+W_y^2)^{1/2}\ 1000\ W_y$$

$$\mathrm{CSET}_y = \frac{1000\ \tau_x}{\rho_w f} = \frac{\rho_a\, c_d}{\rho_w f}\ (W_x^2+W_y^2)^{1/2}\ 1000\ W_x$$

In the equations, ρ_w represents seawater density (1025 kg m^{-3}), ρ_a represents air density (1.22 kg m^{-3}), C_d refers to the drag coefficient ($1.4x10^{-3}$), *W* refers to wind magnitude (m s^{-1}) and *f* represents the Coriolis parameter, inferred from 2 Ω sin(θ); Ω represents the vertical component of the Earth's angular velocity and θ is the local latitude. Negative CSET values indicate upwelling-favourable periods with offshore Ekman transport and conversely, positive values indicate downwelling-favourable periods and onshore Ekman transport.

5.2.3 The effect of infestation on the thermal properties of mussel bed microclimates

The effects of endolithic infestation on mussel bed interstitial spaces were investigated by deploying temperature and humidity data-loggers (hygrochron iButtons DS1923, Maxim Integrated Products, Dallas Semiconductor, USA) inside infested or non-infested beds. These provided relative humidity measurements with a resolution of 0.04% and temperature accuracy of ±0.5 °C and resolution of 0.0625 °C. Loggers were deployed in artificial mussel beds made up of either 100% non-infested (Group A, clean treatment) or heavily infested (Group D, infested treatment) biomimetic mussels (Fig. 5.1). Biomimetic mussels mirror thermal properties of living mussels (Helmuth & Hofmann, 2001) and were used to artificially create mussel beds. They were made by filling empty mussel valves (SL 45 mm ± 5 mm) with silicone sealant and left to dry at ambient temperature for at least 48 h. The beds (n=3 per treatment) were circular (diameter of ca. 16 cm) made up of biomimetic mussels (n~60) arranged vertically, with the umbo of each mussel on the substratum, to mimic their natural position on the shore (Fig. 5.1). Partially rigid, white PVC net (mesh size 1 cm) was placed under and around the beds to prevent biomimetic mussels from falling (see Nicastro *et al.*, 2012). Prior to the experiment, in order to ensure that all artificial beds were exposed to the same environmental conditions (temperature and light), artificial mussel beds were kept in the dark overnight and immersed in water (ca. 18 °C) for 15 min. After emersion, two loggers were immediately inserted into the centre of each bed, recording temperature and humidity data every 5 min. Mussel beds were then placed on white horizontal boards and aerially exposed to ambient sunny conditions for 80 min. The experiment was run twice (on the 17th and 19th August, 2016, referred to as day 1s and day 2s, respectively), during high sun elevation (12 h−15 h) and clear sky conditions at CCMar–Centre of Marine Sciences, Faro, Portugal. Each trial was conducted with different mussel beds to avoid pseudoreplication.

Figure 5.1 – Artificial 100% non-infested (Group A, clean treatment; left) or heavily infested (Group D, infested treatment; right) mussel beds built with biomimetic mussels.

5.2.4 The effect of infestation-induced cooling on the body temperatures of neighbouring mussels

The effect of cooling on neighbouring mussel body temperatures was investigated using robomussels. These were built similarly to biomimetic mussels, described above, with the addition of a temperature data-logger (thermochron iButton DS1921G, Maxim Integrated Products, Dallas Semiconductor, USA; accuracy ±1°C, measurements in 0.5 °C increments) embedded in the inner silicone content. By having a temperature data-logger inside, robomussels capture mussel body temperature (see Helmuth & Hofmann, 2001). Loggers were set to record robomussel body temperatures every 5 min. Clean or infested robomussels were deployed in the centre of 100% clean or infested biomimetic mussel beds. Clean or infested robomussel treatments were tested separately on three distinct days each (clean robomussels: 10th and 17th September and 6th October 2016, referred to as day 1c, day 2c and day 3c, respectively; infested robomussels: 11th and 16th September and 5th October 2016, day 1i, day 2i and day 3i), under clear sky conditions and high sun elevation (12 h−14 h) at CCMar–Centre of Marine Sciences, Faro, Portugal. Each mussel bed (n=6 clean and n=6 infested beds) had a robomussel positioned in the centre and was kept in the dark overnight. Prior to the experiment, mussel beds were immersed in water (ca. 18 ºC) for 15 min and immediately placed on white boards aerially exposed to ambient sunny conditions for 80 min after emersion. New mussel beds were arranged for each trial to avoid pseudoreplication.

5.2.5 Data analyses

The incidence of endoliths was analysed based on the proportion (%) of each degree of infestation (Group A–E) for each site and size class.

Daily CSET data were monthly averaged to reduce the influence of daily anomalies and consequently used to select the annual minimum. The overall mean of upwelling indices (UImean) for the 5-year period was obtained by averaging the five minimum annual CSET (i.e. one value per year). Mean upwelling index of the 5-year period (2011–2015) per site was referred to as upwelling intensity in Spearman's rank correlation analyses.

Spearman's rank correlation was used to evaluate the relationship between infestation frequency (%) and 1) latitude and 2) upwelling intensity of sampling sites. To avoid bias due to uneven distribution of size classes, a Spearman's rank correlation exclusively for mussels belonging to the size class that was common in all quadrats and all sites (SL 20−30 mm) was performed.

Data on temperature and humidity of interstitial spaces in mussel beds were analysed separately using nested ANOVAs with bed (clean or infested) as a fixed factor, bed replicate (3 levels) as a random nested factor and either temperature (°C) or humidity (% relative humidity) as the dependent variable. Temperatures experienced by clean and infested robomussels were analysed separately using one-way ANOVA with bed (clean or infested) as a fixed factor. The nested ANOVAs and one-way ANOVAs were undertaken for two time points (i.e. 40 min and 80 min of sun exposure, representing the mid and endpoints of each experiment).

Data were tested for the prerequisites for parametric analysis (Shapiro's and Cochran's tests) and were analysed using STATISTICA 7.1 software (StatSoft, 2005). When normality or homoscedasticity requirements were not met, analyses were run with the PERMANOVA module (Anderson 2001; McArdle and Anderson 2001), which does not require prior assumptions. In this case, pairwise tests were performed using 999 permutations.

5.3 RESULTS

5.3.1 Degree of infestation along Portugal and Morocco

Severity and prevalence of infestation of *Mytilus galloprovincialis* increased with shell length (SL) throughout the study area (Fig. 5.2). Mussels ranging up to 40-mm SL (size classes 0−10, 10−20, 20−30 and 30−40 mm) were present at all locations (in at least one quadrat) and highlighted a tendency for more severe infestations towards southern locations (e.g. 0% infestation of Group C at MA, the most northerly site, and 67% at site TT, in the extreme south, for the 0−10 mm size class). Initial infestation (Group B) generally appeared in the smallest size class (0−10 mm SL) except for sites VL, FL, IM and ML (Group B infestation started at 10−20 mm SL). Additionally, shells with high levels of erosion and pitting (Group D) were found at all sites except two of the northernmost sites, CT and VL. MA was the only site where endolith-induced shell fractures were detected (Group E; two mussels, 0.2% occurrence in size class 10−20 mm SL).

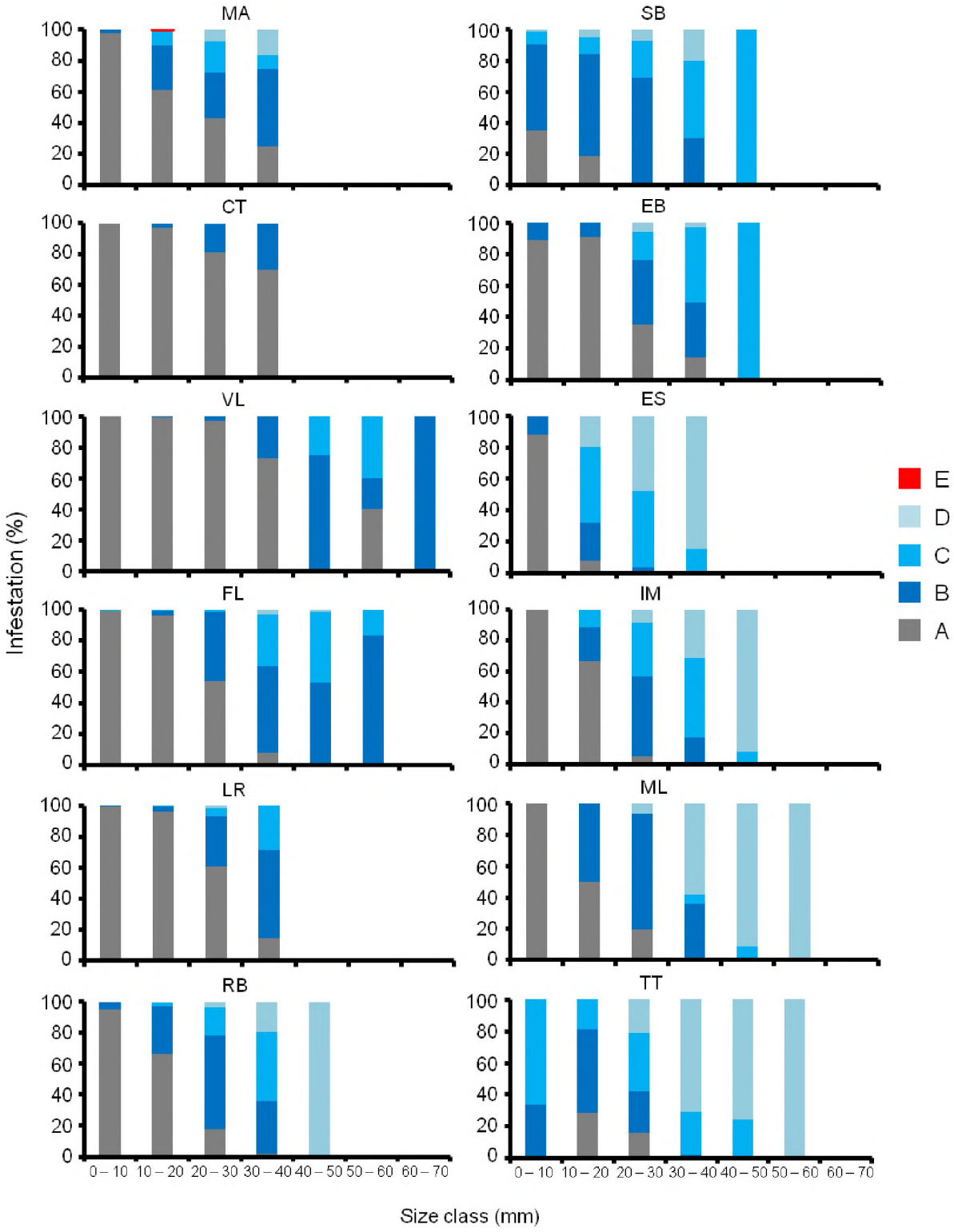

Figure 5.2 – Incidence of endoliths on *M. galloprovincialis* along Portuguese and Moroccan coasts. Proportion (%) of shells infested grouped into 10−mm size classes and classified as distinct degrees of infestation severity (Group A, shells with clean, intact periostracum, to Group E, shells extremely pitted, deformed and brittle, eventually with holes). Sites are arranged north to south (top to bottom and left to right) from MA to TT (MA–FL, Portugal; LR–TT, Morocco; as in Table 5.1). Group E infestation was only found at site MA, in mussels ranging 10–20 mm.

The lowest frequency of endolithic infestation was detected at FL for both size class datasets (all size classes, Fig. 5.3A; 20–30 mm size class Fig. 5.3D). Greatest frequency of infestation was detected at ML (all size classes, Fig. 5.3A) and ES (20–30 mm size class Fig. 5.3D). Infestation significantly increased at lower latitudes (Fig. 5.3B, Spearman's rank correlation: rs=-0.82, n=36, p<0.0001) and towards greater upwelling intensities (more negative values, Spearman's rank correlation: rs=-0.54, n=36, p=0.0001; Fig. 5.3C). This was also true when only the common size class was considered (20−30 mm SL, Spearman's rank correlation: latitude rs=-0.66, n=36, p<0.0001; Fig. 5.3E, upwelling index rs=-0.41, n=36, p=0.013; Fig. 5.3F). Overall, sites VL and ML showed the lowest (2%) and highest (98%) proportion of endolithic infestation, respectively.

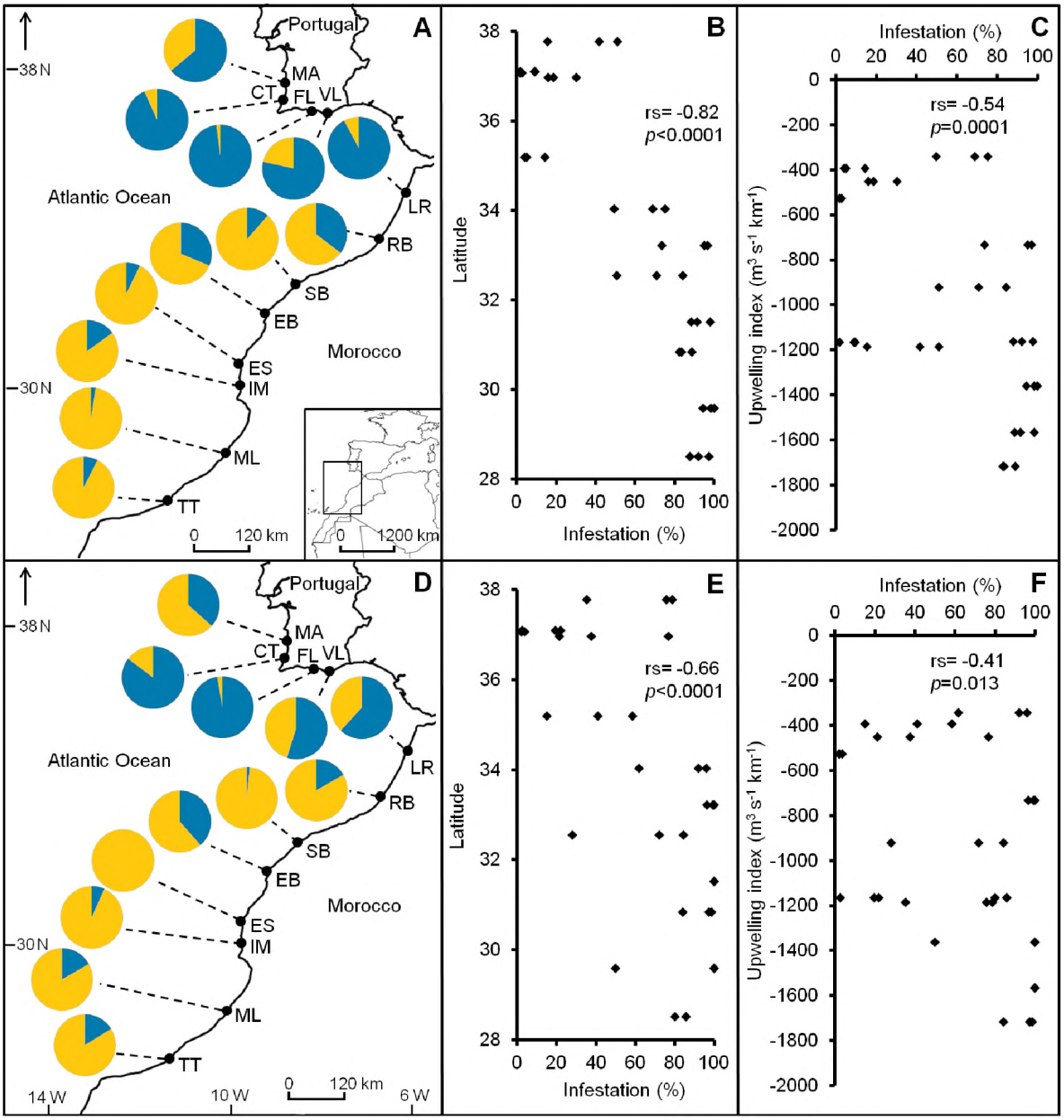

Figure 5.3 – Frequency of endolithic infestation on *M. galloprovincialis* at each sampling site. Location codes as in Table 5.1. Yellow indicates proportion of infested shells: (A) all size classes and (D) 20–30 mm size class only. Correlation between frequency of infestation and latitude: (B) all size classes and (E) 20–30 mm size class only. Correlation between frequency of infestation and upwelling index: (C) all size classes and (F) 20–30 mm size class only.

5.3.2 The effect of infestation on the thermal properties of mussel bed microclimates

The interstitial spaces in clean (non-infested) mussel beds were warmer and less humid than in infested mussel beds (Fig. 5.4, Table 5.2). In general, temperatures in both mussel bed treatments increased through time while humidity decreased. Initial temperature varied between 22.5 and 23.6 ºC on day 1s (Fig. 5.4A) and 20.5 and 21.1 ºC on day 2s

(Fig. 5.4B). Relative humidity (RH) ranged between 87.8−91.9% and 92.8−95.6% on day 1s (Fig. 5.4A) and day 2s (Fig. 5.4B), respectively. Changes in temperature and humidity gradually decreased towards the end of the experiments, generally reaching a plateau at approximately 70−75 min. By the end of the experiment, interstitial temperatures in non-infested and infested beds had increased on average 78% and 72.3% respectively, while relative humidity decreased on average 55.1% and 52.4%. Clean mussel beds generally showed higher temperatures and lower relative humidity than infested beds. At 40 min, non-infested mussel beds exhibited significantly higher temperatures (on average 2.9 °C higher; $p<0.05$ in both cases; Table 5.2) and lower relative humidity (on average 12.7% RH lower; day 1s $p<0.01$; day 2s $p<0.05$; Table 5.2) than infested beds. At 80 min, temperature and relative humidity of non-infested and infested beds did not differ significantly ($p>0.05$ in both cases; Table 5.2).

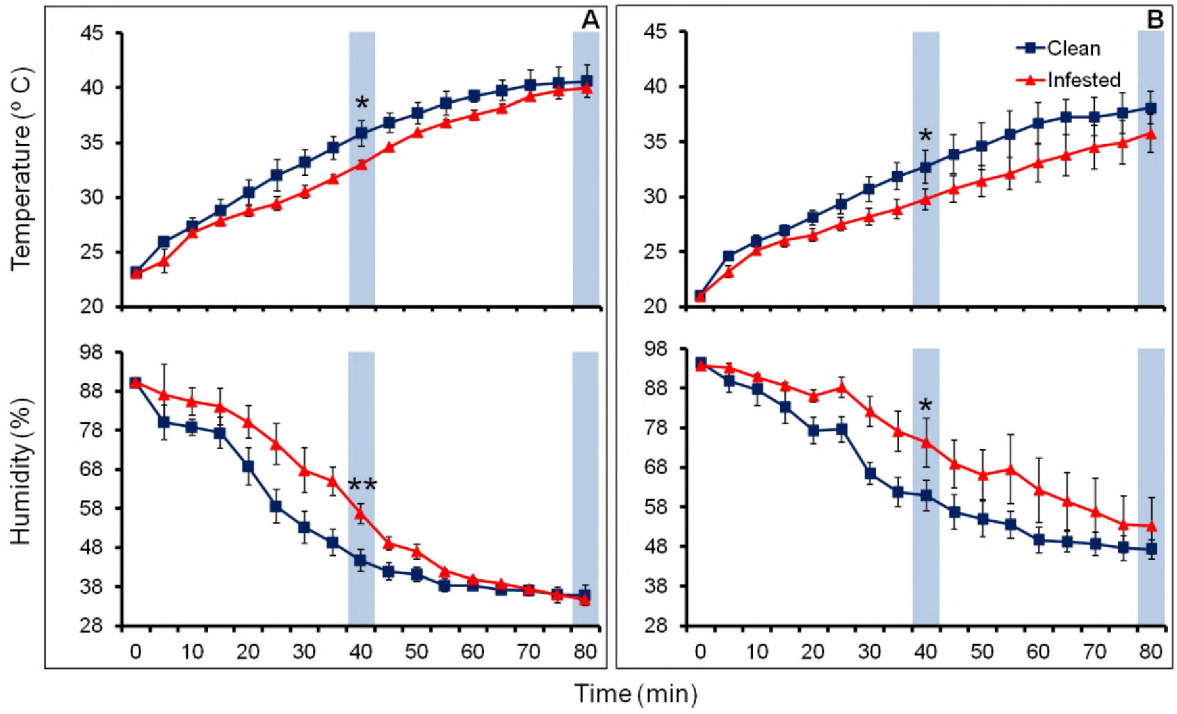

Figure 5.4 – Effect of mussel bed infestation on mean temperature and humidity (n=3; ±SD) within mussel bed interstitial spaces. Results separated by day: A) day 1s, B) day 2s. Top panels represent temperature (°C) and bottom panels represent relative humidity (%). Shade areas depict statistical analyses performed at mid- (40 min) and endpoints (80 min) of the experiment. Statistical significance is represented by * ($p<0.05$) or ** ($p<0.01$).

Table 5.2 – Nested ANOVA on the effect of mussel bed endolithic infestation on temperature and humidity of mussel bed interstitial space at 40 and 80 min after aerial sun exposure on day 1s and day 2s. The nested term is Bed (replicate). Statistically significant values ($p < 0.05$) are in bold.

		Day 1s				Day 2s		
Source	**df**	**MS**	***F*-ratio**	***p*-value**	**df**	**MS**	***F*-ratio**	***p*-value**
Temperature								
40 min								
Bed	1	24.07	16.97	**0.015**	1	25.55	8.144	**0.046**
Bed (replicate)	4	1.42	4.10	0.061	4	3.14	4.413	0.053
Error	6	0.35			6	0.71		
80 min								
Bed	1	1.03	0.443	0.542	1	16.32	3.169	0.150
Bed (replicate)	4	2.33	1.609	0.287	4	5.15	2.430	0.159
Error	6	1.45			6	2.12		
Humidity								
40 min								
Bed	1	431.52	29.781	**0.005**	1	538.85	10.081	**0.034**
Bed (replicate)	4	14.49	0.682	0.629	4	53.45	2.167	0.190
Error	6	21.24			6	24.67		
80 min								
Bed	1	3.11	0.429	0.548	1	103.31	1.8025	0.241
Bed (replicate)	4	7.25	6.951	**0.019**	4	57.32	8.7189	**0.016**
Error	6	1.04			6	6.57		

5.3.3 The effect of infestation-induced cooling on the body temperatures of neighbouring mussels

Clean and infested robomussels experienced lower temperatures when placed in beds composed of infested mussels, than when surrounded by clean, non-infested ones (Fig. 5.5 and 5.6, Table 5.3 and Table 5.4). At the start of the experiments (time 0 min), clean robomussel body temperatures ranged between 19.5–21.0 °C (day 1c, Fig. 5.5A, 20.0–20.5 °C; day 2c, Fig. 5.5B, 20.0–21.0 °C; day 3c, Fig. 5.5C, 19.5–20.5 °C), and increased by an average of 102% and 93.8% in non-infested and infested beds, respectively, by the end of the experiment (Fig. 5.5). At 40 min, clean robomussels deployed in non-infested beds exhibited significantly higher temperatures than those in infested beds (on average 2.2 °C higher; day 2c and day 3c $p<0.05$; Table 5.3), except on day 1c ($p>0.05$, Table 5.3). Generally, after 80 min non-infested robomussels continued to reach higher temperatures when surrounded by non-infested mussels than by infested ones (on

average 2.5 ºC higher; day 2c and day 3c $p<0.05$; Table 5.3), again with the exception of day 1c ($p>0.05$; Table 5.3). At the end of the experiment, non-infested robomussel body temperatures reached 43.1 or 42.2 ºC (day 1c), 42.8 or 40.5 ºC (day 2c) or 37.1 or 34.4 ºC (day 3c) in clean and infested mussel beds respectively.

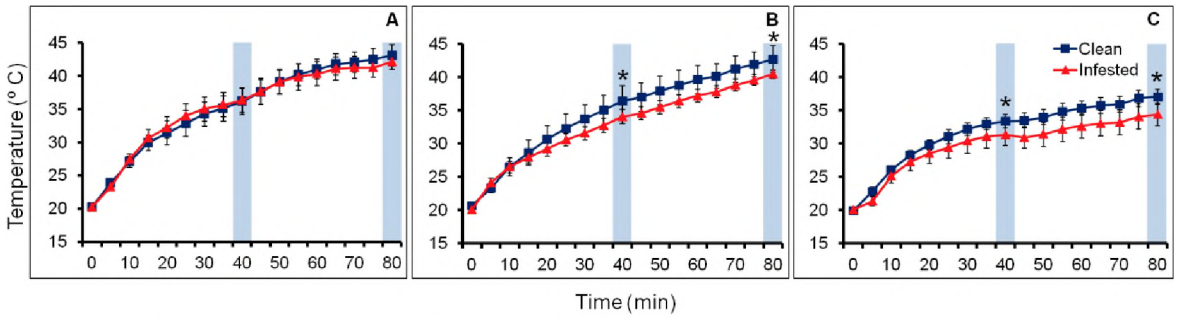

Figure 5.5 – Effect of mussel bed infestation on mean body temperature of clean robomussels (n=6; ±SD). Results separated by day: A) day 1c, B) day 2c, C) day 3c. Shaded areas depict statistical analyses performed at mid (40 min) and endpoints (80 min) of the experiment. Statistical significance is represented by * ($p<0.05$).

Table 5.3 – One-way ANOVA on the effect of mussel bed endolithic infestation on clean robomussel body temperature at 40 and 80 min after aerial sun exposure on day 1c, day 2c and day 3c. Statistical significant values are depicted in bold.

	Day 1c				Day 2c				Day 3c			
Source	**df**	**MS**	***F*-ratio**	***p*-value**	**df**	**MS**	***F*-ratio**	***p*-value**	**df**	**MS**	***F*-ratio**	***p*-value**
40 min												
Bed	1	0.08	0.024	0.881	1	16.33	5.117	**0.047**	1	13.02	7.022	**0.024**
Error	10	3.52			10	3.19			10	1.85		
80 min												
Bed	1	2.52	1.29	0.283	1	15.19	6.788	**0.030**	1	21.33	9.961	**0.010**
Error	10	1.95			10	2.24			10	2.14		

Infested robomussels displayed similar trends, although with lower overall temperatures. Initial body temperatures (time 0 min) of infested robomussels varied between 19.0 and 20.5 ºC (day 1i, Fig. 5.6A, 19.5−20.0 ºC; day 2i, Fig. 5.6B, 19.0−19.5 ºC; day 3i, Fig. 5.6C, 20.0−20.5 ºC) and increased on average 88.6% and 81.8% in non-infested and infested beds, respectively, at the end of the experiment (Fig. 5.6). Significantly higher temperatures were experienced by infested robomussels in clean mussel beds than by those in infested mussel beds at 40 min (on average 2.1 ºC higher; day 1i $p<0.05$ and day 2i $p<0.01$; Table 5.4) except on day 3i ($p>0.05$; Table 5.4). Infested robomussels remained significantly warmer in non-infested mussel beds than in infested ones at the end of the experiment (80 min; on average 1.9 ºC warmer, day 1i $p<0.01$ and day 2i $p<0.05$; Table 5.4) except during the last trial (day 3i, $p>0.05$; Table 5.4). Moreover, at 80

min, infested robomussels reached on average 39.6 or 37.5 ºC (day 1i), 36.3 or 34.8 ºC (day 2i) or 36.4 or 35.6 ºC (day 3i) depending on whether they were surrounded by clean or infested mussels, respectively.

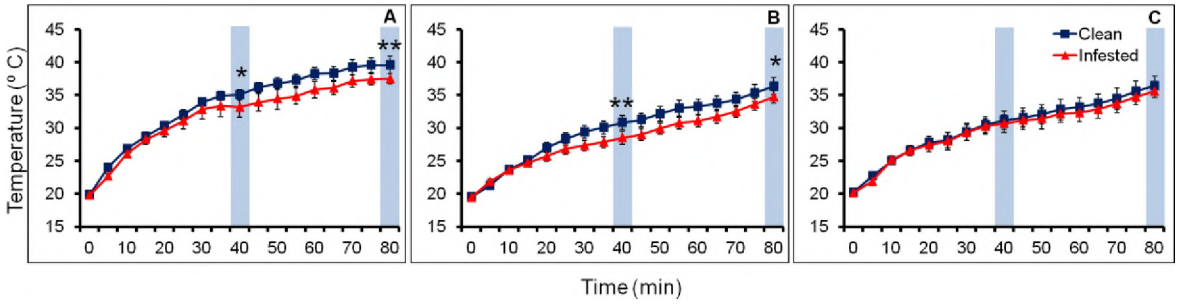

Figure 5.6 – Effect of mussel bed infestation on mean body temperature of infested robomussels (*n*=6; ±SD). Results separated by day: A) day 1i, B) day 2i, C) day 3i. Shaded areas depict statistical analyses performed at mid (40 min) and end (80 min) points of the experiment. Statistical significance is represented by * (p<0.05) or ** (p<0.01).

Table 5.4 – One-way ANOVA on the effect of mussel bed endolithic infestation on infested robomussel body temperature at 40 and 80 min after aerial sun exposure on day 1i, day 2i and day 3i. Statistical significant values are depicted in bold.

	Day 1i				Day 2i				Day 3i			
Source	**df**	**MS**	***F*-ratio**	***p*-value**	**df**	**MS**	***F*-ratio**	***p*-value**	**df**	**MS**	***F*-ratio**	***p*-value**
40 min												
Bed	1	11.02	7.327	**0.022**	1	16.33	15.077	**0.003**	1	0.75	0.413	0.535
Error	10	1.5			10	1.08			10	1.82		
80 min												
Bed	1	13.02	11.12	**0.008**	1	7.52	5.92	**0.035**	1	2.08	1.35	0.272
Error	10	1.17			10	1.27			10	1.54		

5.4 DISCUSSION

This study showed that endolithic infestation of *Mytilus galloprovincialis* significantly modifies the interstitial environment of mussel beds and that the cooling effect provided by phototrophic endoliths extends to neighbouring mussels. Furthermore, intertidal sampling along Portuguese and Moroccan shores revealed increasing endolithic infestations with shell length, upwelling intensity and towards lower latitudes.

5.4.1 Endolith-infested mussels ameliorate mussel beds interstitial microclimate

Parasitic relationships have been documented in a wide range of taxa and their side-effects include changes in host size, shape, colour and behaviour (e.g. Poulin, 1995; Mouritsen & Poulin, 2002). Previous studies have shown that parasitic shell-degrading endoliths significantly reduce mussel condition index, reproductive output, shell and attachment strength and, at sites where their incidence is particularly high, they can be responsible for mass mortalities (e.g. Kaehler & McQuaid, 1999; Zardi *et al.*, 2009; Marquet *et al.*, 2013; Ćurin *et al.*, 2014). Surprisingly, during periods of intense heat stress, shell-degrading endoliths can also have beneficial thermal effects, decreasing the body temperature of mussels (Zardi *et al.*, 2016). This cooling effect is related to shell discolouration. At an initial stage, shells become white through physical damage or removal of the outer layer (periostracum), due to the contact between adjacent mussels or the abrasion by sediment in the water (Kaehler, 1999). After initial damage to the periostracum, endolithic infestation increases shell whitening through chemical dissolution and possibly through redeposition of carbonates (Garcia-Pichel *et al.*, 2010). Advantageous effects of parasitism are not exclusive to mussels. For example, the parasitic trematode *Maritrema* sp. enhances survival of the marine snail *Zeacumantus subcarinatus*, by increasing the host's thermal tolerance (Bates *et al.*, 2011). Here, I further revealed that the thermoregulatory effect of endolithic infestation extends beyond individual mussels to the mussel bed interstitial microclimate. The whitening of mussel shells by endolithic infestation increases reflectance of solar irradiation, reducing the absorption of solar energy, thereby reducing the temperatures of individual mussels and of mussel beds (Zardi *et al.*, 2016). This cooling property, a direct by-product of solar reflectance, leads to greater interstitial relative humidity by reducing evaporative losses. Mussels low on the shore in my study area are typically emerged for ~80 min (pers. obs.). Higher on the shore, aerial exposure lasts longer and exposure to sun irradiance will lead to mussel beds with even lower relative humidities and higher temperatures than those I

report, potentially enhancing the importance of the cooling effect offered by endolith-infested mussel beds. Most intertidal organisms live close to their thermal tolerance limits and face mass mortality as temperatures rise (Sagarin *et al.*, 1999; Stillman & Somero, 2000; Somero, 2002; Harley, 2008; Jones *et al.*, 2010). The bioengineering protection offered by mussel beds to an array of intertidal organisms (Thiel & Ullrich, 2002; O'Donnell, 2008) is likely to be enhanced by endolith-induced improvements in humidity and temperature. Such small scale habitat amelioration could be particularly important under climate warming scenarios.

5.4.2 Endolith-infested mussels thermoregulate neighbouring conspecifics

In this chapter I demonstrate that the advantages of endolithic infestation to members of mussel aggregations extend beyond the cooling of the individual hosts (see Zardi *et al.*, 2016), ameliorating the environment of nearby mussels. My results also showed that mussels surrounded by infested mussels experience lower body temperatures than those with non-infested neighbours, indicating a thermoregulatory effect of neighbouring conspecifics and their role as an element of an individual's thermal environment. A similar thermoregulatory effect of neighbouring individuals has been described from mixed species mussel beds, as *Perna perna* a gaping species (i.e. one that opens and closes the valves during emersion) releases water, cooling the non-gaping species *M. galloprovincialis* (Lathlean *et al.*, 2016b).

Overall, non-significant differences detected during the experiments undertaken on day 1c (non-infested robomussels on non-infested and infested beds) and day 3i (infested robomussels on non-infested and infested beds) were most likely due to high variability in wind speed (Table 5.5), as solar radiation, cloudiness and air temperature were similar. Indeed, wind speed counteracts the effects of increases in air temperature and solar radiation, reducing the exposure to warming experienced by mussels (Helmuth *et al.*, 2011). The fact that the difference between body temperatures of mussels living in clean or infested mussel beds is erased by high wind variability could indicate that the temperature amelioration caused by wind differs with the level of infestation of mussel beds. Nonetheless, under conditions of low wind variability, the cooling effect was observed regardless of whether the robomussel considered was non-infested or infested.

Table 5.5 – Weather data retrieved from Weather Underground (Faro airport station, Portugal) depicting the period during which the experiments on the effects of infestation-induced cooling on the body temperatures of neighbouring mussels took place. * depicts days with a significant statistical difference ($p<0.05$ or $p<0.01$) between infested and non-infested beds both at 40 and 80 min. Global radiation is expressed by accumulated energy (kJ/m^2) and was retrieved from Direcção Regional de Agricultura do Algarve (Regional Agriculture Department of Algarve).

Variable	Time	Day 1c	Day 2c*	Day 3c*	Day 1i*	Day 2i*	Day 3i
Wind speed (km/h)	12h00	11.1	24.1	9.3	14.8	16.7	18.5
	12h30	9.3	24.1	13	13	16.7	20.4
	13h00	16.7	22.2	13	13	16.7	20.4
	13h30	22.2	22.2	13	13	14.8	14.8
	14h00	22.2	22.2	11.1	14.8	13	14.8
	Variability	6.038	1.041	1.660	0.986	1.660	2.829
Air temperature (°C)	12h00	28	29	25	25	21	25
	12h30	29	29	24	25	22	25
	13h00	29	28	24	24	21	25
	13h30	27	28	24	24	21	24
	14h00	27	28	24	25	22	25
	Variability	1	0.548	0.447	0.548	0.548	0.447
Humidity (%)	12h00	37	35	65	69	68	69
	12h30	35	35	69	74	64	69
	13h00	42	37	69	78	68	69
	13h30	54	39	69	78	68	73
	14h00	54	35	69	74	64	69
	Variability	9.127	1.789	1.789	3.715	2.191	1.789
Global radiation (kJ/m^2)	12h00	2750	2714	2281	2664	2678	2379
	13h00	3023	3001	2612	2938	2949	2644
	14h00	3069	3039	2665	2973	2997	2664
	Variability	1601.817	1593.1	1368.48	1549.171	1561.438	1388.872

5.4.3 Endolithic infestation varies with mussel size, latitude and upwelling index

This work supports previous studies demonstrating that endolithic infestation is highly size dependent and increases with mussel size (Kaehler, 1999; Zardi *et al.*, 2009; Marquet *et al.*, 2013; Ćurin *et al.*, 2014). These results most likely reflect a longer period of endolithic infestation, during which the microborers had been intensely excavating the shells of *M. galloprovincialis*, since larger mussels are generally older than smaller mussels when exposed to the same environmental conditions (Sukhotin *et al.*, 2002; Steffani & Branch, 2003; Xavier *et al.*, 2007). Endolithic infestation of intertidal mussels is also likely to exhibit temporal variability. By resurveying two Portuguese locations previously studied by Marquet *et al.* (2013), I highlight changes in overall frequency of infestation in *M. galloprovincialis* and the initial sizes of infestation. Approximately 5 years after the sampling of Marquet *et al.* (2013), the overall frequency of endolithic infestation in Malhão

(site 1 in this chapter, MA in Marquet *et al.*, 2013) more than doubled (36% this chapter and ~15% in Marquet *et al.*, 2013) and infestation started immediately at the smallest sizes (0–10mm; infestation started at 10–20 mm in Marquet *et al.*, 2013). Conversely, Vilamoura (site 3 in this chapter and VL in Marquet *et al.*, 2013) exhibited substantially lower overall endolithic infestation (2% in this chapter and ~20% in Marquet *et al.*, 2013) and infestation started at larger mussel sizes than previously reported (20-30 mm in this chapter; 10–20 mm in Marquet *et al.*, 2013). This temporal variability in endolithic infestation might simply reflect natural changes in the environmental variables along the Portuguese coast (e.g. wave height Soares *et al.*, 1996; Pontes *et al.*, 2005) known to facilitate the spread of endolithic infestation, such as light availability or wave action (Kaehler, 1999; Zardi *et al.*, 2009; Marquet *et al.*, 2013). Nonetheless, Kaehler (1999) has also suggested that the increase in endolithic damage in larger mussels may not only result from increasing infestation severity through time but also from temporal changes (i.e. succession) in the composition of the endolithic community.

The results of this chapter further provide novel insights into the large scale geographical distribution of endolithic infestation. Light increases as cloud cover decreases towards lower latitudes (Wetherald & Manabe, 1980; Warren *et al.*, 1986) and this is consistent with clearer skies and thinner clouds towards my southern sampling locations (http://neo.sci.gsfc.nasa.gov/dataset_index.php#energy). Because photosynthetic endoliths are highly dependent on light, greater endolithic infestation at southern locations could be explained by greater light availability at these sites. These results fit well with previous research showing that infestation in intertidal microhabitats varies with light availability. The intertidal mussel *M. galloprovincialis* is less infested in shaded places than in sun-exposed surfaces (Zardi *et al.*, 2009). While endolithic infestation could be a by-product of wave action due to enhanced shell abrasion (Kaehler, 1999; Zardi *et al.*, 2009), my locations were topographically similar (i.e. all wave-exposed intertidal rocky shores) with no obvious differences in wave action (see also Marquet *et al.*, 2013).

Upwelling phenomena are intimately linked to changes in light availability through increased cloudiness, reducing solar irradiance that reaches the shore by the formation of marine fog or clouds at coastal areas (Tont, 1975; Olivier & Stockton, 1989; Cereceda *et al.*, 2002; Cermak, 2012). As cold upwelling waters reach the surface, they encounter warm air temperatures leading them to cool to dewpoint, producing low clouds and fog (Olivier & Stockton, 1989), which reduce available solar irradiance (Tont, 1975; Olivier & Stockton, 1989; Cereceda *et al.*, 2002). Surprisingly, endolithic infestation was greater at locations characterized by relatively greater upwelling intensity. The unexpected relation between more intense upwelling and greater endolithic infestation might be explained by

an increasing load of nutrients brought to the nearshore by upwelled waters, favouring the activity of endolithic microborers and thus counteracting the expected effect of decreased solar irradiance by upwelling phenomena. In fact, the abundance of phototrophic microborers such as cyanobacteria and algae, and their microbioerosion activity increase with increasing concentrations of nutrients (Carreiro-Silva *et al.*, 2005, 2009, 2012). Despite the strong evidence of the effect of nutrients on phototropic endoliths, I cannot exclude the possibility that the significant correlation between upwelling intensity and endolithic infestation might just mirror the latitudinal gradient effect described above, because the most intense upwelling cells are located at the south of the study area. Future studies investigating the endolithic infestation of intertidal mussels at multiple upwelling regions would allow clarification of this relationship.

Additionally, studies are needed on the variation in endolith species composition over large spatial scales in order to fully comprehend whether it plays a significant role over latitudinal gradients, because endoliths possess a range of functional roles and inhabit different parts of mussel shells (Mao Che *et al.*, 1996; Ćurin *et al.*, 2014; Peharda *et al.*, 2015), potentially causing distinct degrees of infestation. However, the low diversity of endoliths identified for *M. galloprovincialis* in regions as far apart as Portugal and South Africa (Marquet *et al.*, 2013) suggests that the endolithic communities in this study are unlikely to differ significantly.

5.4.4 Final remarks

Greater mussel endolithic infestation towards lower latitudes, where intertidal organisms are exposed to drier and warmer environments, might counterbalance the expected negative effects (e.g. mass mortalities) associated with climate change. Because conditions within beds of infested mussels are ameliorated and individuals in the centre of infested mussel beds experience significantly lower body temperatures, the greater endolithic infestation detected here at lower latitudes might result in an ecological advantage during, for example, heat waves. On the other hand, rising sea temperatures and ocean acidification might facilitate endolithic infestation, as mussel shells suffer periostracum loss and become weaker under warmer temperatures and lower pH (Gazeau *et al.*, 2014). Furthermore, projected changes in wave action (Andrade *et al.*, 2007) will likely affect the frequency of endolithic infestation on intertidal mussels. While it remains unknown whether the cooling effect of endolithic infestation will override the sublethal and lethal effects of parasites on mussels, this parasitic relationship might act as

a thermal buffer, not only for members of the aggregations but also for their associated infauna.

CHAPTER 6

Synthesis

Intertidal rocky shores of Mirleft, Morocco.

6 SYNTHESIS

Throughout this thesis I advanced our knowledge on the influence of upwelling phenomena in determining the composition, distribution and genetic structure of rocky intertidal assemblages under current and forthcoming warming. Specifically, I provide evidence that upwelling: 1) influences the composition of intertidal communities for example by providing refugia against climate warming, 2) does not necessarily drive genetic structure in intertidal species and may 3) influences the incidence of infestation of mussels by phototrophic endoliths.

6.1 Upwelling as refugia for rocky intertidal species in times of climate change

Climate change is considered a major threat to biodiversity (Maclean & Wilson, 2011). In the marine realm, evidence is mounting of its detrimental effects at ecosystem-, species-, and organism-level (Harley *et al.*, 2006; Hoegh-Guldberg & Bruno, 2010; Urban, 2015). In particular, warming has reshuffled the composition of marine communities (Smale & Wernberg, 2013; Vergés *et al.*, 2014) and altered species abundances and range distributions (Poloczanska *et al.*, 2014; Kleisner *et al.*, 2016; Chivers *et al.*, 2017), ultimately causing local extinctions (Graham *et al.*, 2006; Jones *et al.*, 2010). Mass mortalities and sudden contractions in species' distributions after marine heat waves illustrate the large scale consequences and the rapid responses of species to warming (Smale & Wernberg, 2013; Wernberg *et al.*, 2016). Warming has also lead to changes in the genetic diversity of species by partially eroding species genetic lineages through local extinctions (Nicastro *et al.*, 2013). This thesis also highlights that mass mortality due to warming results in local extinctions, consequently causing changes in species abundance and distribution. Alarmingly, the capacity of most species to track climate change is limited (Pearson, 2006; Brown *et al.*, 2016; Chivers *et al.*, 2017 but see Pinsky *et al.*, 2013), therefore safeguarding areas that allow species to persist and preserve their genetic identity are of utmost importance (Hu & Guillemin, 2016). In this thesis, I showed that upwelling regions can act as contemporary climatic refugia for intertidal species by increasing or maintaining species abundance while buffering against present warming. The conclusion in this thesis that upwelling centres have a refugial role is based on: 1) intertidal species exhibiting high abundance at upwelling areas and reduced abundance at non-upwelling areas, 2) intertidal species persisting in upwelling areas while being completely absent from adjacent non-upwelling ones and 3) intertidal species exhibiting different genetic lineages associated with different upwelling cells.

As explored in chapters 2 and 3, upwelling may contribute to greater species abundance, ultimately acting as refugia. Specifically, under strong upwelling conditions (i.e. the

strongest upwelling indices and the lowest sea surface temperatures), upwelling may be particularly important in determining the abundance of intertidal taxa by ameliorating thermal conditions or by increasing the input of nutrients delivered to the nearshore, as demonstrated for example for the opportunistic macroalga *Ulva chlathrata*. This foliose alga reached its greatest relative abundance at the location characterized by the strongest upwelling intensity (site IM). Furthermore, the brown macroalga *Bifurcaria bifurcata*, a warm temperate species that is restricted to tide pools to escape critical thermal extremes (Neiva *et al.*, 2015), showed the same distributional pattern. Likewise, in chapter 3, through exhaustive surveys along Iberian, Moroccan and Western Sahara shores I showed that the abundance of several populations of the macroalga *Fucus guiryi* increased towards upwelling areas and decreased with increasing distance from those centres. The coasts of Atlantic Morocco and Western Sahara include intermittent and quasi-permanent upwelling cells that deliver cold subsurface waters (Marcello *et al.*, 2011; Benazzouz *et al.*, 2014) characterized by high nutrient concentrations (Head *et al.*, 1996) to the nearshore. Therefore, I concluded that the colder, nutrient-rich upwelling waters influence the abundance of intertidal taxa along the study area. As suggested for *B. bifurcata* and for *F. guiryi*, cooler SST delivered by upwelling events may act as a thermal buffer to marine species by ameliorating potentially unfavourable warming rates and promoting an increase in species abundance (see also Riegl & Piller, 2003). Extensive population extinctions of *F. guiryi* were reported from multiple European and African non-upwelling sites presumably due to SST warming, but the species persists within shores affected by upwelled water regardless of upwelling intensity, frequency or geographic area. Moreover, the increase of *U. chlathrata* towards the strongest upwelling centre may also mirror the bottom-up effect resulting from higher concentrations of nutrients associated with upwelling waters that promote the growth of algae (Bustamante *et al.*, 1995). Higher concentrations of nutrients at upwelling areas may also explain the relationship between greater upwelling intensity and more pervasive phototrophic endolithic-infestation of mussels described in chapter 5. Abundance and microbioerosion activity of phototrophic microborers increase with increasing concentrations of nutrients (Carreiro-Silva *et al.*, 2005, 2009, 2012). The abundance of endoliths has not been estimated in this thesis, hence it remains unknown whether such abundance varies with upwelling intensity. However, greater frequency of infestation at sites characterized by stronger upwelling indicates greater endolithic activity, possibly reflecting higher concentrations of nutrients. While disentangling the effects of nutrients and SST on the abundance of intertidal species was beyond the scope of these chapters, I cannot exclude the possibility that both variables may act simultaneously. For example, populations of *F.*

guiryi at upwelling centres may not only benefit from buffered thermal conditions but also from the input of nutrients during upwelling events. Most importantly, the described refugia effect for *F. guiryi* comprises not only the species as a biological unit but also its genetic diversity; different genetic lineages were associated with different upwelling areas. This is of utmost importance for the long-term persistence of the species as a whole, but also for the maintenance of distinct gene pools, which may influence a species' adaptive response to environmental change. Genetic lineages associated with different environmental regimes may display different physiological tolerances to environmental stress and present unique adaptive potential that can be important for overall species survival (Pearson *et al.*, 2009; Zardi *et al.*, 2013; Saada *et al.*, 2016). In the sister species *F. vesiculosus*, the genetic clade inhabiting northern, colder latitudes has lower resilience to heat stress than the neighbouring, southern lineage (Saada *et al.*, 2016). Potentially, each of the *F. guiryi* lineages described in this thesis could display unique ecophysiological responses to their environment, widening the ecological implications of these climatic refugia. Populations of *F. guiryi* from the genetic lineage present along central Portuguese shores are already experiencing reductions in abundance (pers. comm. G. Zardi), though at a lower degree, despite these shores being intermittently affected by upwelling events (Lemos & Pires, 2004). The loss of one or more genetic lineages may therefore represent a threat for the overall adaptive potential of the species, which could result in changes in species distribution and distributional limits.

The environmental niche modelling performed in chapter 4 further highlighted the potential role of upwelling as a form of shelter from unsuitable warm SST for the brown mussel *Perna perna*. While *P. perna* does not seek refuge in temperate upwelling areas along Iberia, Morocco and Western Sahara, the species seems to benefit from thermal amelioration provided by upwelling cells along the warm tropical Atlantic shores of central Africa. In contrast to a general absence from most of the central African coastline (from Gambia to Liberia and from Togo to Gabon), *P. perna* has been reported from the upwelling-influenced shores of Ghana and Ivory Coast (Zabi, 1982; Otchere *et al.*, 2003). Taking into account the lack of reports on the presence of this species from adjacent tropical non-upwelling areas and the extremely low likelihood of its presence from those shores as predicted by the niche modelling (mostly 0 likelihood of presence, Fig. 4.8, chapter 4), I suggested that the long-term persistence of this species is due to thermal refuge provided by the colder waters of the upwelling cells of Ghana and Ivory Coast (Houghton & Mensah, 1978).

Upwelling influences interspecific interactions within intertidal assemblages (Wieters, 2005; Reddin *et al.*, 2015). For example, under the influence of strong upwelling,

herbivore-resistant corticated algae growth faster, outcompeting and suppressing ephemeral algae (Nielsen & Navarrete, 2004). In contrast, with weak upwelling, growth of corticated algae is reduced and ephemeral algae attain higher biomass, which contributes to an increase of density and biomass of herbivores (Nielsen & Navarrete, 2004). Importantly, the role of upwelling areas as climate refugia discussed in this thesis has been demonstrated for species that actively shape intertidal assemblages. Because bioengineers are key foundation organisms that structure intertidal communities by increasing richness and abundance of associated assemblages (Borthagaray & Carranza, 2007; Cole, 2010; Watt & Scrosati, 2013b), the refugial role of upwelling gains increasing importance due to the knock-on effects for associated species. In this sense, the upwelling-driven presence and greater abundance of *F. guiryi* along northern African shores at upwelling centres might dictate the composition of intertidal communities by shaping both lower and higher trophic levels. Watt & Scrosati (2013b) showed that at high and mid intertidal heights, canopies of bioengineer fucoids (e.g. *Ascophyllum nodosum* and *F. vesiculosus*) increased the presence and abundance of associated species, such as the herbivorous gastropod species *Littorina obtusata*. Without thermal refugia, marine species might experience die-offs or go locally extinct, compromising the maintenance of entire communities (Wernberg *et al.*, 2016). For example, following an intense marine heat wave, and in the absence of a thermal buffer, the bioengineer kelp species *Scytothalia dorycarpa* has disappeared from ~100 km of temperate Australian shores, which resulted in structural changes at the community-level, most likely with ecosystem-level implications (Smale & Wernberg, 2013).

6.2 Influence of upwelling on genetic patterns of rocky intertidal species

Upwelling regions preserve genetic diversity of intertidal species, by maintaining different genetic lineages (chapter 3). However, the degree to which upwelling shapes genetic structure of marine species is not consistent; experimental evidence has revealed important contrasting results (i.e. weak and strong genetic structure) leading to divergent conclusions (e.g. Waters & Roy, 2004; Silva *et al.*, 2009; Barshis *et al.*, 2011). Along the Moroccan coast, the strong upwelling cell off Cape Ghir has been considered a major driver of genetic breaks in marine species, as this phenomenon presumably isolates distinct populations, hindering genetic exchange among them (e.g. Chlaida *et al.*, 2009; Neiva *et al.*, 2015). While I have shown that upwelling is crucial for preserving the gene pool of a marine macroalga (chapter 3), I did not find evidence that upwelling cells along Morocco and Western Sahara directly cause strong genetic structure of intertidal species

(chapters 3 and 4). The strong genetic structure of populations of *F. guiryi* (chapter 3) along the study area is better explained by life history traits (i.e. reduced dispersal capacity) and population isolation rather than upwelling forcing genetic differentiation. Once abundant and widespread along Moroccan shores (referred to as *F. spiralis/ F. spiralis platycarpus*, Benhissoune *et al.*, 2002a), populations of *F. guiryi* located outside or at the margin of upwelling cells decreased in abundance or went extinct presumably due to SST warming, resulting in a distributional discontinuity isolating populations that were previously geographically close. Due to the increasing distance between populations and because gene flow of direct-developing structural seaweeds, such as *F. guiryi*, is limited and mainly driven by dispersal via rafting of fertile thalli (Norton, 1992; Kalvas & Kautsky, 1998; Coleman & Brawley, 2005; McKenzie & Bellgrove, 2008), gene flow between populations was most likely dramatically reduced. This has potentially enhanced the importance of site-specific self-recruitment, resulting in separate genetic lineages that are independently associated with distinct upwelling cells.

In contrast to *F. guiryi*, the brown mussel *P. perna* did not display genetic structure along northern Africa and southern Iberia. The unexpected lack of genetic structure in *P. perna* most likely resulted from a combination of species' life history traits (i.e. long dispersal capacity), habitat continuity and stepping stone effects. As a consequence, upwelling cells, along with other potential oceanographic barriers (e.g. the Almeria-Oran Front), do not isolate populations of *P. perna* or discernibly limit genetic exchange between them. If upwelling has the potential to influence genetic patterns of the Brown mussel, it does so, in contrast to my initial hypothesis, by contributing to weak rather than strong genetic structure. As suggested by Barshis *et al.* (2011) for intertidal barnacles, strong upwelling events may increase the off-shore transport of *P. perna* larvae; this could mix larvae from different sources, ultimately homogenizing the pool of recruits and causing a lack of genetic structure.

Although neither model species used in this thesis, whether characterized by reduced dispersal (*F. guiryi*) or long dispersal (*P. perna*), indicated an influence of upwelling in driving the genetic structure of species across the Atlantic Moroccan and Western Sahara coastlines, additional information is needed to confirm these results. Specifically, future studies investigating the genetic patterns of a variety of coastal species with different modes of development (direct or indirect developers) and dispersal capacities (short, medium and long) would greatly increase our understanding of the influence of northern African upwelling cells in shaping species' genetic structure. Studies based on multispecies datasets are particularly useful because species inhabiting the same

geographical region might exhibit contrasting genetic patterns in the face of multiple oceanographic barriers (Kelly & Palumbi, 2010).

6.3 Potential forthcoming biological and environmental changes

How species respond to climate change has been extensively investigated but geographically biased against tropical systems (reviewed in Brown *et al.*, 2016). Tropical and subtropical marine regions, however, are expected to be some of the most important scenes of species distributional shifts (Burrows *et al.*, 2014), as tropical species are highly vulnerable to warming (Nguyen *et al.*, 2011). In such regions, species richness may decline because the species that display distributional shifts may not be replaced (Cheung *et al.*, 2009; Burrows *et al.*, 2014). Forthcoming warming (IPCC, 2014) is likely not only to drive several local populations to extinction but also to alter species distribution and biodiversity patterns (Cheung *et al.*, 2009). Therefore, understanding the velocity of climate change and the distributional shifts of species, as they try to track climate change has gained increasing attention (Burrows *et al.*, 2011; Burrows *et al.*, 2014; Kleisner *et al.*, 2016; Chivers *et al.*, 2017). As an alternative to displaying distributional shifts, species can persist in the face of climate change by adapting to altered environmental conditions (Parmesan, 2006). This is of particular importance for species with reduced mobility that are unable to disperse (Hoffmann & Sgrò, 2011). As climate changes and warming increases, organisms respond based on their physiological and behavioural adaptations (Somero, 2010). In the marine realm, the potential of species to adapt to climate change is generally discussed in a context of thermal optima and tolerance limits, as species cope with a warming environment (Somero, 2010; Reusch, 2014). Often, different intraspecific adaptive potential might be related to species genetic patterns (*F. vesiculosus*, Saada *et al.*, 2016; *P. perna*, Zardi *et al.*, 2015a but see Zardi *et al.*, 2013). For example, individuals of the western (temperate) genetic lineage of the brown mussel *P. perna* inhabiting southern African shores gape (intermittent opening and closure of the valves) less and have lower attachment strength than the eastern (subtropical) lineage (Zardi *et al.*, 2015a). These behavioural and physiological differences represent distinct adaptive responses to high temperatures and help explain vertical zonation and habitat segregation (Zardi *et al.*, 2015a). Ultimately, adaptive potential to climate change helps explain species range and distribution limits. Because the adaptive potential of a species may allow it to cope with the projected consequences of climate change, heritability of adaptive potential by marine species to increasing warming and climate change (Malvezzi *et al.*, 2015; Munday *et al.*, 2017) must be considered when predicting species responses to

climate change (Munday *et al.*, 2017). Upwelling systems, such as the Canary Current system, which encompass both temperate and tropical shores offer ideal conditions to study the responses of marine species to climate change. Because upwelling systems exhibit relatively lower temperatures than the surrounding areas (e.g. Espinosa-Carreon *et al.*, 2004; Marcello *et al.*, 2011), they display contrasting environmental conditions which might be helpful to investigate warming-induced species responses, disentangle the direction (e.g. poleward, equatorward, bottomward) and velocity of distributional shifts of temperate and tropical species in response to warming and also whether differences exist between the two groups of species. The baseline provided in this study contributes to a clarification of the distribution and distributional limits of intertidal northern African species as well as species-specific responses to projected warming.

Along with projected increase in warming rates (IPCC, 2014), upwelling is expected to change at the Canary Current upwelling system, as in other major world upwelling systems (Bakun *et al.*, 2010; Sydeman *et al.*, 2014; García-Reyes *et al.*, 2015; Wang *et al.*, 2015). By the end of the 21st century, upwelling regimes will experience changes in timing, duration, intensity and spatial heterogeneity (Wang *et al.*, 2015), which may consequently result in structural, ecological and genetic changes to coastal communities. Specifically, I suggest that longer, more intense and larger upwelling events may alter species abundances, either by increasing the amount of nutrients or by providing a spatial and temporal thermal buffer. For example, with an increase of nutrients, opportunistic species such as *U. clathrata* (see chapter 2) may outgrow other species and shift the composition and dynamics of intertidal communities. Likewise, small populations of *F. guiryi* may become more abundant, which could benefit associated species or impair competitors. Most importantly, the predicted spatial homogenization of upwelling events at high latitudes (Wang *et al.*, 2015) could potentially enable a recolonization of previously extinct populations of *F. guiryi*, by ameliorating environmental conditions.

Although this thesis does not provide evidence for an active role of upwelling in shaping genetic structure of intertidal species along northern Africa, such a structuring role has been demonstrated for other species (*Sardina pilchardus*, Chlaida *et al.*, 2009; *B. bifurcata,* Neiva *et al.*, 2015) along the same region and for other upwelling systems (e.g. Kelly & Palumbi, 2010). Considering the above contrasting results concerning the influence of upwelling in structuring species genetic patterns, it could be expected that forthcoming intensification of upwelling regimes will further strengthen or promote either intraspecific genetic differentiation or homogenization, as species' population dynamics such as larval transport, recruitment and admixture of recruits might be expected to change. The resulting genetic pattern is likely to be species- and region-specific as it

might interact with additional biological (e.g. life history traits) and geographical (e.g. topography) variables.

As upwelling influences interspecific relationships (Nielsen & Navarrete, 2004; Wieters, 2005; Guerry & Menge, 2017 but see Lany *et al.*, 2017), an intensification of these oceanographic phenomena could trigger changes in the strength and direction of species interactions. For example, Guerry & Menge (2017) showed that under nutrient-rich upwelling influence, grazers have little effect in reducing algal species richness and biomass. Therefore, it might be anticipated that under projected stronger upwelling events, the negative impact of grazers on algal community might further decrease. Furthermore, it might also be expected that an intensification of upwelling might drive changes in other interspecific relationships such as host-parasite interactions. For example, under anomalously strong upwelling conditions, the red tide bloom-forming dinoflagellate species *Akashiwo sanguinea* was able to outgrow its parasite species *Amoebophrya*; most likely as a result of an increasing nutrient supply (Mazzillo *et al.*, 2011). In the future, *Amoebophrya* might not be able to control the occurrence of its host as strong and persistent upwelling may cause faster growth rates of the host than the parasite, consequently developing extreme red tides (Mazzillo *et al.*, 2011). Likewise, the frequency of endolithic infestation on mussels might also change under stronger upwelling events. I suggested that greater endolithic infestation of mussels at sites with strong upwelling index might have been caused by an input of nutrients by upwelled waters because endolithic parasites increase in abundance and activity under nutrient enriched conditions (Carreiro-Silva *et al.*, 2005, 2009, 2012). Therefore, projected intensification of upwelling regimes (Bakun *et al.*, 2010; Wang *et al.*, 2015) could result in longer or greater input of nutrients into the nearshore increasing abundance of endoliths or endolithic activity. The interaction of increased nutrient availability with other environmental variables (i.e. cloud cover, solar irradiance), however, might unveil a more complex biological response to upwelling than previously discussed. As phototrophic endoliths are light-dependent organisms (e.g. Zardi *et al.*, 2009), their geographic distribution and activity might be shaped by environmental variables that control light availability at a larger scale than within the intertidal. Upwelling phenomena are intimately linked to changes in light availability through increased cloudiness, reducing solar irradiance that reaches the shore by the formation of marine fog or clouds at coastal areas (Tont, 1975; Olivier & Stockton, 1989; Cereceda *et al.*, 2002; Cermak, 2012). If the projected intensification of upwelling (Bakun *et al.*, 2010; Wang *et al.*, 2015) also contributes to an increase in cloudiness, endolithic infestation could be expected to decrease rather than intensify. At a first glance, lower levels of endolithic infestation could represent an advantage to marine mussels

because endoliths negatively affect mussels (i.e. reduce mussel condition index, reproductive output, shell and attachment strength, cause mass mortalities, Kaehler & McQuaid, 1999; Zardi *et al.*, 2009; Marquet *et al.*, 2013; Ćurin *et al.*, 2014). A reduction of endolithic infestation on mussels, however, could in contrast mirror disadvantages against projected rising warming because endoliths reduce mussel body temperature and ameliorate the thermal environment (chapter 5, Lourenço *et al.*, 2017), which results in lower mortality rates on infested mussels under heat waves (Zardi *et al.*, 2016). Although these effects are more likely to act at small local scales than to govern changes in the composition of intertidal communities at large regional scales, it remains unknown whether the thermal buffer provided by endolithic infestation will override its negative effects.

Forthcoming climatic changes are also expected to increase the intensity of storms and the frequency of very intense storms (categories 4 and 5, Knutson *et al.*, 2015; Bacmeister *et al.*, 2016), potentially disrupting coastal communities. This might be particularly detrimental for bioengineer organisms that shape intertidal ecosystems, such as the three species studied in detail in this thesis, *F. guiryi*, *P. perna* and *Mytilus galloprovincialis*. Importantly, bioengineer species mitigate climate change consequences on coastal ecosystems for example by dampening waves, reducing current velocity, trapping sediments and increasing soil elevation (Borsje *et al.*, 2011). In particular, reef building species, such as oysters, are of utmost importance for coastal protection because they attenuate the hydrodynamic energy of waves (Piazza *et al.*, 2005). While having a key role in protecting coastal areas, bioengineer species can be severely affected by extreme environmental conditions, and it might be anticipated that under climate change such negative effects will further increase. For example, severe storms significantly altered the structure of a mixed-kelp canopy by greatly reducing the abundance of two out of three kelp species, due to severe wave action dislodgement (Smale & Vance, 2016). Similarly, increases in the severity of storms might pose a risk to the long-term persistence of *F. guiryi* populations, which are already under threat due to SST warming, by damaging individuals (e.g. breaking/dislodging individuals) and reducing species abundance. Increasing intensity of storms might also affect mussel beds and their associated assemblages by promoting mussel dislodgement or mortality by sand inundation. Although differences in stressor tolerance exist between *P. perna* and *M. galloprovincialis*, both mussel species are vulnerable to hydrodynamic disturbance experiencing dislodgement by waves (Rius & McQuaid, 2006; Zardi *et al.*, 2006a); species mortality driven by wave action particularly peaks after severe storms (Rius & McQuaid, 2006; Zardi *et al.*, 2006a). The two species are also susceptible to sand (Zardi *et al.*,

2008; Nicastro *et al.*, 2009), exhibiting high mortality rates driven by sand inundation (Zardi *et al.*, 2006b). Because mussel beds harbour several dozens of species (Hammond & Griffiths, 2004; Borthagaray & Carranza, 2007; Silliman *et al.*, 2011; Arribas *et al.*, 2014), exposure of mussel beds of *P. perna* and *M. galloprovincialis* to increasing wave action or severity of storms might jeopardize their maintenance and the composition of their associated assemblages. In addition to inducing mussel burial, sand and sediment load delivered to the nearshore may damage mussel shells by provoking abrasion and eroding the outer layer of the shell (i.e. the proteinaceous periostracum; Kaehler, 1999), which facilitates infestation by endolithic parasites (Zardi *et al.*, 2009), with potential consequences for the mussel's survival and for the associated assemblages.

As discussed throughout this thesis, intertidal assemblages are already responding to climatic changes regardless of the position on the shore. Due to the complex interaction of biotic and abiotic variables, it remains still unclear which species are likely to persist in the face of forthcoming climatic changes and how their associated assemblages will respond. Although upwelling regions still experience increasing warming, they do so at a lower rate than the adjacent regions (Lima & Wethey, 2012); therefore, they have the ideal environmental conditions for species to retreat and escape projected warming. Despite the potential of deep sea reefs to act as climate refugia against intense storms (Bongaerts *et al.*, 2010), these are likely to shelter only subtidal taxa. Further investigation is therefore needed to understand if coastal intertidal species will be able to counter act the expected increase of storms in frequency and intensity and how will intertidal communities respond to such extreme environmental changes.

6.4 Final remarks

The presented thesis combined distinct methodologies (species distribution surveys, upwelling index estimation, genetic analyses, environmental niche modelling, manipulative experiments) and it was carried out in one of the least explored regions in the world in terms of benthic communities (Decker *et al.*, 2003; Ramos *et al.*, 2015). This approach, based on multiple sources of evidence and developed along intertidal northern African shores, highlights a solid and novel work that contributes to a greater understanding of the environmental, ecological and evolutionary processes shaping intertidal benthic communities inhabiting the upwelling shores of the Canary Current system. Specifically, this study increases our understanding on the influence of upwelling in determining the composition, species distribution and the genetic patterns of intertidal species in a context

of climate change. It also constitutes a baseline for future research aiming to investigate the distribution and distributional changes of intertidal species along northern Africa.

The work developed here is fundamentally important because warming is projected to further rise (IPCC, 2014), which will almost certainly result in novel species distributional shifts, in changes in species gene pool, and in potentially overlapping of interspecific environmental niches that could result in shifts in the composition of intertidal communities. Additionally, warming is likely to interact with other variables (e.g. more intense storms, Knutson *et al.*, 2015; ocean acidification, Poloczanska *et al.*, 2016; habitat loss, Travis, 2003; spread of invasive species, Stachowicz *et al.*, 2002) that greatly endanger species survival. Thus, how species will respond to climate change might be more complex than previously anticipated. Detecting refuge areas where species are able to persist under a changing environment and climate is therefore of paramount importance for the preservation of biodiversity. Upwelling is expected to intensify as a result of changes in greenhouse gas concentrations, land-sea pressure differences and wind patterns (Bakun *et al.*, 2010; Narayan *et al.*, 2010), thus its influence on intertidal communities, particularly as climate change refugia, might be greater than I have shown in this thesis. Large scale studies targeting other upwelling systems and a range of different species and functional groups and investigating how upwelling regimes will change in the future would further clarify and advance our knowledge on how these changes will affect ecosystem functioning and services of coastal ecosystems.

Importantly, this study took place in an interface region, between temperate (northeastern Atlantic) and tropical (eastern Atlantic) systems, marked by significant warming (Lima & Wethey, 2012) and where cold and warmwater species meet their southern and northern distributional limits, respectively (e.g. Zardi *et al.*, 2011b; Smale *et al.*, 2013; Neiva *et al.*, 2015; Assis *et al.*, 2017). Investigating forthcoming distributional shifts of species in this region and whether assemblages associated with bioengineer species differ depending on upwelling intensity would provide clearer evidence on the influence of upwelling in shaping the intertidal communities of northern Africa. Future research focusing on northern African intertidal assemblages is important to evaluating how species will respond to climate change and what the forthcoming ecological and evolutionary consequences are likely to be.

Publication records

The work developed in this thesis has already resulted in three published manuscripts:

- Lourenço *et al.* (2016) in *Journal of Biogeography*, doi: 10.1111/jbi.12744 (Chapter 3)

- Lourenço *et al.* (2017) in *Scientific Reports*, doi: 10.1038/s41598-017-10753-9 (Chapter 4)

- Lourenço *et al.* (2017) in *Marine Biology*, doi: 10.1007/s00227-017-3160-7 (Chapter 5)

7. REFERENCES

Abada-Boudjema, Y.-M. & Davin, J.-C. (1995) Recruitment and life span of two natural mussel populations *Perna perna* (Linnaeus) and *Mytilus galloprovincialis* (Lamarck) from the Algerian coast. *Journal of Molluscan Studies*, **61**, 467-481.

Adams, T.P., Miller, R.G., Aleynik, D. & Burrows, M.T. (2014) Offshore marine renewable energy devices as stepping stones across biogeographical boundaries. *Journal of Applied Ecology*, **51**, 330-338.

Albaina, N., Olsen, J.L., Couceiro, L., Ruiz, J.M. & Barreiro, R. (2012) Recent history of the European *Nassarius nitidus* (Gastropoda): phylogeographic evidence of glacial refugia and colonization pathways. *Marine Biology*, **159**, 1871-1884.

Alberto, F., Raimondi, P.T., Reed, D.C., Coelho, N.C., Leblois, R., Whitmer, A. & Serrão, E.A. (2010) Habitat continuity and geographic distance predict population genetic differentiation in giant kelp. *Ecology*, **91**, 49-56.

Aldenhoven, J.T., Miller, M.A., Corneli, P.S. & Shapiro, M.D. (2010) Phylogeography of ninespine sticklebacks (*Pungitius pungitius*) in North America: glacial refugia and the origins of adaptive traits. *Molecular Ecology*, **19**, 4061-4076.

Allouche, O., Tsoar, A. & Kadmon, R. (2006) Assessing the accuracy of species distribution models: prevalence, kappa and the true skill statistic (TSS). *Journal of Applied Ecology*, **43**, 1223-1232.

Alvarez, I., Gomez-Gesteira, M., deCastro, M., Lorenzo, M.N., Crespo, A.J.C. & Dias, J.M. (2011) Comparative analysis of upwelling influence between the western and northern coast of the Iberian Peninsula. *Continental Shelf Research*, **31**, 388-399.

Anabalón, V., Arístegui, J., Morales, C.E., Andrade, I., Benavides, M., Correa-Ramírez, M.A., Espino, M., Ettahiri, O., Hormazabal, S., Makaoui, A., Montero, M.F. & Orbi, A. (2014) The structure of planktonic communities under variable coastal upwelling conditions off Cape Ghir (31°N) in the Canary Current System (NW Africa). *Progress in Oceanography*, **120**, 320-339.

Anderson, M.J. (2001) A new method for non-parametric multivariate analysis of variance. *Austral Ecology*, **26**, 32-46.

Andrade, C., Pires, H., Taborda, R. & Freitas, M. (2007) Projecting future changes in wave climate and coastal response in Portugal by the end of the 21st century. *Journal of Coastal Research*, **50**, 263-257.

Archambault, J.M., Cope, W.G. & Kwak, T.J. (2014) Survival and behaviour of juvenile unionid mussels exposed to thermal stress and dewatering in the presence of a sediment temperature gradient. *Freshwater Biology*, **59**, 601-613.

Arístegui, J., Barton, E.D., Álvarez-Salgado, X.A., Santos, A.M.P., Figueiras, F.G., Kifani, S., Hernández-León, S., Mason, E., Machú, E. & Demarcq, H. (2009) Sub-regional ecosystem variability in the Canary Current upwelling. *Progress in Oceanography*, **83**, 33-48.

Arribas, L.P., Donnarumma, L., Palomo, M.G. & Scrosati, R.A. (2014) Intertidal mussels as ecosystem engineers: their associated invertebrate biodiversity under contrasting wave exposures. *Marine Biodiversity*, **44**, 203-211.

Ashcroft, M.B. (2010) Identifying refugia from climate change. *Journal of Biogeography*, **37**, 1407-1413.

Assis, J., Coelho, N.C., Alberto, F., Valero, M., Raimondi, P., Reed, D. & Serrão, E.A. (2013) High and distinct range-edge genetic diversity despite local bottlenecks. *PLoS One*, **8**, e68646.

Assis, J., Serrão, E.A., Claro, B., Perrin, C. & Pearson, G.A. (2014) Climate-driven range shifts explain the distribution of extant gene pools and predict future loss of unique lineages in a marine brown alga. *Molecular Ecology* **23**, 2797-2810.

Assis, J., Zupan, M., Nicastro, K.R., Zardi, G.I., McQuaid, C.D. & Serrão, E.A. (2015) Oceanographic conditions limit the spread of a marine invader along southern African shores. *PLoS One*, **10**, e0128124.

Assis, J., Coelho, N.C., Lamy, T., Valero, M., Alberto, F. & Serrão, E.A. (2016) Deep reefs are climatic refugia for genetic diversity of marine forests. *Journal of Biogeography*, **43**, 833-844.

Assis, J., Berecibar, E., Claro, B., Alberto, F., Reed, D., Raimondi, P. & Serrão, E.A. (2017) Major shifts at the range edge of marine forests: the combined effects of climate changes and limited dispersal. *Scientific Reports*, **7**, 44348.

Atarhouch, T., Rami, M., Naciri, M. & Dakkak, A. (2007) Genetic population structure of sardine (*Sardina pilchardus*) off Morocco detected with intron polymorphism (EPIC-PCR). *Marine Biology*, **150**, 521-528.

Bacmeister, J.T., Reed, K.A., Hannay, C., Lawrence, P., Bates, S., Truesdale, J.E., Rosenbloom, N. & Levy, M. (2016) Projected changes in tropical cyclone activity under future warming scenarios using a high-resolution climate model. *Climatic Change*, 1-14.

Badawy, M.I. & Al-Harthy, F. (1991) Hydrocarbons in seawater, sediment, and oyster from the Omani coastal waters. *Bulletin of Environmental Contamination and Toxicology*, **47**, 386-391.

Bakun, A. (1973) Coastal Upwelling Indexes, west coast of North America, 1946–71. NOAA Technical Report NMF, 671, 103 pp.

Bakun, A. & Weeks, S.J. (2008) The marine ecosystem off Peru: What are the secrets of its fishery productivity and what might its future hold? *Progress in Oceanography*, **79**, 290-299.

Bakun, A., Field, D.B., Redondo-Rodriguez, A.N.A. & Weeks, S.J. (2010) Greenhouse gas, upwelling-favorable winds, and the future of coastal ocean upwelling ecosystems. *Global Change Biology*, **16**, 1213-1228.

Bandelt, H.J., Forster, P. & Röhl, A. (1999) Median-joining networks for inferring intraspecific phylogenies. *Molecular Biology and Evolution*, **16**, 37-48.

Barreiro, R., Couceiro, L., Quintela, M. & Ruiz, J.M. (2006) Population genetic structure of the prosobranch *Nassarius reticulatus* (L.) in a ria seascape (NW Iberian Peninsula) as revealed by RAPD analysis. *Marine Biology*, **148**, 1051-1060.

Barshis, D.J., Sotka, E.E., Kelly, R.P., Sivasundar, A., Menge, B.A., Barth, J.A. & Palumbi, S.R. (2011) Coastal upwelling is linked to temporal genetic variability in the acorn barnacle *Balanus glandula*. *Marine Ecology Progress Series*, **439**, 139-150.

Barton, E.D., Arístegui, J., Tett, P., Cantón, M.G.-B., J., Hernández-León, S., Nykjaer, L., Almeida, C., Almunia, J., Ballesteros, S., Basterretxea, G., Escánez, J., García-Weill, L., Hernández-Guerra, A., López-Laatzen, F., Molina, R., Montero, M.F., Navarro-Pérez, E., Rodríguez, J.M., van Lenning, K., Vélez, H. & Wild, K. (1998) The transition zone of the Canary Current upwelling region. *Progress in Oceanography*, **41**, 455-504.

Barton, E.D., Field, D.B. & Roy, C. (2013) Canary current upwelling: more or less? *Progress in Oceanography*, **116**, 167-178.

Bates, A.E., Leiterer, F., Wiedeback, M.L. & Poulin, R. (2011) Parasitized snails take the heat: a case of host manipulation? *Oecologia*, **167**, 613-621.

Bayne, B. (1965) Growth and the delay of metamorphosis of the larvae of *Mytilus edulis* (L.). *Ophelia*, **2**, 1-47.

Beatty, G.E. & Provan, J. (2010) Refugial persistence and postglacial recolonization of North America by the cold-tolerant herbaceous plant *Orthilia secunda*. *Molecular Ecology*, **19**, 5009-5021.

Beatty, G.E. & Provan, J. (2011) Phylogeographic analysis of North American populations of the parasitic herbaceous plant *Monotropa hypopitys* L. reveals a complex history of range expansion from multiple late glacial refugia. *Journal of Biogeography*, **38**, 1585-1599.

Beermann, A.J., Ellrich, J.A., Molis, M. & Scrosati, R.A. (2013) Effects of seaweed canopies and adult barnacles on barnacle recruitment: the interplay of positive and negative influences. *Journal of Experimental Marine Biology and Ecology*, **448**, 162-170.

Belabed, B.E., Laffray, X., Dhib, A., Fertouna-Belakhal, M., Turki, S. & Aleya, L. (2013) Factors contributing to heavy metal accumulation in sediments and in the intertidal mussel *Perna perna* in the Gulf of Annaba (Algeria). *Marine Pollution Bulletin*, **74**, 477-89.

Belanger, C.L., Jablonski, D., Roy, K., Berke, S.K., Krug, A.Z. & Valentine, J.W. (2012) Global environmental predictors of benthic marine biogeographic structure. *Proceedings of the National Academy of Sciences*, **109**, 14046-14051.

Belattmania, Z., Chaouti, A., Machado, M., Engelen, A., Serrão, E.A., Reani, A. & Sabour, B. (2017) *Ampelisca lusitanica* (Crustacea: Amphipoda): new species for the Atlantic coast of Morocco. *Marine Biodiversity Records*, **10**, 7.

Belkhir, K., Borsa, P., Chikhi, L., Raufaste, N. & Bonhomme, F. (2004) GENETIX 4.05, logiciel sous Windows TM pour la génétique des populations. Laboratoire Génome, Populations, Interactions, CNRS UMR 5000, Université de Montpellier II, Montpellier (France).

Belkin, I.M. (2009) Rapid warming of Large Marine Ecosystems. *Progress in Oceanography*, **81**, 207-213.

Bellard, C., Bertelsmeier, C., Leadley, P., Thuiller, W. & Courchamp, F. (2012) Impacts of climate change on the future of biodiversity. *Ecology Letters*, **15**, 365-377.

Belmaker, J. & Jetz, W. (2015) Relative roles of ecological and energetic constraints, diversification rates and region history on global species richness gradients. *Ecology Letters*, **18**, 563-571.

Benazzouz, A., Mordane, S., Orbi, A., Chagdali, M., Hilmi, K., Atillah, A., Pelegrí, J.L. & Demarcq, H. (2014) An improved coastal upwelling index from sea surface temperature using satellite-based approach – The case of the Canary Current upwelling system. *Continental Shelf Research*, **81**, 38-54.

Benhissoune, S., Boudouresque, C.F. & Verlaque, M. (2001) A check-list of marine seaweeds of the Mediterranean and Atlantic coasts of Morocco I. Chlorophyceae Wille s. l. *Botanica Marina*, **44**, 171-182.

Benhissoune, S., Boudouresque, C.F. & Verlaque, M. (2002a) A check-list of marine seaweeds of the Mediterranean and Atlantic coasts of Morocco II. Phaeophyceae. *Botanica Marina*, **45**, 217-230.

Benhissoune, S., Boudouresque, C.F., Perret-Boudoresque, M. & Verlaque, M. (2002b) A check-list of marine seaweeds of the Mediterranean and Atlantic coasts of Morocco III. Rhodophyceae (excluding Ceramiales). *Botanica Marina*, **45**, 391-412.

Benhissoune, S., Boudouresque, C.F., Perret-Boudoresque, M. & Verlaque, M. (2003) A check-list of marine seaweeds of the Mediterranean and Atlantic coasts of Morocco IV. Rhodophyceae - Ceramiales. *Botanica Marina*, **46**, 55-68.

Bennett, K.D. & Provan, J. (2008) What do we mean by 'refugia'? *Quaternary Science Reviews*, **27**, 2449-2455.

Bergamini, A., Ungricht, S. & Hofmann, H. (2009) An elevational shift of cryophilous bryophytes in the last century – an effect of climate warming? *Diversity and Distributions*, **15**, 871-879.

Berger, S., Söhlke, G., Walther, G.-R. & Pott, R. (2007) Bioclimatic limits and range shifts of cold-hardy evergreen broad-leaved species at their northern distributional limit in Europe. *Phytocoenologia*, **37**, 523-539.

Bermejo, R., Ramírez-Romero, E., Vergara, J.J. & Hernández, I. (2015) Spatial patterns of macrophyte composition and landscape along the rocky shores of the Mediterranean–Atlantic transition region (northern Alboran Sea). *Estuarine, Coastal and Shelf Science*, **155**, 17-28.

Berry, P. (1978) Reproduction, growth and production in the mussel *Perna perna* (Linnaeus) on the east coast of South Africa. *Investigational report No. 48, Oceanographic Research Institute*, **48**, 1-28.

Bianchi, C.N., Boero, F., Fraschetti, S. & Morri, C. (2002) La fauna del Mediterraneo. *La fauna in Italia.* , pp. 247-335. Touring Club Italiano, Milan and Ministero dell'Ambiente e della Tutela del Territorio, Rome.

Billard, E., Serrão, E.A., Pearson, G.A., Destombe, C. & Valero, M. (2010) *Fucus vesiculosus* and *spiralis* species complex: a nested model of local adaptation at the shore level. *Marine Ecology Progress Series*, **405**, 163-174.

Blanchette, C.A., Melissa Miner, C., Raimondi, P.T., Lohse, D., Heady, K.E.K. & Broitman, B.R. (2008) Biogeographical patterns of rocky intertidal communities along the Pacific coast of North America. *Journal of Biogeography*, **35**, 1593-1607.

Blanchette, C.A., Wieters, E., Broitman, B., Kinlan, B. & Schiel, D. (2009) Trophic structure and diversity in rocky intertidal upwelling ecosystems: A comparison of community patterns across California, Chile, South Africa and New Zealand. *Progress in Oceanography*, **83**, 107-116.

Bloch, C.P. & Klingbeil, B.T. (2016) Anthropogenic factors and habitat complexity influence biodiversity but wave exposure drives species turnover of a subtropical rocky inter-tidal metacommunity. *Marine Ecology*, **37**, 64-76.

Boaventura, D., Re, P., Cancela da Fonseca, L. & Hawkins, S.J. (2002) Intertidal rocky shore communities of the continental Portuguese coast: analysis of distribution patterns. *Marine Ecology*, **23**, 69-90.

Bongaerts, P., Ridgway, T., Sampayo, E. & Hoegh-Guldberg, O. (2010) Assessing the 'deep reef refugia' hypothesis: focus on Caribbean reefs. *Coral Reefs*, **29**, 309-327.

Borowitzka, M. (1972) Intertidal algal species diversity and the effect of pollution. *Marine and Freshwater Research*, **23**, 73-84.

Borsje, B.W., van Wesenbeeck, B.K., Dekker, F., Paalvast, P., Bouma, T.J., van Katwijk, M.M. & de Vries, M.B. (2011) How ecological engineering can serve in coastal protection. *Ecological Engineering*, **37**, 113-122.

Borthagaray, A.I. & Carranza, A. (2007) Mussels as ecosystem engineers: their contribution to species richness in a rocky littoral community. *Acta Oecologica*, **31**, 243-250.

Bosman, A.L., Hockey, P.A.R. & Siegfried, W.R. (1987) The influence of coastal upwelling on the functional structure of rocky intertidal communities. *Oecologia*, **72**, 226-232.

Boudoresque, C.F., J.G., H. & de Grissac, J. (1986) *Le benthos marin de l'Ile de zembra (Parc National, Tunisie)*. GIS Posidonie, Marseille, France.

Bowcock, A.M., Ruiz-Linares, A., Tomfohrde, J., Minch, E., Kidd, J.R. & Cavalli-Sforza, L.L. (1994) High resolution of human evolutionary trees with polymorphic microsatellites. *Nature*, **368**, 455-457.

Bownes, S.J. & McQuaid, C.D. (2006) Will the invasive mussel *Mytilus galloprovincialis* Lamarck replace the indigenous *Perna perna* L. on the south coast of South Africa? *Journal of Experimental Marine Biology and Ecology*, **338**, 140-151.

Bradshaw, W.E. & Holzapfel, C.M. (2006) Evolutionary response to rapid climate change. *Science*, **312**, 1477-1478.

Brawley, S.H. & Johnson, L.E. (1991) Survival of fucoid embryos in the intertidal zone depends upon developmental stage and microhabitat. *Journal of Phycology*, **27**, 179-186.

Brito, J.C., Godinho, R., Martínez-Freiría, F., Pleguezuelos, J.M., Rebelo, H., Santos, X., Vale, C.G., Velo-Antón, G., Boratyński, Z. & Carvalho, S.B. (2014) Unravelling biodiversity, evolution and threats to conservation in the Sahara-Sahel. *Biological Reviews*, **89**, 215-231.

Broitman, B.R., Navarrete, S.A., Smith, F. & Gaines, S.D. (2001) Geographic variation of southeastern Pacific intertidal communities. *Marine Ecology Progress Series*, **224**, 21-34.

Brown, C.J., O'Connor, M.I., Poloczanska, E.S., Schoeman, D.S., Buckley, L.B., Burrows, M.T., Duarte, C.M., Halpern, B.S., Pandolfi, J.M. & Parmesan, C. (2016) Ecological and methodological drivers of species' distribution and phenology responses to climate change. *Global Change Biology*, **22**, 1548-1560.

Brown, J.H. (2014) Why are there so many species in the tropics? *Journal of Biogeography*, **41**, 8-22.

Bruland, K.W., Rue, E.L. & Smith, G.J. (2001) Iron and macronutrients in California coastal upwelling regimes: Implications for diatom blooms. *Limnology and Oceanography*, **46**, 1661-1674.

Buonomo, R., Assis, J., Fernandes, F., Engelen, A.H., Airoldi, L. & Serrão, E.A. (2017) Habitat continuity and stepping-stone oceanographic distances explain population genetic connectivity of the brown alga *Cystoseira amentacea*. *Molecular Ecology*, **26**, 766-780.

Burgess, S.C., Baskett, M.L., Grosberg, R.K., Morgan, S.G. & Strathmann, R.R. (2016) When is dispersal for dispersal? Unifying marine and terrestrial perspectives. *Biological Reviews*, **91**, 867-882.

Burrows, M.T., Schoeman, D.S., Buckley, L.B., Moore, P., Poloczanska, E.S., Brander, K.M., Brown, C., Bruno, J.F., Duarte, C.M. & Halpern, B.S. (2011) The pace of shifting climate in marine and terrestrial ecosystems. *Science*, **334**, 652-655.

Burrows, M.T., Schoeman, D.S., Richardson, A.J., Molinos, J.G., Hoffmann, A., Buckley, L.B., Moore, P.J., Brown, C.J., Bruno, J.F. & Duarte, C.M. (2014) Geographical limits to species-range shifts are suggested by climate velocity. *Nature*, **507**, 492.

Burt, J.A., Feary, D.A., Bauman, A.G., Usseglio, P., Cavalcante, G.H. & Sale, P.F. (2011) Biogeographic patterns of reef fish community structure in the northeastern Arabian Peninsula. *ICES Journal of Marine Science*, **68**, 1875-1883.

Bush, K.L., Dyte, C.K., Moynahan, B.J., Aldridge, C.L., Sauls, H.S., Battazzo, A.M., Walker, B.L., Doherty, K.E., Tack, J., Carlson, J., Eslinger, D., Nicholson, J., Boyce, M.S., Naugle, D.E., Paszkowski, C.A. & Coltman, D.W. (2011) Population structure and genetic diversity of greater sage-grouse (*Centrocercus urophasianus*) in fragmented landscapes at the northern edge of their range. *Conservation Genetics*, **12**, 527-542.

Bustamante, R.H., Branch, G.M., Eekhout, S., Robertson, B., Zoutendyk, P., Schleyer, M., Dye, A., Hanekom, N., Keats, D., Jurd, M. & McQuaid, C.D. (1995) Gradients of intertidal primary productivity around the coast of South Africa and their relationships with consumer biomass. *Oecologia*, **102**, 189-201.

Bustamante, R.H. & Branch, G.M. (1996a) Large scale patterns and trophic structure of southern African rocky shores: the roles of geographic variation and wave exposure. *Journal of Biogeography*, **23**, 339-351.

Bustamante, R.H. & Branch, G.M. (1996b) The dependence of intertidal consumers on kelp-derived organic matter on the west coast of South Africa. *Journal of Experimental Marine Biology and Ecology*, **196**, 1-28.

Cacciapaglia, C. & van Woesik, R. (2015) Reef-coral refugia in a rapidly changing ocean. *Global Change Biology*, **21**, 2272-2282.

Cahill, A.E., Aiello-Lammens, M.E., Fisher-Reid, M.C., Hua, X., Karanewsky, C.J., Ryu, H.Y., Sbeglia, G.C., Spagnolo, F., Waldron, J.B. & Warsi, O. (2012) How does climate change cause extinction? *Proceedings of the Royal Society B: Biological Sciences*, rspb20121890.

Callapez, P.M., Danielsen, R. & Castilho, A. (2012) Occurrences of the amphi-Atlantic brown mussel *Perna perna* (Linné, 1758)(Mollusca, Bivalvia) in South Portugal since the Atlantic "climatic optimum". *Quaternary Studies*, **8**, 13-21.

Calvo-Ugarteburu, G. & McQuaid, C.D. (1998a) Parasitism and invasive species: effects of digenetic trematodes on mussels. *Marine Ecology Progress Series*, **169**, 149-163.

Calvo-Ugarteburu, G. & McQuaid, C.D. (1998b) Parasitism and introduced species: epidemiology of trematodes in the intertidal mussels *Perna perna* and *Mytilus galloprovincialis*. *Journal of Experimental Marine Biology and Ecology*, **220**, 47-65.

Carreiro-Silva, M., McClanahan, T.R. & Kiene, W.E. (2005) The role of inorganic nutrients and herbivory in controlling microbioerosion of carbonate substratum. *Coral Reefs*, **24**, 214-221.

Carreiro-Silva, M., McClanahan, T.R. & Kiene, W.E. (2009) Effects of inorganic nutrients and organic matter on microbial euendolithic community composition and microbioerosion rates. *Marine Ecology Progress Series*, **392**, 1-15.

Carreiro-Silva, M., Kiene, W.E., Golubic, S. & McClanahan, T.R. (2012) Phosphorus and nitrogen effects on microbial euendolithic communities and their bioerosion rates. *Marine Pollution Bulletin*, **64**, 602-613.

Castilla, J.C., Lagos, N.A. & Cerda, M. (2004) Marine ecosystem engineering by the alien ascidian *Pyura praeputialis* on a mid-intertidal rocky shore. *Marine Ecology Progress Series*, **268**, 119-130.

Cayré, P. (1978) Étude de la moule *Perna perna* L. et des possibilities de Myticulture en République Populaire du Congo. *Cahiers ORSTOM. Serie Oceanographie*, **16**, 9-17.

Cefalì, M.E., Cebrian, E., Chappuis, E., Pinedo, S., Terradas, M., Mariani, S. & Ballesteros, E. (2016) Life on the boundary: Environmental factors as drivers of habitat distribution in the littoral zone. *Estuarine, Coastal and Shelf Science*, **172**, 81-92.

Cereceda, P., Osses, P., Larrain, H., Farıas, M., Lagos, M., Pinto, R. & Schemenauer, R. (2002) Advective, orographic and radiation fog in the Tarapacá region, Chile. *Atmospheric Research*, **64**, 261-271.

Cermak, J. (2012) Low clouds and fog along the southwestern African coast—Satellite-based retrieval and spatial patterns. *Atmospheric Research*, **116**, 15-21.

Chan, B.K., Morritt, D., De Pirro, M., Leung, K.M. & Williams, G.A. (2006) Summer mortality: effects on the distribution and abundance of the acorn barnacle *Tetraclita japonica* on tropical shores. *Marine Ecology Progress Series*, **328**, 195-204.

Chaudhary, C., Saeedi, H. & Costello, M.J. (2016) Bimodality of latitudinal gradients in marine species richness. *Trends in Ecology & Evolution*, **31**, 670-676.

Chefaoui, R.M. & Lobo, J.M. (2008) Assessing the effects of pseudo-absences on predictive distribution model performance. *Ecological Modelling*, **210**, 478-486.

Chefaoui, R.M., Assis, J., Duarte, C.M. & Serrão, E.A. (2016) Large scale prediction of seagrass distribution integrating landscape metrics and environmental factors: the case of *Cymodocea nodosa* (Mediterranean–Atlantic). *Estuaries and Coasts*, **39**, 123-137.

Chen, I.-C., Hill, J.K., Ohlemüller, R., Roy, D.B. & Thomas, C.D. (2011) Rapid range shifts of species associated with high levels of climate warming. *Science*, **333**, 1024-1026.

Cheung, W.W., Lam, V.W., Sarmiento, J.L., Kearney, K., Watson, R. & Pauly, D. (2009) Projecting global marine biodiversity impacts under climate change scenarios. *Fish and Fisheries*, **10**, 235-251.

Chivers, W.J., Walne, A.W. & Hays, G.C. (2017) Mismatch between marine plankton range movements and the velocity of climate change. *Nature Communications*, **8**, 14434.

Chlaida, M., Kifani, S., Lenfant, P. & Ouragh, L. (2006) First approach for the identification of sardine populations *Sardina pilchardus* (Walbaum 1792) in the Moroccan Atlantic by allozymes. *Marine Biology*, **149**, 169-175.

Chlaida, M., Laurent, V., Kifani, S., Benazzou, T., Jaziri, H. & Planes, S. (2009) Evidence of a genetic cline for *Sardina pilchardus* along the Northwest African coast. *ICES Journal of Marine Science*, **66**, 264-271.

Chollett, I., Mumby, P.J. & Cortés, J. (2010) Upwelling areas do not guarantee refuge for coral reefs in a warming ocean. *Marine Ecology Progress Series*, **416**, 47-56.

Chollett, I. & Mumby, P.J. (2013) Reefs of last resort: Locating and assessing thermal refugia in the wider Caribbean. *Biological Conservation*, **167**, 179-186.

Christianen, M.J.A., van der Heide, T., Holthuijsen, S.J., van der Reijden, K.J., Borst, A.C.W. & Olff, H. (2016) Biodiversity and food web indicators of community recovery in intertidal shellfish reefs. *Biological Conservation*, **213**, 317-324.

Clark, P.U. & Mix, A.C. (2002) Ice sheets and sea level of the Last Glacial Maximum. *Quaternary Science Reviews*, **21**, 1-7.

Clarke, K.R. (1993) Non-parametric multivariate analyses of changes in community structure. *Australian Journal of Ecology*, **18**, 117-143.

Clarke, K.R. & Gorley, R.N. (2006) *PRIMER V6: user manual-tutorial*. Plymouth Marine Laboratory.

Clavier, J., Castets, M.-D., Bastian, T., Hily, C., Boucher, G. & Chauvaud, L. (2009) An amphibious mode of life in the intertidal zone: aerial and underwater contribution of

Chthamalus montagui to CO_2 fluxes. *Marine Ecology Progress Series*, **375**, 185-194.

Coelho, N.C., Zardi, G.I., Pearson, G.A., Serrão, E.A. & Nicastro, K.R. (2012) Characterization of ten highly polymorphic microsatellite loci for the intertidal mussel *Perna perna*, and cross species amplification within the genus. *BMC Research Notes*, **5**, 558.

Cole, P.G. & Weltzin, J.F. (2005) Light limitation creates patchy distribution of an invasive grass in eastern deciduous forests. *Biological Invasions*, **7**, 477-488.

Cole, V.J. (2010) Alteration of the configuration of bioengineers affects associated taxa. *Marine Ecology Progress Series*, **416**, 127-136.

Cole, V.J. & McQuaid, C.D. (2010) Bioengineers and their associated fauna respond differently to the effects of biogeography and upwelling. *Ecology*, **91**, 3549-3562.

Cole, V.J., Hutchings, P.A. & Ross, P.M. (2016) Predicting biodiversity changes due to loss of bioengineers from an intertidal landscape, a case study from Sydney Harbour. *Australian zoologist*.

Coleman, M.A. & Brawley, S.H. (2005) Are life history characteristics good predictors of genetic diversity and structure? A case study of the intertidal alga *Fucus spiralis* (Heterokontophyta; Phaephyceae). *Journal of Phycology*, **41**, 753-762.

Coll, M., Piroddi, C., Steenbeek, J., Kaschner, K., Lasram, F.B.R., Aguzzi, J., Ballesteros, E., Bianchi, C.N., Corbera, J. & Dailianis, T. (2010) The biodiversity of the Mediterranean Sea: estimates, patterns, and threats. *PLoS One*, **5**, e11842.

Collins, M., Knutti, R., Arblaster, J., Dufresne, J.-L., Fichefet, T., Friedlingstein, P., Gao, X., Gutowski, W.J., Johns, T., Krinner, G., Shongwe, M., Tebaldi, C., Weaver, A.J. & Wehner, M. (2013) Long-term climate change: projections, commitments and irreversibility. *Climate Change 2013: The Physical Science Basis. Contribution of Working Group I to the Fifth Assessment Report of the Intergovernmental Panel on Climate Change* (ed. by T.F. Stocker, D. Qin, G.-K. Plattner, M. Tignor, S.K. Allen, J. Boschung, A. Nauels, Y. Xia, V. Bex and P.M. Midgley). Cambridge University Press, Cambridge, United Kingdom and New York, NY, USA.

Conde, F. & Seoane, J.A. (1982) Corología de las especies de algas en relación a ciertos factores ecológicos en el litoral Malagueño. *Collectanea Botanica*, **13**, 783-802.

Condit, R., Engelbrecht, B.M.J., Pino, D., Pérez, R. & Turner, B.L. (2013) Species distributions in response to individual soil nutrients and seasonal drought across a community of tropical trees. *Proceedings of the National Academy of Sciences*, **110**, 5064-5068.

Connolly, S.R. & Roughgarden, J. (1998) A latitudinal gradient in northeast Pacific intertidal community structure: evidence for an oceanographically based synthesis of marine community theory. *The American Naturalist*, **151**, 311-326.

Coristine, L.E. & Kerr, J.T. (2015) Temperature-related geographical shifts among passerines: contrasting processes along poleward and equatorward range margins. *Ecology and Evolution*, **5**, 5162-5176.

Costantini, F., Fauvelot, C. & Abbiati, M. (2007) Fine-scale genetic structuring in *Corallium rubrum*: Evidence of inbreeding and limited effective larval dispersal. *Marine Ecology Progress Series*, **340**, 109-119.

Coyer, J.A., Hoarau, G., Beszteri, B., Pearson, G.A. & Olsen, J.L. (2009) Expressed sequence tag-derived polymorphic SSR markers for *Fucus serratus* and amplification in other species of *Fucus*. *Molecular Ecology Resources*, **9**, 168-70.

Coyer, J.A., Hoarau, G., Costa, J.F., Hogerdijk, B., Serrão, E.A., Billard, E., Valero, M., Pearson, G.A. & Olsen, J.L. (2011a) Evolution and diversification within the intertidal brown macroalgae *Fucus spiralis/F. vesiculosus* species complex in the North Atlantic. *Molecular Phylogenetics and Evolution*, **58**, 283-296.

Coyer, J.A., Hoarau, G., Pearson, G.A., Mota, C., Juterbock, A., Alpermann, T., John, U. & Olsen, J.L. (2011b) Genomic scans detect signatures of selection along a salinity gradient in populations of the intertidal seaweed *Fucus serratus* on a 12 km scale. *Marine Genomics*, **4**, 41-9.

Crisp, D., Southward, A. & Southward, E.C. (1981) On the distribution of the intertidal barnacles *Chthamalus stellatus*, *Chthamalus montagui* and *Euraphia depressa*. *Journal of the Marine Biological Association of the United Kingdom*, **61**, 359-380.

Cropper, T.E., Hanna, E. & Bigg, G.R. (2014) Spatial and temporal seasonal trends in coastal upwelling off Northwest Africa, 1981–2012. *Deep Sea Research Part I: Oceanographic Research Papers*, **86**, 94-111.

Cunha, R.L., Nicastro, K.R., Costa, J.F., McQuaid, C.D., Serrão, E.A. & Zardi, G.I. (2014) Wider sampling reveals a non-sister relationship for geographically contiguous lineages of a marine mussel. *Ecology and Evolution*, **4**, 2070-2081.

Ćurin, M., Peharda, M., Calcinai, B. & Golubić, S. (2014) Incidence of damaging endolith infestation of the edible mytilid bivalve *Modiolus barbatus*. *Marine Biology Research*, **10**, 179-189.

D'Aloia, C.C., Bogdanowicz, S.M., Francis, R.K., Majoris, J.E., Harrison, R.G. & Buston, P.M. (2015) Patterns, causes, and consequences of marine larval dispersal. *Proceedings of the National Academy of Sciences*, **112**, 13940-13945.

Dawson, M.N., Hays, C.G., Grosberg, R.K. & Raimondi, P.T. (2014) Dispersal potential and population genetic structure in the marine intertidal of the eastern North Pacific. *Ecological Monographs*, **84**, 435-456.

de Rivera, C.E., Steves, B.P., Fofonoff, P.W., Hines, A.H. & Ruiz, G.M. (2011) Potential for high-latitude marine invasions along western North America. *Diversity and Distributions*, **17**, 1198-1209.

DeCarlo, T.M., Cohen, A.L., Wong, G.T., Davis, K.A., Lohmann, P. & Soong, K. (2017) Mass coral mortality under local amplification of 2° C ocean warming. *Scientific Reports*, **7**, 44586.

Decker, C., Griffiths, C., Prochazka, K., Ras, C. & Whitfield, A. (2003) Marine biodiversity in sub-Saharan Africa: The known and the unknown. *Proceedings of the Marine Biodiversity in Sub-Saharan Africa: The Known and the Unknown*. Cape Town, South Africa, 310 pp.

Demarcq, H., Barlow, R. & Shillington, F. (2003) Climatology and variability of sea surface temperature and surface chlorophyll in the Benguela and Agulhas ecosystems as observed by satellite imagery. *African Journal of Marine Science*, **25**, 363-372.

Dennis, A.B. & Hellberg, M.E. (2010) Ecological partitioning among parapatric cryptic species. *Molecular Ecology*, **19**, 3206-3225.

Diekmann, O.E. & Serrão, E.A. (2012) Range-edge genetic diversity: locally poor extant southern patches maintain a regionally diverse hotspot in the seagrass *Zostera marina*. *Molecular Ecology*, **21**, 1647-1657.

Duarte, L., Viejo, R.M., Martínez, B., Gómez-Gesteira, M. & Gallardo, T. (2013) Recent and historical range shifts of two canopy-forming seaweeds in North Spain and the link with trends in sea surface temperature. *Acta oecologica*, **51**, 1-10.

Dubois, S., Comtet, T., Retière, C. & Thiébaut, E. (2007) Distribution and retention of *Sabellaria alveolata* larvae (Polychaeta: Sabellariidae) in the Bay of Mont-Saint-Michel, France. *Marine Ecology Progress Series*, **346**, 243-254.

Dulvy, N.K., Rogers, S.I., Jennings, S., Stelzenmüller, V., Dye, S.R. & Skjoldal, H.R. (2008) Climate change and deepening of the North Sea fish assemblage: a biotic indicator of warming seas. *Journal of Applied Ecology*, **45**, 1029-1039.

Earl, D.A. & von Holdt, B.M. (2012) STRUCTURE HARVESTER: a website and program for visualizing STRUCTURE output and implementing the Evanno method. *Conservation Genetics Resources*, **4**, 359-361.

Eckert, C.G., Samis, K.E. & Lougheed, S.C. (2008) Genetic variation across species' geographical ranges: the central–marginal hypothesis and beyond. *Molecular Ecology*, **17**, 1170-1188.

Eiríksson, J., Bartels-Jonsdottir, H.B., Cage, A.G., Gudmundsdottir, E.R., Klitgaard-Kristensen, D., Marret, F., Rodrigues, T., Abrantes, F., Austin, W.E. & Jiang, H. (2006) Variability of the North Atlantic Current during the last 2000 years based on shelf bottom water and sea surface temperatures along an open ocean/shallow marine transect in western Europe. *The Holocene*, **16**, 1017-1029.

Elso, M.Z., Manent, P., Luque, A., Ramdani, M. & Robaina, R. (2016) Genetic description and remote sensing techniques as management tools for *Zostera noltii* seagrass populations along the Atlantic Moroccan coast. *Journal of Coastal Research*, **33**, 78-87.

Emanuel, B., Bustamante, R., Branch, G., Eekhout, S. & Odendaal, F. (1992) A zoogeographic and functional approach to the selection of marine reserves on the west coast of South Africa. *South African Journal of Marine Science*, **12**, 341-354.

Engel, C.R., Brawley, S.H., Edwards, K.J. & Serrao, E. (2003) Isolation and cross-species amplification of microsatellite loci from the fucoid seaweeds *Fucus vesiculosus*, *F. serratus* and *Ascophyllum nodosum* (Heterokontophyta, Fucaceae). *Molecular Ecology Notes*, **3**, 180-182.

Engle, J.M. (2008) Unified monitoring protocols for the multi-agency rocky intertidal network. In: *MMS Cooperative Agreement No. 14-35-0001-30761*, p. 84. Marine Science Institute, University if California, Santa Barbara, CA, USA.

Engler, R., Guisan, A. & Rechsteiner, L. (2004) An improved approach for predicting the distribution of rare and endangered species from occurrence and pseudo-absence data. *Journal of Applied Ecology*, **41**, 263-274.

Erasmus, B.F., Van Jaarsveld, A.S., Chown, S.L., Kshatriya, M. & Wessels, K.J. (2002) Vulnerability of South African animal taxa to climate change. *Global Change Biology*, **8**, 679-693.

Erlandsson, J., Pal, P. & McQuaid, C.D. (2006) Re-colonisation rate differs between co-existing indigenous and invasive intertidal mussels following major disturbance. *Marine Ecology Progress Series*, **320**, 169-176.

Escorza-Treviño, S. & Dizon, A.E. (2000) Phylogeography, intraspecific structure and sex-biased dispersal of Dall's porpoise, *Phocoenoides dalli*, revealed by mitochondrial and microsatellite DNA analyses. *Molecular Ecology*, **9**, 1049-1060.

Espinosa-Carreon, T.L., Strub, P.T., Beier, E., Ocampo-Torres, F. & Gaxiola-Castro, G. (2004) Seasonal and interannual variability of satellite-derived chlorophyll pigment, surface height, and temperature off Baja California. *Journal of Geophysical Research: Oceans*, **109**, C3.

Evanno, G., Regnaut, S. & Goudet, J. (2005) Detecting the number of clusters of individuals using the software STRUCTURE: a simulation study. *Molecular Ecology*, **14**, 2611-20.

Excoffier, L., Laval, G. & Schneider, S. (2005) Arlequin ver. 3.0: an integrated software package for population genetics data analysis. *Evolutionary Bioinformatics Online*, **1**, 47-50.

Feare, C.J. (1971) The adaptive significance of aggregation behaviour in the dogwhelk *Nucella lapillus* (L.). *Oecologia*, **7**, 117-126.

Fellous, S. & Salvaudon, L. (2009) How can your parasites become your allies? *Trends in Parasitology*, **25**, 62-66.

Fenberg, P.B., Menge, B.A., Raimondi, P.T. & Rivadeneira, M.M. (2015) Biogeographic structure of the northeastern Pacific rocky intertidal: the role of upwelling and dispersal to drive patterns. *Ecography*, **38**, 83-95.

Fernández, R., Lemer, S., McIntyre, E. & Giribet, G. (2015) Comparative phylogeography and population genetic structure of three widespread mollusc species in the Mediterranean and near Atlantic. *Marine Ecology*, **36**, 701-715.

Fielding, A.H. & Bell, J.F. (1997) A review of methods for the assessment of prediction errors in conservation presence/absence models. *Environmental Conservation*, **24**, 38-49.

Firth, L.B., Knights, A.M. & Bell, S.S. (2011) Air temperature and winter mortality: implications for the persistence of the invasive mussel, *Perna viridis* in the intertidal zone of the southeastern United States. *Journal of Experimental Marine Biology and Ecology*, **400**, 250-256.

Firth, L.B., Mieszkowska, N., Grant, L.M., Bush, L.E., Davies, A.J., Frost, M.T., Moschella, P.S., Burrows, M.T., Cunningham, P.N., Dye, S.R. & Hawkins, S.J. (2015) Historical comparisons reveal multiple drivers of decadal change of an ecosystem engineer at the range edge. *Ecology and Evolution*, **5**, 3210-3222.

Fischer-Piétte, E. (1958) Sur l'écologie intercotidal Ouest-Ibérique. *Comptes Rendus de l'Académie des Sciences (Paris)*, **246**, 1301-1303.

Fischer-Piétte, E. (1963) La distribution des principaux organismes intercotidaux Nord-Iberiques en 1954-1955. *Annals of the Insitute of Oceanography Paris*, **40**, 165-311.

Folkard, A., Davies, P. & Prieur, L. (1994) The surface temperature field and dynamical structure of the Almeria-Oran front from simultaneous shipboard and satellite data. *Journal of Marine Systems*, **5**, 205-222.

Folmer, O., Black, M., Hoeh, W., Lutz, R. & Vrijenhoek, R. (1994) DNA primers for amplification of mitochondrial cytochrome c oxidase subunit I from diverse metazoan invertebrates. *Molecular Marine Biology and Biotechnology*, **3**, 294-299.

Frade, P., De Jongh, F., Vermeulen, F., Van Bleijswijk, J. & Bak, R. (2008) Variation in symbiont distribution between closely related coral species over large depth ranges. *Molecular Ecology*, **17**, 691-703.

Franchimont, J. & Saadaoui, E.M. (2001) National study on biodiversity synthesis report. In. Ministry of Territorial Planning, Water and Environment, Kingdom of Morocco

Francis, A.P. & Currie, D.J. (2003) A globally consistent richness-climate relationship for angiosperms. *The American Naturalist*, **161**, 523-536.

Franco, A., Hill, J.K., Kitschke, C., Collingham, Y.C., Roy, D.B., Fox, R., Huntley, B. & Thomas, C.D. (2006) Impacts of climate warming and habitat loss on extinctions at species' low-latitude range boundaries. *Global Change Biology*, **12**, 1545-1553.

Fratini, S., Ragionieri, L., Deli, T., Harrer, A., Marino, I.A.M., Cannicci, S., Zane, L. & Schubart, C.D. (2016) Unravelling population genetic structure with mitochondrial DNA in a notional panmictic coastal crab species: sample size makes the difference. *BMC Evolutionary Biology*, **16**, 150.

Freeman, B.G. & Class Freeman, A.M. (2014) Rapid upslope shifts in New Guinean birds illustrate strong distributional responses of tropical montane species to global warming. *Proceedings of the National Academy of Sciences*, **111**, 4490-4494.

Garcia-Pichel, F., Ramírez-Reinat, E. & Gao, Q. (2010) Microbial excavation of solid carbonates powered by P-type ATPase-mediated transcellular Ca^{2+} transport. *Proceedings of the National Academy of Sciences*, **107**, 21749-21754.

García-Reyes, M., Sydeman, W.J., Schoeman, D.S., Rykaczewski, R.R., Black, B.A., Smit, A.J. & Bograd, S.J. (2015) Under pressure: climate change, upwelling, and Eastern Boundary Upwelling Ecosystems. *Frontiers in Marine Science*, **2**

Garrity, S.D. (1984) Some adaptations of gastropods to physical stress on a tropical rocky shore. *Ecology*, **65**, 559-574.

Gaspar, R., Pereira, L. & Neto, J.M. (2017) Intertidal zonation and latitudinal gradients on macroalgal assemblages: Species, functional groups and thallus morphology approaches. *Ecological Indicators*, **81**, 90-103.

Gavin, D.G., Fitzpatrick, M.C., Gugger, P.F., Heath, K.D., Rodriguez-Sanchez, F., Dobrowski, S.Z., Hampe, A., Hu, F.S., Ashcroft, M.B., Bartlein, P.J., Blois, J.L., Carstens, B.C., Davis, E.B., de Lafontaine, G., Edwards, M.E., Fernandez, M., Henne, P.D., Herring, E.M., Holden, Z.A., Kong, W.S., Liu, J., Magri, D., Matzke,

N.J., McGlone, M.S., Saltre, F., Stigall, A.L., Tsai, Y.H. & Williams, J.W. (2014) Climate refugia: joint inference from fossil records, species distribution models and phylogeography. *New Phytologist*, **204**, 37-54.

Gazeau, F., Alliouane, S., Bock, C., Bramanti, L., Correa, M.L., Gentile, M., Hirse, T., Pörtner, H.-O. & Ziveri, P. (2014) Impact of ocean acidification and warming on the Mediterranean mussel (*Mytilus galloprovincialis*). *Frontiers in Marine Science*, **1**, 62.

Gerlach, G., Jueterbock, A., Kraemer, P., Deppermann, J. & Harmand, P. (2010) Calculations of population differentiation based on G(ST) and D: forget G(ST) but not all of statistics! *Molecular Ecology* **19**, 3845-3852.

Gilman, S., Hayford., H., Craig, C. & Carrington, E. (2015) Body temperatures of an intertidal barnacle and two whelk predators in relation to shore height, solar aspect, and microhabitat. *Marine Ecology Progress Series,* **536**, 77-88.

Gómez-Gesteira, M., De Castro, M., Álvarez, I., Lorenzo, M.N., Gesteira, J.L.G. & Crespo, A.J.C. (2008) Spatio-temporal upwelling trends along the Canary Upwelling System (1967–2006). *Annals of the New York Academy of Sciences*, **1146**, 320-337.

González García, J.A. & Conde Poyales, F. (1994) Catálogo del macrofitobentos del Mediterráneo de Marruecos. *Acta Botanica Malacitana*, **19**, 5-27.

Goudet, J. (1995) FSTAT (Version 1.2): a computer program to calculate F-Statistics. *Journal of Heredity*, **86**, 485-486.

Graham, M.H., Kinlan, B.P., Druehl, L.D., Garske, L.E. & Banks, S. (2007) Deep-water kelp refugia as potential hotspots of tropical marine diversity and productivity. *Proceedings of the National Academy of Sciences*, **104**, 16576-16580.

Graham, N.A.J., Wilson, S.K., Jennings, S., Polunin, N.V.C., Bijoux, J.P. & Robinson, J. (2006) Dynamic fragility of oceanic coral reef ecosystems. *Proceedings of the National Academy of Sciences*, **103**, 8425-8429.

Gray, J.S. (2002) Species richness of marine soft sediments. *Marine Ecology Progress Series*, **244**, 285-297.

Griffiths, C., Hockey, P., Van Erkom Schurink, C. & Le Roux, P. (1992) Marine invasive aliens on South African shores: implications for community structure and tropillc functioning. *South African Journal of Marine Science*, **12**, 713-722.

Grosberg, C. & Cunningham, C. (2001) Genetic structure in the sea: from populations to communities. *Marine Community Ecology* (ed. by M. Bertness, S. Gaines and M. Hay), pp. 61-84. Sinauer Associates.

Guerry, A.D. & Menge, B.A. (2017) Grazer impacts on algal community structure vary with the coastal upwelling regime. *Journal of Experimental Marine Biology and Ecology*, **488**, 10-23.

Hammond, W. & Griffiths, C. (2004) Influence of wave exposure on South African mussel beds and their associated infaunal communities. *Marine Biology*, **144**, 547-552.

Hampe, A. & Petit, R.J. (2005) Conserving biodiversity under climate change: the rear edge matters. *Ecology Letters*, **8**, 461-467.

Hare, M.P., Guenther, C., Fagan, W.F. & Ó Foighil, D. (2005) Nonrandom larval dispersal can steeepen marine clines. *Evolution*, **59**, 2509-2517.

Harley, C.D.G. (2008) Tidal dynamics, topographic orientation, and temperature-mediated mass mortalities on rocky shores. *Marine Ecology Progress Series*, **371**, 37-46.

Harley, C.D.G. (2011) Climate change, keystone predation, and biodiversity loss. *Science*, **334**, 1124-1127.

Harley, C.D.G. & Helmuth, B.S.T. (2003) Local- and regional-scale effects of wave exposure, thermal stress, and absolute versus effective shore level on patterns of intertidal zonation. *Limnology and Oceanography*, **48**, 1498-1508.

Harley, C.D.G., Randall Hughes, A., Hultgren, K.M., Miner, B.G., Sorte, C.J., Thornber, C.S., Rodriguez, L.F., Tomanek, L. & Williams, S.L. (2006) The impacts of climate change in coastal marine systems. *Ecology Letters*, **9**, 228-241.

Harris, J.M., Branch, G.M., Elliott, B.L., Currie, B., Dye, A.H., McQuaid, C.D., Tomalin, B.J. & Velasquez, C. (1998) Spatial and temporal variability in recruitment of intertidal mussels around the coast of southern Africa. *South African Journal of Zoology*, **33**, 1-11.

Hassoun, M., Salhi, G., Bouksir, H., Moussa, H., Riadi, H. & Kazzaz, M. (2014) *Codium tomentosum var. mucronatum* et son epiphyte *Aglaothamnion pseudobyssoides*, deux nouvelles espèces d'algues benthiques pour la phycoflore du Maroc. *Acta Botanica Malacitana*, **39**, 37-44.

Hassoun, M., Salhi, G., Kazzaz, M., Riadi, H. & Moussa, H. (2016) New records of *Polysiphonia* sensu lato from the Atlantic Ocean in Morocco. *Marine Biodiversity*, **46**, 443-449.

Head, E., Harrison, W., Irwin, B., Horne, E. & Li, W. (1996) Plankton dynamics and carbon flux in an area of upwelling off the coast of Morocco. *Deep Sea Research Part I: Oceanographic Research Papers*, **43**, 1713-1738.

Heino, J. (2001) Regional gradient analysis of freshwater biota: do similar biogeographic patterns exist among multiple taxonomic groups? *Journal of Biogeography*, **28**, 69-76.

Helmuth, B.S. (1998) Intertidal mussel microclimates: predicting the body temperature of a sessile invertebrate. *Ecological Monographs*, **68**, 51-74.

Helmuth, B.S. & Hofmann, G.E. (2001) Microhabitats, thermal heterogeneity, and patterns of physiological stress in the rocky intertidal zone. *The Biological Bulletin*, **201**, 374-384.

Helmuth, B.S., Harley, C.D.G., Halpin, P.M., O'donnell, M., Hofmann, G.E. & Blanchette, C.A. (2002) Climate change and latitudinal patterns of intertidal thermal stress. *Science*, **298**, 1015-1017.

Helmuth, B.S., Broitman, B.R., Blanchette, C.A., Gilman, S., Halpin, P., Harley, C.D.G., O'Donnell, M.J., Hofmann, G.E., Menge, B. & Strickland, D. (2006) Mosaic patterns of termal stress in the rocky intertidal zone: implications for climate change. *Ecological Monographs*, **76**, 461-479.

Helmuth, B.S., Yamane, L., Lalwani, S., Matzelle, A., Tockstein, A. & Gao, N. (2011) Hidden signals of climate change in intertidal ecosystems: what (not) to expect

when you are expecting. *Journal of Experimental Marine Biology and Ecology*, **400**, 191-199.

Helmuth, B.S., Choi, F., Matzelle, A., Torossian, J.L., Morello, S.L., Mislan, K.A.S., Yamane, L., Strickland, D., Szathmary, P.L., Gilman, S.E., Tockstein, A., Hilbish, T.J., Burrows, M.T., Power, A.M., Gosling, E., Mieszkowska, N., Harley, C.D.G., Nishizaki, M., Carrington, E., Menge, B., Petes, L., Foley, M.M., Johnson, A., Poole, M., Noble, M.M., Richmond, E.L., Robart, M., Robinson, J., Sapp, J., Sones, J., Broitman, B.R., Denny, M.W., Mach, K.J., Miller, L.P., O'Donnell, M., Ross, P., Hofmann, G.E., Zippay, M., Blanchette, C., Macfarlan, J.A., Carpizo-Ituarte, E., Ruttenberg, B., Peña Mejía, C.E., McQuaid, C.D., Lathlean, J., Monaco, C.J., Nicastro, K.R. & Zardi, G.I. (2016) Long-term, high frequency in situ measurements of intertidal mussel bed temperatures using biomimetic sensors. *Scientific Data*, **3**, 160087.

Henriques, R., Potts, W.M., Sauer, W.H., Santos, C.V., Kruger, J., Thomas, J.A. & Shaw, P.W. (2016) Molecular genetic, life-history and morphological variation in a coastal warm temperate sciaenid fish: evidence for an upwelling-driven speciation event. *Journal of Biogeography*, **43**, 1820-1831.

Herbert, R.J.H., Ma, L., Marston, A., Farnham, W.F., Tittley, I. & Cornes, R.C. (2016) The calcareous brown alga *Padina pavonica* in southern Britain: population change and tenacity over 300 years. *Marine Biology*, **163**, 46.

Hewitt, G. (2004) Genetic consequences of climatic oscillations in the Quaternary. *Philosophical Transactions of the Royal Society of London B: Biological Sciences*, **359**, 183-195.

Hicks, D.W. & Tunnell, J.W.J. (1993) Invasion of the south Texas coast by the edible brown mussel *Perna perna* (Linnaeus, 1758). *Veliger*, **36**, 92 - 99.

Hicks, D.W. & Tunnell, J.W.J. (1995) Ecological notes and patterns of dispersal in the recently introduced mussel, *Perna perna* (Linneaus, 1758), in the Gulf of Mexico. *American Malacological Bulletin*, **11**, 203-206.

Hicks, D.W. & McMahon, R. (2002) Temperature acclimation of upper and lower thermal limits and freeze resistance in the nonindigenous brown mussel, *Perna perna* (L.), from the Gulf of Mexico. *Marine Biology*, **140**, 1167-1179.

Hiddink, J.G., Burrows, M.T. & García Molinos, J. (2015) Temperature tracking by North Sea benthic invertebrates in response to climate change. *Global Change Biology*, **21**, 117-129.

Hillebrand, H. (2004) On the generality of the latitudinal diversity gradient. *The American Naturalist*, **163**, 192-211.

Hoarau, G., Coyer, J.A., Stam, W.T. & Olsen, J.L. (2007) A fast and inexpensive DNA extraction/purification protocol for brown macroalgae. *Molecular Ecology Notes*, **7**, 191-193.

Hockey, P.A.R. & van Erkom Schurink, C. (1992) The invasive biology of the mussel *Mytilus galloprovincialis* on the southern African coast. *Transactions of the Royal Society of South Africa*, **48**, 123-139.

Hoegh-Guldberg, O. & Bruno, J.F. (2010) The impact of climate change on the world's marine ecosystems. *Science*, **328**, 1523-1528.

Hoffmann, A.A. & Sgrò, C.M. (2011) Climate change and evolutionary adaptation. *Nature*, **470**, 479-485.

Hofmann, G. & Somero, G. (1995) Evidence for protein damage at environmental temperatures: seasonal changes in levels of ubiquitin conjugates and hsp70 in the intertidal mussel *Mytilus trossulus*. *Journal of Experimental Biology*, **198**, 1509-1518.

Homburg, K., Drees, C., Gossner, M.M., Rakosy, L., Vrezec, A. & Assmann, T. (2013) Multiple glacial refugia of the low-dispersal ground beetle *Carabus irregularis*: molecular data support predictions of species distribution models. *PLoS ONE*, **8**, e61185.

Honkoop, P. & van der Meer, J. (1998) Experimentally induced effects of water temperature and immersion time on reproductive output of bivalves in the Wadden Sea. *Journal of Experimental Marine Biology and Ecology*, **220**, 227-246.

Houghton, R.W. & Mensah, M.A. (1978) Physical aspects and biological consequences of Ghanaian coastal upwelling. *Upwelling Ecosystems* (ed. by R. Boje and M. Tomczak), pp. 167-180. Springer Berlin Heidelberg, Berlin, Heidelberg.

Hu, Z.-M. & Guillemin, M.-L. (2016) Coastal upwelling areas as safe havens during climate warming. *Journal of Biogeography*, **43**, 2513-2514.

Hughes, A.R., Schenck, F.R., Bloomberg, J., Hanley, T.C., Feng, D., Gouhier, T.C., Beighley, R.E. & Kimbro, D.L. (2016) Biogeographic gradients in ecosystem processes of the invasive ecosystem engineer *Phragmites australis*. *Biological Invasions*, **18**, 2577-2595.

Hutchings, L., Pitcher, G.C., Probyn, T.A. & Bailey, G.W. (1995) The chemical and biological consequences of coastal upwelling. *Environmental Sciences Research Report*, **18**, 65-82.

Hutchings, L., van Der Lingen, C.D., Shannon, L.J., Crawford, R.J.M., Verheye, H.M.S., Bartholomae, C.H., van der Plas, A.K., Louw, D., Kreiner, A. & Ostrowski, M. (2009) The Benguela Current: An ecosystem of four components. *Progress in Oceanography*, **83**, 15-32.

IPCC (2014) Climate Change 2014: Synthesis Report. Contribution of working groups I, II and III to the Fifth Assessment Report of the Intergovernmental Panel on Climate Change. In: eds. R.K. Pachauri and L.A. Meyer), p. 151. IPCC, Geneva, Switzerland.

Jablonski, D., Roy, K. & Valentine, J.W. (2006) Out of the tropics: evolutionary dynamics of the latitudinal diversity gradient. *Science*, **314**, 102-106.

Jakobsson, M. & Rosenberg, N.A. (2007) CLUMPP: a cluster matching and permutation program for dealing with label switching and multimodality in analysis of population structure. *Bioinformatics*, **23**, 1801-1806.

James, K., Kibele, J. & Shears, N.T. (2015) Using satellite-derived sea surface temperature to predict the potential global range and phenology of the invasive kelp *Undaria pinnatifida*. *Biological Invasions*, **17**, 3393-3408.

Jaspers, C., Møller, L.F. & Kiørboe, T. (2011) Salinity gradient of the Baltic Sea limits the reproduction and population expansion of the newly invaded comb jelly *Mnemiopsis leidyi*. *PLoS One*, **6**, e24065.

Jaziri, H. & Benazzou, T. (2002) Différenciation allozymique multilocus des populations de moule *Mytilus galloprovincialis* Lmk. des côtes marocaines. *Comptes rendus Biologies*, **325**, 1175-1183.

Jin, L. & Chakraborty, R. (1994) Estimation of genetic distance and coefficient of gene diversity from single-probe multilocus DNA fingerprinting data. *Molecular Biology and Evolution*, **11**, 120-127.

John, D.M., Prud'homme van Reine, W.F., Lawson, G., Kostermans, T. & Price, J. (2004) A taxonomic and geographical catalogue of the seaweeds of the western coast of Africa and adjacent islands. *Beihefte zur Nova Hedwigia*, **127**, 1-339.

Johnson, C.R., Banks, S.C., Barrett, N.S., Cazassus, F., Dunstan, P.K., Edgar, G.J., Frusher, S.D., Gardner, C., Haddon, M. & Helidoniotis, F. (2011) Climate change cascades: Shifts in oceanography, species' ranges and subtidal marine community dynamics in eastern Tasmania. *Journal of Experimental Marine Biology and Ecology*, **400**, 17-32.

Jombart, T. (2008) adegenet: a R package for the multivariate analysis of genetic markers. *Bioinformatics*, **24**, 1403-1405.

Jombart, T., Devillard, S. & Balloux, F. (2010) Discriminant analysis of principal components: a new method for the analysis of genetically structured populations. *BMC Genetics*, **11**, 94.

Jones, S.J., Lima, F.P. & Wethey, D.S. (2010) Rising environmental temperatures and biogeography: poleward range contraction of the blue mussel, *Mytilus edulis* L., in the western Atlantic. *Journal of Biogeography*, **37**, 2243-2259.

Jones, S.J., Southward, A.J. & Wethey, D.S. (2012) Climate change and historical biogeography of the barnacle *Semibalanus balanoides*. *Global Ecology and Biogeography*, **21**, 716-724.

Josefson, A.B. (2016) Species sorting of benthic invertebrates in a salinity gradient – importance of dispersal limitation. *PLoS ONE*, **11**, e0168908.

Joshi, H. & Ghose, M. (2003) Forest structure and species distribution along soil salinity and pH gradient in mangrove swamps of the Sundarbans. *Tropical Ecology*, **44**, 195-204.

Jost, L.O.U. (2008) GST and its relatives do not measure differentiation. *Molecular Ecology*, **17**, 4015-4026.

Jourmi, L.E., Amine, A., Alaoui, M.M., Lazar, S., Hmyene, A. & Antri, S.E. (2012) Assessment of water quality in coastal environments of mohammedia applying responses of biochemical biomarkers in the brown mussel *Perna perna*. *International Journal of Computer Science Issues*, **9**, 505-510.

Jueterbock, A., Tyberghein, L., Verbruggen, H., Coyer, J.A., Olsen, J.L. & Hoarau, G. (2013) Climate change impact on seaweed meadow distribution in the North Atlantic rocky intertidal. *Ecology and Evolution*, **3**, 1356-1373.

Jump, A.S., Huang, T.-J. & Chou, C.-H. (2012) Rapid altitudinal migration of mountain plants in Taiwan and its implications for high altitude biodiversity. *Ecography*, **35**, 204-210.

Kaehler, S. (1999) Incidence and distribution of phototrophic shell-degrading endoliths of the brown mussel *Perna perna*. *Marine Biology*, **135**, 505-514.

Kaehler, S. & McQuaid, C.D. (1999) Lethal and sub-lethal effects of phototrophic endoliths attacking the shell of the intertidal mussel *Perna perna*. *Marine Biology*, **135**, 497-503.

Kalvas, A. & Kautsky, L. (1998) Morphological variation in *Fucus vesiculosus* populations along temperature and salinity gradients in Iceland. *Journal of the Marine Biological Association of the United Kingdom*, **78**, 985-1001.

Keenan, K., McGinnity, P., Cross, T.F., Crozier, W.W. & Prodöhl, P.A. (2013) diveRsity: An R package for the estimation and exploration of population genetics parameters and their associated errors. *Methods in Ecology and Evolution*, **4**, 782-788.

Kelaher, B.P. & Castilla, J.C. (2005) Habitat characteristics influence macrofaunal communities in coralline turf more than mesoscale coastal upwelling on the coast of Northern Chile. *Estuarine, Coastal and Shelf Science*, **63**, 155-165.

Kelaher, B.P., Castilla, J.C. & Prado, L. (2007) Is there redundancy in bioengineering for molluscan assemblages on the rocky shores of central Chile? *Revista Chilena de Historia Natural*, **80**, 173-186.

Kelly, R.P. & Palumbi, S.R. (2010) Genetic structure among 50 species of the northeastern Pacific rocky intertidal community. *PLoS One*, **5**, e8594.

Kelly, R.P., Oliver, T.A., Sivasundar, A. & Palumbi, S.R. (2010) A method for detecting population genetic structure in diverse, high gene-flow species. *Journal of Heredity*, 423-436.

Keppel, G., Van Niel, K.P., Wardell-Johnson, G.W., Yates, C.J., Byrne, M., Mucina, L., Schut, A.G.T., Hopper, S.D. & Franklin, S.E. (2012) Refugia: identifying and understanding safe havens for biodiversity under climate change. *Global Ecology and Biogeography*, **21**, 393-404.

Kifani, S., Masski, H. & Faraj, A. (2008) The need of an ecosystem approach to fisheries: The Moroccan upwelling-related resources case. *Fisheries Research*, **94**, 36-42.

Kinlan, B.P. & Gaines, S.D. (2003) Propagule dispersal in marine and terrestrial environments: a community perspective. *Ecology*, **84**, 2007-2020.

Klanderud, K., Vandvik, V. & Goldberg, D. (2015) The importance of biotic vs. abiotic drivers of local plant community composition along regional bioclimatic gradients. *PLoS ONE*, **10**, e0130205.

Kleisner, K.M., Fogarty, M.J., McGee, S., Barnett, A., Fratantoni, P., Greene, J., Hare, J.A., Lucey, S.M., McGuire, C., Odell, J., Saba, V.S., Smith, L., Weaver, K.J. & Pinsky, M.L. (2016) The effects of sub-regional climate velocity on the distribution and spatial extent of marine species assemblages. *PLoS ONE*, **11**, e0149220.

Klouche, M.S., De Deurwaerdère, P., Dellu-Hagedorn, F., Lakhdar-Ghazal, N. & Benomar, S. (2015) Monoamine content during the reproductive cycle of *Perna*

perna depends on site of origin on the Atlantic Coast of Morocco. *Scientific Reports*, **5**, 13715.

Knoll, M., Hernández-Guerra, A., Lenz, B., López Laatzen, F., Machín, F., Müller, T.J. & Siedler, G. (2002) The Eastern Boundary Current system between the Canary Islands and the African Coast. *Deep Sea Research Part II: Topical Studies in Oceanography*, **49**, 3427-3440.

Knutson, T.R., Sirutis, J.J., Zhao, M., Tuleya, R.E., Bender, M., Vecchi, G.A., Villarini, G. & Chavas, D. (2015) Global projections of intense tropical cyclone activity for the late 21st century from dynamical downscaling of CMIP5/RCP4. 5 scenarios. *Journal of Climate*, **28**, 7203-7224.

Kollas, C., Körner, C. & Randin, C.F. (2014) Spring frost and growing season length co-control the cold range limits of broad-leaved trees. *Journal of Biogeography*, **41**, 773-783.

Kooij, J., Engelhard, G.H. & Righton, D.A. (2016) Climate change and squid range expansion in the North Sea. *Journal of Biogeography*, **43**, 2285-2298.

Krug, L.A., Platt, T., Sathyendranath, S. & Barbosa, A.B. (2017) Unravelling region-specific environmental drivers of phytoplankton across a complex marine domain (off SW Iberia). *Remote Sensing of Environment*, in press.

Kruskal, J.B. & Wish, M. (1978) *Multidimensional scaling*. Sage Publications.

Kuo, E.S. & Sanford, E. (2009) Geographic variation in the upper thermal limits of an intertidal snail: implications for climate envelope models. *Marine Ecology Progress Series*, **388**, 137-146.

Lacerda, A.L.F., Kersanach, R., Cortinhas, M.C.S., Prata, P.F.S., Dumont, L.F.C., Proietti, M.C., Maggioni, R. & D'Incao, F. (2016) High connectivity among blue crab (*Callinectes sapidus*) populations in the Western South Atlantic. *PLoS One*, **11**, e0153124.

Ladah, L., Bermudez, R., Pearson, G. & Serrão, E. (2003) Fertilization success and recruitment of dioecious and hermaphroditic fucoid seaweeds with contrasting distributions near their southern limit. *Marine Ecology Progress Series*, **262**, 173-183.

Lal, M.M., Southgate, P.C., Jerry, D.R., Bosserelle, C. & Zenger, K.R. (2017) Swept away: ocean currents and seascape features influence genetic structure across the 18 000 km Indo-Pacific distribution of a marine invertebrate, the black-lip pearl oyster *Pinctada margaritifera*. *BMC Genomics*, **18**, 66.

Lanari, M.d.O. & Coutinho, R. (2014) Reciprocal causality between marine macroalgal diversity and productivity in an upwelling area. *Oikos*, **123**, 630-640.

Langella, O. (2002) *Populations 1.2.30. Population genetic software CNRS UPR9034. [accessed 2017, July, 10] Available from http://bioinformatics.org/~tryphon/populations/.*

Lany, N.K., Zarnetske, P.L., Gouhier, T.C. & Menge, B.A. (2017) Incorporating context dependency of species interactions in species distribution models. *Integrative and Comparative Biology*, **57**, 159-167.

Lasiak, T. & Dye, A. (1989) The ecology of the brown mussel *Perna perna* in Transkei, southern Africa: implications for the management of a traditional food resource. *Biological Conservation*, **47**, 245-257.

Lasiak, T. & Field, J. (1995) Community-level attributes of exploited and non-exploited rocky infratidal macrofaunal assemblages in Transkei. *Journal of Experimental Marine Biology and Ecology*, **185**, 33-53.

Lathlean, J.A., Seuront, L., McQuaid, C.D., Ng, T.P.T., Zardi, G.I. & Nicastro, K.R. (2016a) Size and position (sometimes) matter: small scale patterns of heat stress associated with two co-occurring mussels with different thermoregulatory behaviour. *Marine Biology*, **163**, 189.

Lathlean, J.A., Seuront, L., McQuaid, C.D., Ng, T.P., Zardi, G.I. & Nicastro, K.R. (2016b) Cheating the locals: invasive mussels steal and benefit from the cooling effect of indigenous mussels. *PLoS One*, **11**, e0152556.

Leidenberger, S., De Giovanni, R., Kulawik, R., Williams, A.R. & Bourlat, S.J. (2015) Mapping present and future potential distribution patterns for a meso-grazer guild in the Baltic Sea. *Journal of Biogeography*, **42**, 241-254.

Lemos, R.T. & Pires, H.O. (2004) The upwelling regime off the west Portuguese coast, 1941–2000. *International Journal of Climatology*, **24**, 511-524.

Lenoir, J., Gégout, J.C., Guisan, A., Vittoz, P., Wohlgemuth, T., Zimmermann, N.E., Dullinger, S., Pauli, H., Willner, W. & Svenning, J.C. (2010) Going against the flow: potential mechanisms for unexpected downslope range shifts in a warming climate. *Ecography*, **33**, 295-303.

Leopardas, V., Honda, K., Go, G.A., Bolisay, K., Pantallano, A.D., Uy, W., Fortes, M. & Nakaoka, M. (2016) Variation in macrofaunal communities of sea grass beds along a pollution gradient in Bolinao, northwestern Philippines. *Marine Pollution Bulletin*, **105**, 310-318.

Lett, C., Veitch, J., Van der Lingen, C.D. & Hutchings, L. (2007) Assessment of an environmental barrier to transport of ichthyoplankton from the southern to the northern Benguela ecosystems. *Marine Ecology Progress Series*, **347**, 247-260.

Liaw, A. & Wiener, M. (2002) Classification and regression by randomForest. *R News*, **2**, 18-22.

Librado, P. & Rozas, J. (2009) DnaSP v5: a software for comprehensive analysis of DNA polymorphism data. *Bioinformatics*, **25**, 1451-1452.

Lima, F.P., Queiroz, N., Ribeiro, P.A., Hawkins, S.J. & Santos, A.M. (2006) Recent changes in the distribution of a marine gastropod, *Patella rustica* Linnaeus, 1758, and their relationship to unusual climatic events. *Journal of Biogeography*, **33**, 812-822.

Lima, F.P., Ribeiro, P.A., Queiroz, N., Hawkins, S.J. & Santos, A.M. (2007a) Do distributional shifts of northern and southern species of algae match the warming pattern? *Global Change Biology*, **13**, 2592-2604.

Lima, F.P., Ribeiro, P.A., Queiroz, N., Xavier, R., Tarroso, P., Hawkins, S.J. & Santos, A.M. (2007b) Modelling past and present geographical distribution of the marine

gastropod *Patella rustica* as a tool for exploring responses to environmental change. *Global Change Biology*, **13**, 2065-2077.

Lima, F.P., Queiroz, N., Ribeiro, P.A., Xavier, R., Hawkins, S.J. & Santos, A.M. (2009) First record of *Halidrys siliquosa* on the Portuguese coast: counter-intuitive range expansion? *Marine Biodiversity Records*, **2**, e1.

Lima, F.P. & Wethey, D.S. (2012) Three decades of high-resolution coastal sea surface temperatures reveal more than warming. *Nature Communications*, **3**, 704.

Lima, F.P., Gomes, F., Seabra, R., Wethey, D.S., Seabra, M.I., Cruz, T., Santos, A.M. & Hilbish, T.J. (2016) Loss of thermal refugia near equatorial range limits. *Global Change Biology*, **22**, 254-263.

Ling, S.D., Johnson, C.R., Ridgway, K., Hobday, A.J. & Haddon, M. (2009) Climate-driven range extension of a sea urchin: inferring future trends by analysis of recent population dynamics. *Global Change Biology*, **15**, 719-731.

Lodola, A., Ferrario, J. & Occhipinti-Ambrogi, A. (2015) Further Mediterranean expansion of the non-indigenous bryozoan Celleporaria brunnea: multiple records along the Italian coasts. *Scientia Marina*, **79**, 263-274.

Loehr, J., Worley, K., Grapputo, A., Carey, J., Veitch, A. & Coltman, D.W. (2006) Evidence for cryptic glacial refugia from North American mountain sheep mitochondrial DNA. *Journal of Evolutionary Biology*, **19**, 419-430.

Losos, J.B. (2011) Convergence, adaptation, and constraint. *Evolution*, **65**, 1827-40.

Lourenço, C.R. (2012) *First record of the intertidal mussel Perna perna along the European coast: long overlooked or a recent range expansion?* University of Algarve, Faro, Portugal.

Lourenço, C.R., Nicastro, K.R., Serrão, E.A. & Zardi, G.I. (2012) First record of the brown mussel (*Perna perna*) from the European Atlantic coast. *Marine Biodiversity Records*, **5**, e39.

Lourenço, C.R., Nicastro, K.R., Serrão, E.A., Castilho, R. & Zardi, G.I. (2015) Behind the mask: cryptic genetic diversity of *Mytilus galloprovincialis* along southern European and northern African shores. *Journal of Molluscan Studies*, **81**, 380-387.

Lourenço, C.R., Zardi, G.I., McQuaid, C.D., Serrão, E.A., Pearson, G.A., Jacinto, R. & Nicastro, K.R. (2016) Upwelling areas as climate change refugia for the distribution and genetic diversity of a marine macroalga. *Journal of Biogeography*, **43**, 1595-1607.

Lourenço, C.R., Nicastro, K.R., McQuaid, C.D., Sabour, B. & Zardi, G.I. (2017) Latitudinal incidence of phototrophic shell-degrading endoliths and their effects on mussel bed microclimates. *Marine Biology*, **164**, 129.

Ludford, A., Cole, V.J., Porri, F., McQuaid, C.D., Motebang, D., Nakin, V. & Erlandsson, J. (2012) Testing source-sink theory: the spill-over of mussel recruits beyond marine protected areas. *Landscape Ecology*, **27**, 859-868.

Lutjeharms, J.R. (2006) The coastal oceans of southeastern Africa (15, W). *The sea, the global coastal ocean, interdisciplinary regional studies and syntheses* (ed. by A.R.B. Robinson, Kenneth H), pp. 783-834. Harvard University Press, Cambridge, MA.

Lyrholm, T., Leimar, O., Johanneson, B. & Gyllensten, U. (1999) Sex–biased dispersal in sperm whales: contrasting mitochondrial and nuclear genetic structure of global populations. *Proceedings of the Royal Society of London B: Biological Sciences*, **266**, 347-354.

Macho, G., Woodin, S.A., Wethey, D.S. & Vázquez, E. (2016) Impacts of sublethal and lethal high temperatures on clams exploited in European fisheries. *Journal of Shellfish Research*, **35**, 405-419.

Maclean, I.M.D. & Wilson, R.J. (2011) Recent ecological responses to climate change support predictions of high extinction risk. *Proceedings of the National Academy of Sciences*, **108**, 12337-12342.

Macpherson, E. (2002) Large–scale species–richness gradients in the Atlantic Ocean. *Proceedings of the Royal Society of London B: Biological Sciences*, **269**, 1715-1720.

Maggs, C.A., Castilho, R., Foltz, D., Henzler, C., Jolly, M.T., Kelly, J., Olsen, J., Perez, K.E., Stam, W., Väinölä, R., Viard, F. & Wares, J. (2008) Evaluating signatures of glacial refugia for North Atlantic benthic marine taxa. *Ecology*, **89**, S108-S122.

Magri D., Vendramin, G.G., Comps, B., Dupanloup, I., Geburek, T., Gomory, D., Latalowa, M., Litt, T., Paule, L., Roure, J.M., Tantau, I., van der Knaap, W.O., Petit, R.J. & de Beaulieu, J.-L.. (2006) A new scenario for the Quaternary history of European beech populations: palaeobotanical evidence and genetic consequences. *New Phytologist*, **171**, 199–221.

Malvezzi, A.J., Murray, C.S., Feldheim, K.A., DiBattista, J.D., Garant, D., Gobler, C.J., Chapman, D.D. & Baumann, H. (2015) A quantitative genetic approach to assess the evolutionary potential of a coastal marine fish to ocean acidification. *Evolutionary Applications*, **8**, 352-362.

Mann, M.E., Zhang, Z., Rutherford, S., Bradley, R.S., Hughes, M.K., Shindell, D., Ammann, C., Faluvegi, G. & Ni, F. (2009) Global signatures and dynamical origins of the Little Ice Age and Medieval Climate Anomaly. *Science*, **326**, 1256-1260.

Mannion, P.D., Upchurch, P., Benson, R.B.J. & Goswami, A. (2014) The latitudinal biodiversity gradient through deep time. *Trends in Ecology & Evolution*, **29**, 42-50.

Manuel, S.A., Coates, K.A., Kenworthy, W.J. & Fourqurean, J.W. (2013) Tropical species at the northern limit of their range: composition and distribution in Bermuda's benthic habitats in relation to depth and light availability. *Marine Environmental Research*, **89**, 63-75.

Mao Che, L., Le Campion-Alsumard, T., Boury-Esnault, N., Payri, C., Golubic, S. & Bézac, C. (1996) Biodegradation of shells of the black pearl oyster, *Pinctada margaritifera var. cumingii*, by microborers and sponges of French Polynesia. *Marine Biology*, **126**, 509-519.

Marcello, J., Hernández-Guerra, A., Eugenio, F. & Fonte, A. (2011) Seasonal and temporal study of the northwest African upwelling system. *International Journal of Remote Sensing*, **32**, 1843-1859.

Margalet, J.L., Almaraz, T., Navarro, M.J. & Pérez-Ruzafa, I.M. (1993) Mapas de distribución de algas marinas de la Península Ibérica. III. *Fucus ceranoides L.*, *F.*

serratus L., *F. spiralis L.* y *F. vesiculosus L.* (Fucales, Fucophyceae)*. *Botanica Complutensis*, **18**, 267-290.

Marquet, N., Nicastro, K.R., Gektidis, M., McQuaid, C.D., Pearson, G.A., Serrão, E.A. & Zardi, G.I. (2013) Comparison of phototrophic shell-degrading endoliths in invasive and native populations of the intertidal mussel *Mytilus galloprovincialis*. *Biological Invasions*, **15**, 1253-1272.

Marshall, K.E. & Baltzer, J.L. (2015) Decreased competitive interactions drive a reverse species richness latitudinal gradient in subarctic forests. *Ecology*, **96**, 461-470.

Martínez, B., Viejo, R.M., Carreno, F. & Aranda, S.C. (2012) Habitat distribution models for intertidal seaweeds: responses to climatic and non-climatic drivers. *Journal of Biogeography*, **39**, 1877-1890.

Martínez, B., Arenas, F., Trilla, A., Viejo, R.M. & Carreño, F. (2015) Combining physiological threshold knowledge to species distribution models is key to improving forecasts of the future niche for macroalgae. *Global Change Biology*, **21**, 1422-1433.

Martins, C.S., Hammann, M. & Fiúza, A.F.G. (2002) Surface circulation in the eastern North Atlantic, from drifters and altimetry. *Journal of Geophysical Research*, **107**, 3217.

Matschiner, M. & Salzburger, W. (2009) TANDEM: integrating automated allele binning into genetics and genomics workflows. *Bioinformatics*, **25**, 1982-1983.

Mazzillo, F.F., Ryan, J.P. & Silver, M.W. (2011) Parasitism as a biological control agent of dinoflagellate blooms in the California Current System. *Harmful Algae*, **10**, 763-773.

McArdle, B.H. & Anderson, M.J. (2001) Fitting mulltivariate models to community data: a coment on distance-based redudancy analysis. *Ecology*, **82**, 290-297.

McCarty, J.P. (2001) Ecological consequences of recent climate change. *Conservation Biology*, **15**, 320-331.

McGregor, H.V., Dima, M., Fischer, H.W. & Mulitza, S. (2007) Rapid 20th-century increase in coastal upwelling off northwest Africa. *Science*, **315**, 637-9.

McKenzie, P.F. & Bellgrove, A. (2008) Dispersal of *Hormosira banksii* (Phaeophyceae) via detached fragments: reproductive viability and longevity *Journal of Phycology*, **44**, 1108-1115.

McQuaid, C.D. & Phillips, T.E. (2000) Limited wind-driven dispersal of intertidal mussel larvae: in situ evidence from the plankton and the spread of the invasive species *Mytilus galloprovincialis* in South Africa. *Marine Ecology Progress Series*, **201**, 211-220.

Medina, M., Scolaro, A., Méndez-De la Cruz, F., Sinervo, B. & Ibargüengoytía, N. (2011) Thermal relationships between body temperature and environment conditions set upper distributional limits on oviparous species. *Journal of Thermal Biology*, **36**, 527-534.

Meiri, M., Lister, A.M., Higham, T.F., Stewart, J.R., Straus, L.G., Obermaier, H., Gonzalez Morales, M.R., Marin-Arroyo, A.B. & Barnes, I. (2013) Late-glacial recolonization

and phylogeography of European red deer (*Cervus elaphus* L.). *Molecular Ecology*, **22**, 4711-4722.

Mejías, J.A., Arroyo, J. & Maranón, T. (2007) Ecology and biogeography of plant communities associated with the post Plio-Pleistocene relict *Rhododendron ponticum subsp. baeticum* in southern Spain. *Journal of Biogeography*, **34**, 456-472.

Menge, B.A., Blanchette, C., Raimondi, P., Freidenburg, T., Gaines, S., Lubchenco, J., Lohse, D., Hudson, G., Foley, M. & Pamplin, J. (2004) Species interaction strength: testing model predictions along an upwelling gradient. *Ecological Monographs*, **74**, 663-684.

Mhamada, M., Cheihk, M.O.M., Khannous, S., Dartige, A. & Hassan, E.-R. (2015) Metallic contamination assessment of the Lévrier Bay (Mauritanian Atlantic coast), using *Perna perna* and *Venus rosalina*. *Journal of Environmental Solutions*, **3**, 1-10.

Mieszkowska, N., Kendall, M., Hawkins, S., Leaper, R., Williamson, P., Hardman-Mountford, N. & Southward, A. (2006) Changes in the range of some common rocky shore species in Britain–a response to climate change? *Hydrobiologia*, **555**, 241-251.

Mieszkowska, N., Firth, L. & Bentley, M. (2013) Impacts of climate change on intertidal habitats. *Marine Climate Change Impacts Partnership: Science Review*, **4**, 180-192.

Migliore, J., Baumel, A., Juin, M., Fady, B., Roig, A., Duong, N. & Medail, F. (2013) Surviving in mountain climate refugia: new insights from the genetic diversity and structure of the relict shrub *Myrtus nivellei* (Myrtaceae) in the Sahara Desert. *PLoS One*, **8**, e73795.

Millot, C. (1999) Circulation in the western Mediterranean Sea. *Journal of Marine Systems*, **20**, 423-442.

Mislan, K.A.S., Helmuth, B. & Wethey, D.S. (2014) Geographical variation in climatic sensitivity of intertidal mussel zonation. *Global Ecology and Biogeography*, **23**, 744-756.

Mock, K.E. & Miller, M. (2005) Patterns of molecular diversity in naturally occurring and refugial populations of the least chub. *Transactions of the American Fisheries Society*, **134**, 267-278.

Molinos, J.G., Halpern, B.S., Schoeman, D.S., Brown, C.J., Kiessling, W., Moore, P.J., Pandolfi, J.M., Poloczanska, E.S., Richardson, A.J. & Burrows, M.T. (2016) Climate velocity and the future global redistribution of marine biodiversity. *Nature Climate Change*, **6**, 83-88.

Monteiro, S., Chapman, M. & Underwood, A. (2002) Patches of the ascidian *Pyura stolonifera* (Heller, 1878): structure of habitat and associated intertidal assemblages. *Journal of Experimental Marine Biology and Ecology*, **270**, 171-189.

Morelli, T.L., Daly, C., Dobrowski, S.Z., Dulen, D.M., Ebersole, J.L., Jackson, S.T., Lundquist, J.D., Millar, C.I., Maher, S.P., Monahan, W.B., Nydick, K.R., Redmond, K.T., Sawyer, S.C., Stock, S. & Beissinger, S.R. (2016) Managing climate change refugia for climate adaptation. *PLoS ONE*, **11**, e0159909.

Morin, X., Viner, D. & Chuine, I. (2008) Tree species range shifts at a continental scale: new predictive insights from a process-based model. *Journal of Ecology*, **96**, 784-794.

Morley, S.A., Griffiths, H.J., Barnes, D.K. & Peck, L.S. (2010) South Georgia: a key location for linking physiological capacity to distributional changes in response to climate change. *Antarctic Science*, **22**, 774-781.

Morueta-Holme, N., Engemann, K., Sandoval-Acuña, P., Jonas, J.D., Segnitz, R.M. & Svenning, J.-C. (2015) Strong upslope shifts in Chimborazo's vegetation over two centuries since Humboldt. *Proceedings of the National Academy of Sciences*, **112**, 12741-12745.

Mouritsen, K.N. & Poulin, R. (2002) Parasitism, community structure and biodiversity in intertidal ecosystems. *Parasitology*, **124**, 101-117.

Moyano, M., Rodríguez, J.M., Benítez-Barrios, V.M. & Hernández-León, S. (2014) Larval fish distribution and retention in the Canary Current system during the weak upwelling season. *Fisheries Oceanography*, **23**, 191-209.

Mueter, F.J. & Litzow, M.A. (2008) Sea ice retreat alters the biogeography of the Bering Sea continental shelf. *Ecological Applications*, **18**, 309-320.

Muir, A.P., Nunes, F.L., Dubois, S.F. & Pernet, F. (2016) Lipid remodelling in the reef-building honeycomb worm, *Sabellaria alveolata*, reflects acclimation and local adaptation to temperature. *Scientific Reports*, **6**, 35669.

Munday, P.L., Donelson, J.M. & Domingos, J.A. (2017) Potential for adaptation to climate change in a coral reef fish. *Global Change Biology*, **23**, 307-317.

Narayan, N., Paul, A., Mulitza, S. & Schulz, M. (2010) Trends in coastal upwelling intensity during the late 20th century. *Ocean Science*, **6**, 815-823.

Neethling, M., Matthee, C.A., Bowie, R.C. & von der Heyden, S. (2008) Evidence for panmixia despite barriers to gene flow in the southern African endemic, *Caffrogobius caffer* (Teleostei: Gobiidae). *BMC Evolutionary Biology*, **8**, 325.

Nei, M. (1987) *Molecular evolutionary genetics*. Columbia University Press, New York.

Neiva, J., Pearson, G.A., Valero, M. & Serrão, E.A. (2012) Fine-scale genetic breaks driven by historical range dynamics and ongoing density-barrier effects in the estuarine seaweed *Fucus ceranoides* L. *BMC Evolutionary Biology*, **12**, 78.

Neiva, J., Assis, J., Fernandes, F., Pearson, G.A., Serrão, E.A. & Maggs, C. (2014) Species distribution models and mitochondrial DNA phylogeography suggest an extensive biogeographical shift in the high-intertidal seaweed *Pelvetia canaliculata*. *Journal of Biogeography*, **41**, 1137-1148.

Neiva, J., Assis, J., Coelho, N.C., Fernandes, F., Pearson, G.A. & Serrão, E.A. (2015) Genes left behind: climate change threatens cryptic genetic diversity in the canopy-forming seaweed *Bifurcaria bifurcata*. *PLoS One*, **10**, e0131530.

Nguyen, K.D.T., Morley, S.A., Lai, C.-H., Clark, M.S., Tan, K.S., Bates, A.E. & Peck, L.S. (2011) Upper temperature limits of tropical marine ectotherms: Global warming implications. *PLoS ONE*, **6**, e29340.

Nicastro, K.R., Zardi, G.I., McQuaid, C.D., Teske, P.R. & Barker, N.P. (2008) Coastal topography drives genetic structure in marine mussels. *Marine Ecology Progress Series*, **368**, 189-195.

Nicastro, K.R., Zardi, G.I. & McQuaid, C.D. (2009) Differential reproductive investment, attachment strength and mortality of invasive and indigenous mussels across heterogeneous environments. *Biological Invasions*, **12**, 2165-2177.

Nicastro, K.R., Zardi, G.I., McQuaid, C.D., Pearson, G.A. & Serrão, E.A. (2012) Love thy neighbour: group properties of gaping behaviour in mussel aggregations. *PLoS One*, **7**, e47382.

Nicastro, K.R., Zardi, G.I., Teixeira, S., Neiva, J., Serrao, E.A. & Pearson, G.A. (2013) Shift happens: trailing edge contraction associated with recent warming trends threatens a distinct genetic lineage in the marine macroalga *Fucus vesiculosus*. *BMC Biology*, **11**, 6.

Nielsen, K.J. & Navarrete, S.A. (2004) Mesoscale regulation comes from the bottom-up: intertidal interactions between consumers and upwelling. *Ecology Letters*, **7**, 31-41.

Norton, T.A. (1992) Dispersal by macroalgae. *British Phycological Journal*, **27**, 293-301.

Nye, J.A., Link, J.S., Hare, J.A. & Overholtz, W.J. (2009) Changing spatial distribution of fish stocks in relation to climate and population size on the Northeast United States continental shelf. *Marine Ecology Progress Series*, **393**, 111-129.

O'Donnell, M.J. (2008) Reduction of wave forces within bare patches in mussel beds. *Marine Ecology Progress Series*, **362**, 157-167.

Ocaña, O., Brito, A. & González, G. (2005) The genus *Actinia* in the Macaronesian archipelagos: a general perspective of the genus focussed on the North-oriental Atlantic and Mediterranean species (Actiniaria: Actiniidae). *Vieraea*, **33**, 477-494.

Olivier, J. & Stockton, P.L. (1989) The influence of upwelling extent upon fog incidence at Lüderitz, southern Africa. *International Journal of Climatology*, **9**, 69-75.

Oomen, R.A., Reudink, M.W., Nocera, J.J., Somers, C.M., Green, M.C. & Kyle, C.J. (2011) Mitochondrial evidence for panmixia despite perceived barriers to gene flow in a widely distributed waterbird. *Journal of Heredity*, **102**, 584-592.

Ormond, R.F.G. & Banaimoon, S.A. (1994) Ecology of intertidal macroalgal assemblages on the Hadramout coast of southern Yemen, an area of seasonal upwelling. *Marine Ecology Progress Series*, **105**, 105-120.

Otchere, F.A., Joiris, C.R. & Holsbeek, L. (2003) Mercury in the bivalves *Anadara* (*Senilia*) *senilis*, *Perna perna* and *Crassostrea tulipa* from Ghana. *The Science of The Total Environment*, **304**, 369-375.

Ouazzani, K.C., Benazzou, T., Charouki, N., Bonhomme, F. & Chlaida, M. (2017) Genetic differentiation of European anchovy (*Engraulis encrasicolus*) along the Moroccan coast reveals a phylogeographic break around the 25th parallel North. *Marine Biology Research*, **13**, 1-9.

Palumbi, S.R. (1996) Nucleic acids II: the polymerase chain reaction. *Molecular Systematics* (ed. by D.M. Hillis, C. Moritz and B.K. Mable). Sinauer Associates: Sunderland, MA.

Palumbi, S.R. & Baker, C.S. (1994) Contrasting population structure from nuclear intron sequences and mtDNA of humpback whales. *Molecular Biology and Evolution*, **11**, 426-435.

Pardo, P.C., Padín, X.A., Gilcoto, M., Farina-Busto, L. & Pérez, F.F. (2011) Evolution of upwelling systems coupled to the long-term variability in sea surface temperature and Ekman transport. *Climate Research*, **48**, 231-246.

Parmesan, C. (2006) Ecological and evolutionary responses to recent climate change. *Annual Review of Ecology, Evolution, and Systematics*, **37**, 637-669.

Parmesan, C. & Yohe, G. (2003) A globally coherent fingerprint of climate change impacts across natural systems. *Nature*, **421**, 37.

Parrish, J.K. & Edelstein-Keshet, L. (1999) Complexity, pattern, and evolutionary trade-offs in animal aggregation. *Science*, **284**, 99-101.

Patarnello, T., Volckaert, F.A. & Castilho, R. (2007) Pillars of Hercules: is the Atlantic-Mediterranean transition a phylogeographical break? *Molecular Ecology*, **16**, 4426-44.

Patti, B., Guisande, C., Riveiro, I., Thejll, P., Cuttitta, A., Bonanno, A., Basilone, G., Buscaino, G. & Mazzola, S. (2010) Effect of atmospheric CO_2 and solar activity on wind regime and water column stability in the major global upwelling areas. *Estuarine, Coastal and Shelf Science*, **88**, 45-52.

Pearson, G.A., Lago-Leston, A. & Mota, C. (2009) Frayed at the edges: selective pressure and adaptive response to abiotic stressors are mismatched in low diversity edge populations. *Journal of Ecology*, **97**, 450-462.

Pearson, R.G. (2006) Climate change and the migration capacity of species. *Trends in Ecology & Evolution*, **21**, 111-113.

Peharda, M., Calcinai, B., Puljas, S., Golubic, S., Arapov, J. & Thebault, J. (2015) Endoliths in *Lithophaga lithophaga* shells -variation in intensity of infestation and species occurrence. *Marine Environmental Research*, **108**, 91-99.

Pelegrí, J., Arístegui, J., Cana, L., González-Dávila, M., Hernández-Guerra, A., Hernández-León, S., Marrero-Díaz, A., Montero, M., Sangrà, P. & Santana-Casiano, M. (2005) Coupling between the open ocean and the coastal upwelling region off northwest Africa: water recirculation and offshore pumping of organic matter. *Journal of Marine Systems*, **54**, 3-37.

Pereira, S.G., Lima, F.P., Queiroz, N.C., Ribeiro, P.A. & Santos, A.M. (2006) Biogeographic patterns of intertidal macroinvertebrates and their association with macroalgae distribution along the Portuguese coast. *Hydrobiologia*, **555**, 185-192.

Pereira, T.R., Engelen, A.H., Pearson, G.A., Valero, M. & Serrão, E.A. (2015) Contrasting timing of life stages across latitudes–a case study of a marine forest-forming species. *European Journal of Phycology*, **50**, 361-369.

Pérez-Portela, R., Rius, M. & Villamor, A. (2017) Lineage splitting, secondary contacts and genetic admixture of a widely distributed marine invertebrate. *Journal of Biogeography*, **44**, 446-460.

Perrin, C., Daguin, C., Vliet, M.V.D., Engel, C.R., Pearson, G.A. & Serrão, E.A. (2007) Implications of mating system for genetic diversity of sister algal species: *Fucus*

spiralis and *Fucus vesiculosus* (Heterokontophyta, Phaeophyceae). *European Journal of Phycology*, **42**, 219-230.

Perry, A.L., Low, P.J., Ellis, J.R. & Reynolds, J.D. (2005) Climate change and distribution shifts in marine fishes. *Science*, **308**, 1912-1915.

Peterson, A.T., Ortega-Huerta, M.A., Bartley, J., Sanchez-Cordero, V., Soberon, J., Buddemeier, R.H. & Stockwell, D.R.B. (2002) Future projections for Mexican faunas under global climate change scenarios. *Nature*, **416**, 626-629.

Petes, L.E., Menge, B.A., Chan, F. & Webb, M.A. (2008) Gonadal tissue color is not a reliable indicator of sex in rocky intertidal mussels. *Aquatic biology*, **3**, 63-70.

Petit, R.J., Aguinagalde, I., de Beaulieu, J.-L., Bittkau, C., Brewer, S., Cheddadi, R., Ennos, R., Fineschi, S., Grivet, D., Lascoux, M., Mohanty, A., Müller-Starck, G., Demesure-Musch, B., Palmé, A., Martín, J.P., Rendell, S. & Vendramin, G.G. (2003) Glacial Refugia: hotspots but not melting pots of genetic diversity. *Science*, **300**, 1563-1565.

Piazza, B.P., Banks, P.D. & La Peyre, M.K. (2005) The potential for created oyster shell reefs as a sustainable shoreline protection strategy in Louisiana. *Restoration Ecology*, **13**, 499-506.

Picaut, J. (1983) Propagation of the seasonal Upwelling in the Eastern Equatorial Atlantic. *Journal of Physical Oceanography*, **13**, 18-37.

Piñeiro-Corbeira, C., Barreiro, R. & Cremades, J. (2016) Decadal changes in the distribution of common intertidal seaweeds in Galicia (NW Iberia). *Marine Environmental Research*, **113**, 106-115.

Pinsky, M.L., Worm, B., Fogarty, M.J., Sarmiento, J.L. & Levin, S.A. (2013) Marine taxa track local climate velocities. *Science*, **341**, 1239-1242.

Plicanti, A., Domínguez, R., Dubois, S.F. & Bertocci, I. (2016) Human impacts on biogenic habitats: Effects of experimental trampling on *Sabellaria alveolata* (Linnaeus, 1767) reefs. *Journal of Experimental Marine Biology and Ecology*, **478**, 34-44.

Poloczanska, E.S., Babcock, R., Butler, A., Hobday, A., Hoegh-Guldberg, O., Kunz, T., Matear, R., Milton, D., Okey, T. & Richardson, A. (2007) Climate change and Australian marine life. *Oceanography and marine biology*, **45**, 407.

Poloczanska, E.S., Brown, C.J., Sydeman, W.J., Kiessling, W., Schoeman, D.S., Moore, P.J., Brander, K., Bruno, J.F., Buckley, L.B. & Burrows, M.T. (2013) Global imprint of climate change on marine life. *Nature Climate Change*, **3**, 919-925.

Poloczanska, E.S., Hoegh-Guldberg, O., Cheung, W., Pörtner, H.O. & Burrows, M.T. (2014) Crosss-chapter box on observed global responses of marine biogeography, abundance, and phenology to climate change. *Climate Change 2014: Impacts, Adaptation, and Vulnerability. Part A: Global and Sectoral Aspects. Contribution of Working Group II to the Fifth Assessment Report of the Intergovernmental Panel on Climate Change*, pp. 123-127. Cambridge University Press.

Poloczanska, E.S., Burrows, M.T., Brown, C.J., García Molinos, J., Halpern, B.S., Hoegh-Guldberg, O., Kappel, C.V., Moore, P.J., Richardson, A.J., Schoeman, D.S. & Sydeman, W.J. (2016) Responses of marine organisms to climate change across oceans. *Frontiers in Marine Science*, **3**, 62.

Pontes, M.T., Aguiar, R. & Pires, H.O. (2005) A nearshore wave energy atlas for Portugal. *Journal of Offshore Mechanics and Arctic Engineering*, **127**, 249-255.

Porri, F., Jackson, J.M., Von der Meden, C.E., Weidberg, N. & McQuaid, C.D. (2014) The effect of mesoscale oceanographic features on the distribution of mussel larvae along the south coast of South Africa. *Journal of Marine Systems*, **132**, 162-173.

Pörtner, H.O. & Knust, R. (2007) Climate change affects marine fishes through the oxygen limitation of thermal tolerance. *Science*, **315**, 95-97.

Posada, D. (2008) jModelTest: phylogenetic model averaging. *Molecular Biology and Evolution*, **25**, 1253-6.

Poulin, R. (1995) "Adaptive" changes in the behaviour of parasitized animals: a critical review. *International Journals for Parasitology*, **25**, 1371-1383.

Pritchard, J.K., Stephens, M. & Donnelly, P. (2000) Inference of population structure using multilocus genotype data. *Genetics*, **155**, 945-959.

Provan, J. & Bennett, K. (2008) Phylogeographic insights into cryptic glacial refugia. *Trends in Ecology & Evolution*, **23**, 564-571.

Provan, J. & Maggs, C.A. (2012) Unique genetic variation at a species' rear edge is under threat from global climate change. *Proceedings of the Royal Society B: Biological Sciences*, **279**, 39-47.

Quesada, H., Beynon, C.M. & Skibinski, D.O. (1995) A mitochondrial DNA discontinuity in the mussel *Mytilus galloprovincialis* Lmk: pleistocene vicariance biogeography and secondary intergradation. *Molecular Biology and Evolution*, **12**, 521-524.

Quinteiro, J., Rodríguez-Castro, J. & Rey-Méndez, M. (2007) Population genetic structure of the stalked barnacle *Pollicipes pollicipes* (Gmelin, 1789) in the northeastern Atlantic: influence of coastal currents and mesoscale hydrographic structures. *Marine Biology*, **153**, 47-60.

R Core Team (2012) R: A language and environment for statistical computing. R Foundation for Statistical Computing, Vienna, Austria. URL http://www.R-project.org/.

Ramos, A., Ramil, F., Mohamed, S. & Barry, A. (2015) The benthos of Northwest Africa. *Oceanographic and biological features in the Canary Current Large Marine Ecosystem* (ed. by L. Valdés and I. Déniz-González), pp. 231-244. IOC Technical Series, IOC-UNESCO, Paris.

Raybaud, V., Beaugrand, G., Goberville, E., Delebecq, G., Destombe, C., Valero, M., Davoult, D., Morin, P. & Gevaert, F. (2013) Decline in Kelp in West Europe and Climate. *PLoS ONE*, **8**, e66044.

Reddin, C.J., Docmac, F., O'Connor, N.E., Bothwell, J.H. & Harrod, C. (2015) Coastal upwelling drives intertidal assemblage structure and trophic ecology. *PLoS ONE*, **10**, e0130789.

Reid, K., Hoareau, T.B., Graves, J.E., Potts, W.M., dos Santos, S.M.R., Klopper, A.W. & Bloomer, P. (2016) Secondary contact and asymmetrical gene flow in a cosmopolitan marine fish across the Benguela upwelling zone. *Heredity*, **117**, 307-315.

Reiss, H., Cunze, S., König, K., Neumann, H. & Kröncke, I. (2011) Species distribution modelling of marine benthos: a North Sea case study. *Marine Ecology Progress Series*, **442**, 71-86.

Relvas, P. & Barton, E.D. (2002) Mesoscale patterns in the Cape São Vicente (Iberian Peninsula) upwelling region. *Journal of Geophysical Research*, **107**, 3164.

Reniers, J., Vanschoenwinkel, B., Rabet, N. & Brendonck, L. (2013) Mitochondrial gene trees support persistence of cold tolerant fairy shrimp throughout the Pleistocene glaciations in both southern and more northerly refugia. *Hydrobiologia*, **714**, 155-167.

Reum, J.C., Essington, T.E., Greene, C.M., Rice, C.A. & Fresh, K.L. (2011) Multiscale influence of climate on estuarine populations of forage fish: the role of coastal upwelling, freshwater flow and temperature. *Marine Ecology Progress Series*, **425**, 203-215.

Reusch, T.B.H. (2014) Climate change in the oceans: evolutionary versus phenotypically plastic responses of marine animals and plants. *Evolutionary Applications*, **7**, 104-122.

Ribeiro, P.A., Branco, M., Hawkins, S.J. & Santos, A.M. (2010) Recent changes in the distribution of a marine gastropod, *Patella rustica*, across the Iberian Atlantic coast did not result in diminished genetic diversity or increased connectivity. *Journal of Biogeography*, **37**, 1782-1796.

Ricciardi, A., Whoriskey, F.G. & Rasmussen, J.B. (1997) The role of the zebra mussel (*Dreissena polymorpha*) in structuring macroinvertebrate communities on hard substrata. *Canadian Journal of Fisheries and Aquatic Sciences*, **54**, 2596-2608.

Ridgway, K.R. (2007) Long-term trend and decadal variability of the southward penetration of the East Australian Current. *Geophysical Research Letters*, **34**, L13613.

Riegl, B. & Piller, W.E. (2003) Possible refugia for reefs in times of environmental stress. *International Journal of Earth Sciences*, **92**, 520-531.

Riera, R., Sangil, C. & Sansón, M. (2015) Long-term herbarium data reveal the decline of a temperate-water algae at its southern range. *Estuarine, Coastal and Shelf Science*, **165**, 159-165.

Riginos, C., Hickerson, M.J., Henzler, C.M. & Cunningham, C.W. (2004) Differential patterns of male and female mtDNA exchange across the Atlantic Ocean in the blue mussel, *Mytilus edulis*. *Evolution*, **58**, 2438-2451.

Rius, M. & McQuaid, C.D. (2006) Wave action and competitive interaction between the invasive mussel *Mytilus galloprovincialis* and the indigenous *Perna perna* in South Africa. *Marine Biology*, **150**, 69-78.

Rivadeneira, M.M. & Fernández, M. (2005) Shifts in southern endpoints of distribution in rocky intertidal species along the southeastern Pacific coast. *Journal of Biogeography*, **32**, 203-209.

Rivera, A., Weidberg, N., Pardiñas, A.F., González-Gil, R., García-Flórez, L. & Acuña, J.L. (2013) Role of upwelling on larval dispersal and productivity of goseneck barnacle

populations in the Cantabrian Sea: management implications. *PLoS One*, **8**, e78482.

Robinson, A.R., Golnaraghi, M., Leslie, W.G., Artegiani, A., Hecht, A., Lazzoni, E., Michelato, A., Sansone, E., Theocharis, A. & Ünlüata, Ü. (1991) The eastern Mediterranean general circulation: features, structure and variability. *Dynamics of Atmospheres and Oceans*, **15**, 215-240.

Robinson, T.B., Branch, G.M., Griffiths, C.L., Govender, A. & Hockey, P.A. (2007) Changes in South African rocky intertidal invertebrate community structure associated with the invasion of the mussel *Mytilus galloprovincialis*. *Marine Ecology Progress Series*, **340**, 163-171.

Rojas, J.M., Castillo, S.B., Escobar, J.B., Shinen, J.L. & Bozinovic, F. (2013) Huddling up in a dry environment: the physiological benefits of aggregation in an intertidal gastropod. *Marine Biology*, **160**, 1119-1126.

Roméo, M., Sidoumou, Z. & Gnassia-Barelli, M. (2000) Heavy metals in various molluscs from the Mauritanian coast. *Bulletin of Environmental Contamination and Toxicology*, **65**, 269-276.

Rouhi, A., Sif, J., Ferssiwi, A. & Chemaa, A. (2007) Bioaccumulation de quelques éléments métalliques par deux espèces d'Annélides Polychètes du littoral de Jorf Lasfar (région d'El Jadida, Maroc). *Bulletin de l'Institut Scientifique*, **29**, 81-87.

Rubal, M., Veiga, P., Cacabelos, E., Moreira, J. & Sousa-Pinto, I. (2013) Increasing sea surface temperature and range shifts of intertidal gastropods along the Iberian Peninsula. *Journal of Sea Research*, **77**, 1-10.

Sá-Pinto, A., Branco, M.S., Alexandrino, P.B., Fontaine, M.C. & Baird, S.J.E. (2012) Barriers to gene flow in the marine environment: Insights from two common intertidal limpet species of the Atlantic and Mediterranean. *PLoS ONE*, **7**, e50330.

Saada, G., Nicastro, K.R., Jacinto, R., McQuaid, C.D., Serrão, E.A., Pearson, G.A. & Zardi, G.I. (2016) Taking the heat: distinct vulnerability to thermal stress of central and threatened peripheral lineages of a marine macroalga. *Diversity and Distributions*, **22**, 1060-1068.

Sabour, B., Reani, A., El-Magouri, H. & Haroun, R. (2013) *Sargassum muticum* (Yendo) Fensholt (Fucales, Phaeophyta) in Morocco, an invasive marine species new to the Atlantic coast of Africa. *Aquatic Invasions*, **8**, 97-102.

Sabri, H., Cherifi, O., Maarouf, A., Cheggour, M., Bertrand, M. & Mandi, L. (2017) Wastewater impact on macroalgae biodiversity in Essaouira coast (Morocco). *Journal of Materialls and Environmental Sciences*, **8**, 857-862.

Sagarin, R.D., Barry, J.P., Gilman, S.E. & Baxter, C.H. (1999) Climate-related change in an intertidal community over short and long time scales. *Ecological Monographs*, **69**, 465-490.

Sakko, A. (1998) The influence of the Benguela upwelling system on Namibia's marine biodiversity. *Biodiversity and Conservation*, **7**, 419-433.

Sambrook, J., Fritshch, E.F. & Maniatis, T. (1989) *Molecular cloning: a laboratory manual*. Cold Spring Harbor Laboratory Press, New York.

Sammarco, P.W., Brazeau, D.A. & Sinclair, J. (2012) Genetic connectivity in scleractinian corals across the northern Gulf of Mexico: oil/gas platforms, and relationship to the Flower Garden Banks. *PLoS ONE*, **7**, e30144.

Sancinetti, G.S., Azevedo, A., Castilho, A.L., Fransozo, A. & Costa, R.C. (2014) How marine upwelling influences the distribution of *Artemesia longinaris* (Decapoda: Penaeoidea)? *Latin American Journal of Aquatic Research*, **42**, 322-331.

Sanford, E. & Swezey, D.S. (2008) Response of predatory snails to a novel prey following the geographic range expansion of an intertidal barnacle. *Journal of Experimental Marine Biology and Ecology*, **354**, 220-230.

Santos, A.M.P., Kazmin, A.S. & Peliz, A. (2005) Decadal changes in the Canary upwelling system as revealed by satellite observations: their impact on productivity. *Journal of Marine Research*, **63**, 359-379.

Schemske, D.W. & Mittelbach, G.G. (2017) "Latitudinal gradients in species diversity": Reflections on Pianka's 1966 article and a look forward. *The American Naturalist*, **189**, 599-603.

Schluter, D. & Pennell, M.W. (2017) Speciation gradients and the distribution of biodiversity. *Nature*, **546**, 48-55.

Schmitt, T. & Varga, Z. (2012) Extra-Mediterranean refugia: The rule and not the exception? *Frontiers in Zoology*, **9**, 22.

Schoch, G., Menge, B.A., Allison, G., Kavanaugh, M., Thompson, S.A. & Wood, S.A. (2006) Fifteen degrees of separation: Latitudinal gradients of rocky intertidal biota along the California Current. *Limnology and Oceanography*, **51**, 2564-2585.

Seoane-Camba, J. (1965) Estudios sobre las algas bentónicas en la costa sur de la Península Ibérica (litoral de Cádiz). *Investigacion Pesquera*, **29**, 3-216.

Shafee, M. (1989) Reproduction of *Perna picta* (Mollusca: Bivalvia) from the Atlantic coast of Morocco. *Marine Ecology Progress Series*, **53**, 235-245.

Shanks, A.L., Grantham, B.A. & Carr, M.H. (2003) Propagule dispersal distance and the size and spacing of marine reserves. *Ecological Applications*, **13**, S159-S169.

Sheehy, D.J. & Vik, S.F. (2010) The role of constructed reefs in non-indigenous species introductions and range expansions. *Ecological Engineering*, **36**, 1-11.

Shemesh, E., Huchon, D., Simon-Blecher, N. & Achituv, Y. (2009) The distribution and molecular diversity of the Eastern Atlantic and Mediterranean chthamalids (Crustacea, Cirripedia). *Zoologica Scripta*, **38**, 365-378.

Short, J., Foster, T., Falter, J., Kendrick, G.A. & McCulloch, M.T. (2015) Crustose coralline algal growth, calcification and mortality following a marine heatwave in Western Australia. *Continental Shelf Research*, **106**, 38-44.

Sidoumou, Z., Gnassia-Barelli, M., Siau, Y., Morton, V. & Romeo, M. (2006) Heavy metal concentrations in molluscs from the Senegal coast. *Environment International*, **32**, 384-387.

Sigurdsson, J.B. (1976) The dispersal of young post-larval bivalve molluscs by byssus threads. *Nature*, **262**, 386-387.

Silliman, B.R., Bertness, M.D., Altieri, A.H., Griffin, J.N., Bazterrica, M.C., Hidalgo, F.J., Crain, C.M. & Reyna, M.V. (2011) Whole-community facilitation regulates biodiversity on Patagonian rocky shores. *PLoS ONE*, **6**, e24502.

Silva, I.C., Mesquita, N., Schubart, C.D., Alves, M.J. & Paula, J. (2009) Genetic patchiness of the shore crab *Pachygrapsus marmoratus* along the Portuguese coast. *Journal of Experimental Marine Biology and Ecology*, **378**, 50-57.

Sink, K.J., Branch, G.M. & Harris, J.M. (2005) Biogeographic patterns in rocky intertidal communities in KwaZulu-Natal, South Africa. *African Journal of Marine Science*, **27**, 81-96.

Smale, D.A. & Wernberg, T. (2013) Extreme climatic event drives range contraction of a habitat-forming species. *Proceedings of the Royal Society of London B: Biological Sciences*, **280**, 20122829.

Smale, D.A., Burrows, M.T., Moore, P., O'Connor, N. & Hawkins, S.J. (2013) Threats and knowledge gaps for ecosystem services provided by kelp forests: a northeast Atlantic perspective. *Ecology and Evolution*, **3**, 4016-4038.

Smale, D.A. & Vance, T. (2016) Climate-driven shifts in species' distributions may exacerbate the impacts of storm disturbances on Northeast Atlantic kelp forests. *Marine and Freshwater Research*, **67**, 65-74.

Smale, D.A., Wernberg, T. & Vanderklift, M.A. (2017) Regional-scale variability in the response of benthic macroinvertebrate assemblages to a marine heatwave. *Marine Ecology Progress Series*, **568**, 17-30.

Soares, C.G., Ferreira, A. & Cunha, C. (1996) Linear models of the time series of significant wave height on the Southwest Coast of Portugal. *Coastal Engineering*, **29**, 149-167.

Sokołowski, A., Bawazir, A.S., Sokołowska, E. & Wołowicz, M. (2010) Seasonal variation in the reproductive activity, physiological condition and biochemical components of the brown mussel *Perna perna* from the coastal waters of Yemen (Gulf of Aden). *Aquatic Living Resources*, **23**, 177-186.

Soltis, D.E., Morris, A.B., McLachlan, J.S., Manos, P.S. & Soltis, P.S. (2006) Comparative phylogeography of unglaciated eastern North America. *Molecular Ecology*, **15**, 4261-4293.

Somero, G.N. (2002) Thermal physiology and vertical zonation of intertidal animals: optima, limits, and costs of living. *Integrative and Comparative Biology*, **42**, 780-789.

Somero, G. (2010) The physiology of climate change: how potentials for acclimatization and genetic adaptation will determine 'winners' and 'losers'. *Journal of Experimental Biology*, **213**, 912-920.

Sorte, C.J., Williams, S.L. & Carlton, J.T. (2010) Marine range shifts and species introductions: comparative spread rates and community impacts. *Global Ecology and Biogeography*, **19**, 303-316.

Sousa, M.C., Alvarez, I., deCastro, M., Gomez-Gesteira, M. & Dias, J.M. (2017a) Seasonality of coastal upwelling trends under future warming scenarios along the

southern limit of the Canary upwelling system. *Progress in Oceanography*, **153**, 16-23.

Sousa, M.C., deCastro, M., Alvarez, I., Gomez-Gesteira, M. & Dias, J.M. (2017b) Why coastal upwelling is expected to increase along the western Iberian Peninsula over the next century? *Science of the Total Environment*, **592**, 243-251.

Southward, A.J. (1976) On the taxonomic status and distribution of *Chthamalus stellatus* (Cirripedia) in the northeast Atlantic region: with a key to the common intertidal barnacles of Britain. *Journal of the Marine Biological Association of the United Kingdom*, **56**, 1007-1028.

Southward, A.J., Langmead, O., Hardman-Mountford, N.J., Aiken, J., Boalch, G.T., Dando, P.R., Genner, M.J., Joint, I., Kendall, M.A. & Halliday, N.C. (2004) Long-term oceanographic and ecological research in the western English Channel. *Advances in Marine Biology*, **47**, 1-105.

Spalding, M.D., Fox, H.E., Allen, G.R., Davidson, N., Ferdaña, Z.A., Finlayson, M., Halpern, B.S., Jorge, M.A., Lombana, A., Lourie, S.A., Martin, K.D., McManus, E., Molnar, J., Recchia, C.A. & Robertson, J. (2007) Marine ecoregions of the world: A bioregionalization of coastal and shelf areas. *BioScience*, **57**, 573-583.

Stachowicz, J.J., Terwin, J.R., Whitlatch, R.B. & Osman, R.W. (2002) Linking climate change and biological invasions: Ocean warming facilitates nonindigenous species invasions. *Proceedings of the National Academy of Sciences*, **99**, 15497-15500.

Stanichny, S. (2005) Wind driven upwelling along the African coast of the Strait of Gibraltar. *Geophysical Research Letters*, **32**, L04604.

Steffani, C.N. & Branch, G.M. (2003) Growth rate, condition, and shell shape of *Mytilus galloprovincialis*: responses to wave exposure. *Marine Ecology Progress Series*, **246**, 197-209.

Stephenson, E.H., Steneck, R.S. & Seeley, R.H. (2009) Possible temperature limits to range expansion of non-native Asian shore crabs in Maine. *Journal of Experimental Marine Biology and Ecology*, **375**, 21-31.

Steven, B., Gallegos-Graves, L.V., Belnap, J. & Kuske, C.R. (2013) Dryland soil microbial communities display spatial biogeographic patterns associated with soil depth and soil parent material. *FEMS Microbiology Ecology*, **86**, 101-113.

Stewart, J.R., Lister, A.M., Barnes, I. & Dalén, L. (2010) Refugia revisited: individualistic responses of species in space and time. *Proceedings of the Royal Society B: Biological Sciences*, **277**, 661-671.

Stillman, J.H. (2002) Causes and consequences of thermal tolerance limits in rocky intertidal porcelain crabs, genus *Petrolisthes*. *Integrative and Comparative Biology*, **42**, 790-796.

Stillman, J.H. & Somero, G.N. (2000) A comparative analysis of the upper thermal tolerance limits of eastern Pacific porcelain crabs, genus *Petrolisthes*: influences of latitude, vertical zonation, acclimation, and phylogeny. *Physiological and Biochemical Zoology*, **73**, 200-208.

Stock, C.A., John, J.G., Rykaczewski, R.R., Asch, R.G., Cheung, W.W., Dunne, J.P., Friedland, K.D., Lam, V.W., Sarmiento, J.L. & Watson, R.A. (2017) Reconciling

fisheries catch and ocean productivity. *Proceedings of the National Academy of Sciences*, **114**, E1441-E1449.

Storey, J.D. (2002) A direct approach to false discovery rates. *Journal of the Royal Statistical Society Series B*, **64**, 479-498.

Sukhotin, A.A., Abele, D. & Pörtner, H.-O. (2002) Growth, metabolism and lipid peroxidation in *Mytilus edulis*: age and size effects. *Marine Ecology Progress Series*, **226**, 223-234.

Sunday, J.M., Bates, A.E. & Dulvy, N.K. (2012) Thermal tolerance and the global redistribution of animals. *Nature Climate Change*, **2**, 686-690.

Sunday, J.M., Popovic, I., Palen, W.J., Foreman, M.G.G. & Hart, M.W. (2014) Ocean circulation model predicts high genetic structure observed in a long-lived pelagic developer. *Molecular Ecology*, **23**, 5036-5047.

Sydeman, W., García-Reyes, M., Schoeman, D., Rykaczewski, R., Thompson, S., Black, B. & Bograd, S. (2014) Climate change and wind intensification in coastal upwelling ecosystems. *Science*, **345**, 77-80.

Szefer, P. & Geldon, J. (1997) Distribution and association of trace metals in soft tissue and byssus of mollusc *Perna perna* from the Gulf of Aden, Yemen. *Environment International*, **23**, 53-61.

Tagliarolo, M. & McQuaid, C.D. (2015) Sub-lethal and sub-specific temperature effects are better predictors of mussel distribution than thermal tolerance. *Marine Ecology Progress Series*, **535**, 145-159.

Tagliarolo, M., Montalto, V., Sarà, G., Lathlean, J.A. & McQuaid, C.D. (2016) Low temperature trumps high food availability to determine the distribution of intertidal mussels *Perna perna* in South Africa. *Marine Ecology Progress Series*, **558**, 51-63.

Tamura, K., Peterson, D., Peterson, N., Stecher, G., Nei, M. & Kumar, S. (2011) MEGA5: molecular evolutionary genetics analysis using maximum likelihood, evolutionary distance, and maximum parsimony methods. *Molecular Biology and Evolution*, **28**, 2731-9.

Tapia, F.J., Largier, J.L., Castillo, M., Wieters, E.A. & Navarrete, S.A. (2014) Latitudinal discontinuity in thermal conditions along the nearshore of Central-Northern Chile. *PLoS ONE*, **9**, e110841.

Tateno, R. & Takeda, H. (2003) Forest structure and tree species distribution in relation to topography-mediated heterogeneity of soil nitrogen and light at the forest floor. *Ecological Research*, **18**, 559-571.

Taulman, J.F. & Robbins, L.W. (2014) Range expansion and distributional limits of the nine-banded armadillo in the United States: an update of Taulman & Robbins (1996). *Journal of Biogeography*, **41**, 1626-1630.

Tavares, A.I., Cabezas, M.P., Xavier, R., Branco, M., Lima, F.P., Seabra, R., Ribeiro, P.A., Lopes, E.P. & Santos, A.M. (2017) Phylogeography and phylogeny of the genus *Acanthonyx* (Decapoda, Epialtidae) in the northeast Atlantic and Mediterranean. *Zoologica Scripta*, **46**, 571–583.

Teske, P.R., Papadopoulos, I., Newman, B.K., Dworschak, P.C., McQuaid, C.D. & Barker, N.P. (2008) Oceanic dispersal barriers, adaptation and larval retention: an interdisciplinary assessment of potential factors maintaining a phylogeographic break between sister lineages of an African prawn. *BMC Evolutionary Biology*, **8**, 341.

Teske, P.R., Papadopoulos, I., Barker, N.P. & McQuaid, C.D. (2012) Mitochondrial DNA paradox: sex-specific genetic structure in a marine mussel - despite maternal inheritance and passive dispersal. *BMC Genet*, **13**, 45.

Teske, P.R., Papadopoulos, I., Barker, N.P., McQuaid, C.D. & Beheregaray, L.B. (2014) Mitonuclear discordance in genetic structure across the Atlantic/Indian Ocean biogeographical transition zone. *Journal of Biogeography*, **41**, 392-401.

Thiel, M. & Ullrich, N. (2002) Hard rock versus soft bottom: the fauna associated with intertidal mussel beds on hard bottoms along the coast of Chile, and considerations on the functional role of mussel beds. *Helgoland Marine Research*, **56**, 21-30.

Thompson, S.A., Sydeman, W.J., Santora, J.A., Black, B.A., Suryan, R.M., Calambokidis, J., Peterson, W.T. & Bograd, S.J. (2012) Linking predators to seasonality of upwelling: using food web indicators and path analysis to infer trophic connections. *Progress in Oceanography*, **101**, 106-120.

Thuiller, W., Georges, D. & Engler, R. (2014) biomod2: Ensemble platform for species distribution modeling. R package version 3.1-64. *Available at: http://CRAN. R-project. org/package= biomod2 (accessed January 2016)*,

Tintore, J., La Viollete, P.E., Blade, I. & Cruzado, A. (1988) A study of an intense density front in the Eastern Alboran Sea: the Almeria-Oran Front. *Journal of Physical Oceanography*, **18**, 1384-1397.

Tomanek, L. & Somero, G.N. (1999) Evolutionary and acclimation-induced variation in the heat-shock responses of congeneric marine snails (genus *Tegula*) from different thermal habitats: implications for limits of thermotolerance and biogeography. *Journal of Experimental Biology*, **202**, 2925-2936.

Tont, S.A. (1975) The effect of upwelling on solar irradiance near the coast of southern California. *Journal of Geophysical Research*, **80**, 5031-5034.

Tont, S.A. (1981) Upwelling: effects on air temperatures and solar irradiance. *Coastal and Estuarine Sciences*, **1**, 57-62.

Traill, L.W., Lim, M.L.M., Sodhi, N.S. & Bradshaw, C.J.A. (2010) Mechanisms driving change: altered species interactions and ecosystem function through global warming. *Journal of Animal Ecology*, **79**, 937-947.

Travis, J. (2003) Climate change and habitat destruction: a deadly anthropogenic cocktail. *Proceedings of the Royal Society of London B: Biological Sciences*, **270**, 467-473.

Tuya, F., Cacabelos, E., Duarte, P., Jacinto, D., Castro, J.J., Silva, T., Bertocci, I., Franco, J.N., Arenas, F., Coca, J. & Wernberg, T. (2012) Patterns of landscape and assemblage structure along a latitudinal gradient in ocean climate. *Marine Ecology Progress Series*, **466**, 9-19.

Tyberghein, L., Verbruggen, H., Pauly, K., Troupin, C., Mineur, F. & De Clerck, O. (2012) Bio-ORACLE: a global environmental dataset for marine species distribution modelling. *Global Ecology and Biogeography*, **21**, 272-281.

Underwood, G., Phillips, J. & Saunders, K. (1998) Distribution of estuarine benthic diatom species along salinity and nutrient gradients. *European Journal of Phycology*, **33**, 173-183.

Unesco (2015) Oceanographic and biological features in the Canary Current Large Marine Ecosystem. In: eds. L. Valdés and I. Déniz-González), p. 389. Intergovernmental Oceanographic Commission

Urban, M.C. (2015) Accelerating extinction risk from climate change. *Science*, **348**, 571-573.

Vakily, J.M. (1989) *The biology and culture of mussels of the genus Perna*. International center for living aquatic resources management, Manila, Philippines / Deutsche gesellschaft fur technische zusammenarbeit (GTZ) eschborn, Germany.

van de Koppel, J., Gascoigne, J.C., Theraulaz, G., Rietkerk, M., Mooij, W.M. & Herman, P.M.J. (2008) Experimental evidence for spatial self-organization and its emergent effects in mussel bed ecosystems. *Science*, **322**, 739-742.

van Hooidonk, R., Maynard, J. & Planes, S. (2013) Temporary refugia for coral reefs in a warming world. *Nature Climate Change*, **3**, 508-511.

van Oosterhout, C., Hutchinson, W., Wills, D. & Shipley, P. (2004) Micro-checker: software for identifying and correcting genotyping errors in microsatellite data. *Molecular Ecology Notes*, **4**, 535 - 538.

Varela, R., Alvarez, I., Santos, F., deCastro, M. & Gomez-Gesteira, M. (2015) Has upwelling strengthened along worldwide coasts over 1982-2010? *Scientific Reports*, **5**, 10016.

Varney, R.L., Sackett, R.E. & Wilbur, A.E. (2016) Analysis of spatiotemporal genetic variability in eastern oyster *Crassostrea virginica* (Gmelin, 1791) MtDNA 16S sequences among North Carolina populations. *Journal of Shellfish Research*, **35**, 329-342.

Vergés, A., Steinberg, P.D., Hay, M.E., Poore, A.G.B., Campbell, A.H., Ballesteros, E., Heck, K.L., Booth, D.J., Coleman, M.A., Feary, D.A., Figueira, W., Langlois, T., Marzinelli, E.M., Mizerek, T., Mumby, P.J., Nakamura, Y., Roughan, M., van Sebille, E., Gupta, A.S., Smale, D.A., Tomas, F., Wernberg, T. & Wilson, S.K. (2014) The tropicalization of temperate marine ecosystems: climate-mediated changes in herbivory and community phase shifts. *Proceedings of the Royal Society B: Biological Sciences*, **281**, 20140846.

Vilaça, S.T., Biosa, D., Zachos, F., Iacolina, L., Kirschning, J., Alves, P.C., Paule, L., Gortazar, C., Mamuris, Z., Jędrzejewska, B., Borowik, T., Sidorovich, V.E., Kusak, J., Costa, S., Schley, L., Hartl, G.B., Apollonio, M., Bertorelle, G., Scandura, M. & Linder, P. (2014) Mitochondrial phylogeography of the European wild boar: the effect of climate on genetic diversity and spatial lineage sorting across Europe. *Journal of Biogeography*, **41**, 987-998.

Villamor, A., Costantini, F. & Abbiati, M. (2014) Genetic structuring across marine biogeographic boundaries in rocky shore invertebrates. *PLoS One*, **9**, e101135.

Villesen, P. (2007) FaBox: an online toolbox for fasta sequences. *Molecular Ecology Notes*, **7**, 965-968.

Visser, M.E. (2008) Keeping up with a warming world; assessing the rate of adaptation to climate change. *Proceedings of the Royal Society B: Biological Sciences*, **275**, 649-659.

Wallace, A.L., Klein, A.S. & Mathieson, A.C. (2004) Determining the affinities of salt marsh Fucoids using microsatellite markers: evidence of hybridization and introgression between two Species of *Fucus* (Phaeophyta) in a Maine estuary. *Journal of Phycology*, **40**, 1013-1027.

Walther, G.-R., Post, E., Convey, P., Menzel, A., Parmesan, C., Beebee, T.J.C., Fromentin, J.-M., Hoegh-Guldberg, O. & Bairlein, F. (2002) Ecological responses to recent climate change. *Nature*, **416**, 389-395.

Wang, D., Gouhier, T.C., Menge, B.A. & Ganguly, A.R. (2015) Intensification and spatial homogenization of coastal upwelling under climate change. *Nature*, **518**, 390-4.

Warren, S.G., Hahn, C.J., London, J., Chervin, R.M. & Jenne, R.L. (1986) *Global distribution of total cloud cover and cloud type amonts over land*. NCAR Technical Note TN-273+STR, Boulder, CO, USA.

Waters, J.M. & Roy, M.S. (2004) Phylogeography of a high-dispersal New Zealand sea-star: does upwelling block gene-flow? *Molecular Ecology*, **13**, 2797-2806.

Waters, J.M., Condie, S.A. & Beheregaray, L.B. (2014) Does coastal topography constrain marine biogeography at an oceanographic interface? *Marine and Freshwater Research*, **65**, 969-977.

Watt, C.A. & Scrosati, R.A. (2013a) Regional consistency of intertidal elevation as a mediator of seaweed canopy effects on benthic species richness, diversity, and composition. *Marine Ecology Progress Series*, **491**, 91-99.

Watt, C.A. & Scrosati, R.A. (2013b) Bioengineer effects on understory species richness, diversity, and composition change along an environmental stress gradient: Experimental and mensurative evidence. *Estuarine, Coastal and Shelf Science*, **123**, 10-18.

Weber, L.I. & Hawkins, S.J. (2005) *Patella aspera* and *P. ulyssiponensis*: genetic evidence of speciation in the northeast Atlantic. *Marine Biology*, **147**, 153-162.

Weir, B.S. & Cockerham, C.C. (1984) Estimating F-Statistics for the analysis of population structure. *Evolution* **38**, 1358-1370.

Wernberg, T., Russell, B.D., Moore, P.J., Ling, S.D., Smale, D.A., Campbell, A., Coleman, M.A., Steinberg, P.D., Kendrick, G.A. & Connell, S.D. (2011) Impacts of climate change in a global hotspot for temperate marine biodiversity and ocean warming. *Journal of Experimental Marine Biology and Ecology*, **400**, 7-16.

Wernberg, T., Bennett, S., Babcock, R.C., de Bettignies, T., Cure, K., Depczynski, M., Dufois, F., Fromont, J., Fulton, C.J., Hovey, R.K., Harvey, E.S., Holmes, T.H., Kendrick, G.A., Radford, B., Santana-Garcon, J., Saunders, B.J., Smale, D.A., Thomsen, M.S., Tuckett, C.A., Tuya, F., Vanderklift, M.A. & Wilson, S. (2016)

Climate-driven regime shift of a temperate marine ecosystem. *Science*, **353**, 169-172.

Wetherald, R.T. & Manabe, S. (1980) Cloud cover and climate sensitivity. *Journal of the Atmospheric Sciences*, **37**, 1485-1510.

Wethey, D.S. (2002) Biogeography, competition, and microclimate: the barnacle *Chthamalus fragilis* in New England. *Integrative and Comparative Biology*, **42**, 872-880.

Whittaker, R.J., Araújo, M.B., Jepson, P., Ladle, R.J., Watson, J.E.M. & Willis, K.J. (2005) Conservation Biogeography: assessment and prospect. *Diversity and Distributions*, **11**, 3-23.

Wieters, E.A. (2005) Upwelling control of positive interactions over mesoscales: a new link between bottom-up and top-down processes on rocky shores. *Marine Ecology Progress Series*, **301**, 43-54.

Wieters, E.A., Broitman, B.R. & Brancha, G.M. (2009) Benthic community structure and spatiotemporal thermal regimes in two upwelling ecosystems: Comparisons between South Africa and Chile. *Limnology and Oceanography*, **54**, 1060-1072.

Williams, G.A., De Pirro, M., Leung, K.M. & Morritt, D. (2005) Physiological responses to heat stress on a tropical shore: the benefits of mushrooming behaviour in the limpet *Cellana grata*. *Marine Ecology Progress Series*, **292**, 213-224.

Wood, A.R., Apte, S., MacAvoy, E.S. & Gardner, J.P. (2007) A molecular phylogeny of the marine mussel genus *Perna* (Bivalvia: Mytilidae) based on nuclear (ITS1&2) and mitochondrial (COI) DNA sequences. *Molecular Phylogenetics and Evolution*, **44**, 685-698.

Woodworth-Jefcoats, P.A., Polovina, J.J. & Drazen, J.C. (2016) Climate change is projected to reduce carrying capacity and redistribute species richness in North Pacific pelagic marine ecosystems. *Global Change Biology*, **23**, 1000-1008.

Xavier, B.M., Branch, G.M. & Wieters, E.A. (2007) Abundance, growth and recruitment of *Mytilus galloprovincialis* on the west coast of South Africa in relation to upwelling. *Marine Ecology Progress Series*, **346**, 189-201.

Yamano, H., Sugihara, K. & Nomura, K. (2011) Rapid poleward range expansion of tropical reef corals in response to rising sea surface temperatures. *Geophysical Research Letters*, **38**, GL046474.

Yap, W.G., Young, A.I., Orano, C.E.F. & Castro, M.T. (1979) Manual on mussel fanning. *Aquaculture Extension Manual No.6.*, p. 17, Southeast Asian Development Center, Aquaculture Department, Iloilo, Philippines.

Zabi, S.G. (1982) Répartition et abondance des espèces de la macrofaune benthique de la lagune Ebrié (Côte d'Ivoire). *Document Scientifique du Centre de Recherche Océanographique, Abidjan*, **13**, 73-96.

Zacherl, D., Gaines, S.D. & Lonhart, S.I. (2003) The limits to biogeographical distributions: insights from the northward range extension of the marine snail, *Kelletia kelletii* (Forbes, 1852). *Journal of Biogeography*, **30**, 913-924.

Zardi, G.I., Nicastro, K.R., McQuaid, C.D., Rius, M. & Porri, F. (2006a) Hydrodynamic stress and habitat partitioning between indigenous (*Perna perna*) and invasive

(*Mytilus galloprovincialis*) mussels: constraints of an evolutionary strategy. *Marine Biology*, **150**, 79-88.

Zardi, G.I., Nicastro, R.K., Porri, F. & McQuaid, D.C. (2006b) Sand stress as a non-determinant of habitat segregation of indigenous (*Perna perna*) and invasive (*Mytilus galloprovincialis*) mussels in South Africa. *Marine Biology*, **148**, 1031-1038.

Zardi, G.I., McQuaid, C.D., Teske, P.R. & Barker, N.P. (2007) Unexpected genetic structure of mussel populations in south Africa: indigenous *Perna perna* and invasive *Mytilus galloprovincialis*. *Marine Ecology Progress Series*, **337**, 135 - 144.

Zardi, G.I., Nicastro, K.R., McQuaid, C.D. & Erlandsson, J. (2008) Sand and wave induced mortality in invasive (*Mytilus galloprovincialis*) and indigenous (*Perna perna*) mussels. *Marine Biology*, **153**, 853-858.

Zardi, G.I., Nicastro, K.R., McQuaid, C.D. & Gektidis, M. (2009) Effects of endolithic parasitism on invasive and indigenous mussels in a variable physical environment. *PLoS One*, **4**, e6560.

Zardi, G.I., Nicastro, K.R., McQuaid, C.D., Hancke, L. & Helmuth, B. (2011a) The combination of selection and dispersal helps explain genetic structure in intertidal mussels. *Oecologia*, **165**, 947-958.

Zardi, G.I., Nicastro, K.R., Canovas, F., Costa, J.F., Serrão, E.A. & Pearson, G.A. (2011b) Adaptive traits are maintained on steep selective gradients despite gene flow and hybridization in the intertidal zone. *PLoS One*, **6**, e19402.

Zardi, G.I., Nicastro, K.R., Costa, J.F., Serrão, E.A. & Pearson, G.A. (2013) Broad scale agreement between intertidal habitats and adaptive traits on a basis of contrasting population genetic structure. *Estuarine, Coastal and Shelf Science*, **131**, 140-148.

Zardi, G.I., Nicastro, K.R., McQuaid, C.D., Castilho, R., Costa, J.F., Serrão, E.A. & Pearson, G.A. (2015a) Intraspecific genetic lineages of a marine mussel show behavioural divergence and spatial segregation over a tropical/subtropical biogeographic transition. *BMC Evolutionary Biology*, **15**, 100.

Zardi, G.I., Nicastro, K.R., Serrão, E.A., Jacinto, R., Monteiro, C.A. & Pearson, G.A. (2015b) Closer to the rear edge: ecology and genetic diversity down the core-edge gradient of a marine macroalga. *Ecosphere*, **6**, art23.

Zardi, G.I., Nicastro, K.R., McQuaid, C.D., Ng, T.P., Lathlean, J. & Seuront, L. (2016) Enemies with benefits: parasitic endoliths protect mussels against heat stress. *Scientific Reports*, **6**, 31413.

Zhan, A., Hu, J., Hu, X., Zhou, Z., Hui, M., Wang, S., Peng, W., Wang, M. & Bao, Z. (2009) Fine-scale population genetic structure of Zhikong scallop (*Chlamys farreri*): do local marine currents drive geographical differentiation? *Marine Biotechnology*, **11**, 223-235.

Zhang, H.-M., Bates, J.J. & Reynolds, R.W. (2006) Assessment of composite global sampling: Sea surface wind speed. *Geophysical Research Letters*, **33**, GL027086.

Ziadi, B., Dhib, A., Turki, S. & Aleya, L. (2015) Bivalve and barnacle larvae distribution driven by water temperature in a Mediterranean lagoon. *Environmental science and pollution research international*, **22**, 7002.

Zizzari, Z.V. & Ellers, J. (2011) Effects of exposure to short-term heat stress on male reproductive fitness in a soil arthropod. *Journal of Insect Physiology*, **57**, 421-426.

8 APPENDICES

8.1 Tables

Table A1 – Presence/absence records of *P. perna* used for the environmental niche modelling approach.

Country	Location	Coordinates	Presence	Reference
Tunisia	Zembra Island	37°08'25.96"N; 10°48'28.94"E	Present	Boudoresque *et al.*, 1986
Tunisia	Korbous	36°49'29.04"N; 10°33'59.97"E	Present	This thesis
Tunisia	La Goulette	36°49'18.84"N; 10°18'42.14"E	Present	Boudoresque *et al.*, 1986
Tunisia	Bizerte	37°15'10.41"N; 09°56'41.15"E	Present	This thesis
Tunisia	Tabarka	36°57'39.05"N; 08°45'02.62"E	Present	Boudoresque *et al.*, 1986
Algeria	La Kyenne Beach	36°58'02.00"N; 07°46'24.00"E	Present	Belabed *et al.*, 2013
Algeria	Saint Cloud Beach	36°55'22.20"N; 07°45'50.20"E	Present	Belabed *et al.*, 2013
Algeria	Sunrise Beach	36°54'33.90"N; 07°46'20.90"E	Present	Belabed *et al.*, 2013
Algeria	Sidi Salem Beach	36°52'02.00"N; 07°46'26.60"E	Present	Belabed *et al.*, 2013
Algeria	Annaba Bay	36°50'32.48"N; 07°51'17.48"E	Present	This thesis
Algeria	Boubouaou El Bahri	36°46'33.56"N; 03°23'15.41"E	Present	Abada-Boudjema & Davin, 1995
Algeria	Bordj El Kiffan	36°45'37.72"N; 03°12'45.24"E	Present	Abada-Boudjema & Davin, 1995
Spain	Cullera	39°11'16.26"N; 00°13'17.20"W	Absent	This thesis
Spain	Dénia	38°57'50.66"N; 00°07'43.58"W	Absent	This thesis
Spain	Cape de la Nau	38°43'51.27"N; 00°13'08.85"E	Absent	This thesis
Spain	Calpe	38°38'25.71"N; 00°03'56.53"E	Absent	This thesis
Spain	Alicante	38°21'07.64"N; 00°24'40.40"W	Absent	This thesis
Spain	Santa Pola	38°11'18.94"N; 00°33'06.45"W	Absent	This thesis
Spain	Guardamar del Segura	38°06'37.33"N; 00°38'27.07"W	Absent	This thesis
Spain	Cape Palos	37°38'00.94"N; 00°41'23.95"W	Absent	This thesis
Spain	Portman	37°34'50.35"N; 00°51'13.23"W	Absent	This thesis
Spain	Puerto de Mazarron	37°33'28.51"N; 01°17'10.24"W	Absent	This thesis
Spain	Cape Cope	37°26'12.49"N; 01°29'02.88"W	Absent	This thesis
Spain	Calabardina	37°25'53.29"N; 01°30'27.11"W	Absent	This thesis
Spain	Aguilas (beach)	37°24'15.16"N; 01°33'56.64"W	Absent	This thesis
Spain	Villaricos	37°14'49.74"N; 01°46'15.80"W	Absent	This thesis
Spain	Garrucha	37°10'21.02"N; 01°49'18.30"W	Absent	This thesis
Spain	La Isleta (village)	36°48'47.17"N; 02°03'05.46"W	Absent	This thesis
Spain	La Isleta (beach)	36°47'53.54"N; 02°03'42.64"W	Absent	This thesis
Spain	Cape Gata	36°44'00.26"N; 02°12'14.70"W	Present	This thesis
Spain	Aguadulce	36°48'40.91"N; 02°34'00.66"W	Absent	This thesis
Spain	Roquetas de Mar	36°45'27.41"N; 02°36'15.26"W	Absent	This thesis
Spain	Balerma	36°41'56.20"N; 02°51'33.99"W	Present	This thesis
Spain	Almuñecar	36°43'39.84"N; 03°41'39.86"W	Present	This thesis
Spain	La Araña	36°42'41.35"N; 04°19'37.50"W	Present	This thesis
Spain	Torreguadiaro	36°18'00.14"N; 05°16'04.77"W	Present	This thesis
Spain	Los Palmones	36°10'34.28"N; 05°25'28.26"W	Present	This thesis
Spain	Tarifa	36°00'27.89"N; 05°36'26.09"W	Absent	This thesis
Spain	Paloma Baja	36°03'49.70"N; 05°43'39.89"W	Absent	This thesis
Spain	Atlanterra	36°05'24.78"N; 05°48'43.02"W	Present	This thesis

Spain	Barbate	36°11'00.22"N; 05°56'10.82"W	Absent	This thesis
Spain	Puerto Sherry	36°34'48.65"N; 06°15'55.07"W	Absent	This thesis
Spain	Rota	36°36'55.50"N; 06º21'27.85"W	Absent	This thesis
Spain	Huelva	37°07'45.19"N; 06º51'09.43"W	Absent	This thesis
Spain	Punta Umbria	37°09'53.78"N; 06º56'54.38"W	Absent	This thesis
Spain	Punta del Moral	37°10'57.76"N; 07º19'46.83"W	Present	This thesis
Portugal	V. R. S. António	37°10'03.78"N; 07º24'09.03"W	Present	This thesis
Portugal	Tavira	37°06'41.06"N; 07º36'57.99"W	Present	This thesis
Portugal	Farol	36°58'29.95"N; 07º51'42.17"W	Present	This thesis
Portugal	Vilamoura	37°04'05.50"N; 08º06'42.64"W	Present	This thesis
Portugal	Albufeira	37°05'21.03"N; 08°11'29.76"W	Absent	This thesis
Portugal	Pintadinho	37°06'32.07"N; 08°31'11.63"W	Absent	This thesis
Portugal	Lagos	37°06'01.04"N; 08°40'02.80"W	Absent	This thesis
Portugal	Sagres	37°00'23.69"N; 08º56'55.80"W	Present	This thesis
Portugal	Castelejo	37°06'08.00"N; 08º56'44.29"W	Present	This thesis
Portugal	Amoreira	37°20'59.18"N; 08º50'53.15"W	Absent	This thesis
Portugal	V. N. Milfontes	37°43'04.79"N; 08º47'27.73"W	Absent	This thesis
Portugal	Malhão	37°46'44.64"N; 08º48'09.35"W	Absent	This thesis
Portugal	Lizandro	38°56'28.13"N; 09°25'02.28"W	Absent	This thesis
Portugal	Ericeira	38°57'21.03"N; 09°25'00.97"W	Absent	This thesis
Portugal	Viana do Castelo	41°41'57.85"N; 08°51'23.81"W	Absent	This thesis
Morocco	Punta Negri	35°16'46.33"N; 03º08'06.63"W	Present	This thesis
Morocco	Larache	35°11'48.14"N; 06°09'30.61"W	Present	This thesis
Morocco	Bouknadel	34°07'40.74"N; 06°45'14.63"W	Present	Klouche *et al.*, 2015
Morocco	Rabat	34°01'57.26"N; 06°50'27.96"W	Present	This thesis
Morocco	Skhirat	33°52'15.84"N; 07°03'54.72"W	Present	Jourmi *et al.*, 2012
Morocco	Mohammedia	33°42'13.04"N; 07°24'49.62"W	Present	Klouche *et al.*, 2015
Morocco	Casablanca	33°39'07.22"N; 07°29'03.11"W	Present	This thesis
Morocco	Sidi Bouzid	33°13'06.11"N; 08°34'23.19"W	Present	This thesis
Morocco	El Beddouza	32°32'42.33"N; 09°16'55.34"W	Present	This thesis
Morocco	Essaouira	31°30'42.78"N; 09°46'24.31"W	Present	This thesis
Morocco	Imsouane	30°50'24.43"N; 09°49'21.92"W	Present	This thesis
Morocco	Anza	30°27'00.18"N; 09°39'44.47"W	Present	This thesis
Morocco	Mirleft	29°35'06.58"N; 10°02'50.78"W	Present	This thesis
Morocco	Tan-Tan	28°30'05.58"N; 11°20'06.38"W	Present	This thesis
Morocco	Tarfaya	27°45'33.64"N; 13°02'40.40"W	Absent	This thesis
Western Sahara	Boujdour	26°07'38.95"N; 14º30'02.38"W	Present	This thesis
Western Sahara	Nouifed	24°54'30.29"N; 14º49'45.36"W	Present	This thesis
Western Sahara	Hassi El kraa	24°41'06.18"N; 14°54'08.87"W	Present	This thesis
Western Sahara	Dakhla	23°46'06.97"N; 15º55'32.16"W	Present	This thesis
Mauritania	Cansado–IMROP	20°51'27.19"N; 17°01'52.10"W	Present	Mhamada *et al.*, 2015
Mauritania	Cansado–COMECA	20°50'19.68"N; 17°02'01.57"W	Present	Mhamada *et al.*, 2015
Mauritania	Cansado–Oil port	20°49'54.71"N; 17°02'07.66"W	Present	Mhamada *et al.*, 2015
Mauritania	Nouadhibou	20°58'27.91"N; 17°00'32.18"W	Present	Roméo *et al.*, 2000
Mauritania	Nouakchott	18°05'09.87"N; 16°01'35.15"W	Present	Roméo *et al.*, 2000

Senegal	Dakar	14°40'47.39"N; 17°28'11.23"W	Present	Sidoumou *et al.*, 2006
Ivory Coast	Ebrie Lagoon	05°17'36.29"N; 04°00'37.57"W	Present	Zabi, 1982
Ghana	Benya lagoon	05°04'57.21"N; 01°20'48.94"W	Present	Otchere *et al.*, 2003
Ghana	Sakumo lagoon	05°31'02.85"N; 00°16'52.32"W	Present	Otchere *et al.*, 2003
Congo	Pointe-Noire	04°45'32.64"S; 11°50'13.97"E	Present	Cayré, 1978
Angola	Luanda	08°52'11.28"S; 13°11'42.93"E	Present	This thesis
Namibia	Rocky Point	18°59'36.13"S; 12°28'36.54"E	Present	This thesis
Namibia	Mowey Bay	19°22'22.61"S; 12°42'19.38"E	Present	This thesis
Namibia	Terrace Bay	19°59'49.09"S; 13°02'01.24"E	Present	This thesis
Namibia	Swakopmound	22°40'07.52"S; 14°31'23.08"E	Present	This thesis
Namibia	Walvis Bay	22°55'28.69"S 14°31'03.66"E	Present	This thesis
Namibia	Sylvia Hill	25°08'46.62"S; 14°50'43.44"E	Present	This thesis
Namibia	Luderitz	26°38'43.31"S; 15°05'25.62"E	Absent	This thesis
South Africa	Alexander Bay	28°40'05.74"S; 16°30'20.35"E	Absent	This thesis
South Africa	Port Nolloth	29°15'01.53"S; 16°52'02.30"E	Absent	This thesis
South Africa	Brand-se-Baai	31°17'30.09"S; 17°52'46.86"E	Absent	This thesis
South Africa	Paternoster	32°48'07.22"S 17°53'51.95"E	Absent	This thesis
South Africa	Elands Bay	32°18'59.49"S; 18°18'54.50"E	Absent	This thesis
South Africa	Saldanha Bay	33°01'34.14"S; 17°56'30.55"E	Absent	This thesis
South Africa	Yzerfontein	33°21'14.99"S; 18°09'01.07"E	Absent	This thesis
South Africa	Bloubergstrand	33°48'06.18"S; 18°27'30.45"E	Absent	This thesis
South Africa	Camps Bay	33°57'11.26"S; 18°22'27.61"E	Absent	This thesis
South Africa	Scarborough	34°11'55.95"S; 18°22'16.49"E	Present	This thesis
South Africa	Outland Point	34°14'20.82"S; 18°28'38.02"E	Present	This thesis
South Africa	Pringle Bay	34°20'16.52"S; 18°49'41.04"E	Present	This thesis
South Africa	Betty's Bay	34°21'23.82"S; 18°55'59.54"E	Present	This thesis
South Africa	Kleinmond	34°20'37.84"S; 19°02'12.05"E	Present	This thesis
South Africa	Hermanus	34°24'40.64"S; 19°15'40.67"E	Present	This thesis
South Africa	Gans Bay	34°33'17.92"S; 19°21'49.38"E	Present	This thesis
South Africa	Cape Aghullas	34°49'26.40"S; 20°01'01.59"E	Present	This thesis
South Africa	Arniston	34°40'08.12"S; 20°14'05.13"E	Present	This thesis
South Africa	Mossel Bay-lighthouse	34°10'58.42"S; 22°09'30.73"E	Present	This thesis
South Africa	Mossel Bay-Dias strand	34°10'27.36"S; 22°08'09.70"E	Present	This thesis
South Africa	Mossel Bay-Hartenbos	34°09'56.22"S; 22°06'51.08"E	Present	This thesis
South Africa	Glentana	34°03'07.41"S; 22°19'19.01"E	Present	This thesis
South Africa	Wilderness	33°59'49.68"S; 22°33'57.53"E	Present	This thesis
South Africa	Sedgefield	34°01'44.56"S; 22°46'05.08"E	Present	This thesis
South Africa	Brenton-on-Sea	34°04'28.83"S; 23°01'12.56"E	Present	This thesis
South Africa	Robberg-open	34°06'08.06"S; 23°22'52.92"E	Present	This thesis
South Africa	Robberg-in	34°05'57.04"S; 23°22'37.86"E	Present	This thesis
South Africa	Plettenberg Bay-Beacon Isle	34°03'35.65"S; 23°22'50.22"E	Present	This thesis
South Africa	Plettenberg Bay-Lookout	34°03'06.08"S; 23°22'39.02"E	Present	This thesis
South Africa	Pletternberg Bay-Keurboomstrand	34°00'17.78"S; 23°27'18.61"E	Present	This thesis
South Africa	Oubosstrand	34°04'22.88"S; 24°13'29.60"E	Present	This thesis
South Africa	Seal Point	34°12'35.27"S; 24°49'31.96"E	Present	This thesis
South Africa	Sea Vista	34°10'15.24"S; 24°50'05.23"E	Present	This thesis
South Africa	Jeffrey's Bay	34°03'37.00"S; 24°55'43.64"E	Present	This thesis
South Africa	Noordkloofspunt	34°01'34.07"S; 24°55'50.90"E	Present	This thesis
South Africa	Kini Bay	34°01'17.91"S; 25°22'48.39"E	Present	This thesis
South Africa	Skoenmakerskop	34°02'28.06"S; 25°32'01.70"E	Present	This thesis
South Africa	Chelsea Point	34°02'45.66"S; 25°38'04.55"E	Present	This thesis
South Africa	Port Elizabeth-Bird Rock	33°59'00.57"S; 25°40'17.17"E	Present	This thesis
South Africa	Port Elizabeth-Shark Rock	33°58'47.18"S; 25°39'28.38"E	Present	This thesis

South Africa	Port Elizabeth-Deal Park	33°52'54.56"S; 25°37'37.39"E	Present	This thesis
South Africa	Hougham Park	33°45'17.09"S; 25°46'01.20"E	Present	This thesis
South Africa	Kenton-on-Sea	33°41'37.49"S; 26°40'13.70"E	Present	This thesis
South Africa	Old Womans	33°28'56.45"S; 27°09'06.98"E	Present	This thesis
South Africa	Kayser's Beach	33°12'44.21"S; 27°36'41.05"E	Present	This thesis
South Africa	Kidd's Beach	33°08'49.12"S; 27°42'11.29"E	Present	This thesis
South Africa	Gonubie	32°56'18.43"S; 28°01'58.06"E	Present	This thesis
South Africa	Glen Muir	32°53'04.40"S; 28°06'00.23"E	Present	This thesis
South Africa	Haga Haga	32°45'54.29"S; 28°14'56.51"E	Present	This thesis
South Africa	Morgan Bay	32°42'36.11"S; 28°20'30.00"E	Present	This thesis
South Africa	Kei mounth	32°41'03.70"S; 28°22'56.63"E	Present	This thesis
South Africa	Port St Johns	31°39'15.23"S; 29°30'56.40"E	Present	This thesis
South Africa	Port Edward	31°03'15.39"S; 30°13'42.30"E	Present	This thesis
South Africa	Durban	29°51'10.77"S; 31°02'27.68"E	Present	This thesis
South Africa	Ballito	29°32'42.96"S; 31°12'57.11"E	Present	This thesis
South Africa	Mapelane	28°24'27.04"S; 32°25'37.35"E	Present	This thesis
South Africa	Kosi Bay	27°00'45.82"S; 32°52'02.40"E	Present	This thesis
South Africa	Marion Island	46°49'57.95"S; 37°47'13.61"E	Absent	This thesis
Mozambique	Punta Douro	26°50'39.15"S; 32°53'41.39"E	Present	This thesis
Mozambique	Praia de Xai-Xai	25°06'42.09"S; 33°45'17.90"E	Present	This thesis
Mozambique	Praia de Závora	24°31'15.10"S; 35°12'22.40"E	Present	This thesis
Mozambique	Baía de Inhambane	23°52'04.68"S; 35°22'47.26"E	Absent	This thesis
Mozambique	Chicamane	21°53'09.91"S; 35°18'18.13"E	Absent	This thesis
Mozambique	Macunhe	21°50'30.97"S; 35°17'43.32"E	Absent	This thesis
Mozambique	Nhagonzo	21°43'50.44"S; 35°17'01.16"E	Absent	This thesis
Mozambique	Bazaruto	21°32'25.26"S; 35°28'14.60"E	Absent	This thesis
Yemen	Ash-shehr	14°44'49.88"N; 49°35'31.46"E	Present	Sokołowski *et al.*, 2010
Yemen	Bandar Fuqum	12°44'52.37"N; 44°49'31.63"E	Present	Szefer & Geldon, 1997
Yemen	Ras Marbat	12°47'08.56"N; 44°58'17.13"E	Present	Szefer & Geldon, 1997
Yemen	Sira Island	12°46'37.04"N; 45°02'55.42"E	Present	Szefer & Geldon, 1997
Oman	Salalah - Raysut	16°59'49.12"N; 54°05'23.18"E	Present	Badawy & Al-Harthy, 1991
Oman	Muscat	23°37'19.37"N; 58°35'22.14"E	Present	Cunha *et al.*, 2014

Table A2 – Confidence intervals (95%) of pairwise F_{ST} (above) and Jost's D (below) comparisons of *P. perna* populations. Location codes as in Table 4.2.

	KR	BZ	OR	PN	CG	BM	AM	LA	TG	LP	AT	PM	TV	VL	SG	LR	RB	CB	SB	EB	ES	IM	ML	TT	BJ	LB	DK
KR		(-0.014 - 0.012)	(-0.013 - 0.022)	(-0.011 - 0.017)	(-0.021 - 0.021)	(-0.010 - 0.014)	(-0.010 - 0.015)	(-0.014 - 0.010)	(-0.013 - 0.009)	(-0.097 - 0.076)	(-0.013 - 0.016)	(-0.016 - 0.019)	(-0.011 - 0.015)	(-0.014 - 0.011)	(-0.031 - 0.100)	(-0.015 - 0.009)	(-0.011 - 0.015)	(-0.013 - 0.014)	(-0.011 - 0.018)	(-0.013 - 0.011)	(-0.012 - 0.013)	(-0.008 - 0.021)	(-0.008 - 0.023)	(-0.014 - 0.010)	(-0.010 - 0.017)	(-0.013 - 0.008)	(-0.012 - 0.016)
BZ	(-0.027 - 0.046)		(-0.015 - 0.016)	(-0.010 - 0.021)	(-0.025 - 0.017)	(-0.011 - 0.012)	(-0.012 - 0.012)	(-0.016 - 0.010)	(-0.009 - 0.015)	(-0.101 - 0.078)	(-0.012 - 0.017)	(-0.017 - 0.010)	(-0.014 - 0.013)	(-0.013 - 0.010)	(-0.037 - 0.109)	(-0.013 - 0.013)	(-0.014 - 0.010)	(-0.013 - 0.020)	(-0.013 - 0.011)	(-0.012 - 0.013)	(-0.013 - 0.010)	(-0.012 - 0.013)	(-0.014 - 0.008)	(-0.014 - 0.008)	(-0.014 - 0.010)	(-0.013 - 0.010)	(-0.015 - 0.010)	(-0.013 - 0.015)
OR	(-0.035 - 0.062)	(-0.023 - 0.049)		(-0.016 - 0.018)	(-0.029 - 0.020)	(-0.016 - 0.012)	(-0.013 - 0.018)	(-0.019 - 0.009)	(-0.015 - 0.020)	(-0.089 - 0.105)	(-0.016 - 0.016)	(-0.016 - 0.020)	(-0.009 - 0.033)	(-0.014 - 0.020)	(-0.05- 0.102)	(-0.014 - 0.021)	(-0.016 - 0.011)	(-0.016 - 0.015)	(-0.012 - 0.015)	(-0.016 - 0.014)	(-0.014 - 0.019)	(-0.009 - 0.021)	(-0.008 - 0.025)	(-0.010 - 0.023)	(-0.013 - 0.025)	(-0.018 - 0.016)	(-0.016 - 0.017)
PN	(-0.028 - 0.062)	(-0.024 - 0.071)	(-0.028 - 0.052)		(-0.021 - 0.030)	(-0.010 - 0.016)	(-0.012 - 0.013)	(-0.013 - 0.011)	(-0.010 - 0.016)	(-0.096 - 0.080)	(-0.012 - 0.015)	(-0.011 - 0.029)	(-0.004 - 0.031)	(-0.012 - 0.020)	(-0.045 - 0.109)	(-0.010 - 0.020)	(-0.008 - 0.016)	(-0.011 - 0.015)	(-0.005 - 0.026)	(-0.008 - 0.021)	(-0.010 - 0.018)	(-0.004 - 0.029)	(-0.004 - 0.031)	(-0.009 - 0.019)	(-0.008 - 0.026)	(-0.009 - 0.021)	(-0.012 - 0.015)
CG	(-0.039 - 0.080)	(-0.039 - 0.074)	(-0.043 - 0.070)	(-0.044 - 0.088)		(-0.022 - 0.023)	(-0.026 - 0.020)	(-0.023 - 0.020)	(-0.018 - 0.025)	(-0.121 - 0.101)	(-0.026 - 0.015)	(-0.026 - 0.021)	(-0.023 - 0.023)	(-0.020 - 0.021)	(-0.051 - 0.108)	(-0.024 - 0.018)	(-0.025 - 0.014)	(-0.022 - 0.022)	(-0.025 - 0.018)	(-0.017 - 0.022)	(-0.023 - 0.019)	(-0.020 - 0.024)	(-0.021 - 0.024)	(-0.022 - 0.019)	(-0.021 - 0.022)	(-0.023 - 0.019)	(-0.026 - 0.024)
BM	(-0.034 - 0.044)	(-0.024 - 0.043)	(-0.026 - 0.045)	(-0.026 - 0.053)	(-0.047 - 0.078)		(-0.013 - 0.009)	(-0.014 - 0.006)	(-0.011 - 0.016)	(-0.083 - 0.091)	(-0.015 - 0.008)	(-0.015 - 0.018)	(-0.008 - 0.020)	(-0.011 - 0.013)	(-0.048 - 0.093)	(-0.013 - 0.010)	(-0.012 - 0.010)	(-0.013 - 0.014)	(-0.011 - 0.011)	(-0.011 - 0.011)	(-0.011 - 0.012)	(-0.013 - 0.010)	(-0.010 - 0.015)	(-0.014 - 0.011)	(-0.007 - 0.024)	(-0.015 - 0.010)	(-0.013 - 0.011)
AM	(-0.036 - 0.052)	(-0.031 - 0.043)	(-0.031 - 0.055)	(-0.030 - 0.043)	(-0.042 - 0.077)	(-0.037 - 0.036)		(-0.014 - 0.007)	(-0.009 - 0.017)	(-0.106 - 0.077)	(-0.016 - 0.010)	(-0.014 - 0.020)	(-0.013 - 0.016)	(-0.016 - 0.009)	(-0.051 - 0.098)	(-0.013 - 0.011)	(-0.012 - 0.009)	(-0.014 - 0.012)	(-0.010 - 0.016)	(-0.009 - 0.017)	(-0.015 - 0.009)	(-0.011 - 0.016)	(-0.012 - 0.013)	(-0.014 - 0.009)	(-0.008 - 0.022)	(-0.014 - 0.009)	(-0.015 - 0.011)
LA	(-0.022 - 0.040)	(-0.027 - 0.038)	(-0.023 - 0.039)	(-0.030 - 0.044)	(-0.038 - 0.071)	(-0.038 - 0.022)	(-0.040 - 0.028)		(-0.013 - 0.014)	(-0.095 - 0.080)	(-0.013 - 0.013)	(-0.014 - 0.020)	(-0.010 - 0.022)	(-0.015 - 0.012)	(-0.046 - 0.092)	(-0.014 - 0.010)	(-0.014 - 0.007)	(-0.014 - 0.008)	(-0.015 - 0.008)	(-0.014 - 0.010)	(-0.015 - 0.011)	(-0.010 - 0.015)	(-0.013 - 0.015)	(-0.013 - 0.011)	(-0.011 - 0.020)	(-0.015 - 0.012)	(-0.015 - 0.010)
TG	(-0.031 - 0.045)	(-0.024 - 0.056)	(-0.030 - 0.048)	(-0.028 - 0.051)	(-0.044 - 0.082)	(-0.037 - 0.045)	(-0.037 - 0.050)	(-0.040 - 0.035)		(-0.108 - 0.065)	(-0.010 - 0.020)	(-0.011 - 0.023)	(-0.008 - 0.021)	(-0.013 - 0.012)	(-0.033 - 0.117)	(-0.011 - 0.013)	(-0.007 - 0.019)	(-0.011 - 0.017)	(-0.012 - 0.020)	(-0.013 - 0.010)	(-0.011 - 0.015)	(-0.007 - 0.025)	(-0.009 - 0.021)	(-0.009 - 0.013)	(-0.011 - 0.018)	(-0.013 - 0.010)	(-0.011 - 0.018)
LP	(-0.085 - 0.194)	(-0.093 - 0.194)	(-0.094 - 0.248)	(-0.075 - 0.175)	(-0.102 - 0.230)	(-0.101 - 0.227)	(-0.088 - 0.205)	(-0.100 - 0.203)	(-0.084 - 0.149)		(-0.082 - 0.082)	(-0.105 - 0.095)	(-0.082 - 0.088)	(-0.084 - 0.086)	(-0.174 - 0.209)	(-0.087 - 0.080)	(-0.089 - 0.085)	(-0.097 - 0.064)	(-0.089 - 0.082)	(-0.096 - 0.079)	(-0.091 - 0.092)	(-0.080 - 0.112)	(-0.080 - 0.093)	(-0.083 - 0.090)	(-0.091 - 0.077)	(-0.08 - 0.093)	(-0.105 - 0.090)
AT	(-0.041 - 0.058)	(-0.036 - 0.054)	(-0.039 - 0.062)	(-0.039 - 0.048)	(-0.047 - 0.066)	(-0.050 - 0.029)	(-0.052 - 0.031)	(-0.042 - 0.044)	(-0.044 - 0.058)	(-0.101 - 0.214)		(-0.015 - 0.022)	(-0.012 - 0.020)	(-0.013 - 0.013)	(-0.044 - 0.094)	(-0.017 - 0.006)	(-0.014 - 0.009)	(-0.016 - 0.011)	(-0.010 - 0.018)	(-0.012 - 0.014)	(-0.012 - 0.018)	(-0.013 - 0.017)	(-0.010 - 0.021)	(-0.014 - 0.015)	(-0.007 - 0.027)	(-0.016 - 0.011)	(-0.014 - 0.015)
PM	(-0.033 - 0.053)	(-0.042 - 0.033)	(-0.031 - 0.055)	(-0.042 - 0.063)	(-0.045 - 0.086)	(-0.036 - 0.061)	(-0.044 - 0.058)	(-0.035 - 0.056)	(-0.038 - 0.062)	(-0.101 - 0.243)	(-0.041 - 0.064)		(-0.015 - 0.019)	(-0.016 - 0.019)	(-0.033 - 0.106)	(-0.015 - 0.021)	(-0.014 - 0.018)	(-0.013 - 0.031)	(-0.013 - 0.017)	(-0.014 - 0.017)	(-0.016 - 0.015)	(-0.016 - 0.015)	(-0.014 - 0.014)	(-0.015 - 0.016)	(-0.014 - 0.015)	(-0.017 - 0.017)	(-0.017 - 0.021)
TV	(-0.038 - 0.056)	(-0.030 - 0.046)	(-0.037 - 0.088)	(-0.007 - 0.096)	(-0.044 - 0.080)	(-0.037 - 0.062)	(-0.032 - 0.052)	(-0.028 - 0.064)	(-0.021 - 0.072)	(-0.089 - 0.212)	(-0.043 - 0.066)	(-0.034 - 0.065)		(-0.015 - 0.012)	(-0.026 - 0.112)	(-0.013 - 0.013)	(-0.011 - 0.018)	(-0.011 - 0.024)	(-0.007 - 0.022)	(-0.005 - 0.027)	(-0.010 - 0.016)	(-0.011 - 0.021)	(-0.014 - 0.012)	(-0.013 - 0.015)	(-0.011 - 0.017)	(-0.014 - 0.014)	(-0.009 - 0.027)
VL	(-0.032 - 0.049)	(-0.030 - 0.044)	(-0.037 - 0.067)	(-0.040 - 0.053)	(-0.041 - 0.078)	(-0.031 - 0.046)	(-0.034 - 0.039)	(-0.038 - 0.047)	(-0.038 - 0.050)	(-0.095 - 0.209)	(-0.049 - 0.049)	(-0.043 - 0.060)	(-0.034 - 0.052)		(-0.029 - 0.120)	(-0.015 - 0.011)	(-0.010 - 0.013)	(-0.016 - 0.012)	(-0.010 - 0.015)	(-0.012 - 0.012)	(-0.016 - 0.008)	(-0.008 - 0.019)	(-0.014 - 0.015)	(-0.011 - 0.013)	(-0.012 - 0.015)	(-0.017 - 0.005)	(-0.012 - 0.017)
SG	(-0.167 - 0.220)	(-0.157 - 0.221)	(-0.121 - 0.225)	(-0.118 - 0.263)	(-0.141 - 0.226)	(-0.136 - 0.193)	(-0.133 - 0.220)	(-0.138 - 0.213)	(-0.158 - 0.241)	(-0.175 - 0.279)	(-0.135 - 0.228)	(-0.153 - 0.222)	(-0.179 - 0.213)	(-0.152 - 0.236)		(-0.041 - 0.090)	(-0.042 - 0.092)	(-0.052 - 0.087)	(-0.050 - 0.084)	(-0.043 - 0.093)	(-0.037 - 0.109)	(-0.032 - 0.110)	(-0.028 - 0.110)	(-0.037 - 0.104)	(-0.021 - 0.119)	(-0.034 - 0.112)	(-0.046 - 0.108)
LR	(-0.027 - 0.053)	(-0.029 - 0.052)	(-0.043 - 0.070)	(-0.038 - 0.072)	(-0.046 - 0.080)	(-0.032 - 0.054)	(-0.036 - 0.048)	(-0.028 - 0.049)	(-0.032 - 0.048)	(-0.106 - 0.228)	(-0.058 - 0.025)	(-0.044 - 0.066)	(-0.032 - 0.053)	(-0.044 - 0.051)	(-0.144 - 0.213)		(-0.013 - 0.011)	(-0.014 - 0.011)	(-0.012 - 0.013)	(-0.012 - 0.010)	(-0.010 - 0.016)	(-0.011 - 0.018)	(-0.014 - 0.012)	(-0.015 - 0.007)	(-0.011 - 0.018)	(-0.016 - 0.007)	(-0.013 - 0.018)
RB	(-0.027 - 0.048)	(-0.021 - 0.037)	(-0.025 - 0.043)	(-0.017 - 0.058)	(-0.035 - 0.064)	(-0.023 - 0.036)	(-0.023 - 0.036)	(-0.019 - 0.032)	(-0.026 - 0.047)	(-0.088 - 0.224)	(-0.027 - 0.037)	(-0.030 - 0.059)	(-0.038 - 0.056)	(-0.024 - 0.052)	(-0.142 - 0.221)	(-0.026 - 0.050)		(-0.016 - 0.010)	(-0.008 - 0.015)	(-0.011 - 0.010)	(-0.010 - 0.014)	(-0.012 - 0.014)	(-0.011 - 0.013)	(-0.013 - 0.012)	(-0.010 - 0.020)	(-0.014 - 0.010)	(-0.014 - 0.010)
CB	(-0.036 - 0.060)	(-0.035 - 0.060)	(-0.036 - 0.057)	(-0.025 - 0.058)	(-0.050 - 0.077)	(-0.041 - 0.050)	(-0.036 - 0.042)	(-0.026 - 0.047)	(-0.038 - 0.054)	(-0.093 - 0.188)	(-0.049 - 0.044)	(-0.049 - 0.074)	(-0.041 - 0.064)	(-0.053 - 0.041)	(-0.135 - 0.234)	(-0.032 - 0.059)	(-0.027 - 0.046)		(-0.007 - 0.022)	(-0.010 - 0.015)	(-0.011 - 0.020)	(-0.007 - 0.027)	(-0.008 - 0.023)	(-0.012 - 0.016)	(-0.008 - 0.027)	(-0.018 - 0.009)	(-0.014 - 0.015)
SB	(-0.034 - 0.056)	(-0.026 - 0.040)	(-0.027 - 0.051)	(-0.041 - 0.073)	(-0.044 - 0.064)	(-0.032 - 0.047)	(-0.028 - 0.067)	(-0.035 - 0.035)	(-0.038 - 0.060)	(-0.098 - 0.225)	(-0.048 - 0.060)	(-0.037 - 0.056)	(-0.017 - 0.081)	(-0.038 - 0.053)	(-0.123 - 0.217)	(-0.040 - 0.053)	(-0.020 - 0.050)	(-0.025 - 0.082)		(-0.013 - 0.009)	(-0.012 - 0.013)	(-0.009 - 0.014)	(-0.011 - 0.011)	(-0.011 - 0.014)	(-0.012 - 0.019)	(-0.012 - 0.017)	(-0.009 - 0.021)
EB	(-0.024 - 0.045)	(-0.025 - 0.049)	(-0.028 - 0.052)	(-0.016 - 0.064)	(-0.040 - 0.077)	(-0.026 - 0.039)	(-0.029 - 0.054)	(-0.027 - 0.040)	(-0.023 - 0.035)	(-0.080 - 0.202)	(-0.035 - 0.053)	(-0.032 - 0.057)	(-0.007 - 0.105)	(-0.030 - 0.045)	(-0.124 - 0.202)	(-0.027 - 0.047)	(-0.026 - 0.041)	(-0.029 - 0.058)	(-0.031 - 0.042)		(-0.010 - 0.017)	(-0.009 - 0.014)	(-0.009 - 0.014)	(-0.009 - 0.015)	(-0.007 - 0.023)	(-0.013 - 0.010)	(-0.012 - 0.016)
ES	(-0.030 - 0.044)	(-0.025 - 0.036)	(-0.039 - 0.056)	(-0.035 - 0.045)	(-0.048 - 0.071)	(-0.035 - 0.045)	(-0.047 - 0.029)	(-0.048 - 0.026)	(-0.036 - 0.050)	(-0.089 - 0.218)	(-0.053 - 0.056)	(-0.039 - 0.048)	(-0.029 - 0.049)	(-0.045 - 0.029)	(-0.147 - 0.222)	(-0.043 - 0.065)	(-0.030 - 0.043)	(-0.043 - 0.060)	(-0.034 - 0.048)	(-0.032 - 0.050)		(-0.009 - 0.020)	(-0.011 - 0.016)	(-0.010 - 0.016)	(-0.011 - 0.016)	(-0.014 - 0.010)	(-0.012 - 0.018)
IM	(-0.030 - 0.053)	(-0.024 - 0.041)	(-0.029 - 0.062)	(-0.016 - 0.077)	(-0.042 - 0.076)	(-0.029 - 0.040)	(-0.029 - 0.053)	(-0.027 - 0.043)	(-0.031 - 0.063)	(-0.100 - 0.241)	(-0.036 - 0.049)	(-0.030 - 0.057)	(-0.038 - 0.056)	(-0.019 - 0.056)	(-0.149 - 0.196)	(-0.029 - 0.057)	(-0.022 - 0.035)	(-0.032 - 0.063)	(-0.025 - 0.049)	(-0.016 - 0.043)	(-0.023 - 0.061)		(-0.011 - 0.016)	(-0.012 - 0.013)	(-0.007 - 0.026)	(-0.012 - 0.015)	(-0.009 - 0.020)
ML	(-0.040 - 0.075)	(-0.029 - 0.040)	(-0.030 - 0.076)	(-0.043 - 0.075)	(-0.050 - 0.090)	(-0.037 - 0.060)	(-0.039 - 0.051)	(-0.041 - 0.059)	(-0.043 - 0.066)	(-0.102 - 0.219)	(-0.047 - 0.067)	(-0.040 - 0.055)	(-0.034 - 0.047)	(-0.043 - 0.063)	(-0.148 - 0.205)	(-0.033 - 0.052)	(-0.029 - 0.049)	(-0.038 - 0.063)	(-0.032 - 0.045)	(-0.029 - 0.053)	(-0.046 - 0.056)	(-0.03 - 0.058)		(-0.014 - 0.013)	(-0.008 - 0.021)	(-0.012 - 0.013)	(-0.012 - 0.021)
TT	(-0.031 - 0.044)	(-0.022 - 0.038)	(-0.025 - 0.059)	(-0.037 - 0.051)	(-0.035 - 0.073)	(-0.037 - 0.039)	(-0.031 - 0.038)	(-0.032 - 0.036)	(-0.031 - 0.038)	(-0.082 - 0.200)	(-0.036 - 0.056)	(-0.038 - 0.048)	(-0.027 - 0.055)	(-0.028 - 0.049)	(-0.144 - 0.209)	(-0.022 - 0.041)	(-0.022 - 0.035)	(-0.031 - 0.051)	(-0.034 - 0.045)	(-0.020 - 0.053)	(-0.031 - 0.052)	(-0.022 - 0.036)	(-0.035 - 0.042)		(-0.009 - 0.019)	(-0.013 - 0.007)	(-0.015 - 0.012)
BJ	(-0.027 - 0.054)	(-0.022 - 0.042)	(-0.038 - 0.067)	(-0.022 - 0.073)	(-0.041 - 0.077)	(-0.026 - 0.066)	(-0.026 - 0.069)	(-0.026 - 0.054)	(-0.028 - 0.058)	(-0.087 - 0.186)	(-0.045 - 0.075)	(-0.031 - 0.056)	(-0.028 - 0.061)	(-0.037 - 0.057)	(-0.156 - 0.255)	(-0.039 - 0.069)	(-0.029 - 0.062)	(-0.034 - 0.077)	(-0.034 - 0.054)	(-0.024 - 0.068)	(-0.030 - 0.055)	(-0.019 - 0.068)	(-0.026 - 0.072)	(-0.023 - 0.059)		(-0.013 - 0.017)	(-0.008 - 0.026)
LB	(-0.024 - 0.042)	(-0.022 - 0.039)	(-0.048 - 0.038)	(-0.024 - 0.069)	(-0.047 - 0.075)	(-0.036 - 0.034)	(-0.028 - 0.041)	(-0.029 - 0.046)	(-0.031 - 0.047)	(-0.094 - 0.227)	(-0.049 - 0.036)	(-0.032 - 0.056)	(-0.030 - 0.058)	(-0.039 - 0.027)	(-0.136 - 0.228)	(-0.048 - 0.028)	(-0.023 - 0.039)	(-0.028 - 0.051)	(-0.035 - 0.066)	(-0.029 - 0.046)	(-0.036 - 0.047)	(-0.025 - 0.043)	(-0.033 - 0.053)	(-0.020 - 0.033)	(-0.039 - 0.056)		(-0.013 - 0.014)
DK	(-0.029 - 0.054)	(-0.025 - 0.045)	(-0.024 - 0.052)	(-0.022 - 0.046)	(-0.038 - 0.076)	(-0.029 - 0.038)	(-0.033 - 0.040)	(-0.035 - 0.038)	(-0.034 - 0.045)	(-0.082 - 0.198)	(-0.043 - 0.047)	(-0.036 - 0.058)	(-0.022 - 0.096)	(-0.037 - 0.056)	(-0.127 - 0.223)	(-0.032 - 0.065)	(-0.020 - 0.033)	(-0.037 - 0.057)	(-0.038 - 0.055)	(-0.032 - 0.049)	(-0.035 - 0.046)	(-0.019 - 0.051)	(-0.041 - 0.060)	(-0.025 - 0.041)	(-0.018 - 0.067)	(-0.028 - 0.044)	

Table A3 – Pairwise ϕ_{ST} comparison of male (below) and female (above) *P. perna* datasets. All *p*-values were corrected and non-significant. Location codes as in Table 4.2.

	BM	LR	ES	IM	ML	TT	BJ	LB	DK
BM	-	0.000	0.045	0.014	0.011	0.037	0.055	0.000	0.000
LR	0.014	-	0.002	0.000	0.000	0.007	0.008	0.000	0.000
ES	0.005	0.004	-	0.054	0.000	0.016	0.038	0.000	0.046
IM	0.000	0.004	0.003	-	0.019	0.019	0.026	0.000	0.040
ML	0.000	0.000	0.000	0.001	-	0.001	0.019	0.000	0.013
TT	0.000	0.000	0.000	0.000	0.000	-	0.000	0.000	0.082
BJ	0.005	0.001	0.000	0.015	0.000	0.008	-	0.010	0.101
LB	0.001	0.000	0.000	0.000	0.000	0.000	0.000	-	0.000
DK	0.012	0.000	0.000	0.014	0.000	0.000	0.005	0.000	-

Table A4 – AMOVA of male (A) and female (B) individuals from nine populations of *P. perna* distributed over four groups, based on mitochondrial COI.

A

Source of variation	df	Sum of squares	Variance components	Percentage of variation	ϕ-statistics	*p*-value
Among groups	3	1.874	-0.0061	-0.87	-0.0087	0.80
Among populations within groups	5	4.095	0.0079	1.11	0.0110	0.21
Within populations	124	87.233	0.7035	99.76	0.0024	0.33
Total	132	93.203	0.7052			

B

Source of variation	df	Sum of squares	Variance components	Percentage of variation	ϕ-statistics	*p*-value
Among groups	3	1.826	-0.0049	-0.81	-0.0081	0.75
Among populations within groups	5	3.833	0.0112	1.85	0.0183	0.06
Within populations	126	75.467	0.5989	98.96	0.0104	0.12
Total	134	81.126	0.6052			

Table A5 – Pairwise F_{ST} (above) and Jost's D (below) comparisons of male (A) and female (B) *P. perna* datasets. All *p*-values of F_{ST} and Jost's D were corrected and non-significant. Location codes as in Table 4.2.

A

Males	BM	LR	ES	IS	ML	TT	BJ	LB	DK
BM	-	0.014	0.005	0.000	0.000	0.000	0.005	0.001	0.012
LR	0.145	-	0.004	0.004	0.000	0.000	0.001	0.000	0.000
ES	0.108	0.000	-	0.003	0.000	0.000	0.000	0.000	0.000
IS	0.006	0.060	0.068	-	0.001	0.000	0.015	0.000	0.014
ML	0.000	0.000	0.000	0.037	-	0.000	0.000	0.000	0.000
TT	0.000	0.000	0.000	0.000	0.000	-	0.008	0.000	0.000
BJ	0.045	0.051	0.015	0.069	0.000	0.054	-	0.000	0.005
LB	0.045	0.000	0.054	0.007	0.000	0.000	0.000	-	0.000
DK	0.121	0.029	0.000	0.118	0.000	0.000	0.098	0.067	-

B

Females	BM	LR	ES	IS	ML	TT	BJ	LB	DK
BM	-	0.000	0.002	0.000	0.005	0.009	0.007	0.000	0.005
LR	0.000	-	0.000	0.002	0.000	0.000	0.000	0.000	0.000
ES	0.000	0.000	-	0.000	0.007	0.005	0.000	0.000	0.005
IS	0.006	0.022	0.009	-	0.000	0.000	0.000	0.000	0.004
ML	0.103	0.016	0.074	0.003	-	0.000	0.001	0.005	0.005
TT	0.042	0.051	0.106	0.032	0.003	-	0.000	0.000	0.010
BJ	0.029	0.000	0.000	0.036	0.012	0.039	-	0.000	0.009
LB	0.000	0.000	0.000	0.000	0.085	0.061	0.000	-	0.000
DK	0.052	0.017	0.005	0.026	0.044	0.054	0.111	0.000	-

Table A6 – AMOVA of male (a) and female (b) individuals from nine populations of *P. perna* distributed over four groups, based on seven microsatellite markers.

A

Source of variation	df	Sum of squares	Variance components	Percentage of variation	ϕ-statistics	*p*-value
Among groups	3	7.504	-0.0021	-0.08	-0.0008	0.64
Among populations within groups	5	13.178	0.0002	0.01	0.0001	0.50
Within populations	261	686.633	2.6308	100.07	-0.0007	0.58
Total	269	707.315	2.6289			

B

Source of variation	df	Sum of squares	Variance components	Percentage of variation	ϕ-statistics	*p*-value
Among groups	3	7.644	0.0022	0.09	0.0009	0.34
Among populations within groups	5	12.033	-0.0028	-0.11	-0.0011	0.87
Within populations	261	650.2	2.4912	100.02	-0.0003	0.88
Total	269	669.878	2.4906			

8.2 Figures

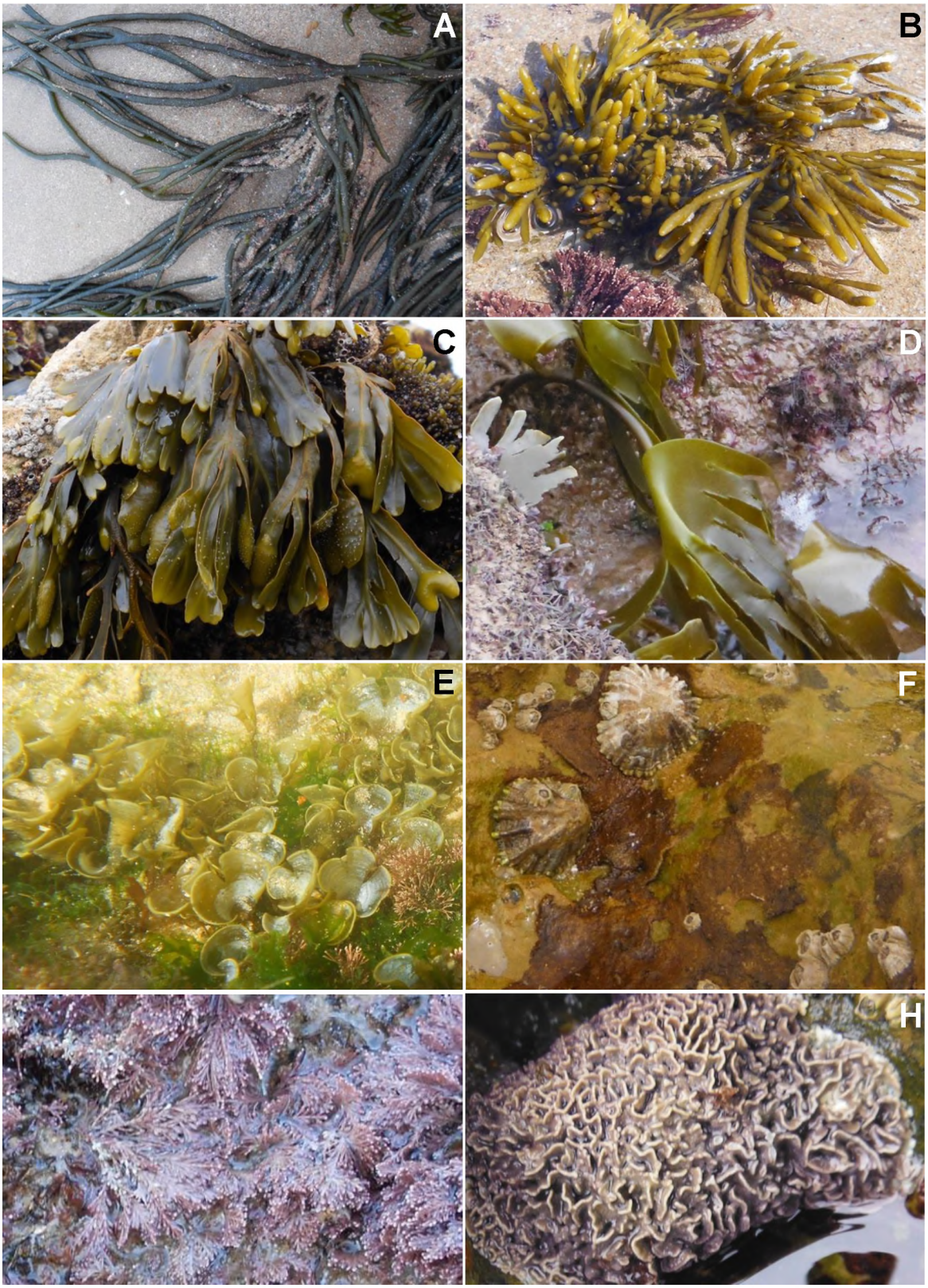

Figure A1 – Examples of alga species present on Moroccan and Western Sahara shores. A) *Codium tomentosum var. mucronatum*, B) *Bifurcaria bifurcata*, C) *Fucus guiryi*, D) *Laminaria ochroleuca*, E) *Padina pavonica*, F) *Ralfsia verrucosa*, G) *Corallina caespitosa*, H) *Litophyllum byssoides*. A) green alga; B-F) brown algae and G-H) red algae.

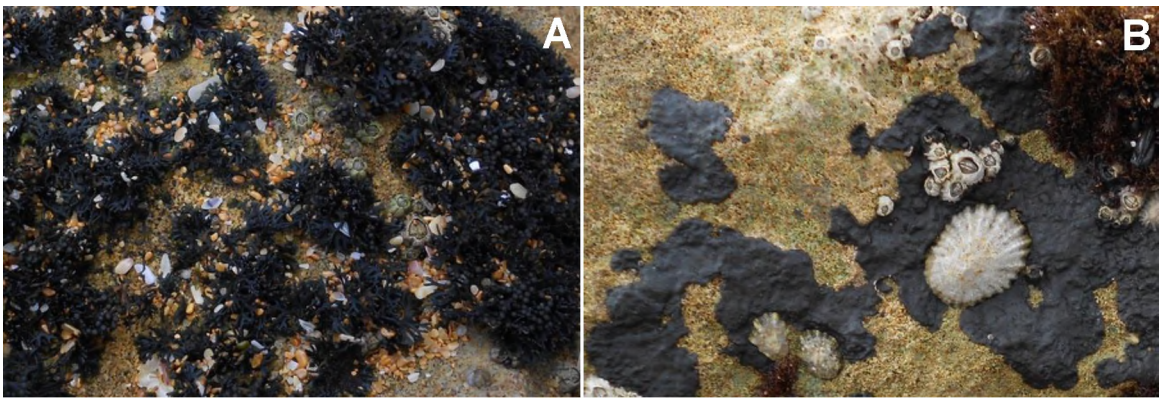

Figure A2 – Ascomycota (lichen) species identified from Moroccan and Western Sahara shores. A) *Lichina pygmaea*, B) *Verrucaria maura*.

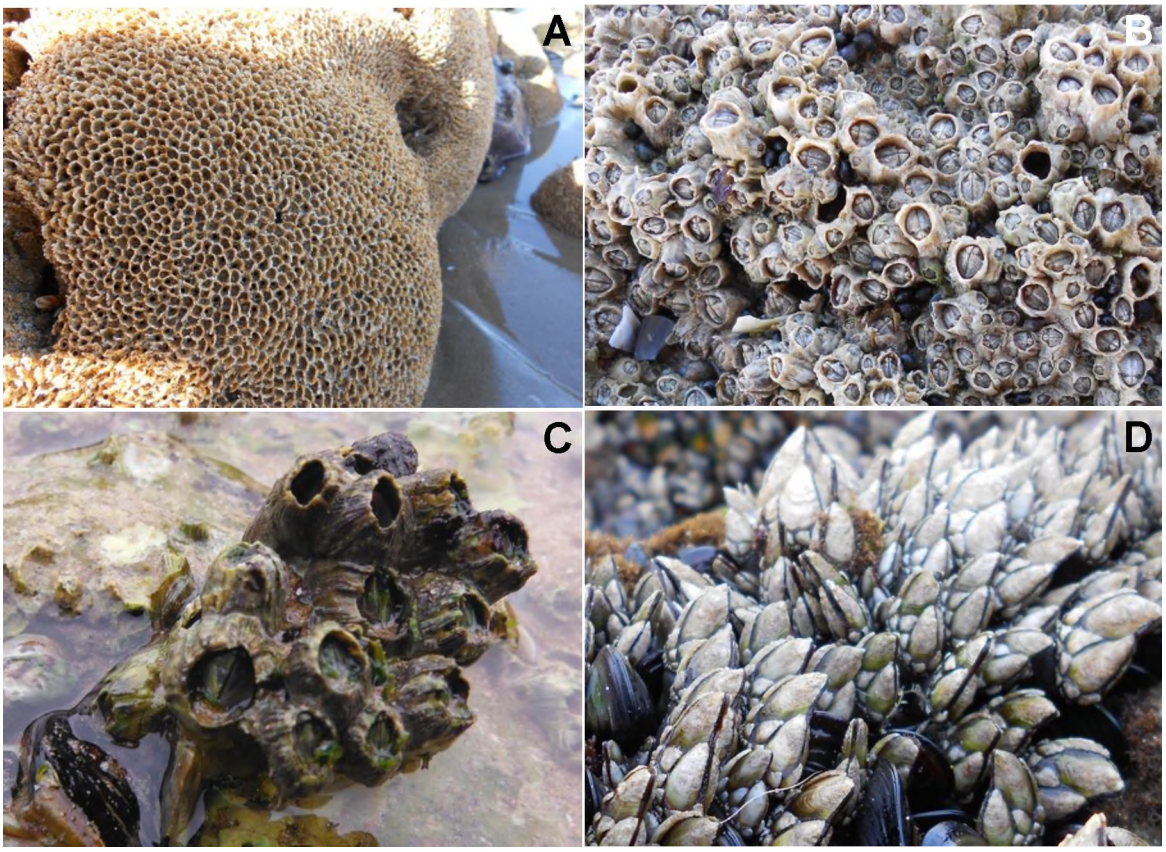

Figure A3 – Anellida (A) and Arthropoda (B-D) species identified from Moroccan and Western Sahara shores. A) *Sabellaria alveolata*, B) *Chthamalus* spp, C) *Perforatus perforatus*, D) *Pollicipes pollicipes*.

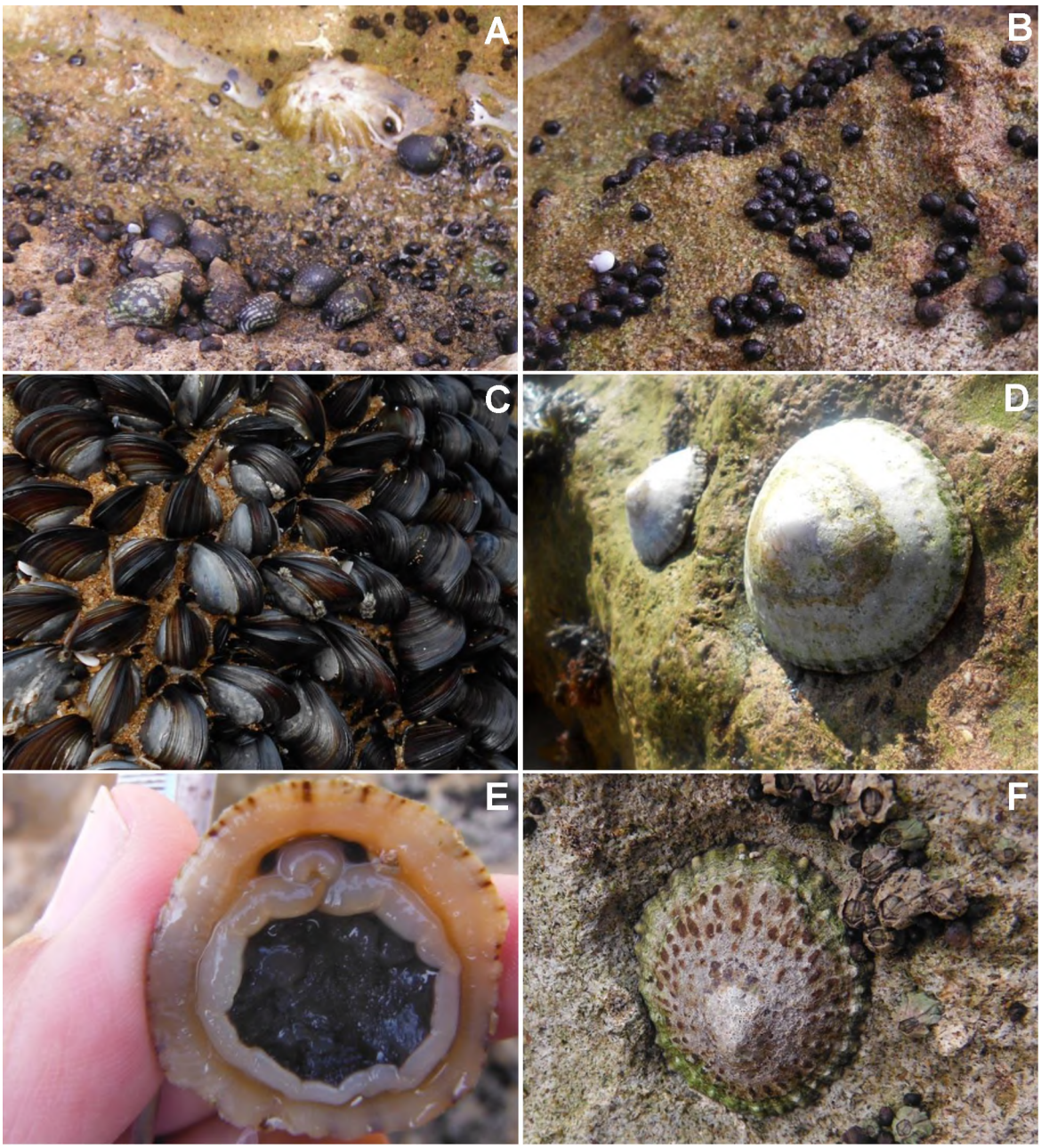

Figure A4 – Examples of Mollusca species identified from Moroccan and Western Sahara shores. A) *Echinolittorina punctata*, B) *Melarhaphe neritoides*, C) *Mytilus galloprovincialis*, D) *Cymbula nigra*, E) *Patella depressa*, F) *Pat. rustica*.

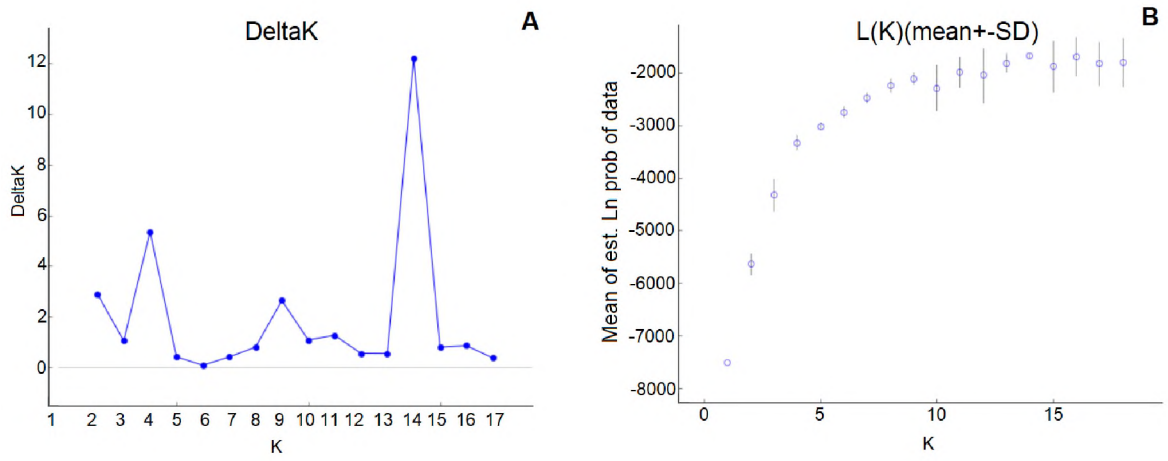

Figure A5 – Selection of best-fitting K (number of clusters) proposed for the genetic structure of *F. guiry* populations. A) Best-fitting K based on ΔK method of Evanno *et al.* (2005), i.e. K=4, B) Best-fitting K based on Ln(K), i.e. K=4.

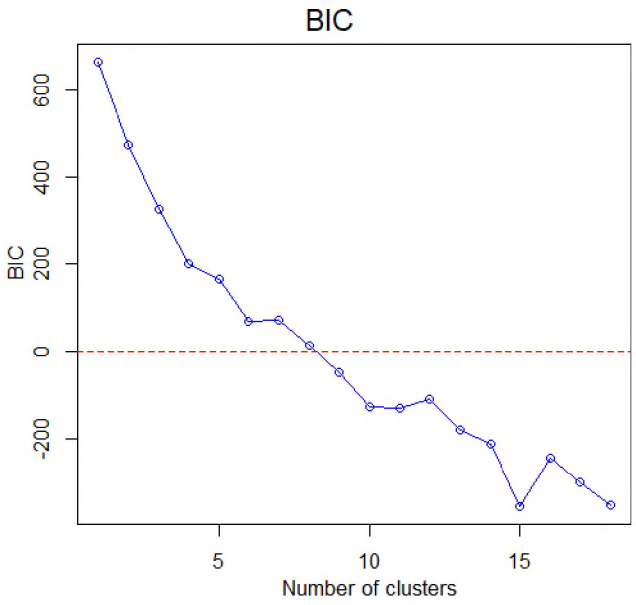

Figure A6 – Discriminant analyses of principal components (DAPC) results. Selection of best fitting K (K=4) based on Bayesian Information Criterion (BIC),

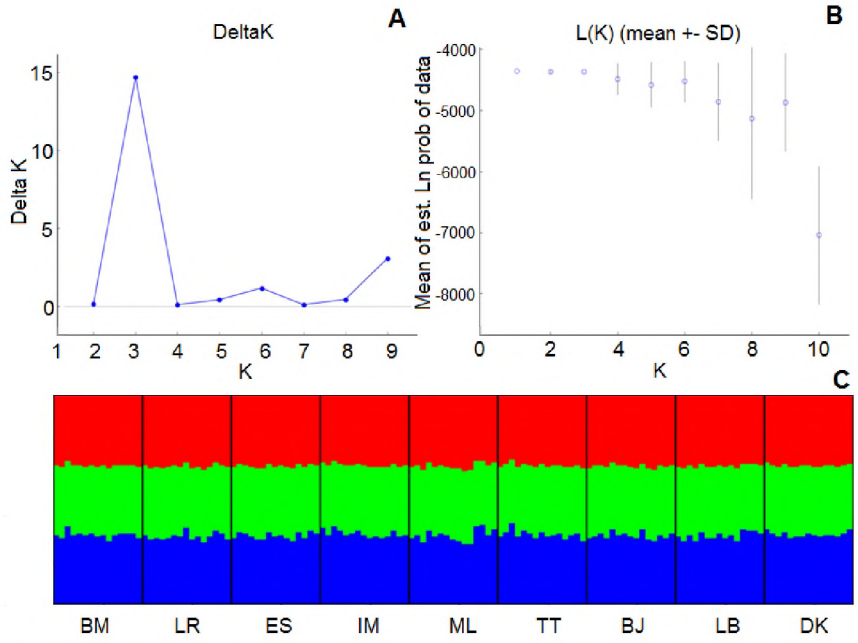

Figure A7 – Selection of best-fitting K (number of clusters) proposed for the genetic structure of the male dataset of *P. perna* populations. A) Best-fitting K based on ΔK method of Evanno *et al.* (2005), i.e. K=3, B) Best-fitting K based on Ln(K), i.e. K=1, C) Bayesian analysis summary plot (each bar represents one individual) obtained from STRUCTURE i.e. K=3. Coloured bars depict expected genetic clusters. Bars of different widths indicate different populations and are composed of single bars for each individual.

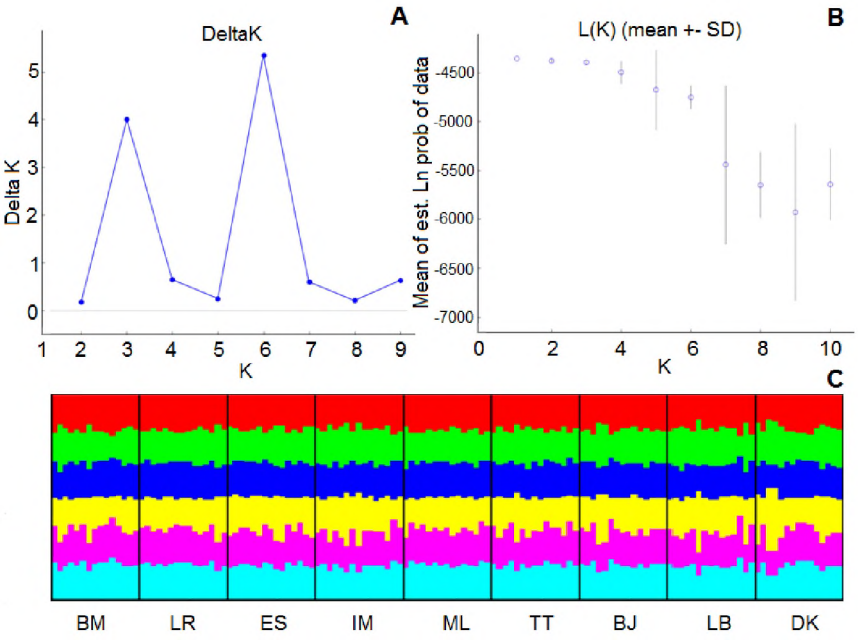

Figure A8 – Selection of best-fitting K (number of clusters) proposed for the genetic structure of the male dataset of *P. perna* populations. A) Best-fitting K based on ΔK method of Evanno *et al.* (2005), i.e. K=3, B) Best-fitting K based on Ln(K), i.e. K=1, C) Bayesian analysis summary plot (each bar represents one individual) obtained from STRUCTURE i.e. K=3. Coloured bars depict expected genetic clusters. Bars of different widths indicate different populations and are composed of single bars for each individual.